Histamine H$_3$ receptor antagonists with multitargeting properties at GPCRs and enzymes

Inaugural-Dissertation

zur Erlangung des Doktorgrades
der Mathematisch-Naturwissenschaftlichen Fakultät
der Heinrich-Heine-Universität Düsseldorf

vorgelegt von

Stefanie Hagenow

aus Seesen

Düsseldorf, Juli 2018

Angefertigt am Institut für Pharmazeutische und Medizinische Chemie der Heinrich-Heine-Universität Düsseldorf.

To my father
        and grandfather

Contents

Abbreviations

5-HT	5-Hydroxytryptamine (Serotonin)
6-OHDA	6-Hydroxydopamine
Aβ	Amyloid β peptides
$A_x R$	Adenosine A_x receptor
AC	Adenylyl cyclase
ACh	Acetylcholine
AChE	Acetylcholinesterase
AChEI	Acetylcholinesterase inhibitor
AD	Alzheimer's disease
ADHD	Attention-deficit hyperactivity syndrome
ATP	Adenosine triphosphate
APP	Amyloid precursor protein
BACE 1	β-Secretase
BBB	Blood-brain barrier
cAMP	Cyclic adenosine monophosphate
ChE	Cholinesterase
ChEI	Cholinesterase inhibitor
CNS	Central nervous system
COMT	Catechol-O-methyltransferase
CREB	cAMP response element-binding protein
CYP	Cytochrome P450
$D_x R$	Dopamine D_x receptor
EDS	Excessive daytime sleepiness
EMA	European Medicines Agency
ERK	Extracellular signal-regulated kinase
FAD	Flavin adenine dinucleotide
FDA	Food and Drug Administration
GABA	γ-Aminobutyric acid
GIRK	G-Protein-gated inwardly rectifying potassium channel
GPCR	G-Protein coupled receptor
GP_e	Globus pallidus externa
GP_i	Globus pallidus interna
GSK3β	Glycogen synthase kinase 3β
GTP	Guanosine triphosphate
HDC	Histidine decarboxylase
$HDC^{-/-}$	HDC knock out/deficiency
hERG	Human Ether-a-go-go related gene
HNMT	Histamine *N*-methyltransferase
HxR	Histamine H_x receptor
$H_3 R^{-/-}$	$H_3 R$ knock out/deficiency

IP$_3$	Inositol-1,4,5-trisphosphate
L-DOPA	L-3,4-Dihydroxyphenylalanine
LID	L-DOPA-induced dyskinesia
MAO	Monoamine oxidase
MAPK	Mitogen-activated protein kinase
MCH	Melanin-concentrating hormone
MCHR1	Melanin-concentrating hormone receptor 1
MCHR1$^{-/-}$	MCHR1 knock out/deficiency
MPTP	N-Methyl-4-phenyl-1,2,3,6-tetrahydropyridine
mRNA	Messenger ribonucleic acid
MTL	Multitargeting ligand
NMDA	N-Methyl-D-aspartate
NMDAR	N-Methyl-D-aspartate receptor
OSA	Obstructive sleep apnea
PD	Parkinson's disease
PI3K	Phosphoinositol-3-kinase
PLA$_2$	Phospholipase A$_2$
RAMH	R-α-Methylhistamine
ROS	Reactive oxygen species
SAR	Structure-activity relationships
SN	Substantia nigra
SNpc	Substantia nigra pars compacta
STN	Subthalamic nucleus
TM	Transmembrane domain
TMN	Tuberomammilary nucleus

Zusammenfassung

In den letzten Jahrzehnten wurde das Design von Multitargeting-Liganden (MTLs) zu einem bedeutenden Forschungsgebiet in der medizinischen Chemie. Mit der Entwicklung von Wirkstoffen zur synergistischen Modulation mehrerer Targets, wurde ein neues Kapitel in der Therapie von multifaktoriellen Erkrankungen aufgeschlagen, die mit klassischen selektiven Wirkstoffen nur unzureichend therapiert werden können. Störungen des zentralen Nervensystems (ZNS), beispielsweise bei neurodegenerativen Erkrankungen, sind typischerweise multifaktoriell und weisen insbesondere unter Berücksichtigung des demographischen Wandels unserer Gesellschaft einen hohen medizinischen Bedarf auf. Angesichts des ständig wachsenden Verständnisses der Ursachen und vielen Faktoren, die an diesen Krankheiten beteiligt sind, setzen Forscher große Hoffnungen in Multitargeting-Medikamente als revolutionäre Pharmakotherapie. Histamin-H_3-Rezeptoren (H_3R) leisten einen großen Beitrag bei der Regulation verschiedenster Neurotransmittersysteme. Folglich besitzen Antagonisten/Inverse Agonisten, welche den H_3R blockieren, eine therapeutische Relevanz für eine Vielzahl von ZNS-Störungen, wie kürzlich durch Zulassung von Pitolisant als "Orphan Drug" für Narkolepsie unter Beweis gestellt. Gleichzeitig liefert ihr Einsatz im Rahmen von Multitargeting-Medikamenten ein erweitertes therapeutisches Spektrum.

Die Publikationen in dieser Arbeit umfassen die Identifizierung und zielgerichtete Entwicklung von H_3R-MTLs, die entweder als Liganden G-Protein-gekoppelter Rezeptoren (GPCRs) oder Inhibitoren von Neurotransmitter-abbauenden Enzymen wirken. Aufgrund des therapeutischen Potenzials von Monoaminooxidase (MAO) A/B-Inhibitoren bei neurodegenerativen Prozessen, wurden H_3R/MAO-MTLs strukturell basierend auf Ciproxifan entworfen. Dieser bekannte H_3R-Inversen Agonist zeigt moderate MAO-Inhibition, welche hier erstmals beschrieben wurde. Durch Anwendung eines wissensbasierten MTL-Ansatzes wurde ein allgemein akzeptierter H_3R-Pharmakophor mit Strukturelementen von MAO A/B-Inhibitoren verknüpft oder verschmolzen. Dabei wurden H_3R-MTLs charakterisiert, welche entweder eine reversible oder ein irreversible MAO-Inhibition aufweisen. Representative MTLs zeigten eine vielversprechende Dual- oder Multitargeting-Wirksamkeit, sowie therapeutisches Potenzial bei der Behandlung von neurodegenerativen Erkrankungen wie Morbus Alzheimer oder Parkinson. Um unterschiedliche therapeutische Kombinationsmöglichkeiten zu demonstrieren, wurden darüber hinaus H_3R-MTLs, die als Antagonisten des Melanin-konzentrierenden Hormonrezeptors 1 (MCHR1) fungieren, über einen computergestützten Liganden-basierten Data-Mining-Ansatz entwickelt. Da beide Targets zur Regulierung der Energiehomöostase und der Nahrungsaufnahme beitragen, stellen H_3R/MCHR1-MTLs einen innovativen Ansatz für die Behandlung von Essstörungen dar.

Zusammenfassend liefert diese Arbeit erste präklinische Belege für die therapeutische Relevanz von H_3R-Antagonisten als Multitargeting-Wirkstoffe bei der Behandlung von multifaktoriellen Erkrankungen, wie beispielsweise neurodegenerativen Erkrankungen.

Summary

Over the last decades the design of multitargeting ligands (MTLs) has become a significant research field in medicinal chemistry. With the approach of designing drugs which specifically modulate multiple targets in a synergistic manner, a new leaf was turned over in therapy of multifactorial diseases, being insufficiently addressed by target-selective drugs in the classical "one drug - one target" mode. Central nervous system (CNS) disorders, such as neurodegenerative diseases, are prominent representatives of multifactorial diseases, having a high medical need especially within the demographic shift of our society. With the constantly growing understanding of initial causes and multiple factors involved in these diseases, researchers pin high hopes on multitargeting drug design as revolutionary pharmacotherapy. Histamine H_3 receptors (H_3R) have a great share in overall regulation of various neurotransmitter systems. Thus, antagonists/inverse agonists that block H_3Rs have a therapeutic relevance in a variety of CNS disruptions as shown by pitolisant, a recently approved orphan drug for narcolepsy. When used in multitargeting drug design, H_3R antagonists will have an even larger spectrum of indications.

The compiled publications in this thesis comprise the initial identification and straightforward design of H_3R MTLs, either acting as antagonists of additional G-protein coupled receptors (GPCRs) or as inhibitors of neurotransmitter-catabolizing enzymes. With the potential utility of monoamine oxidase (MAO) A/B inhibitors in fighting neurodegeneration, H_3R/MAO B MTLs were structurally designed based on ciproxifan, a common H_3R antagonist with herein described moderate MAO inhibition capacities. A strategy of knowledge-based MTL design was pursued by fusing or merging a general accepted H_3R pharmacophore with key structural elements of MAO A/B inhibitors. H_3R MTLs showing reversible and irreversible modes of MAO A/B inhibition with promising dual- or multitargeting efficacy were characterized, providing a therapeutic potential for treatment of neurodegenerative diseases such as Alzheimer's or Parkinson's disease.

Additionally, to expand their therapeutic repertoire, H_3R MTLs showing antagonism of melanin-concentrating hormone receptors 1 (MCHR1) were designed via a computational ligand-based data mining approach. With both targets playing a part in energy and food intake homeostasis, these H_3R/MCHR1 MTLs may provide an innovative approach for treatment of eating disorders.

In conclusion, this thesis provides initial preclinical evidence for the therapeutic relevance of multitargeting H_3R antagonists/inverse agonists in the treatment of multifactorial neurodegenerative diseases.

1 Introduction

1.1 Multitargeting Approach

Due to the extraordinary complexity of the central nervous system (CNS) and its multiple and various tasks in physiological regulation, it is inevitable that CNS disorders display a similar complexity. Accordingly, treatment of CNS-originated diseases represents a remarkable challenge not only in human medicine.[1] Medicinal progress in technology, diagnostics and pharmaceutics provide steadily growing scientific insights into neurological diseases, thus, putting together the puzzle piece by piece. For example, for neurodegenerative diseases various determinants have already been identified, while the exact mechanisms still need to be elucidated. As a consequence, dysregulated processes might appear much more complex after considering any new data input. Adjustment to this medicinal progress forced pharmacologists and medicinal chemists to face these diseases with more innovative strategies to combat the multifactorial mechanisms. Over the last decades, the development of multitargeting ligands (MTLs) emerged to be an effective approach in therapy of neurological diseases.[2,3] While former drug development focused on selective drugs modulating a specific target, typified by Paul Ehrlich's "magic bullet", MTLs are designed to regulate several targets, which might interact with each other. For some marketed and well-characterized drugs, multitargeting properties have been discovered retrospectively.[2] Initially named as "dirty drugs", for some of them their multitargeting behaviour turned out to be favourable or even the reason for pharmacological advantages compared to highly selective compounds within a drug class.[4] For instance, the atypical antipsychotic clozapine possesses a diverse target portfolio, leading to multiple side effects e.g. by histamine H_1 or adrenergic receptor affinity. Its affinity at both dopamine and serotonin receptors, defines its advanced therapeutic value in treatment of psychotic disorders.[5,6] Subsequently, the development of a new generation of antipsychotics was initiated such as aripiprazole which, was approved in 2002 by the Food and Drug Administration (FDA). These representative MTLs modulate multiple specific dopamine and serotonin receptor subtypes, exhibiting a reduced risk to cause extrapyramidal symptoms compared to first generation antipsychotics.[4,7] Moreover, the general assumption favouring selective drugs to lower the risk for side effects was challenged due to frequent observations of their limited in vivo efficacy, in particular to treat the more complex diseases.[8]

Assessing multitargeting drugs, however, requires a more extensive pharmacological characterization of a set of targets as well as earliest mechanism-based off-target identification. Synthetic adjustments and target-specific pharmacological evaluations have to be combined in a continuous iterative process, where medici-

nal chemists have to struggle with reduced flexibility in terms of target balancing and lead optimization to obtain the desired promiscuous character. Depending on the targets and their biochemical and topographical relation, this process can be manifold and challenging.[2] In comparison with application of drug cocktails (co-pharmacotherapy, co-medication) to address multifactorial diseases, the use of MTLs would improve complex pharmacokinetic issues, since onset-time, half-life and metabolism would be aligned for MTLs. Risk factors like potential drug resistances are minimized, while drug-drug interactions will be entirely omitted in best cases.[5,9] This simplifies the therapeutic regimen for patients, promoting compliance, which is especially low in numerous neurological diseases, e.g. patients suffering from depression or cognitive impairment. Another advantage of MTLs is an optimized cost and time efficiency of the drug development process, where safety and risk assessment in drug combinations must be performed for each drug and again for their combination. Most appreciable, with MTLs the pharmacodynamic possibility to achieve higher therapeutic efficacy by synergistic or additive effects is enhanced, something which needs to be more carefully elucidated in case of drug combination therapies with respect to dose adjustment and drug interactions.[2]

To identify sufficient MTL lead compounds, two options are possible: Random or focussed screening (serendipitous approach), in the case of limited access to target-specific pharmacophores or knowledge-based approaches evaluating previously described target affinities.[2] The chemical realization of rational multitargeting drug design may start from a lead structure with any proven multiple target efficacy or from at least two target-selective compounds (Figure 1).[10] The first strategy means target balancing or refinement of multitargeting properties based on one lead compound, e.g. applicable on retrospectively classified MTLs. The latter strategy includes three main synthetic approaches: i) linking, ii) fusing or iii) merging of two pharmacophores,[5,10,11] which are defined as ensemble of steric and electronic features, necessary to ensure the optimal supramolecular interactions with a specific biological target structure to trigger (or block) its biological response.[12]

Linked multitargeting drugs may be connected either via metabolizable (e.g. ester-based) linkers to release two ligands interacting with their respective targets independently or via metabolically stable (non-cleavable) linkers, which have their pharmacological eligibility in specific targeting and characterization of hetero-oligomers.[5] (Hetero)oligomerization represents a common phenomenon in G-Protein coupled receptor (GPCR) research, in which receptors can influence each other's binding and signalling, and is gaining more and more importance for understanding of receptor function and associated pathologies.[13–15] However, linked MTLs may suffer from inadequate physicochemical properties depending on mole-
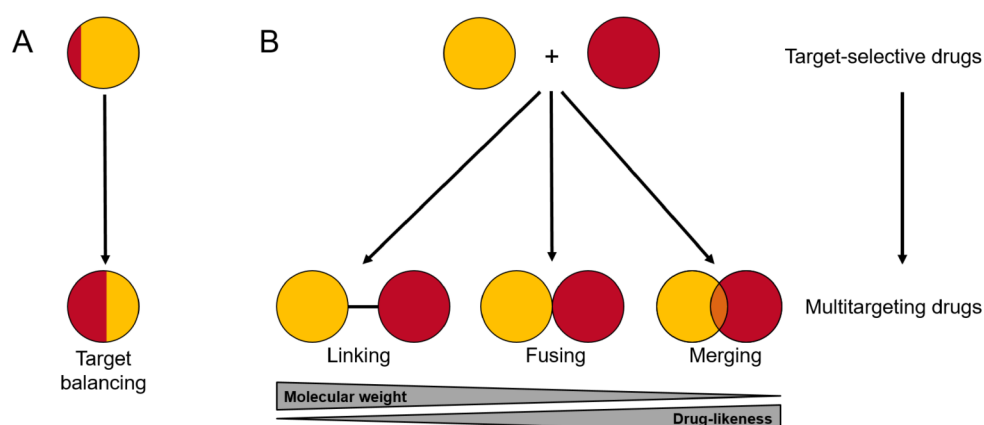
Figure 1 – Multitargeting drug design strategies starting from (A) one lead structure with known multitarget affinities or (B) two target-selective compounds (adapted from ref. 10).

cular weight of the two pharmacophores. On the other hand, fusing and merging of two pharmacophores results in a remarkable decrease of the molecular size, most probably leading to more favourable drug-likeness of MTLs.[16] Over decades of applied multitargeting drug design it appeared that small and less complex molecules are non-selective and most likely to bind multiple targets, explainable by lower target-mismatching.[8,10,11,16] For successful design of MTLs, the pioneers Morphy and Rankovic defined valuable requirements such as adequate understanding of in vitro/in vivo relationships, indication of structure-activity relationship (SAR)-based "arbitrary regions" for fusing or merging and sufficient drug-like properties, ideally evidenced by drug market maturity of either "starting compounds" or related substructures.

For CNS diseases, many drugs are approved, but showing therapeutical limitations in addressing the multifactorial pathologies, e.g. associated with the multiple neurotransmitter systems involved. Furthermore, CNS drugs have a high rate of clinical failure, where candidates often do not show the desired therapeutical efficacy.[1] Nevertheless, continuous effort has been made in identification of new mechanisms and targets as well as the drug's modes of action. These facts, together with an urgent need for more comprehensive pharmacotherapy, strongly suggest consideration of combination therapies and MTLs based on approved drugs or candidates not effective in single-drug applications.[1] Addressing several neurotransmitter systems involved in these diseases should be a promising approach to treat main but also cormobid symptoms. Among them, the histaminergic system, despite having received less attention compared to other neurotransmitter systems, was identified as key player in numerous pathophysiological conditions observed in CNS disorders, i.e. regulation of sleep, energy balance, motor functions, cognition and attention.[17]
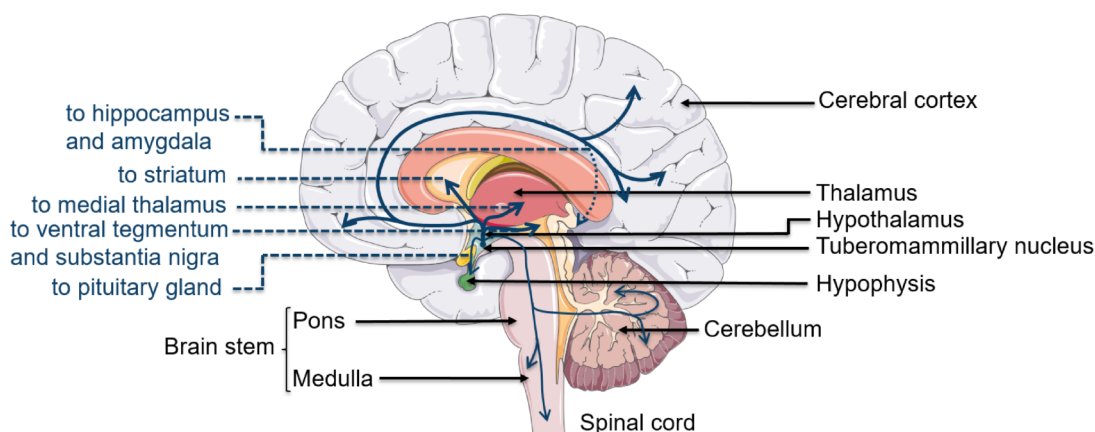
Figure 2 – Histaminergic projections (blue arrows) originating in the tuberomammillary nucleus (TMN) and innervating the major parts of the human brain, i.e. cerebral cortex, amygdala, substantia nigra and striatum, with one descending pathway to the brain stem, cerebellum and the spinal cord (modified from ref. 21, 22).

1.2 The Histamine H$_3$ Receptor

For a long time, histamine was known for its peripheral rather than for CNS functions, namely mediation of inflammatory or allergic reactions and gastric acid secretion. Initially classified as a tissue mediator, histamine became generally recognized as a neurotransmitter in the 1980's, when histaminergic neurons were visualized for the first time.[18-20] This was a fundamental evidence of histamine's role in neurotransmission, something already assumed since the discovery of sedating effects observed for "classical" antiallergic antihistamines. The tuberomammillary nucleus (TMN), located in the hypothalamus, was identified as the origin of various projections of the histaminergic system (Figure 2).[21,22]

Histaminergic innervations cover almost the entire CNS, while highest densities were found in the amygdala, cerebral cortex, striatum and the substantia nigra. By now, the pivotal and manifold contribution of neuronal histamine in regulation of basic physiologic functions such as drinking/feeding behaviour and energy homeostasis, but also waking, attention and cognition is ascertained beyond any doubt.[21,23] In the TMN, the only site of neuronal histamine biosynthesis, histidine decarboxylases (HDC; EC 4.1.1.22) convert L-histidine to histamine. Stored in vesicles, histamine can be released into the synaptic cleft, where its half-life is about thirty minutes but may change quickly due to neuronal activity.[21]

The inactivation of released histamine involves two enzyme-catalysed pathways: (a) oxidative deamination by diamine oxidases (DAO; EC 1.4.3.22) in the periphery or by (b) N^{τ}-methylation of the imidazole by cytosolic histamine N-methyltransferases (HNMT; EC 2.1.1.8) after cellular reuptake. In the brain, the latter is
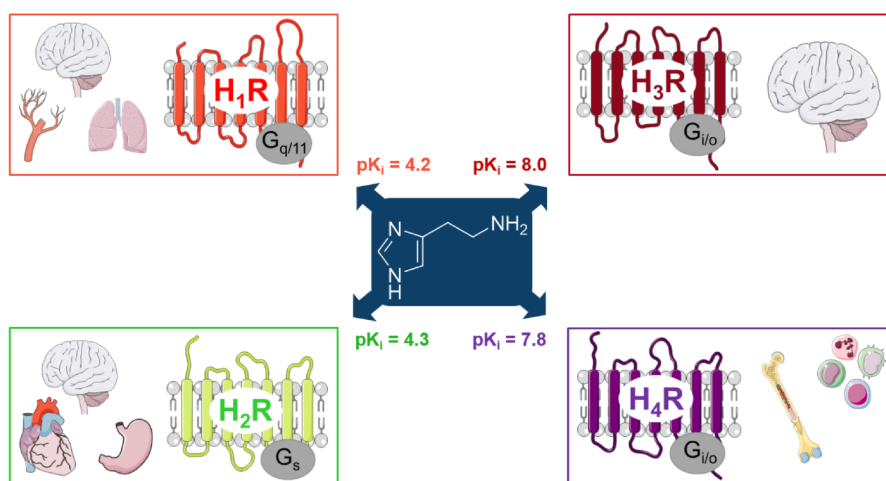
Figure 3 – The four histamine receptor subtypes and their most abundant localizations. Histamine has distinct affinities (given as pK_i values) at the histamine receptor subtypes.[25,26]

the major path of histamine degradation, leading to conversion into the inactive metabolite N^τ-methylhistamine, which will be further converted by monoamine oxidase B via oxidative deamination.[18,24] Histamine can act via four different G-protein coupled histamine receptors (H_1-H_4) (Figure 3) but it shows highest affinity at histamine H_3 receptors (H_3Rs).[25,26] For the first three identified receptor subtypes, a wide but distinct expression in the CNS could be demonstrated. H_3Rs show the most exclusive CNS expression with limited but mentionable peripheral distribution, e.g. in the cardiovascular system.[26,27]

The histamine H_1 receptor (H_1R) represents a main target for therapy of allergic reactions as well as insomnia, while the histamine H_2 receptor (H_2R) plays a key role in gastric acid secretion. Thus, H_1R antagonists ("H_1-Antihistamines") represent a common drug class of over-the-counter antiallergics and hypnotics. H_2R antagonists, inhibiting gastric acid secretion, have been used in the treatment of peptic ulcers or acid reflux disorders. The most recent discovered histamine H_4 receptor (H_4R) is primary connected to inflammation and immune responses due to its high expression on immune cells, whereas a localization in the CNS is still disputed.[26] With the discovery of the H_3R in 1983 by Arrang et al.,[28] the comprehensive modulative capacity of neuronal histamine became clearly evident, representing a milestone in recognition of histamine receptors as a useful tool for neurological disorders.[29]

The H_3R and all other histamine receptor subtypes belong to the rhodopsin-like class A GPCRs with the classical seven transmembrane regions (TM). Due to its $G_{i/o}$ coupling, activation of the H_3R results in inhibition of adenylyl cyclase (AC) and consequent decreased conversion of adenosine triphosphate (ATP) to cyclic adenosine monophosphate (cAMP) (Figure 4).[26,30] The signal transduc-
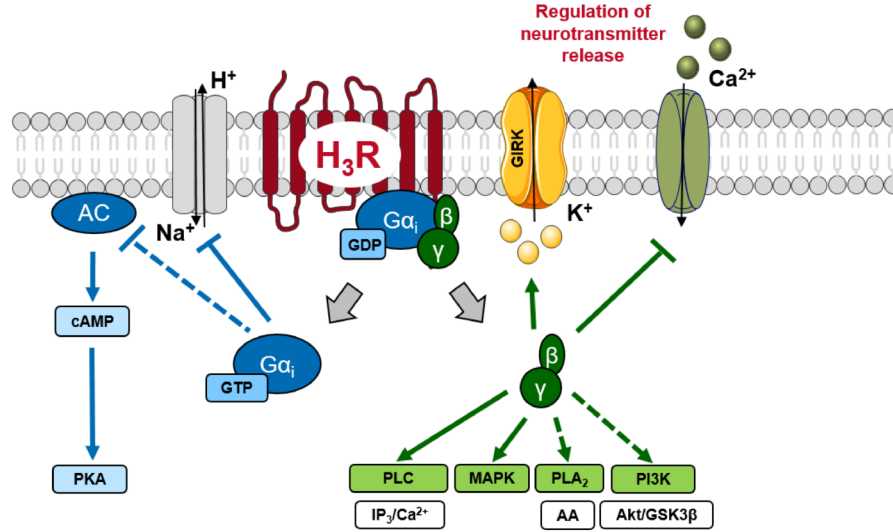
Figure 4 – Prominent signalling pathways of activated histamine H$_3$ receptors.[34] Profound constitutive activity is indicated with a dashed line. AA, arachidonic acid, AC, adenylyl cyclase, cAMP, cyclic adenosine monophosphate, GIRK, G-protein-gated inwardly rectifying potassium channel, GDP/GTP, guanosine di-/triphosphate, GSK3β, glycogen synthase kinase 3β, IP$_3$, inositol-1,4,5-trisphosphate, MAPK, mitogen-activated protein kinase, PI3K, phosphoinositol-3-kinase, PKA, proteinkinase A, PLA$_2$/PLC, phospholipase A$_2$/C.

tion of H$_3$Rs encompasses activation of the phospholipase C (PLC) pathway, triggering intracellular calcium (Ca^{2+}) release via inositol-1,4,5-trisphosphate (IP$_3$) formation and extracellular signal-regulated kinase (ERK) 1/2 phosphorylation (probably arrestin-independent).[31] An isoform and cell-type dependent modulation of mitogen-activated protein kinase (MAPK),[30,32] as well as phospholipase A$_2$ (PLA$_2$) and phosphoinositol-3-kinase (PI3K) activation via the G$_{\beta\gamma}$ subunit was reported. PLA$_2$ activation results in cellular release of multiple lipid mediators and precursor molecules such as arachidonic acid, pathologically relevant in neuroinflammatory processes.[33] Cell-type-dependent H$_3$R-mediated PI3K activation triggers the Akt/glycogen synthase kinase 3β (GSK3β) pathway, which is probably involved in neuronal cell migration and survival, suggesting neuroprotective features of H$_3$Rs.[30,32] H$_3$R activation influences also cellular cation homeostasis by downregulation of Ca^{2+} influx, a pathway most likely linked to regulation of neurotransmitter release.[21,34] Furthermore, activation of G-protein-gated inwardly rectifying potassium channels (GIRK), e.g. GIRK1 and GIRK4, as well as inhibition of Na$^+$/H$^+$ exchangers was described.[30,34] As GIRKs are found to inhibit synaptic transmission, activation of presynaptic GIRKs may contribute to H$_3$R-mediated modulation of neurotransmitter release, while postsynaptically H$_3$Rs can also influence neuronal levels e.g. of the neuropeptide melanin-concentrating hormone (MCH).[34,35] The "constitutive activity" (or "basal activity") of H$_3$Rs, displayed for

distinct signalling pathways (e.g. for AC or PLA_2 signalling), is defined as spontaneous transduction without activation by the endogenous ligand.[36] This phenomenon, widely found in a large number of GPCRs, resulted in reclassification of several H_3R antagonists. Thus, ligands inhibiting the H_3R behave differently from normal antagonists by reducing constitutive activity rather than abolishing activation by competing with the endogenous ligand. Accordingly, these antagonists are defined as "inverse agonists",[37] being further discussed in the following paragraph.

Despite the fact that the H_1R and H_2R, discovered in 1966 and 1972, were known for a long time, more than ten years went by prior to identification of the H_3R, most probably hampered by its low identity to the previous described histamine receptors.[28] When Lovenberg and colleagues were finally able to clone the human H_3R in 1999,[38] the human H_4R was cloned shortly afterwards due to its high amino acid sequence identity to the H_3R (about 40%, and about 60% in TM regions).[39] Initiated with the cloning of the human subtype, H_3Rs of other species used in preclinical studies have been cloned, such as guinea pig,[40] rat,[41] mouse,[42] dog,[43] monkey[44] or even zebrafish.[45] These studies provide relevant information of inter-species differences on the molecular level, revealing an overall high sequence similarity with monkey and rodents H_3Rs (>90%), dog (75%) or zebrafish (50%).[34,45] The H_3R provides a large amount of splice variants in humans (resulting in at least 20 protein isoforms),[26,46] but also in other species e.g. rat, mouse or monkey.[47,48] The full length human isoform $H_3(445)$ and the seven additional isoforms $H_3(453)$, $H_3(415)$, $H_3(413)$, $H_3(409)$, $H_3(373)$, $H_3(365)$ and $H_3(329)$ were found to be functionally competent, varying mainly in the third intracellular loop, whereas the TM regions are highly conserved.[48] Accordingly, they differ in ligand binding, constitutive activity and coupling behaviour.[30] The full length human $H_3(445)$ and the $H_3(365)$ are the most abundant isoforms almost evenly distributed in various human brain regions, while the full length H_3R still represents the most characterized isoform.[30,48] Although the full length isoform $H_3(445)$ encoded in rodents demonstrate high similarity to the human isoform, different signalling as well as ligand binding for a number of H_3R antagonists (e.g. ciproxifan) has been shown, particularly demonstrated for rat $H_3(445)$.[34,48,49] The impact of these various isoforms on usage of H_3R ligands as pharmacological tools needs to be elucidated further. Also isoforms may have different roles in distinct (patho)physiologies,[48] similar to previously investigated H_3R gentic variations/polymorphisms.[50]

Initially, H_3Rs were identified as presynaptic autoreceptors by Arrang and colleagues, regulating neuronal histamine release and synthesis in a negative feedback loop.[51,52] Later on it was observed, that this feedback regulation on release of presynaptic H_3Rs is not limited to histamine itself, but affects, as heteroreceptor, also other neurotransmitters such as noradrenaline, dopamine or acetylcholine to

name a few.[53-56] In some brain regions H_3Rs are expressed to a higher extent post-synaptically, e.g. in the striatum, hypothetically involved in dopamine signalling. Nevertheless, the majority of its pharmacological capacities are linked to its presynaptic-mediated neurotransmitter regulation, while several studies evidence a potential pharmacological utility also for postsynaptic H_3Rs in the treatment of neurological diseases.[57] In contrast to the other histamine receptor subtypes, the H_3R shows an exclusively high localization in the brain with minor distribution in the periphery, which represents a valuable speciality to avoid at least CNS-absent side effects.[48] The H_3R is widely expressed in the basal ganglia, a brain region commonly associated with cognitive functions, learning and memory as well as locomotor activity.[58,59] Autoradiography studies showed distributions with highest concentrations in the substantia nigra, the putamen and the globus pallidus.[60] H_3Rs were also found in the frontal cortex, hypothalamus or hippocampus.[30,48] The number and expression patterns of the functional isoforms may vary in different species, while the overall distribution of H_3Rs shows a high overlap among different species, e.g. in human and rat. These findings provide at least a basis for use of distinct pharmacological animal models of neurological diseases to investigate therapeutic effects of H_3 ligands.[26,48]

1.3 Histamine H$_3$ Receptor Antagonists/Inverse Agonists

During the last decades, great effort has been brought to the development of potent H_3R ligands. Historically, these ligands were structurally highly related to histamine, bearing an imidazole moiety as central core. In addition to the endogenous ligand histamine, 4-substituted imidazoles like N^α-methylhistamine, (R)-α-methylhistamine (RAMH), imetit and immepip/methimmepip are characterized as potent H_3R agonists. All these compounds are common pharmacological tools and frequently used in numerous in vitro and in vivo studies. A variety of possible indications for H_3R agonists has been suggested such as migraine, inflammation, pain, ischaemic arrhythmias or insomnia.[61] However, none of the H_3R agonists described so far proceeded to therapeutic application. Thus, research on H_3R agonists awaits further investigational steps to reveal substantial insights into pharmaceutical relevance.

On the contrary, large progress has been made in case of H_3R antagonists. With the discovery of the receptor's constitutive activity (agonist-independent activity), researches were forced to reconsider the functional potency of H_3R antagonists described so far. As previously mentioned, this resulted in reclassification of these ligands as "inverse agonists", representing a special type of antagonists. In contrast to neutral antagonism, defined as abolishment of an agonist-induced receptor activation, inverse agonism is a term reserved for receptors with constitutive activity.
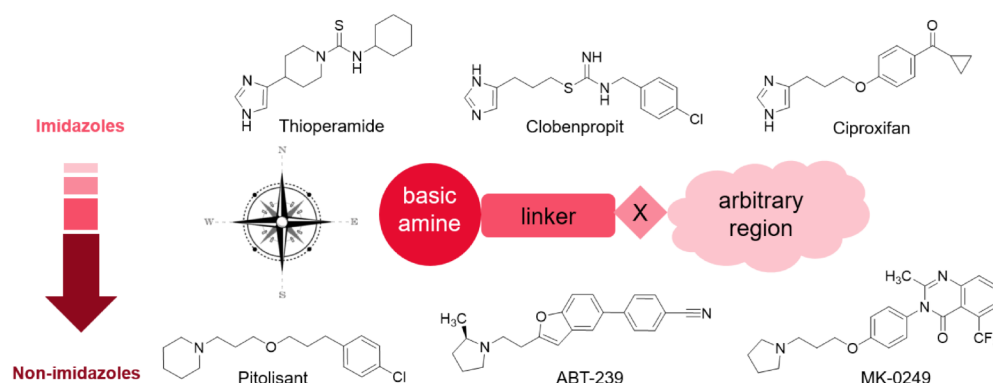
Figure 5 – First generation imidazole and advanced non-imidazole H_3R antagonists fitting the general H_3R pharmacophor. Heteroatom X = N, O, S.

It describes the behaviour of ligands to promote an effect opposite to agonists by stabilizing the inactive state of the receptor, reducing its basal or constitutive activity. In the absence of constitutive activity, inverse agonists act as neutral antagonists.[37,62] The constitutive activity of the H_3R may complicate its role as pharmacological target, but the functional difference of neutral antagonists and inverse agonists, henceforth referred as "H_3R antagonists", may provide distinct physiological and therapeutic capacities.[63]

Early developed ligands like thioperamide, clobenpropit or ciproxifan are representatives of the imidazole-bearing first generation H_3R antagonists (Figure 5). Most disadvantageously, as discovered later, the majority of these antagonists show only low subtype selectivity between H_3Rs and the later discovered and most homologous H_4Rs (e.g. thioperamide, clobenpropit).[22,26,64] Thus, early pharmacological effects thought to be H_3R-related need to be reviewed carefully, especially regarding peripheral effects. Further, the pharmacological inconvenience of many imidazole-containing compounds such as low CNS penetration or cytochrome P450 (CYP) enzyme interaction led to design of numerous bioisosteric structural motifs for H_3R antagonists.[64–66] Nevertheless, the first generation H_3R antagonists remain popular pharmacological tools in vitro and in rodent animal studies, providing high H_3R potency and a great history of pharmacological characterization.[22] The first description of non-imidazole H_3R antagonists/inverse agonists in 1998 and subsequent imidazole-replacement studies with first generation ligands pioneered a great impetus in non-imidazole H_3R antagonist development.[66–69] In the following years, comprehensive SAR studies were performed,[22,70] revealing a general accepted blue print for H_3R antagonists (Figure 5). A basic moiety, providing interaction with Asp114 in TM3, is connected via an alkyl linker (e.g. trimethylene) to an arbitrary region in the eastern part of the molecule, often bearing a central aromatic core. Most commonly the basic moiety, mimicking the imidazole, is represented by

cyclic aliphatic amines such as pyrrolidine or piperidine. In the arbitrary region, diverse variations have been shown to be tolerated by the H_3R, e.g. high lipophilic, polar, additional basic or even acidic moieties.[22] This new generation of non-imidazole H_3R antagonists provides selectivity over H_4Rs as well as more favourable pharmacological properties, i.e. increased drug-likeness and a reduced side effect potential. To date, a steadily growing number of non-imidazole H_3R antagonists have been described, offering a reliable stage for these ligands antagonists in drug development.

1.4 Therapeutic Potential of H_3R Antagonists

The ubiquitous CNS distribution of the H_3R and especially its heteroreceptor capacity modulating several neurotransmitter levels in the human brain led to suggestion of H_3R antagonists as possible treatment for a great variety of neurological diseases involving disruption of one or more neurotransmitter systems. To name only a few, beside obesity, addiction, depression, Tourette's syndrome, Huntigton's disease or multiple sclerosis, H_3R antagonists are intensively discussed for the treatment of cognitive impairment, i.e. as main or partial aspect in Alzheimer's disease, schizophrenia and attention-deficit hyperactivity disorder (ADHD). Additionally, they are described to positively influence the condition of excessive daytime sleepiness (EDS) manifested in sleeping disorders such as narcolepsy and obstructive sleep apnea (OSA) or Parkinson's disease.[57,64,71] Within this broad spectrum of possible applications, the latter ones, i.e. cognitive and sleep impairment, are the most frequently examined conditions.

Numerous in vitro studies, but also in vivo animal models have proven the wake-promoting and pro-cognitive effects of H_3R antagonists and a number are in clinical trials for various conditions (Figure 6).[22] While only pitolisant (Figure 5) is currently implemented in phase III studies, a handful H_3R antagonists completed clinical phase II trials for previously mentioned CNS disorders, predominantly without any disclosed results (clinicaltrials.gov). Noteworthy, GSK-239512 shows positive outcomes in Alzheimer's disease patients (phase II, NCT01009255), and completed also a clinical efficacy, kinetic and safety study on lesion remyelination in patients with relapsing-remitting multiple sclerosis.[72] Nevertheless, with exception of pitolisant, the initial euphoria on the therapeutic potential of H_3R antagonists was dampened or delayed, since several postulated preclinical therapeutic effects could not be validated when transferred to human trials. Thus, a number of H_3R antagonists failed demonstrating clinical efficacy (for at least one indication), and trials were terminated, sometimes without any reasons disclosed. To date, pitolisant, the only H_3R inverse agonist to make it to the drug market, is also being investigated for its wake-promoting effect in OSA (phase III,
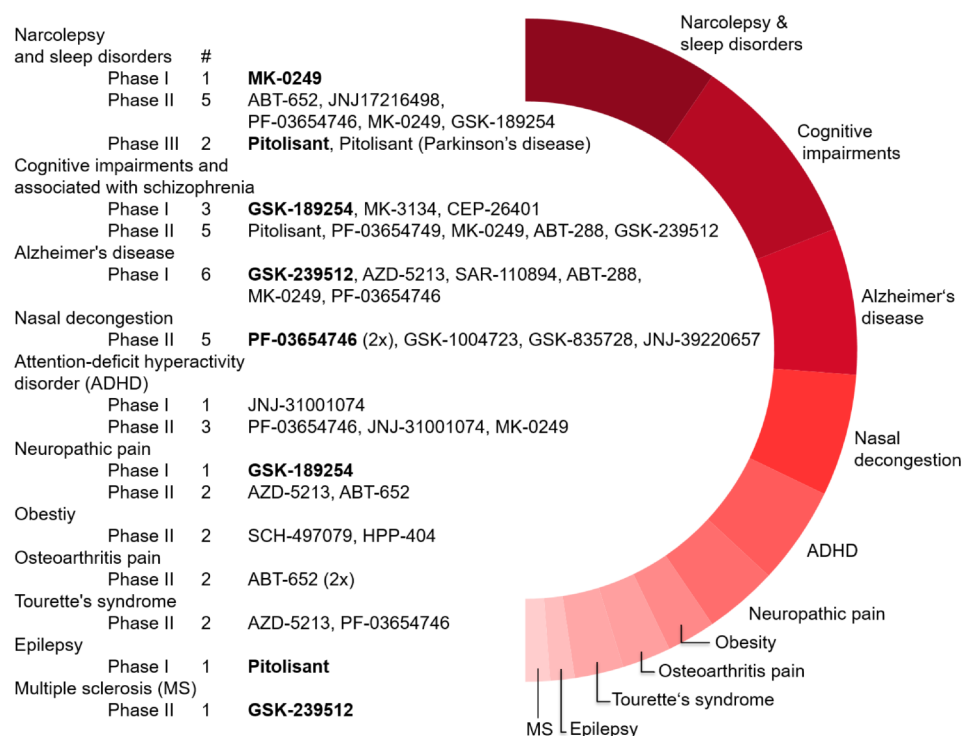
Narcolepsy
and sleep disorders #
  Phase I   1   **MK-0249**
  Phase II   5   ABT-652, JNJ17216498,
                  PF-03654746, MK-0249, GSK-189254
  Phase III 2   **Pitolisant**, Pitolisant (Parkinson's disease)
Cognitive impairments and
associated with schizophrenia
  Phase I   3   **GSK-189254**, MK-3134, CEP-26401
  Phase II   5   Pitolisant, PF-03654749, MK-0249, ABT-288, GSK-239512
Alzheimer's disease
  Phase I   6   **GSK-239512**, AZD-5213, SAR-110894, ABT-288,
                  MK-0249, PF-03654746
Nasal decongestion
  Phase II   5   **PF-03654746** (2x), GSK-1004723, GSK-835728, JNJ-39220657
Attention-deficit hyperactivity
disorder (ADHD)
  Phase I   1   JNJ-31001074
  Phase II   3   PF-03654746, JNJ-31001074, MK-0249
Neuropathic pain
  Phase I   1   **GSK-189254**
  Phase II   2   AZD-5213, ABT-652
Obestiy
  Phase II   2   SCH-497079, HPP-404
Osteoarthritis pain
  Phase II   2   ABT-652 (2x)
Tourette's syndrome
  Phase II   2   AZD-5213, PF-03654746
Epilepsy
  Phase I   1   **Pitolisant**
Multiple sclerosis (MS)
  Phase II   1   **GSK-239512**

Figure 6 – Histamine H₃R antagonists in clinical trials for multiple diseases (Number of candidates # per clinical phase). Candidates with positive outcomes appear in bold.[22]

NCT01072968) and Parkinson's disease (phase III, NCT01066442). Additionally, it completed a clinical phase II trial for cognitive impairment in schizophrenia (NCT00690274) and demonstrated anti-epileptic efficacy in patients.[73,74] The approval of pitolisant (Wakix®) by the European Medicines Agency (EMA) in 2016 as orphan drug for the treatment narcolepsy with and without cataplexy represents a hallmark in H₃R research. Accordingly, the treatment of sleep impairment in CNS diseases may represent the most promising and progressive indication for H₃R antagonists. A number of candidates are currently implemented in phase II studies for sleep disorders, however, they were either terminated (GSK-189254, MK-0249), do not have available results (JNJ-17216498) or show no significant improvement (PF-03654746).[22,75]

More rarely investigated, by addressing rather H₃R autoreceptors than heteroreceptors, H₃R antagonists were shown to demonstrate anti-obese potential in preclinical studies,[76] with a few compounds currently in clinical trials. SCH-497079 completed an efficacy and safety study (phase II, NCT00642993) in obese participants, while a phase II dose-range study with HPP-404 (NCT01540864), proven to be well tolerated in healthy individuals, was terminated without reasons disclosed.[77]

So far, with limited success of selective H₃R antagonists reaching the drug market but proven roles in various CNS functions, H₃Rs were promoted as an attractive

target in MTL design for combination with established targets in CNS disorders, probably enlarging the spectrum of their aforementioned indications.[78] From the medicinal chemistry point of view, H$_3$Rs are valuable targets in multitargeting drug design due to decisive SAR for H$_3$R ligands and the high tolerability for structural variations in the ligands arbitrary region. Thus, numerous potent H$_3$R MTLs have been described as possible medications for distinct CNS disorders, showing auxiliary activity at other GPCRs (e.g. dopamine, serotonin, muscarine receptors), enzymes (e.g. HNMT, cholinesterases), neurotransmitter transporters or even signalling molecules such as nitrogen monoxide.[78]

Of particular interest for neurodegenerative diseases, H$_3$R antagonists may counterbalance the neurotransmitter dysregulation due to neurodegeneration, by inducing heteroreceptor-mediated release of several neurotransmitters, i.e. dopamine or acetylcholine. Thus, selective and multitargeting H$_3$R antagonists may provide therapeutic potential and relevance in both Alzheimer's and Parkinson's disease, the most prevalent neurodegenerative diseases, by especially addressing cognitive and/or sleep symptomologies.

1.4.1 Alzheimer's Disease

Alzheimer's disease (AD), characterized by significant loss of memory and cognitive functions, affects more than 35 million people worldwide, representing the most prevalent neurodegenerative disease. Elderly people have an especially high risk to develop AD with a steadily increasing incidence at an age above 65 years.[79,80] The exact mechanisms of this progressive neurodegenerative disease are not fully understood, but a number of key determinants has been identified.[79] Accumulation of misfolded amyloid β peptides (Aβ) and tau proteins results in formation of Aβ plaques and neurofibrillary tangles, respectively, representing the main pathological findings thought to be associated with AD.[79,81] However, the early and soluble peptide aggregates were identified to be the toxic species as the appearance of larger insoluble plaques alone did not correlate with cognitive impairment.[82] Toxic Aβ causes a significant and progressive loss of especially cholinergic neuronal cells in the brain, mostly the cerebral cortex, inducing cognitive defects.[83] Inhibiting the cytochrome c oxidase, Aβ accumulation leads to overall mitochondrial impairment, promoting oxidative stress and apoptosis of neuronal cells due to cytochrome c release.[79] The loss (e.g. in the hippocampus) and Aβ-mediated disruption of synapses results in a decrease of presynaptic neurotransmitter release, especially affecting the acetylcholine (ACh) signalling, which plays a key role in memory and other cognitive functions.[79,81]

To date, therapeutical options are symptomatic treatments, i.e. with cholinesterase (ChE) inhibitors or *N*-methyl-D-aspartate (NMDA) receptor antagonist

memantine for mild to severe and moderate to severe AD, respectively, both with limited efficacy due to the multifactorial character and progression of AD. Over the last decades, numerous additional targets have been identified, which can be roughly divided into "symptomatic" (e.g. neurotransmitter receptors, neurotransmitter-catabolizing enzymes) and "disease-modifying" targets (e.g. involved in Aβ production, transport and degradation).[84] Based on these various targets and their underlying mechanisms of action, Cummings and colleagues recently distinguished different approaches within an overview of the therapeutic AD pipeline in 2017, i.e. tau-/amyloid-related (including immune therapy), neurotransmitter-based, neuroprotective/antioxidative or anti-inflammatory approaches.[85] Especially the development of immunotherapeutics (e.g. Aβ antibodies) is the subject of the disease-modifying strategies, currently being investigated with increased effort to decelerate AD progression in early stages.

The symptomatic pharmacotherapy, in contrast, is primary represented by small molecule drug design.[85] The majority of small molecules in clinical phase II and III belong to the class of neurotransmitter-based approaches, including neurotransmitter-catabolizing enzyme inhibitors (e.g. monoamine oxidase (MAO) or acetyl-choline-/butyrylcholinesterase inhibitors) or receptor ligands (e.g. muscarinic M_1 receptor agonists). Hence, the development of drugs regulating neurotransmitter levels still represents a common approach in symptomatic therapy of psychotic and cognitive issues. So far, acetylcholinesterase (AChE) inhibitors (AChEI), enhancing ACh levels in the synaptic cleft by prevention of ACh degradation, represent the most reliable therapeutic treatment of cognitive impairment in AD.[86] AChEIs like rivastigmine (Exelon®) or donepezil (Aricept®), both approved for AD, are also approved or in late clinical stages for Parkinson's disease related dementia, respectively.[87] As disease-modifying strategies, neuroprotective and antioxidative agents have actually a great share in clinical phase II trials. Counteracting the cytotoxicity of Aβ e.g. by reducing oxidative stress helps to prevent neuronal cell death and probably to provide deceleration of AD progression. Beside compounds showing radical scavenging properties ("antioxidants"), inhibitors of MAO A/B are discussed as potent neuroprotectives, a property which is assumed for multiple approved MAO B inhibitors.[88,89] Application of MAO B inhibitors also represent a main strategy in the treatment of Parkinson's disease and will be described more extensively in the following paragraph. In brief, MAOs are mitochondrial enzymes being considered as source of oxidative stress as they generate reactive oxygen species (ROS) as a second product. Thus, inhibitors of MAO might prevent mitochondrial disruption and progression of neurodegeneration.[90] The marketed MAO inhibitor rasagiline (Azilect®) just entered a phase II clinical trial for evaluation of its effects on the regional brain metabolism in mild to moderate AD

(NCT02359552). During AD neurodegeneration, neurofibrillary tangles accumulate in the brain and the TMN is affected in early stages, with a significant high loss of histaminergic neurons (>50%) in TMN region.[91-93] Additionally, enhanced expression of HNMT and H_3R mRNA in the prefrontal cortex was observed, but surprisingly only in female AD patients,[93] while no significant differences in H_3R densities were observed comparing AD and control brains.[94] However, estimating the capacities of H_3R antagonists for AD therapy, the blockade of H_3Rs results in enhanced ACh concentrations due to its heteroreceptor activity similar to AChE inhibition.[55] In contrast to AChEs, this effect will be established predominantly in the brain due to their more exclusive localization in the CNS.

The H_3R was already identified as a potential target for treatment of cognitive impairment in numerous studies.[83,95-97] Significant reduction of memory capacity in rodent models could be observed for several H_3R agonists (e.g. RAMH or imetit[56]) inhibiting the release of ACh. In addition, studies performed with H_3R knock out ($H_3R^{-/-}$) mice revealed reduced response to memory deficits caused by the muscarinic acetylcholine receptor antagonist scopolamine.[98] Numerous H_3R antagonists, such as thioperamide, ciproxifan, ABT-239 or pitolisant (Figure 5),[99-103] were shown to stimulate ACh transmission and demonstrate pro-cognitive and memory-enhancing effects in rodents.[97] The potent H_3R antagonist GSK-239512 reached clinical phase II for treatment of mild to moderate AD (NCT01009255), showing improvement of episodic memory, but failed to enhance cognitive deficits in working memory or any other domains of cognition.[104] A few other H_3R antagonists proceeded to clinical phase II studies, i.e. MK-0249[105] and ABT-288[106] or SAR-110894 (combined with donepezil; NCT01266525), showing no efficacy or lacking disclosed results, respectively.[97,107] In 2015, a meta-analysis of clinical trials for H_3R antagonists disclosed no clinical efficacy in AD therapy.[108] However, only few placebo-controlled clinical trials were performed so far, hence, a final judgement on the therapeutic relevance of H_3R antagonists for cognitive impairment in AD cannot be made yet.[108]

Despite the previously described symptomatically driven approach, a few preclinical studies indicate that H_3R antagonists may contribute to decelerate AD progression by neuroprotective mechanisms against Aβ toxicity or attenuation of tau protein hyperphosphorylation.[110,111] The H_3R-mediated neurotransmitter release stimulate postsynaptic signalling leading to increased phosphorylation of CREB, a transcription factor involved in cognitive processes and GSK3β inhibition via the constitutive active Akt pathway, which contributes to tau hyperphosphorylation.[83] These effects were shown for ABT-239,[110] a representative with limited clinical relevance due to severe side effects (e.g. QT prolongation).[96,112] More recently, SAR-110894 was proven to decrease tau hyperphosphorylation preventing subse-
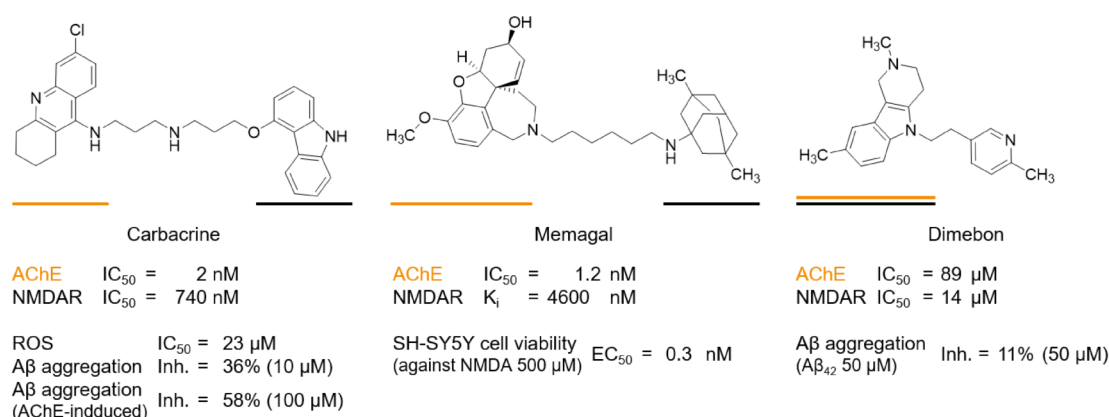
Figure 7 – Multitargeting acetylcholinesterase (AChE)/NMDA receptor (NMDAR) inhibitors for the treatment of Alzheimer's disease with proposed neuroprotective, disease-modifying capacities.[109] Pharmacophoric structural elements are underlined in orange (AChE) and black (NMDAR). Aβ, amyloid β peptides, Inh., inhibition, ROS, reactive oxygen species.

quent memory deficits in transgenic mice, thus, may have disease-modifying capacities in long-term treatment of neurodegenerative tauopathies.[113]

In AD therapy, multitargeting drug design was initially considered as rational approach, to combine in one drug the symptomatic treatment demonstrated by AChEIs together with neuroprotective, disease-modifying capacities exemplified by the NMDA receptor (NMDAR) antagonist memantine.[109] Accordingly, one of the proof-of-concept MTL carbacrine (Figure 7) was developed by fusing the pharmacophoric element of the AChEI tacrine with the carbazole moiety of carvedilol, to preserve NMDAR antagonism, antioxidant and Aβ aggregation inhibition properties.[114] With carbacrine, demonstrating the desired multitargeting capacities,[115] a number of AChE/NMDAR MTLs were published (Figure 7). Memagal was designed based on memantine and galantamine (AChEI), two drugs acting pro-cognitive in co-administration therapy. It shows nanomolar activity at both targets as well as neuroprotective properties in human neuroblastoma cells (SH-SY5Y) intoxicated with NMDA.[109] Based on dimebon, an antihistamine found to possess remarkable pro-cognitive efficacy in clinical trial,[116] bivalent derivatives were designed showing improved anti-AD capacities.[109]

Moreover, numerous MTLs were developed showing inhibition of ChEs with additional properties,[80] such as anti-Aβ-aggregation,[117,118] β-secretase (BACE 1) inhibition,[119–122] MAO inhibition,[123–126] 5-HT₄ binding,[127,128] phosphodiesterase 5(A) inhibition[129,130] and/or antioxidative effects.[131] Most promising, ladostigil (Figure 8), a combined ChE/MAO A/B inhibitor obtained by fusing pharmacophores of rivastigmine and rasagiline,[86] completed two clinical phase II studies for cognitive impairment (NCT01429623, NCT01354691), tending to be effec-
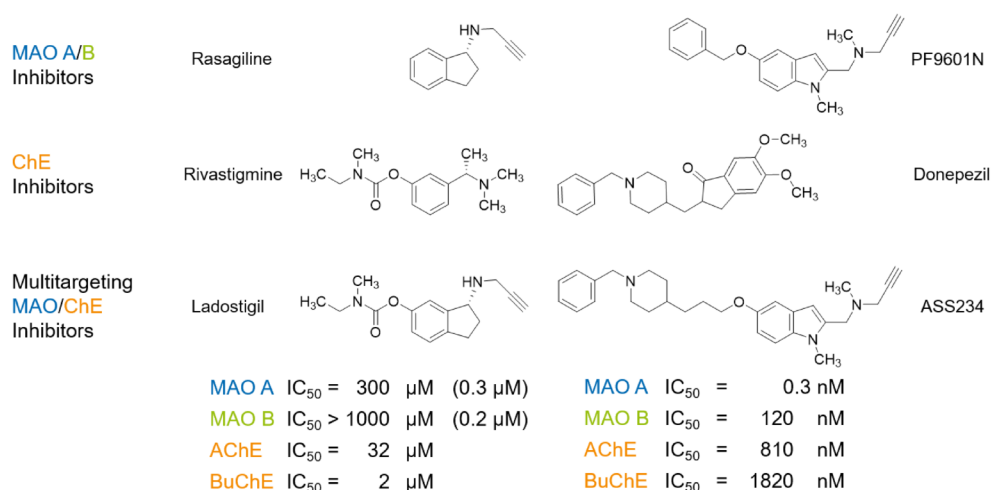
Figure 8 – Target affinity profiles of knowledge-based designed MTLs ladostigil (affinities of active metabolite given in parenthesis)[123] and ASS234,[142] developed for treatment of Alzheimer's disease by combining monoamine oxidase (MAO) A/B and acetyl-/butyrylcholinesterase (AChE/BuChE) inhibition.

tive against neurodegeneration but failing to meet primary outcome measures, i.e. prevention of progression from mild cognitive impairment to AD. Nevertheless, overall observations suggest further clinical development of ladostigil as stated by Avraham Pharma (www.avphar.com). The fact that ladostigil contains a propargyl moiety to ensure neuroprotective features already demonstrated for rasagiline,[86,132,133] brought great impetus to the design of multitargeting propargyl amines for treatment of neurodegenerative diseases. For example, the multitargeting ChE/MAO inhibitor ASS234 (Figure 8),[124,134] exhibits antioxidative, neuroprotective and anti-Aβ-aggregation properties. In rodents, it improved scopolamine-induced cognitive impairment and working memory in a model of vascular dementia as well as plaque burden in a transgenic mouse model of AD.[135–137] Despite most frequent investigated ChE MTLs, multiple MAO inhibitors demonstrating antioxidant, anti-Aβ-aggregation as well as metal chelating properties have been suggested as anti-AD agents.[86,138–140] Divalent metal ions such as Cu^{2+}, Fe^{2+} or Zn^{2+}, accumulated in AD brains, are thought to accelerate formation of Aβ aggregates and neurofibrillary tangles as well as neuronal oxidative stress.[139,140] However, the mechanism and benefits of metal chelation therapy in AD has been controversially discussed, stressing that metal chelators in AD therapy may alter metal-protein interactions rather than removing metal ion overload observed in AD.[141]

Due to the pro-cognitive abilities of H_3Rs a number of MTLs possessing H_3R antagonism were proposed for the treatment of AD. With some structural overlap in AChE and H_3R pharmacophores, initially described $H_3R/HNMT$ MTLs were identified to be potent ChE inhibitors,[143,144] enabling the possible modulation

of brain ACh levels via two distinct, probably synergistic acting mechanisms.[145] As H$_3$R antagonists, in contrast to AChE, increase ACh predominantly in the brain, MTLs addressing both targets may provide efficacy with reduced peripheral side effects, often observed for selective AChEIs.[146] UW-MD-71, a dualtargeting AChE/H$_3$R representative, display nanomolar activity at both targets and was found to enhance memory function in rats.[146][147] Furthermore, a small series of AChE/H$_3$R MTLs was synthesized, showing additional inhibition of BACE 1.[148] This enzyme plays a central role in Aβ formation and represents one of the most promising targets in current disease-modifying AD therapies.[85] Another combined symptomatic/disease-modifying approach was suggested by Lepailleur and colleagues, investigating H$_3$R/5-HT$_4$ MTLs for AD therapy, where 5-HT$_4$ receptors provide neuroprotective capacities via regulation of α-secretases responsible for non-amyloidogenic amyloid precursor protein (APP) cleavage.[149] The most promising H$_3$R antagonist/5-HT$_4$ agonist within this series showed nanomolar affinity at both targets and reversal of scopolamine-induced amnesia in mice indicating a potential of H$_3$R MTLs for treatment of AD.[150]

1.4.2 Parkinson's Disease

After AD, Parkinson's disease (PD) represents nowadays the second most common neurodegenerative disease. PD, originally described by James Parkinson in 1817,[151] is a mostly age-related, idiopathic neurological disease.[152] Fitting Parkinson's initial naming "Shaking Palsy", PD patients most obviously suffer from locomotor dysfunctions, demonstrated by the cardinal symptoms i.e. resting tremor, mostly affecting the hands first, the forward-flexed posture and shuffling gait as well as bradykinesia and muscle rigidity.[151][153] Similar to AD, protein misfolding (e.g. of α-synuclein and Aβ) leads to accumulation of intracellular inclusions ("Lewy bodies"), which represents a histological hallmark in PD patients.[152] Evidently, the motor impairment in PD patients is strongly associated with a progressive loss of dopaminergic neurons in the substantia nigra pars compacta (SNpc), a part of the basal ganglia, which significantly contribute to body movement. The neuronal management of voluntary movements in a normal brain involves balanced but interacting striatal output projections via two different pathways (direct and indirect) connected in a basal ganglia circuit, where the direct pathway promotes and the indirect pathway attenuates movement (Figure 9). In the direct pathway, the striatum receives initiating (excitatory) signals from the motor cortex inhibiting the globus pallidus interna (GP$_i$) via GABAergic (γ-aminobutyric acid) projections, thus, leading to less inhibition of the thalamus. Since the thalamus controls the motor cortex via excitatory projections, less inhibition of the thalamus results in activation of the motor cortex. In the indirect pathway, striatal
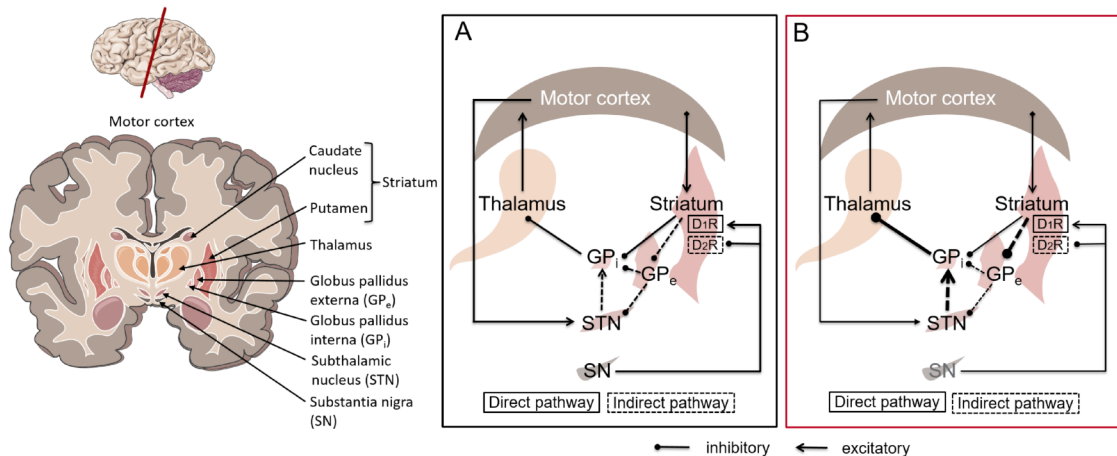
Figure 9 – A simplified scheme of the basal ganglia circuit regulating motor activity
under (A) normal dopamine-mediated conditions and (B) in Parkinson's disease
with a loss of dopaminergic modulation.[155]

neurons inhibit the globus pallidus externa (GP_e) GABA-mediated, which in turn
results in less inhibition of the subthalamic nucleus (STN). The STN projects to
the GP_i via excitatory effects, thus increasing activity of GP_i firing. Contrary to
the direct pathway, an enhanced activation of the GP_i would result in an increased
inhibition of the thalamus and inhibition of the motor cortex.[152,154] In PD, a sub-
sequent decrease of dopamine, implemented in the basal ganglia circuit, leads to
dysregulation in excitability of striatal neurons.[152] Dopamine acts via five different
GPCR subtypes, divided into D_1-like (D_1, D_5) and D_2-like (D_2, D_3, D_4) receptor
classes due to their adenylyl cyclase stimulating (G_s) and inhibiting ($G_{i/o}$) coupling
behaviour.[156] In healthy people, dopamine released from SNpc neurons stimulates
the direct pathway via dopamine D_1-like receptors, while inhibiting the indirect
pathway via dopamine D_2-like receptors at the same time, hence, inducing motor
activity. In PD patients, the loss of dopaminergic signalling from the SNpc affects
both pathways and leads to overall decreased motor activity.

To overcome motor symptoms associated with PD, application of dopaminergic
drugs represents the most common therapy for PD patients.[157] Since its introduc-
tion, L-3,4-dihydroxyphenylalanine (L-DOPA, levodopa) as dopamine prodrug,
represents the gold standard in treatment, especially improving motor symptoms
in PD patients. Due to extensive peripheral metabolism it is applied with DOPA
decarboxylase (DDC) inhibitors (e.g. benserazide or carbidopa), which signifi-
cantly increase the bioavailability and CNS concentration of L-DOPA. Adjunctive
dosing with catechol-O-methyltransferase (COMT; EC 2.1.1.6) inhibitors, i.e. enta-
capone (Comtan®), helps to prevent excessive peripheral inactivation of L-DOPA
to its metabolite 3-*O*-methyldopa (3-methoxy-4-hydroxy-L-phenylalanine).[158] In
the CNS, conversion of L-DOPA to dopamine by the DDCs results in enhanced or

normalized dopamine levels in the synaptic cleft. However, although L-DOPA is sufficient and useful in stages of PD where some endogenous dopamine is still available, its short half-life combined with progression of PD leads to insufficient and reduced responsiveness after three to five years of therapy or in later PD stages. A large number of PD patients develop motor fluctuations (ON/OFF periods) and/or L-DOPA-induced dyskinesia (LID). These complications are poorly understood, being hypothetically associated with disease progression and caused by pharmacokinetic alterations e.g. loss of presynaptic storage capacity of L-DOPA or intestinal absorption.[159,160] Subsequent dosing adjustments or adjunctive pharmacotherapies (e.g. with COMT or MAO inhibitors[161]) can help restore the therapeutic efficacy.

As an alternative, dopamine receptor agonists represent a therapeutic option as monotherapy for early stages with mild to moderate motor symptoms, being comparably effective with L-DOPA in younger patients (<65-70 years), but with a reduced potential for dyskinesias. They can be also combined with L-DOPA in advanced PD stages to increase therapeutic efficiency.[162–164] Dopamine receptor agonists mimic dopamine's effects via stimulation of postsynaptic dopamine receptors, preferentially D_2/D_3 receptors (D_2R/D_3R).[164] Dopamine receptor agonists are structurally divided into ergoline derivatives, having a long history in PD, and more recently developed non-ergolines. Ergolines, such as bromocriptine (Perlodel®), show less dopamine receptor subtype selectivity compared that of non-ergoline agonists and most disadvantageously also interact with various off-target GPCRs like serotonergic or adrenergic receptors leading to numerous adverse effects. Non-ergolines, in contrast, predominantly target D_2-like receptor subtypes with high selectivity over distinct aminergic receptors, thus, having a more favourable side effect profile.[165,166] For many non-ergolines, e.g. pramipexole, neuroprotective features have been demonstrated in preclinical studies, probably due to antioxidant and anti-apoptotic effects. However, these suggested disease-modifying effects could not be proved in patients so far.[164] To date, pramipexole (Mirapex®), a D_3R-preferring agonist with well-defined efficacy and safety profile, is the most prescribed dopamine agonist for PD worldwide.[167]

Monoamine oxidase (MAO; EC 1.4.3.4) B inhibitors (Figure 10), such as selegiline (Eldepryl®), rasagiline (Azilect®) or the most recently approved safinamide (Xadago®), are predominantly used as adjunctive therapy, but can be also applied as monotherapy in early stages of PD.[157] MAOs are flavin adenine dinucleotide (FAD)-containing enzymes, localized in the mitochondria outer membrane, which metabolize various neurotransmitters after cellular reuptake from the synaptic cleft. Two isoforms can be distinguished, MAO A and MAO B, differing in their CNS and cellular localization as well as their substrate and inhibitor selectivity.

Most relevant for pharmacotherapy, MAO B, localized mainly in glial cells but also serotonergic neurons, metabolizes dopamine, while the MAO A isoform, expressed in all other neurons, predominantly degrades serotonin (5-HT) in the human brain. However, in absence of MAO B, MAO A can take over the degradation of dopamine.[168,169] The initial MAO-dependent neurotransmitter breakdown, exemplified for dopamine (Figure 10), involves oxidative deamination, while intermediate products will be rapidly metabolised.[168] Inhibition of MAO B would decrease dopamine catabolism and enhance dopamine availability, representing an indirect dopaminergic pharmacotherapy in PD. The age-dependent increase and enhanced MAO B expression in AD and PD patients suggests a key role in neurodegenerative diseases.[90] As MAOs are mitochondrial enzymes, their pathophysiological capacity is associated with overall mitochondrial dysfunction, a proposed determining factor in neurodegeneration.[170-172] This may lead to disruption of cellular energy, i.e. adenosine triphosphate (ATP) supply, and drives oxidative stress, which might overwhelm the antioxidative capacity of the cell. Neuronal cells have high energetic ATP demands, so they are especially sensitive to mitochondrial dysfunction.[169,171]

Historical interesting, anticholinergic drugs represented the only pharmacotherapy for PD before the introduction of L-DOPA in 1969. As the loss of dopaminergic signalling occurs during PD progression, the striatal excitatory cholinergic system, implemented and connected with dopamine in the basal ganglia circuit, gains the upper hand. However, complex interactions between these neurotransmitters within the basal ganglia circuit (and sub-circuits) are poorly understood,[173] while a intra-striatal dopamine/ACh imbalance is believed to at least partly affect PD motor symptomology, particularly tremors and muscle stiffness. Unfortunately, due to a progressive loss of striatal cholinergic markers accompanying PD, side effects on cognitive performance have been described for anticholinergic drugs.[173] Nowadays anticholinergic therapy was proven to be of limited value for the majority of PD patients with dominating side effects.[152,163]

Noteworthy, the main difference between James Parkinson's and the current understanding of PD, is the overall recognition of a great variety of PD-associated non-motor symptoms, which often appear prior to motor symptoms, but tend to worsen with disease progression. Beside gastrointestinal and cardiovascular complications from common autonomic dysfunctions and depression, anxiety, dementia or psychosis, sleep impairment represents one of the main CNS-related non-motor symptoms which can also occur as long-term side effects after dopaminergic treatment.[160,174,175] Non-motor symptoms, especially psychiatric ones, exhibit a high level of suffering and may lead to reduced compliance and cooperativity of PD patients, therefore need to be therapeutically addressed with similar effort to motor complications. A broad spectrum of common pharmacotherapeutics, i.e.
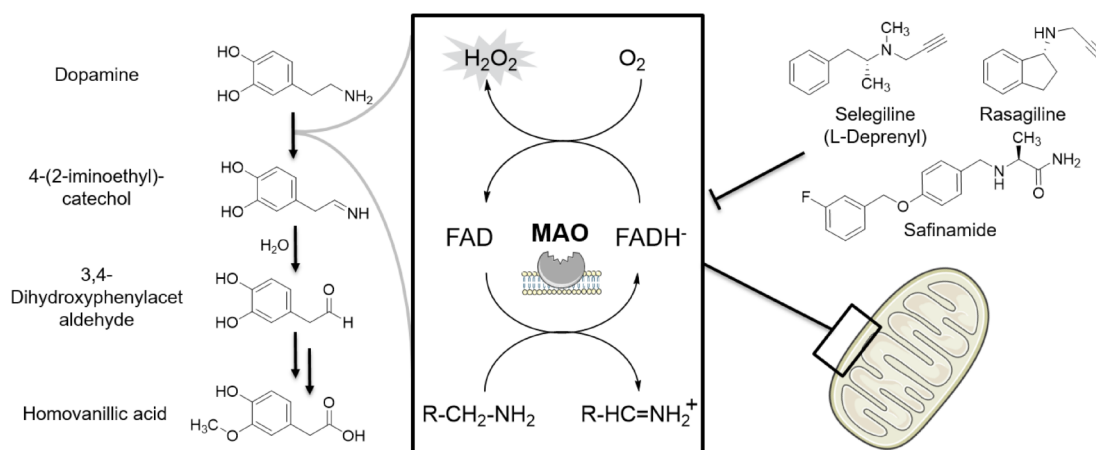
Figure 10 – The dopamine degradation process including oxidative deamination catalysed by monoamine oxidases (MAO). These enzymes, localized in the outer mitochondria membrane, catalyse the oxidation of amines to imines, thereby producing hydrogen peroxide (H_2O_2) as second product during the enzyme recovery process.[168] FAD/FADH⁻, flavin adenine dinucleotide (anion).

antipsychotics or antidepressants, has been suggested as adjunctive therapies to improve the patient's quality of life. To name only a few, the cholinergic AChEI rivastigmine is approved for mild to moderate dementia in PD,[90,175] while the atypical antipsychotic clozapine remains the most frequent applied drug in PD-related psychosis.[160,175,176] In general, sufficient therapeutic options for non-motor symptoms are limited and their overall relevance as well as their safety remains contradictory, therefore, their application require a careful monitoring of the patients.[175]

Over the last decades, increasing effort has been brought to investigate and establish suitable pharmacotherapies for non-motor symptoms. Aforementioned symptoms like mood, cognitive or sleep impairments are most frequently observed,[175] being evidently influenced by histaminergic transmission.[17] In PD, significant alterations of the histaminergic system have been described, suggesting an essential role in disease pathology.[93] Increased histamine levels as well as altered histaminergic fibre morphology and density in different brain regions were observed, including the SNpc of PD patients.[60,177,178] Noteworthy, despite the fact that Lewy bodies are abundantly formed in TMN, the brain histamine biosynthesis site, no alterations were found in TMN neurons of PD patients, neither in their number nor their HDC expression.[179] In accordance, elevated histamine concentrations could be shown also in 6-hydroxydopamine (6-OHDA)-lesioned rats, a classical rodent PD model.[180] These findings suggest a direct modulation of histamine as a consequence of dopaminergic depletion, while histamine biosynthesis remains relatively unaffected.[17,93] Interestingly, increased histamine levels were shown to further exaggerate degeneration of dopaminergic neurons via H₁R activation.[181] This effect

is hypothetically compensated by increased HNMT expression in affected brain regions.[93]

In normal brain, H_3Rs demonstrate a considerably high distribution in the basal ganglia, i.e. striatum and SN,[60] especially on GABAergic neurons.[59] Studies showed a significant elevation of H_3R mRNA and H_3R binding in PD patients and 6-OHDA-lesioned rats, but no functional activity alteration (in $GTP\gamma^{35}S$-binding assay) was found compared to that of normal brains.[17,60,182] While H_3Rs evidently control glutamate and GABA release in the basal ganglia (probably dopamine-dependent), the expression and modulation in dopaminergic neurons is controversial discussed.[54,182-184] The modulation of dopamine release by H_3R antagonists and agonists in rodent basal ganglia under certain conditions, was claimed to be indirectly via inhibition of dopamine synthesis, influencing local dopamine availability.[185,186] H_3Rs can also form functional heterodimers with D_1Rs and D_2Rs with mutual manipulation. This may result in inhibition or at least decreased agonist binding at activated D_1Rs or D_2Rs, respectively.[187-189] Consequently, H_3R activation may decrease pathologic hyperactivity of the indirect pathway (turn-down of motor activity) similar to D_2R activation, but suppress the D_1R-mediated direct pathway (turn-up of motor activity).[189] However, whether one of these interactions may have relevance on modulation of motor activity in PD needs to be elucidated.

In behavioural studies, $H_3R^{-/-}$ mice demonstrated reduced locomotor and wheel-running activity.[98] In the 6-OHDA-lesioned rat PD model, thioperamide decreased locomotor activity, while H_1R and H_2R antagonists were ineffective.[180] In the same test model, the H_3R agonist as well as H_1R and H_2R antagonists decreased apomorphine-induced turning behaviour.[190] These studies suggest a complex but strong influence of 6-OHDA treatment on the histaminergic system, but may also indicate a potential utility of histaminergic drugs in basal ganglia disorders. Additionally, several H_3R antagonists, e.g. ciproxifan,[103,191-193] thioperamide,[99] JNJ-39220675[194] or ABT-239,[101] were shown to increase or at least modulate hyperactivity and locomotor behaviour in rodents, induced by dopaminergic psychostimulants like methamphetamine or the similar acting NMDAR blocker MK-801. Ciproxifan, applied to haloperidol-treated rats, accelerated locomotor activity suggesting synergistic interactions between D_2Rs and H_3Rs.[192] H_3R blockade by thioperamide resulting in potentiation of D_1R and D_2R agonist-induced locomotor activity in mice, support a direct postsynaptic interaction of these receptors, potentially by heterodimerization.[187] Confirmative, the H_3R agonists RAMH and immepip attenuated D_1R agonist-induced locomotor activation.[32] Neither H_3R activation, nor inhibition alone e.g. by ciproxifan or thioperamide did interfere with locomotor behaviour.[192,195] When applied together with L-DOPA, the H_3R agonist immepip reduced LID, rather affecting chorea but not dystonia in non-human primates. The

same concentration of immepip alone resulted in significant acceleration of parkinsonian effects.[196] In conclusion, studies on H_3R activation/blockade to modulate locomotor activity remain controversial due to inconsistent reports. To date, there is no evidence, that H_3R antagonists alone are able to improve motor symptoms in PD itself, whereas a positive influence on dopaminergic treatments is likely.

A large number of PD patients (about 75%) develop serious cognitive dysfunction and dementia with neurodegenerative disease progression,[175] which often means the loss of autonomy in their daily life. Due to similar ongoing pathogenesis, PD-related dementia can often be treated with common AD therapeutics. As comprehensively discussed in the previous paragraph, H_3R antagonists provide pro-cognitive effects, most probably by ACh modulation.[95,97] Therefore, these compounds might be effective in PD-accompanying dementia.

Sleep impairment is often experienced by PD patients.[175] EDS, manifested as sudden-onset sleep during the day, represents the most prevalent sleep disruption in PD patients, having a severe impact on quality of life. Typically, EDS accompanies or became aggravated by dopaminergic treatment, especially by dopamine agonists but may also occur occasionally in untreated or L-DOPA patients.[153,160,175] These dysfunctions might appear as a consequence of progressing brain pathology, evidently also resulting in alterations within the histaminergic system.[17,60,178] Histamine is a key player in sleep-wake regulation and circadian rhythm, where the histaminergic system maintains the waking state, demonstrating increased neuronal firing rates.[23,197-199] CNS-penetrating H_1R antagonists can have sedative effects but lack therapeutical relevance for sleep disorders due to long half-lives and peripheral side effects. As later discovered, H_3Rs modulate wakefulness, raising great expectations for the therapeutic application of H_3R ligands in sleep-wake disorders.[29] $H_3R^{-/-}$ mice show chronical enhanced histamine neurotransmission resulting in, among other phenotypes, sleep-wake abnormalities due to abolishment of the negative feedback on histamine release via H_3R autoreceptors.[200] Accordingly, compounds impairing histaminergic release enhances sleep, which was demonstrated e.g. for the histamine synthesis inhibitor α-fluoromethylhistidine as well as H_3R autoreceptor agonists.[23,199,200] A number of imidazole-based H_3R antagonists, e.g. ciproxifan, exhibit significant wake-promoting effects in various animal models.[198,201-203] Recently, thioperamide was shown to modulate the circadian rhythm, but also improve cognitive deficits in the 6-OHDA mouse model.[203]

The clinical efficiency of H_3R antagonists for sleep disorders was finally confirmed by the approval of pitolisant as an orphan drug for the treatment of narcolepsy with and without cataplexy in 2016. This successful application awaked further enthusiasm for investigating H_3R antagonists as treatment option for sleep disorders. Consequently, additional compounds (e.g. JNJ-17216498) entered clinical trials as discussed previously. Pitolisant finished a clinical phase III study for EDS in PD patients, but without disclosed results as yet (NCT01036139).[107] Additionally, a safety and tolerability phase I study for ABT-652 in patients with EDS was completed (no results disclosed so far, NCT01124851).

Similar to AD, the pathological mechanisms of PD are manifold, justifying a utility of multitargeting drugs as innovative approach for PD treatment. With some commonalities in disease progression or symptoms for AD and PD, i.e. cognitive impairment, a few previous mentioned MTL strategies might be applicable for PD as well.[90] MTLs addressing simultaneously ChEs and MAOs, especially MAO B, may improve motor and non-motor symptoms of PD at the same time.[126,204] Accordingly, ladostigil as well as M30, a MAO inhibitor with metal chelation properties, were investigated for antiparkinsonian capabilities, showing neuroprotective and -restorative properties.[204] For example, M30 restored dopamine depletion and metabolism in PD animal models, i.e. N-methyl-4-phenyl-1,2,3,6-tetrahydropyridine (MPTP)-lesioned mice.[205] A different concept focuses on development of multitargeting adenosine receptor ligands, i.e. adenosine A_{2A} receptor ($A_{2A}R$) and to a lesser extent adenosine A_1 receptor (A_1R) antagonists, in combination with established dopaminergic targets such as D_2R[206,207] or MAO B.[208-210] $A_{2A}Rs$ were shown to affect PD motor symptoms via functional interaction with D_2Rs in the indirect pathway of the basal ganglia circuit. Within multiple rodent and non-human primate models of PD, promising antiparkinsonian potencies could be demonstrated for $A_{2A}R/(A_1R)$ antagonists.[211-214] Either as monotherapy or co-administrated with L-DOPA, $A_{2A}R$ antagonists improved motor symptoms or positively influenced L-DOPA wearing off and lowered effective L-DOPA dosage, respectively. In 2013, the $A_{2A}R$ antagonist istradefylline was approved in Japan, reducing the OFF periods when applied with L-DOPA. Several other $A_{2A}R$ antagonists reached phase II and phase III clinical trials, however, more often being investigated in patients with advanced PD receiving additional antiparkinsonian medications.[214] Overall, these findings clearly prove their potential for PD treatment, at least for late stage PD. Notably, some improvement of posture abnormalities, a hardly addressed issue in PD patients, could be demonstrated for istradefylline just recently.[215] Interestingly, it could be shown that presynaptic H_3Rs modulate $A_{2A}R$-mediated GABA release in the GP, suggesting an indirect contribution of H_3Rs in control of motor function,[216] however, no H_3R MTL for PD was previously published.

1.4.3 Obesity

Obesity affects millions of people worldwide, becoming a pandemic-like public health problem with growing morbidity and being associated with numerous serious conditions such as hypertension, diabetes mellitus or stroke.[217,218] While guided changing of lifestyle and eating behaviour are the first choice treatment, for a large number of patients pharmacotherapy is necessary to combat obesity. Despite considerable efforts by pharmaceutical companies, to date only a handful of drugs are approved with distinct mechanisms of action or even unknown mechanisms. The first approved and only peripheral acting compound, orlistat (Alli®, Xenical®) inhibits gastrointestinal lipases so that about a quarter of dietary fat will be defecated undigested. The other drugs act centrally by affecting the feeling of appetite and satiety, e.g. lorcaserin (Belviq®) a 5-HT$_{2C}$ receptor agonist, liraglutide (Saxenda®) a glucagon-like peptide 1 receptor agonist or naltrexone (opioid receptor antagonist) and bupropion (dopamine and noradrenaline reuptake inhibitor), latter ones applied as combination preparation (Mysimba®). Furthermore, a number of new targets for the treatment of obesity have emerged over the last decades,[218] such as antagonists of the G-protein coupled neuropeptide receptors, i.e. neuropeptide Y1/5 or melanin-concentrating hormone receptors 1 (MCHR1).[77] A potential therapeutic benefit of the latter one was assumed due to the hyperactive and enhanced energy expenditure of MCHR1$^{-/-}$ mice, being resistant to diet-induced obesity.[219] In rodents, MCHR1 antagonists were shown to reduce body weight gain via decreasing food intake induced by the orexigenic neuropeptide MCH.[220,221] With a high number of investigated MCHR1 antagonists, only a few have entered clinical trials, however, being discontinued due to safety and pharmacokinetic liabilities or missing efficacy.[218]

The histaminergic system plays a crucial role in eating behaviour by regulating the feeling of appetite and satiety as well as peripheral metabolic processes.[76] By definition, obesity is characterized by a chronical imbalance between energy intake and expenditure. A complex and sensitive homeostasis controls the body weight, where only marginal changes are able to cause overweight.[76] Affecting the energy homeostasis, histaminergic receptors represent an interesting target for anti-obesity drugs. The early hypothesis of brain histamine influencing the eating behaviour based on in vivo studies, where histamine injection into the brain resulted in abnormal food intake, e.g. in cats and rodents.[222] In addition, HDC$^{-/-}$ mice demonstrating neuronal histamine-deficiency show 13-20% increase of body weight compared to that of wild type mice (but just at 16 to 30 weeks of age) as well as an increased risk for developing high-fat-induced obesity.[223,224] The direct influence of neuronal histamine on appetite could be shown, either by neuronal activation in the histaminergic TMN, occurring directly before feeding of

food-scheduled rats or by an increase of hypothalamic histamine in hungry rats trained to access a food reservoir.[225-227] These changes on histamine or histamine turnover could not be demonstrated in ad libitum fed rats, thus, being connected to a state of arousal or expectation of food only.[226] Among histamine receptors, especially H_1Rs and H_3Rs are investigated regarding eating behaviour.[76,228] $H_1R^{-/-}$ mice show increased food intake and visceral adiposity.[229] A similar obese phenotype was observed by Takahashi and colleagues in $H_3R^{-/-}$ mice.[230] However, contradictory observations were made by other working groups claiming no significant alteration in body weight of $H_3R^{-/-}$ mice.[98,228] As excessive histamine stimulation via postsynaptic H_1Rs normally results in reduced weight gain, the manifestation of overweight in $H_3R^{-/-}$ mice seems paradox considering the absence of histamine release modulation via presynaptic H_3Rs. However, this circumstance may be explicable by histamine overstimulation resulting in desensitization of postsynaptic receptors.[230] In conclusion, these observations may already reflect a higher complexity of histamine receptor-mediated food intake and energy expenditure, in particular for H_3Rs as pan-receptor modulators. The highly potent and central acting H_1R agonist 2-(3-(trifluoromethyl)phenyl)histamine reduced daily food intake, as did a few H_1R antagonists (e.g. chlorpheniramine and pyrilamine). In contrast, numerous H_1R antagonists, i.e. antiallergics, enhanced it.[76] Furthermore, schizophrenic patients treated with atypical antipsychotics show an increased incidence of obesity with highest weight gain observed for clozapine and olanzapine, a side effect hampering patients compliance.[231] This observation, initially considered as co-incidence, was later connected to an extraordinary high affinity with antagonistic behaviour of clozapine and olanzapine at H_1R receptors (K_i = 1.2 nM and K_i = 2.0 nM, respectively[232]).[231,233]

A more congruent experimental situation may be observed for H_3R antagonists, where numerous first generation imidazole-based (ciproxifan, thioperamide, clobenpropit) and more recent representatives such as ABT-239 decrease food intake in rodents, even though, thioperamide, being extensively studied, lack anti-obese efficacy in a few studies.[76] Thioperamide was also shown to suppress hyperphagia induced by the orexigenic neuropeptide Y in multiple studies,[234,235] an effect which can be attenuated by H_1R antagonists such as the antipsychotic olanzapine stimulating the same pathway.[236] Just recently pitolisant was also found to reduce body weight and furthermore improve metabolic parameters (i.e. plasma triglyceride levels) in obese mice,[237] in accordance with previous observations of pitolisant counteracting olanzapine-induced hypertriglicerydemia.[238] Thus, a number of H_3R antagonists, particularly non-imidazoles, were developed and investigated for their anti-obesity potential in diet-induced obese rodents. The most progressed representatives were developed by Novo Nordisk, a company holding several patent

applications of H_3R antagonists as anti-obesity drugs.[228] Among two published candidates showing anti-obese capacities in rats after oral application, NNC 38 1202 was proven to be effective also in rhesus monkeys.[239,240] Unfortunately, strong ability for CYP interaction and hERG inhibition was demonstrated for NNC 38 1202, hence, a structural modified class of (piperazine-1-yl)-(piperidine-1-yl)-methanones was developed with an improved side effect profile.[241,242] Since then, Novo Nordisk made no further attempts and H_3R antagonists do not appear in their actual obesity pipeline (www.novonordisk.com). Currently, only two selective H_3R antagonists are still listed in clinical trial database (clinicaltrials.gov) for treatment of obesity. Schering-Plough, acquired by Merck in 2009, developed SCH-497079, which completed a clinical trial phase II with no effect on any outcome measure (NCT00642993, updated 2016), thus being discontinued and do not appear in their current pipeline (www.merckgroup.com). Another phase II clinical trial of HPP-404 (TransTechPharma) was terminated without explanation (NCT01540864). A more promising approach for treatment of obesity and drug-induced weight gain is demonstrated by betahistine, a dualtargeting H_1R agonist and mixed H_3R inverse agonist/agonist.[243] Being used for the treatment of vertigo in Meniére's disease for several years with a negligible tendency for adverse side effects, it was investigated as potential anti-obesity drug in numerous preclinical and clinical studies.[76] In vitro, it shows a higher affinity at H_3Rs, while even metabolites of betahistine bind to H_3Rs but not to central H_1Rs.[244] Despite its H_1R agonism, the H_3R autoreceptor modulation is presumed to be substantial for betahistine's histaminergic modulation. Detailed investigations of betahistine's H_3R functional potencies revealed a H_3R inverse agonism within nanomolar concentrations at both rat and human recombinant receptors.[243] Unfortunately, betahistine could not fulfil expectations in obese, otherwise healthy, patients.[245,246] More promising, schizophrenic patients showed either a stagnation of weight gain after two weeks or less weight gain at all after co-administration of betahistine with olanzapine or olanzapine and reboxetine (norepinephrine reuptake inhibitor), respectively.[247,248] A clinical study assessing the effect of betahistine on working memory in healthy women demonstrated no significant influence.[249] With the current scientific knowledge, the therapeutical efficacy of betahistine might be beneficial in patients with abnormal H_3R-mediated histaminergic signalling as observed in schizophrenia.[76,250]

In conclusion, these overall, partly controversial, preclinical and clinical observations do not allow a definite decision on the utility of H_3R antagonists in treatment of obesity, but they still remain a considerable basis for further evaluations, presumably more promising in multitargeting or co-medication concepts.

2 Scope and Objectives

The design of multitargeting ligands (MTLs) represent a novel, highly promising approach for treatment of multifactorial diseases, such as neurodegenerative diseases, with a high need for more comprehensive pharmacotherapy options. MTLs may provide higher efficacy by addressing synergistically multiple targets, thus, representing a valuable alternative to classical combination therapies applied in multifactorial diseases.[2,3]

The G-protein coupled histamine H_3 receptor (H_3R) demonstrate a unique pan-neurotransmitter regulation capacity, showing a broad spectrum of possible applications in central nervous system (CNS) disorders, especially cognitive and sleep disorders.[64] In particular, as target in multitargeting drug design a promising therapeutic utility for H_3R ligands is assumed, e.g. in therapy of neurodegenerative diseases.

This cumulative thesis aims to present explorative approaches of H_3R-based multitargeting drug design to combat multifactorial CNS diseases via simultaneous blockade of the H_3R and either other G-protein coupled receptors (GPCRs) or neurotransmitter-catabolizing enzymes. Combined targets to be addressed with H_3Rs include therapeutically established targets, i.e. monoamine oxidases or cholinesterase in Parkinson's or Alzheimer's disease therapy, but also more innovative targets proposed in literature for the respective disorders. Strategies for lead identification in multitargeting drug design based either on compound screening, in this case a condensed library of H_3R antagonists (serendipitous approach), or on valid st7ructure-activity relationship (SAR) assumptions e.g. verified historically and/or computational-assisted (knowledge-based approach).[5,10] Subsequent optimization of identified leads and initial proof-of-concept in vivo studies may provide a substantial evidence for utility of H_3R MTLs in therapy of CNS disorders.

3 Publications

3.1 Publication 1

Ciproxifan, a histamine H₃ receptor antagonist, reversibly inhibits monoamine oxidase A and B

Hagenow, S.[1], Stasiak, A.[2], Ramsay, R. R.[3], Stark, H.[1]

[1] Institute of Pharmaceutical and Medicinal Chemistry, Heinrich Heine University Duesseldorf, Universitaetsstr. 1, 40225 Duesseldorf, Germany. [2] Department of Hormone Biochemistry, Medical University of Lodz, Zeligowskiego 7/9, Pl 90-752 Lodz, Poland. [3] Biomedical Sciences Research Complex, University of St Andrews, North Haugh, St Andrews KY16 9ST, United Kingdom.

Abstract

Ciproxifan is a well-investigated histamine H₃ receptor (H₃R) inverse agonist/antagonist, showing an exclusively high species-specific affinity at rodent compared to human H₃R. It is well studied as reference compound for H₃R in rodent models for neurological diseases connected with neurotransmitter dysregulation, e.g. attention deficit hyperactivity disorder or Alzheimer's disease. In a screening for potential monoamine oxidase A and B inhibition ciproxifan showed efficacy on both enzyme isoforms. Further characterization of ciproxifan revealed IC_{50} values in a micromolar concentration range for human and rat monoamine oxidases with slight preference for monoamine oxidase B in both species. The inhibition by ciproxifan was reversible for both human isoforms. Regarding inhibitory potency of ciproxifan on rat brain MAO, these findings should be considered, when using high doses in rat models for neurological diseases. As the H₃R and monoamine oxidases are all capable of affecting neurotransmitter modulation in brain, we consider dual targeting ligands as interesting approach for treatment of neurological disorders. Since ciproxifan shows only moderate activity at human targets, further investigations in animals are not of primary interest. On the other hand, it may serve as starting point for the development of dual targeting ligands.

SCIENTIFIC REP**O**RTS

Ciproxifan, a histamine H$_3$ receptor antagonist, reversibly inhibits monoamine oxidase A and B

S. Hagenow[1], A. Stasiak[2], R. R. Ramsay[3] & H. Stark[1]

Ciproxifan is a well-investigated histamine H$_3$ receptor (H3R) inverse agonist/antagonist, showing an exclusively high species-specific affinity at rodent compared to human H3R. It is well studied as reference compound for H3R in rodent models for neurological diseases connected with neurotransmitter dysregulation, e.g. attention deficit hyperactivity disorder or Alzheimer's disease. In a screening for potential monoamine oxidase A and B inhibition ciproxifan showed efficacy on both enzyme isoforms. Further characterization of ciproxifan revealed IC$_{50}$ values in a micromolar concentration range for human and rat monoamine oxidases with slight preference for monoamine oxidase B in both species. The inhibition by ciproxifan was reversible for both human isoforms. Regarding inhibitory potency of ciproxifan on rat brain MAO, these findings should be considered, when using high doses in rat models for neurological diseases. As the H3R and monoamine oxidases are all capable of affecting neurotransmitter modulation in brain, we consider dual targeting ligands as interesting approach for treatment of neurological disorders. Since ciproxifan shows only moderate activity at human targets, further investigations in animals are not of primary interest. On the other hand, it may serve as starting point for the development of dual targeting ligands.

Ciproxifan (cyclopropyl 4-(3-(1*H*-imidazol-4-yl)propyloxy)phenyl methanone) is a well characterized species-specific histamine H$_3$ receptor (H3R) inverse agonist/antagonist (Fig. 1). It shows exclusively high affinity at rodent H3R in a sub-nanomolar range (K$_i$ (rH3R) = 0.4–6.2 nM and K$_i$ (mH3R) = 0.5–0.8 nM), while binding to human H3R is only moderate (K$_i$ = 46–180 nM) with negligible selectivity e.g. over human adrenergic α_{2A} and α_{2C} receptors[1–3] (Table 1). Ciproxifan's inverse agonism/antagonism at histamine H$_3$ receptors is manifested in improvement of wakefulness and attention *in vivo*[4,5]. It is commonly used as reference H3R antagonist, e.g. in rodent models studying cognitive impairment[6], Alzheimer's disease[7] or attention deficit hyperactivity disorder (ADHD)[8]. It was also tested in animal models for schizophrenia[9], sleeping disorders[10] or most recently autism[11].

The H3R (for review, e.g. see Sander *et al.*[5] or Gemkow *et al.*[12]), a G-protein coupled receptor displaying constitutive activity (basal activity without binding of an agonist), inhibits the release of several neurotransmitters like dopamine, histamine, serotonin or acetylcholine[4]. In consequence, inverse agonism/antagonism of the H$_3$ receptor leads to accelerated release of mentioned neurotransmitters which is why H$_3$ receptor inverse agonists/ antagonists like ciproxifan are recognized as promising therapeutics for treatment of several neuropathological diseases[13]. During a screening for monoamine oxidase A (MAO A) and B (MAO B) inhibitors, ciproxifan was found to be an inhibitor for both enzyme isoforms. MAOs are expressed in neurons and glial cells, localized in the cell on the outer membrane of mitochondria and critically involved in degradation of neurotransmitters in the brain. In humans MAO A is predominantly found in adrenergic, catecholaminergic and dopaminergic neurons and deactivates serotonin, dopamine, norepinephrine and epinephrine. Human MAO B participates in dopamine degradation and is mainly expressed in serotonergic neurons and glial cells[14,15]. Therefore, MAO inhibitors are frequently investigated for treatment of depression and Parkinson's disease[16]. In this study, we further investigated ciproxifan's capability to inhibit human MAO A and MAO B *in vitro* by determination of IC$_{50}$ values and reversibility of its inhibition.

[1]Heinrich Heine University Duesseldorf, Institute of Pharmaceutical and Medicinal Chemistry, Universitaetsstr. 1, 40225 Duesseldorf, Germany. [2]Department of Hormone Biochemistry, Medical University of Lodz, Zeligowskiego 7/9, Pl 90-752 Lodz, Poland. [3]Biomedical Sciences Research Complex, University of St Andrews, North Haugh, St Andrews KY16 9ST, United Kingdom. Correspondence and requests for materials should be addressed to H.S. (email: stark@hhu.de)
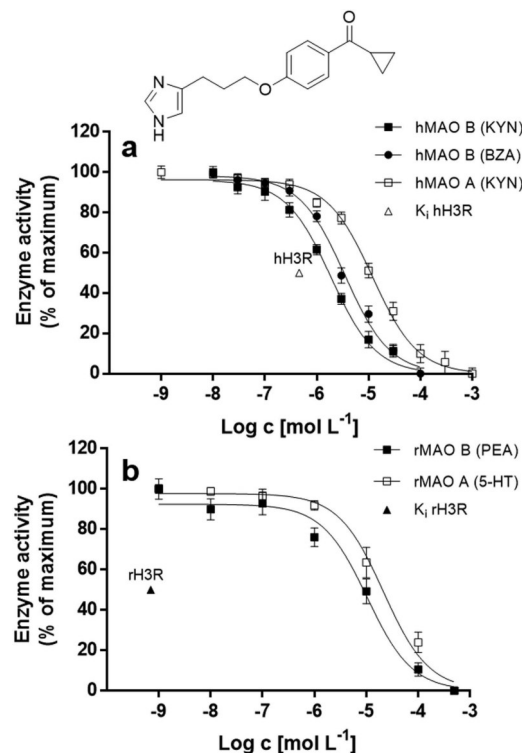
Figure 1. (**a**) Inhibition curves for ciproxifan obtained with a spectrophotometric assay using human recombinant membrane-bound MAO A and MAO B. (**b**) Inhibition curves for ciproxifan in rat brain MAO A and MAO B measured radiometrically. Kynuramine (KYN, **a**) or serotonin (5-HT, **b**) were used as MAO A substrates. Kynuramine (KYN, **a**), benzylamine (BZA, **a**) or phenylethylamine (PEA, **b**) were used as MAO B substrates. Data represent mean ± s.e.m. of at least n = 3 independent experiments each performed at least in duplicates (global fit). The K_i values of ciproxifan for human histamine H_3 receptors (hH3R, Δ) and rat histamine H_3 receptors (rH3R, ▲) are indicated in the graphs[1].

Receptor	K_i [nM]	Receptor	K_i [nM]
rH_3R	0.4–6.2[2,3,27–29]	$gp\beta_1$[b]	12589[2]
$mH3R$	0.5–0.8[30]	gp M_3[c]	3162[2]
mkH_3R	41[27]	gp5-HT_3[c]	>3,162[2]
hH_3R	46–180[1,3,27]	gp5-HT_{1B}[d]	>10,000[2]
hH_1R	>10,000[3]	r5-HT_1	16598[31]
hH_2R	>10,000[3]	r5-HT_{2A}[e]	15848[2]
hH_4R	1862[3]	r5-HT_3	302[3]
$h\alpha_{2C}$	63[3]	r5-HT_4[f]	>1,995[2]
$h\alpha_{2A}$	43[3]		
$r\alpha_{1D}$[a]	3,981[2]		

Table 1. Published affinity data for ciproxifan. gp = guinea pig, h = human, m = mouse, mk = monkey, r = rat. [a]rat aorta. [b]guinea pig atrium. [c]guinea pig ileum. [d]guinea pig iliac. [e]rat tail. [f]rat esophagus.

Results

IC$_{50}$ determinations for human MAO. The IC$_{50}$ values of ciproxifan for human membrane-bound MAO (hMAO) were measured spectrophotometrically using kynuramine (KYN) and benzylamine (BZA) as MAO B substrates, while for MAO A only KYN was used. We found IC$_{50}$ values for ciproxifan in a micromolar range

	IC$_{50}$ [μM] ± s.e.m (n)			IC$_{50}$ [μM] ± s.e.m (n)		
	hMAO			rMAO		
	A		**B**	**A**	**B**	**Inhibition Type**
Substrate	KYN	BZA	KYN	5-HT	PEA	
Ciproxifan	11.4 ± 1.2 (5)	4.3 ± 0.7 (5)	2.1 ± 0.3 (9)	37.5 ± 0.2 (3)	15.4 ± 0.3 (3)	Reversible
Safinamide	n.d.	n.d.	0.049 ± 0.001 (4)	n.d.	n.d.	Reversible[20]
Moclobemide	568 ± 115 (3)	n.d.	n.d.	n.d.	n.d.	Reversible[32]
ʟ-Deprenyl	29.6 ± 3.9 (9)	n.d.	0.037 ± 0.004 (5)	n.d.	n.d.	Mixed/Irreversible[33]
Clorgyline	0.008 ± 0.001 (4)	n.d.	1.3 ± 0.2 (4)	n.d.	n.d.	Mixed/Irreversible[33]

Table 2. IC$_{50}$ values and type of inhibition for ciproxifan, ʟ-deprenyl, clorgyline, safinamide and moclobemide using kynuramine (KYN) or serotonin (5-HT) and benzylamine (BZA) or phenylethylamine (PEA) as MAO A and MAO B substrates, respectively. IC$_{50}$ values are given as means ± standard errors of means (s.e.m.) of n independent experiments, each performed at least in duplicates. n.d. = not determined, ʟ-deprenyl IC$_{50}$ = 0.036 μM[33], clorgyline IC$_{50}$ = 0.0065 μM[33], safinamide IC$_{50}$ = 0.048 μM[20], moclobemide IC$_{50}$ = 361 μM[32].

(IC$_{50, \text{MAO A}}$ = 11 μM and IC$_{50, \text{MAO B}}$ = 2 μM), showing an about 5-fold higher preference for MAO B (IC$_{50, \text{MAO B}}$/IC$_{50, \text{MAO A}}$ = 0.2) (Fig. 1, Table 2).

ʟ-Deprenyl, clorgyline, safinamide and moclobemide were tested as reference compounds using the same spectrophotometric method. The irreversible MAO B selective inhibitor ʟ-deprenyl showed an IC$_{50}$ value of 37 nM for MAO B (Table 2). For clorgyline, an irreversible MAO A selective inhibitor, an IC$_{50}$ value of 8 nM for MAO A were found. The reversible inhibitors safinamide and moclobemide gave IC$_{50}$ values of 49 nM (MAO B) and 568 μM (MAO A), respectively (Table 2).

IC$_{50}$ determinations for rat brain MAO. The IC$_{50}$ values of ciproxifan for rat brain MAO (rMAO) were obtained radiometrically using serotonin (5-HT) and phenylethylamine (PEA) as MAO A and MAO B substrates, respectively. Similar to hMAO, ciproxifan displayed IC$_{50}$ values in the micromolar concentration range (IC$_{50, \text{MAO A}}$ = 38 μM and IC$_{50, \text{MAO B}}$ = 15 μM), again with slight preference for MAO B (IC$_{50, \text{MAO B}}$/IC$_{50, \text{MAO A}}$ = 0.4) (Table 2).

Reversibility of human MAO inhibition. In order to determine whether ciproxifan shows a reversible or irreversible inhibition type, dilution experiments using the spectrophotometric assay were performed, where hMAOs were preincubated with ciproxifan (10 × IC$_{50}$). After preincubation probes were diluted 100-fold, measured at saturated substrate conditions and the remaining enzyme activity was compared to that of MAO preincubated without ciproxifan. For both hMAO isoforms no considerable decrease in enzyme activity after preincubation with ciproxifan compared to control (set to 100%) were observed, suggesting a reversible inhibition type (Table 2). The remained enzyme activities for hMAO A and hMAO B preincubated with ciproxifan were 107.7 ± 3.4% and 91.4 ± 9.7%, respectively. In order to verify the test procedure, ʟ-deprenyl was tested in the same manner showing decreased remaining enzyme activity of hMAO B (51.1 ± 2.9%) after preincubation.

Discussion

Ciproxifan is frequently used as the reference histamine H$_3$ receptor (H3R) antagonist in rodent models for neurological diseases like cognition[6], Alzheimer's disease[7] or sleep-wake disorders[10,17], because of its explicit high affinity and efficacy in rodent H3R (K$_i$ < 1.0 nM) which is about 30- to 100-fold lower than that at the human H3R. In our study we showed an additional property of ciproxifan. It inhibits human and rat MAO A and MAO B reversibly in a micromolar concentration range with a slight preference for MAO B.

We consider a combined activity pattern of ligands at H3R and MAO as new interesting approach for the treatment of neurological diseases. These are often associated with a neurotransmitter dysregulation, assumed to be adjustable by H3R blockade[12]. Neurotransmitter levels could be also modulated by inhibition of their degradation. MAOs are enzymes involved in oxidative deamination of neurotransmitters in neuronal cells after reuptake from the synaptic cleft. Therefore, deactivation of MAO A or MAO B is a principle well established in therapy of neurological disorders like depression and Parkinson's disease[18]. Additionally, MAOs are thought to promote oxidative stress when highly expressed in neuronal tissues. This can force increased neuronal cell death, a condition observed in Alzheimer's disease[19]. Thus, we hypothesize that reversible or more probably irreversible MAO inhibitors and H3R inverse agonists/antagonists can have overlapping pharmacological utilities, suggesting ligands, interacting with both targets, as promising candidates for treatment of neurodegenerative diseases. Concerning ciproxifan, which displays IC$_{50}$ values for both hMAO isoforms only in a micromolar range, we found its inhibition far too low for therapeutic efficacy in humans, which is anyway limited by its low affinity at human H3R. For example, safinamide, a MAO B selective reversible inhibitor most recently approved as first add-on treatment of Parkinson's disease, is active in submicromolar concentration ranges (IC$_{50}$ = 0.048–0.112 μM for hMAO B; IC$_{50, \text{MAO B}}$/IC$_{50, \text{MAO A}}$ < 0.001[20–22]). Additionally, imidazole-containing drugs like ciproxifan are potential inhibitors of cytochrome P450 enzymes by coordination of the heme iron atom[23]. So, it may only serve as prospective starting

point for investigation of dual targeting ligands in the future. Since ciproxifan is frequently used in rodent models for several neurological diseases, its MAO inhibition should be taken into consideration in retrospect or in the future using rodent models as possible accompanying effect. Ciproxifan has about four orders of magnitude higher activity at rH3R compared to the in-cell target rMAO. However, with a calculated log P value of 2.76[24] we assume good membrane penetration by ciproxifan[23]. Additionally, it could be shown that ciproxifan can reach brain concentrations up to approximately $10\,\mu M$ when applied i.p. to rats[17], evidencing that partial rMAO inhibition is at least conceivable under test conditions.

Taken together, the moderate and reversible MAO inhibitory properties of ciproxifan are interesting newly described properties which may interact with some previous animal screening data at high ciproxifan dosages. It can still be taken as a reference H3R antagonist, but its MAO A and MAO B inhibitory properties may be considered in retrospect on high dosage screenings.

Nevertheless, ciproxifan may serve as starting point for the design of dual targeting ligands combining H_3 receptor inverse agonism/antagonism and MAO inhibition, possibly favourable in treatment various neurological diseases. Since ciproxifan inhibited rat brain MAO also in micromolar concentration ranges, its activity has to be take into consideration in the future as a possible accompanying effect, when using it in rat models for neurological diseases. In retrospect, some of its effects explored in different species were probably contributed by its MAO A/B inhibitory properties.

Methods

All authors confirmed that all methods were carried out in accordance with relevant guidelines and regulations.

Spectrophotometric IC$_{50}$ determination using human MAO. Enzyme studies were carried out using human recombinant membrane-bound MAO A and MAO B (Sigma-Aldrich, St. Louis, MO). Pipetting of assays were fully automated using a pipetting robot in a total assay volume of $100\,\mu L$ or performed manually in a total assay volume of $200\,\mu L$. IC$_{50}$ values were obtained by measuring enzymatic conversion rates at inhibitor concentrations between $10^{-9}\,M$ and $10^{-3}\,M$ in the presence of kynuramine ($K_M = 40\,\mu M$ for MAO A and $K_M = 25\,\mu M$ for MAO B) or benzylamine ($K_M = 165\,\mu M$) using $2 \times K_M$ substrate concentrations, while reactions were started by addition of MAO A ($10\,ng\,\mu L^{-1}$) or MAO B ($12.5\,ng\,\mu L^{-1}$). For optimal enzyme activity all assays were carried out under potassium phosphate buffered conditions ($50\,mM$, pH = 7.4). Initial velocities were determined spectrophotometrically by a microplate reader at $30\,°C$ by following product formation of 5-hydroxyquinoline and benzaldehyde at 316 nm and 250 nm, respectively, over a period of at least 30 minutes (interval of 20–30 seconds). Initial velocities, expressed as mAU min^{-1}, were obtained from the linear phase of product formation (see Supplementary Information, Fig. 1). Data were analysed using GraphPad PRISM version 6. For IC$_{50}$ determinations initial velocities for each experiment were normalized (expressed as percentage), plotted against inhibitor concentrations and fitted using the non-linear regression "log inhibitor vs. response (three parameters)". IC$_{50}$ values were determined in at least three independent experiments, each performed at least in duplicates.

Radiometric IC$_{50}$ determination using rat brain MAO. Wistar male rats were sacrificed, the brains were quickly excised from the skulls, cleaned of residual meninges and frozen on dry ice. For each experiment the crude homogenates prepared from pooled brain from three rats were used. Enzyme activity of MAO A or MAO B was measured using radioactive substrate (PerkinElmer/NEN): serotonin (5-[2-^{14}C]-hydroxytryptamine binoxalate) or β-[ethyl-1-^{14}C]-phenyl-ethyl-amine hydrochloride (PEA), respectively, with the procedure described by Fowler and Tipton 1981[25] with some modification according to Gómez *et al.*[26]. IC$_{50}$ values were determined using six different concentrations of ciproxifan between $10^{-9}\,M$ and $5 \times 10^{-4}\,M$ at fixed concentration of substrate ($200\,\mu M$ serotonin or $20\,\mu M$ PEA). For IC$_{50}$ determinations values were normalized (expressed as percentage), plotted against inhibitor concentrations and fitted using the non-linear regression "log inhibitor vs. response (three parameters)". IC$_{50}$ values were determined in three independent experiments, each performed in duplicates.

Reversibility of human MAO inhibition. Reversibility of hMAO inhibition by ciproxifan was assessed by dilution experiments. Supplied MAOs ($5\,mg\,mL^{-1}$ in potassium phosphate $100\,mM$, sucrose $0.25\,M$, EDTA $0.1\,mM$, glycerol 5%) were preincubated with inhibitor ($10 \times IC_{50}$) or water at $30\,°C$ for 15 minutes in a water bath. The inhibitor volume represented one-tenth of the total preincubation volume. After preincubation, probes were 100-fold diluted with potassium phosphate buffer ($100\,mM$, pH = 7.4) to yield a final concentration of 12.5 ng μL^{-1} for the enzyme. Enzymatic conversion rates were determined in the presence of kynuramine for hMAO A and benzylamine for hMAO B at saturating substrate concentrations ($10 \times K_M$) under potassium phosphate buffer conditions ($50\,mM$, pH = 7.4). Spectrophotometric measurements were carried out as described for IC$_{50}$ determinations over a period of at least 30 minutes for hMAO A and hMAO B, respectively (interval of 20–30 seconds). Initial velocities, obtain from the linear phase of product formation, of hMAO preincubated with inhibitor ($10 \times IC_{50}$) were compared to hMAO preincubated with water (control) to define reversible or irreversible inhibition mode (see Supplementary Information, Fig. 2). Initial velocities, expressed as mAU min^{-1}, were normalized and given as percent of control.

References

1. Ligneau, X. *et al.* Distinct pharmacology of rat and human histamine H(3) receptors: role of two amino acids in the third transmembrane domain. *Br J Pharmacol* **131**, 1247–1250 (2000).
2. Ligneau, X. *et al.* Neurochemical and behavioral effects of ciproxifan, a potent histamine H3-receptor antagonist. *J. Pharmacol. Exp. Ther.* **287**, 658–666 (1998).

3. Esbenshade, T. & Krueger, K. Two novel and selective nonimidazole histamine H3 receptor antagonists A-304121 and A-317920: I. *In vitro* pharmacological effects. *J. Pharmacol. Exp. Ther.* **305,** 887–896 (2003).

4. Leurs, R., Bakker, R. A., Timmerman, H. & de Esch, I. J. P. The histamine H3 receptor: from gene cloning to H3 receptor drugs. *Nat. Rev. Drug Discov.* **4,** 107–120 (2005).

5. Sander, K., Kottke, T. & Stark, H. Histamine H3 receptor antagonists go to clinics. *Biol. Pharm. Bull.* **31,** 2163–2181 (2008).

6. Fox, G. B. *et al.* Cognition enhancing effects of novel H3 receptor (H3R) antagonists in several animal models. *Inflamm Res* **53,** S49–S50 (2004).

7. Bardgett, M. E., Davis, N. N., Schultheis, P. J & Griffith, M. S. Ciproxifan, an H3 receptor antagonist, alleviates hyperactivity and cognitive deficits in the APPTg2576 mouse model of Alzheimer's disease. *Neurobiol. Learn. Mem.* **95,** 64–72 (2011).

8. Fox, G. B. *et al.* Effects of histamine H3 receptor ligands GT-2331 and ciproxifan in a repeated acquisition avoidance response in the spontaneously hypertensive rat pup. *Behav. Brain Res.* **131,** 151–161 (2002).

9. Mahmood, D., Khanam, R., Pillai, K. K. & Akhtar, M. Protective effects of histamine H3 -receptor ligands in schizophrenic behaviors in experimental models. *Pharmacol. Reports* **64,** 191–204 (2012).

10. Gondard, E. *et al.* Enhanced histaminergic neurotransmission and sleep-wake alterations, a study in histamine H3-receptor knock-out mice. *Neuropsychopharmacology* **38,** 1015–1031 (2013).

11. Baronio, D. *et al.* Effects of an H3R antagonist on the animal model of autism induced by prenatal exposure to valproic acid. *PLoS One* **10,** 1–11 (2015).

12. Gemkow, M. J. *et al.* The histamine H3 receptor as a therapeutic drug target for CNS disorders. *Drug Discov. Today* **14,** 509–515 (2009).

13. Passani, M. B. & Blandina, P. Histamine receptors in the CNS as targets for therapeutic intervention. *Trends Pharmacol. Sci.* **32,** 242–249 (2011).

14. Wang, C. C., Billett, E., Borchert, A., Kuhn, H. & Ufer, C. Monoamine oxidases in development. *Cell. Mol. Life Sci.* **70,** 599–630 (2013).

15. Ramsay, R. R. Monoamine oxidases: the biochemistry of the proteins as targets in medicinal chemistry and drug discovery. *Curr. Top. Med. Chem.* **12,** 2189–2209 (2012).

16. Youdim, M. B. H. & Riederer & P. F. In *Handbook of Clinical Neurology* (eds. Koller, W. C. & Melamed, E.) 84, 93–120 (Elsevier B.V., 2007).

17. Le, S., Gruner, J. a, Mathiasen, J. R., Marino, M. J. & Schaffhauser, H. Correlation between *ex vivo* receptor occupancy and wake-promoting activity of selective H3 receptor antagonists. *J. Pharmacol. Exp. Ther.* **325,** 902–909 (2008).

18. Finberg, J. P. M. Update on the pharmacology of selective inhibitors of MAO-A and MAO-B: focus on modulation of CNS monoamine neurotransmitter release. *Pharmacol. Ther.* **143,** 133–152 (2014).

19. Xie, S. *et al.* Synthesis and evaluation of selegiline derivatives as monoamine oxidase inhibitor, antioxidant and metal chelator against Alzheimer's disease. *Bioorg. Med. Chem.* **23,** 3722–3729 (2015).

20. Mostert, S., Petzer, A. & Petzer, J. P. Inhibition of monoamine oxidase by benzoxathiolone analogues. *Bioorganic Med. Chem.* **26,** 1200–1204 (2016).

21. Choi, J. W. *et al.* Synthesis of a series of unsaturated ketone derivatives as selective and reversible monoamine oxidase inhibitors. *Bioorg. Med. Chem.* **23,** 6486–6496 (2015).

22. Stocchi, F. & Torti, M. Adjuvant therapies for Parkinson's disease: critical evaluation of safinamide. *Drug Des. Devel. Ther.* **10,** 609–618 (2016).

23. Rydzewski, R. M. *A Chemist's Guide to Biotech and Pharmaceutical Research.* (Elsevier, 2008).

24. Molsoft L. L. C., Drug-Likeness and Molecular Property Prediction. http://molsoft.com/mprop/ (accessed Nov. 3, 2016).

25. Fowler, C. J & Tipton, K. F. Concentration dependence of the oxidation of tyramine by the two forms of rat liver mitochondrial monoamine oxidase. *Biochem. Pharmacol.* **30,** 3329–3332 (1981).

26. Gómez, N., Balsa, D. & Unzeta, M. A comparative study of some kinetic and molecular properties of microsomal and mitochondrial monoamine oxidase. *Biochem. Pharmacol.* **37,** 3407–3413 (1988).

27. Yao, B. B., Sharma, R., Cassar, S., Esbenshade, T. A. & Hancock, A. A. Cloning and pharmacological characterization of the monkey histamine H3 receptor. *Eur. J. Pharmacol.* **482,** 49–60 (2003).

28. Medhurst, A. D. *et al.* GSK189254, a novel H3 receptor antagonist that binds to histamine H3 receptors in Alzheimer's disease brain and improves cognitive performance in preclinical. *J. Pharmacol. Exp. Ther.* **321,** 1032–1045 (2007).

29. Wulff, B. S., Hastrup, S. & Rimvall, K. Characteristics of recombinantly expressed rat and human histamine H3 receptors. *Eur. J. Pharmacol.* **453,** 33–41 (2002).

30. Rouleau, A. *et al.* Cloning and expression of the mouse histamine H3 receptor: evidence for multiple isoforms. *J. Neurochem.* **90,** 1331–1338 (2004).

31. Zhao, C. *et al.* The alkaloid conessine and analogues as potent histamine H3 receptor antagonists. *J. Med. Chem.* **51,** 5423–5430 (2008).

32. Alcaro, S. *et al.* Chromone-2- and -3-carboxylic acids inhibit differently monoamine oxidases A and B. *Bioorganic Med. Chem. Lett.* **20,** 2709–2712 (2010).

33. Chaurasiya, N. D., Ibrahim, M. A., Muhammad, I., Walker, L. A. & Tekwani, B. L. Monoamine oxidase inhibitory constituents of propolis: Kinetics and mechanism of inhibition of recombinant human MAO-A and MAO-B. *Molecules* **19,** 18936–18952 (2014).

Acknowledgements

Author Contributions

H.S. provided ciproxifan maleate. S.H., A.S., H.S. and R.R.R. contributed to the experimental design. A.S. performed the radiometric IC_{50} determinations of ciproxifan with rat brain MAO. S.H. performed the biological evaluation of ciproxifan with human MAO, wrote the main manuscript text and prepared figure and tables. All authors reviewed the manuscript.

Additional Information

Supplementary information accompanies this paper at http://www.nature.com/srep

Competing financial interests: The authors declare no competing financial interests.

How to cite this article: Hagenow, S. *et al.* Ciproxifan, a histamine H$_3$ receptor antagonist, reversibly inhibits monoamine oxidase A and B. *Sci. Rep.* **7,** 40541; doi: 10.1038/srep40541 (2017).

Publisher's note: Springer Nature remains neutral with regard to jurisdictional claims in published maps and institutional affiliations.

Supplementary Informations

Ciproxifan, a histamine H_3 receptor antagonist, reversibly inhibits monoamine oxidase A and B

S. Hagenow[1], A. Stasiak[2], R. R. Ramsay[3] and H. Stark[1]*

[1] Heinrich Heine University Duesseldorf, Institute of Pharmaceutical and Medicinal Chemistry, Universitaetsstr. 1, 40225 Duesseldorf, Germany; e-mail: stark@hhu.de, Fax +49 211 8113359, phone: +49 211 8110478.

[2] Department of Hormone Biochemistry, Medical University of Lodz, Poland Zeligowskiego 7/9, Pl 90-752 Lodz.

[3] Biomedical Sciences Research Complex, University of St Andrews, North Haugh, St Andrews KY16 9ST, United Kingdom.

*Correspondence to stark@hhu.de

Spectrophotometric IC_{50} determination using human MAO
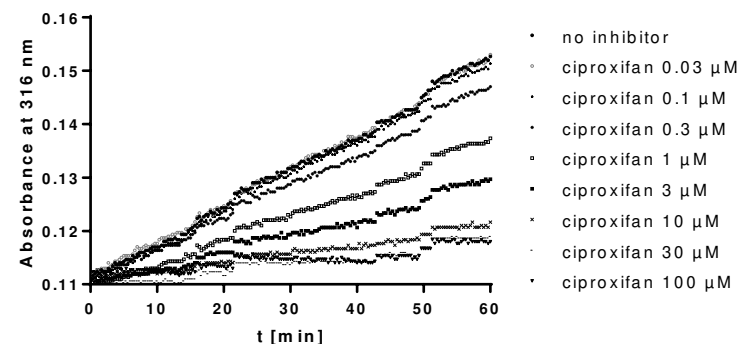
Figure 1. Kinetic measurements of one representative experiment of ciproxifan (eight concentrations, 3×10^{-11} to 10^{-4} M) with MAO B using kynuramine ($2 \times K_M$, 50 µM). Enzyme conversion rates were given as mAU min^{-1} over a period of 60 minutes ($R^2 > 0.97$).

Reversibility of human MAO inhibition
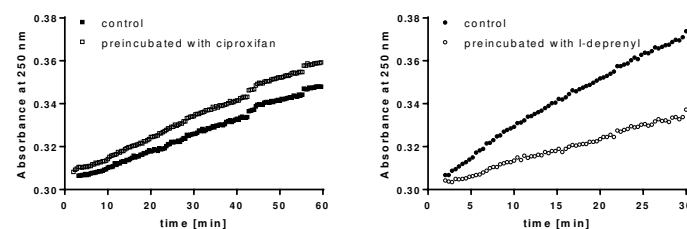
Figure 2. Kinetic measurements of reversibility studies for ciproxifan (left) and L-deprenyl (right) with MAO B. Graphs show one representative experiment for ciproxifan and l-deprenyl each. MAO B were preincubated with water (control) and inhibitor ($10 \times IC_{50}$) for 15 minutes at 30°C. After preincubation samples were diluted ($100 \times$) and enzyme conversion rates were measured as mAU min^{-1} (at 215 nm) in the presence of benzylamine ($10 \times K_M$).

3.2 Publication 2

Novel indanone derivatives as MAO B/H$_3$R dual-targeting ligands for treatment of Parkinson's disease

Affini, A.[1*], Hagenow, S.[1*], Zivkovic, A.[1], Marco-Contelles, J.[2], Stark, H.[1]

[1] Institute of Pharmaceutical and Medicinal Chemistry, Heinrich Heine University Duesseldorf, Universitaetstr. 1, 40225 Duesseldorf, Germany. [2] Laboratory of Medicinal Chemistry (IQOG, CSIC), C/ Juan de la Cierva 3, 28006-Madrid, Spain.
[*]These authors have contributed equally to this work.

Abstract

The design of multi-targeting ligands was developed in the last decades as an innovative therapeutic concept for Parkinson's disease (PD) and other neurodegenerative disorders. As the monoamine oxidase B (MAO B) and the histamine H$_3$ receptor (H$_3$R) are promising targets for dopaminergic regulation, we synthetized dual-targeting ligands (DTLs) as non-dopaminergic receptor approach for the treatment of PD. Three series of compounds were developed by attaching the H$_3$R pharmacophore to indanone-related MAO B motifs, leading to development of MAO B/H$_3$R DTLs. Among synthesized indanone DTLs, compounds bearing the 2-benzylidene-1-indanone core structure showed MAO B preferring inhibition capabilities along with nanomolar hH$_3$R affinity. Substitution of C5 and C6 position of the 2-benzylidene-1-indanones with lipophilic substituents revealed three promising candidates exhibiting inhibitory potencies for MAO B with IC$_{50}$ values ranging from 1931 nM to 276 nM and high affinities at hH$_3$R (K$_i$ < 50 nM). Compound **3f** ((E)-5-((4-bromobenzyl)oxy)-2-(4-(3-(piperidin-1-yl)propoxy)benzy-lide-ne)-2,3-dihydro-1H-inden-1-one, MAO B IC$_{50}$ = 276 nM, hH$_3$R K$_i$ = 6.5 nM) showed highest preference for MAO B over MAO A (SI > 36). Interestingly, IC$_{50}$ determinations after preincubation of enzyme and DTLs revealed also nanomolar MAO B potency for **3e** (MAO B IC$_{50}$ = 232 nM), a structural isomer of **3f**, and **3d** (MAO B IC$_{50}$ = 541 nM), suggesting time-dependent inhibition modes. Reversibility of inhibition for all three compounds were confirmed by dilution studies in excess of substrate. Thus, indanone-substituted derivatives are promising lead structures for the design of MAO B/hH$_3$R DTLs as novel therapeutic approach of PD therapy.

Contents lists available at ScienceDirect

European Journal of Medicinal Chemistry

Research paper

Novel indanone derivatives as MAO B/H₃R dual-targeting ligands for treatment of Parkinson's disease

Anna Affini [a,1], Stefanie Hagenow [a,1], Aleksandra Zivkovic [a], Jose Marco-Contelles [b], Holger Stark [a,*]

[a] *Heinrich Heine University Duesseldorf, Institute of Pharmaceutical and Medicinal Chemistry, Universitaetstr. 1, 40225 Duesseldorf, Germany*
[b] *Laboratory of Medicinal Chemistry (IQOG, CSIC), C/ Juan de la Cierva 3, 28006, Madrid, Spain*

ARTICLE INFO

ABSTRACT

The design of multi-targeting ligands was developed in the last decades as an innovative therapeutic concept for Parkinson's disease (PD) and other neurodegenerative disorders. As the monoamine oxidase B (MAO B) and the histamine H₃ receptor (H₃R) are promising targets for dopaminergic regulation, we synthetized dual-targeting ligands (DTLs) as non-dopaminergic receptor approach for the treatment of PD. Three series of compounds were developed by attaching the H₃R pharmacophore to indanone-related MAO B motifs, leading to development of MAO B/H₃R DTLs. Among synthesized indanone DTLs, compounds bearing the 2-benzylidene-1-indanone core structure showed MAO B preferring inhibition capabilities along with nanomolar hH₃R affinity. Substitution of C5 and C6 position of the 2-benzylidene-1-indanones with lipophilic substituents revealed three promising candidates exhibiting inhibitory potencies for MAO B with IC_{50} values ranging from 1931 nM to 276 nM and high affinities at hH₃R ($K_i < 50$ nM). Compound **3f** ((E)-5-((4-bromobenzyl)oxy)-2-(4-(3-(piperidin-1-yl)propoxy)benzylidene)-2,3-dihydro-1H-inden-1-one, MAO B $IC_{50} = 276$ nM, hH₃R $K_i = 6.5$ nM) showed highest preference for MAO B over MAO A (SI > 36). Interestingly, IC_{50} determinations after preincubation of enzyme and DTLs revealed also nanomolar MAO B potency for **3e** (MAO B $IC_{50} = 232$ nM), a structural isomer of **3f**, and **3d** (MAO B $IC_{50} = 541$ nM), suggesting time-dependent inhibition modes. Reversibility of inhibition for all three compounds were confirmed by dilution studies in excess of substrate. Thus, indanone-substituted derivatives are promising lead structures for the design of MAO B/hH₃R DTLs as novel therapeutic approach of PD therapy.

---

1. Introduction

Parkinson's disease (PD) is one of the most common central nervous system (CNS) disorder affecting 1.5% of the global population older than 65 years. Recognizing PD as high complex and multifactorial dysregulation forced researchers to come up with more and more imaginative approaches for medicinal therapy. Challenging the "one-drug one-target" paradigm, showing mostly inadequate therapeutical efficacy, the development of multi-targeting ligands attracted notice over the last decades, where only a few entered the drug market. Due to the fact that multi-targeting drugs, addressing more than one target simultaneously, promise several improvements compared to selective drugs, i.e. potential synergistic efficacy, less drug-drug interactions, easier dosing schedule, and a unified pharmacokinetic profile [1–4], great effort has been brought to the design of such ligands for treatment of PD. As a common strategy in PD therapy monoamine oxidase

(MAO) B inhibitors are approved as mono- and add-on therapy [5,6]. MAOs are mitochondrial membrane-bound FAD-containing enzymes playing a key role in neurotransmitter degradation. In addition to their localizations in brain regions, the two isoforms A and B differ in substrate and inhibitor specificities. While MAO A inhibitors are used in treatment of depression, the MAO B isoform predominantly degrades dopamine in human brain, thus, representing a well-established target for PD therapy. Among irreversible inhibitors like L-deprenyl or rasagiline, safinamide is the only approved reversible MAO B inhibitor in PD therapy. As dual-targeting approach for PD treatment, ligands addressing MAO B and adenosine A_{2A} receptors, a G-protein coupled receptor (GPCR), were recently suggested as indirect non-dopaminergic therapy [7]. The human histamine H_3 receptor (hH_3R), a class A GPCR predominantly expressed in the CNS, serves as pan-neurotransmitter modulator in the human brain due to its heteroreceptor activity. Activation of presynaptic H_3Rs may decrease the release of dopamine and other neurotransmitters [8,9], meaning that H_3R inverse agonism/antagonism might provide a hitherto hardly investigated opportunity for the treatment of PD [10]. Although their exact utility in PD treatment can be hardly estimated so far, H_3R antagonists show promising features to improve motor but especially non-motor symptoms, i.e. cognitive or sleep impairment [11,12]. As H_3Rs are co-expressed with dopamine D_1 and D_2 receptors in the basal ganglia [12], Ferrada et al. demonstrated the potentiation of dopamine agonist-induced locomotor activation by the H_3R antagonist thioperamide [13], indicating a potential benefit of H_3R

antagonists on motor control in PD patients when applied with dopamine agonists. Recently, thioperamide was also proven to counteract memory and sleep impairment in a 6-OHDA PD mouse model [14], while wake-promoting effects for thioperamide and numerous other H_3R antagonists could be also shown previously in vivo and clinical trials [15,16]. To date, pitolisant (Wakix®) is the only H_3R inverse agonist/antagonist on the drug market approved for the treatment of narcolepsy with and without cataplexy and already in Phase III clinical trials for excessive daytime sleepiness in PD patients (clinicaltrials.gov). Numerous H_3R ligands are described, showing additional affinity to other GPCRs, ion channels, transporters or even enzymes [2]. Additionally, the dopamine modulation capacities of MAO B and H_3R as well as their co-localization especially in the substantia nigra [12,13], which is predominantly affected by loss of dopaminergic neurons in PD patients, strongly encouraged us to design MAO B/H_3R dual-targeting ligands (DTL) as possible and innovative approach to modulate the dopamine imbalance in PD patients. To overcome drawbacks associated with irreversible MAO inhibition, such as slow recovery of MAO expression levels after inactivation, we have focussed on reversible MAO B inhibition strategies. Numerous structural classes of MAO B inhibitors are described, while especially structural related (benzylidene-)chromones and coumarine derivatives [17] as well as recently described (2-benzylidene-) indanones [18,19] showed highly selective and reversible inhibition properties in nanomolar concentration ranges. Compounds **I** and **II** (Fig. 1) are potent and selective reversible MAO B inhibitors,
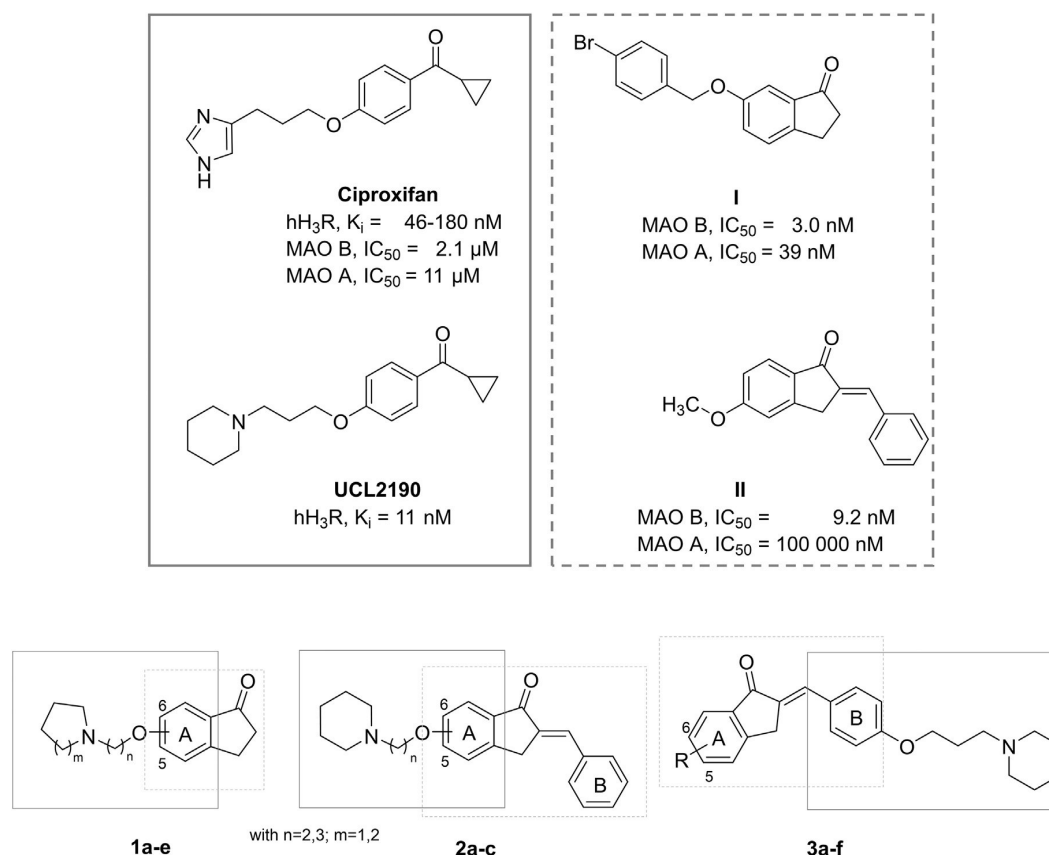

Fig. 1. H_3R antagonists/inverse agonists ciproxifan [20] and UCL2190 (hH_3R Ki = 1.6 nM [^{125}I]iodoproxyfan replacement studies [24]), as well as potent reversible (2-benzylidene-) indanone MAO B inhibitors (I and II) [18,19] taken as lead structures for three series of potential dual-targeting ligands (DTLs).

showing IC_{50} values in low nanomolar concentrations ranges [18,19]. We recently found ciproxifan (Fig. 1), a common reference H_3R inverse agonist/antagonist, to have MAO B preferring inhibition potency (MAO B $IC_{50} = 2.1 \mu M$) [20], while the probability of MAO inhibition by already described H_3R ligands could be also shown elsewhere [21]. Preserving the alkyloxyphenyl linker of ciproxifan, the imidazole moiety, associated with adverse side effects, was replaced by piperidine as shown for UCL2190 [22] (Fig. 1) fitting a pharmacologically more favourable H_3R pharmacophore [22,23]. Accordingly, three series of DTLs were synthetized by attaching piperidine- or pyrrolidine(alkyloxy)phenyl H_3R structural elements to already described (2-benzylidene-)indanone MAO B inhibitor scaffolds in different positions. The first series of MAO B/H_3R DTLs (**1a-e**) were synthesized by attachment of the H_3R motif to the C5 or C6 position of an indanone core structure related to compound **I**. Variations in alkyl chain length between the aromatic core A and the amine as well as in size of the aliphatic heterocycle (piperidino or pyrrolidino group) were performed. A second set of DTLs were obtained by introduction of the H_3R pharmacophore in either C5 or in C6 position of the more lipophilic 2-benzylidene-indanone derivative **II** (**2a-c**). A third series of compounds (**3a-f**) was received by connecting the H_3R pharmacophore to the benzylidene ring B at the C4' position [19].

2. Chemistry

In the present study, the commercially available 5- and 6-methoxy-1-indanone were used for the synthesis of the corresponding hydroxy derivatives. The demethylation of phenol ethers was achieved with yields higher than 90% [25]. Precursors were then synthesized by alkylation of piperidine with 2-chloroethan-1-ol or 3-chloropropan-1-ol [26]. UCL2190 was obtained with 60% yield via nucleophilic exchange between 3-(piperidin-1-yl)propan-1-ol and cyclopropyl 4-fluorophenyl methanone (Scheme 1) [22,27]. Precursors were obtained after chlorination of the alcohol derivatives in quantitative yield [28,29]. Williamson ether reaction was then performed to alkylate 6- or 7-hydroxy-1-indanone with 1-(2-chloroethyl)piperidine/pyrrolidine or 1-(3-chloropropyl)piperidine/pyrrolidine [30]. The first series of compounds, **1a-e**, was obtained with a yield ranging from 72% to 85% (Scheme 1).

Afterwards, some of the latter compounds were combined with benzaldehyde via aldol condensation to obtain the corresponding 2-benzylidene-1-indanone derivatives **2a-c** in good yields (80—90%) (Scheme 2) [31]. The synthesis of compounds **3a-f** started with the alkylation of the commercially available 4-hydroxybenzaldehyde with 1-(3-chloropropyl)piperidine hydrochloride. The obtained aldehyde was converted into several 2-benzylidene-1-indanone derivatives via aldol condensation with the corresponding commercially available indanones (Scheme 2). For the synthesis of these compounds the same procedure described for the second series of products were used. For 2-benzylidene-1-indanone derivatives the isomers were determined to be in *E*-conformation using 2D NMR (NOESY) [32]. The structures of final compounds were confirmed by ^1H NMR, ^{13}C NMR and ESI-HRMS, while their purities were verified by elementary analysis.

3. Pharmacology

All compounds were screened for MAO A/B inhibition at one concentration (usually $10 \mu M$) and revealed mostly MAO B preferring inhibitory potencies, while series three DTLs (**3a-f**) were the most potent ones (**1a-e** < **2a-c** < **3a-f**) (Table 1). Concerning their affinity at hH_3R, first series of compounds (**1a-e**) showed only poor hH_3R affinity ($K_i > 100$ nM). This could be improved in second (**2a-c**) and third series (**3a-f**) of DTLs yielding desired nanomolar H_3R affinities. DTLs providing more than 76% (+++) inhibition for MAO B and high affinity for hH_3R ($K_i < 100$ nM) were further characterized to obtain IC_{50} values for both isoforms as well as modes of inhibition (Table 2).

4. Discussion

In our study, we could obtain the final products in high yields, by performing only few synthetic steps. In general, synthesis of precursor molecules was the most laborious part, while combining the H_3R pharmacophore with the indanone or the benzylic moiety could be easily performed by Williamson ether reaction. For lead structure optimization, based on our prior description of ciproxifan possessing only moderate MAO and hH_3R activities [20], its
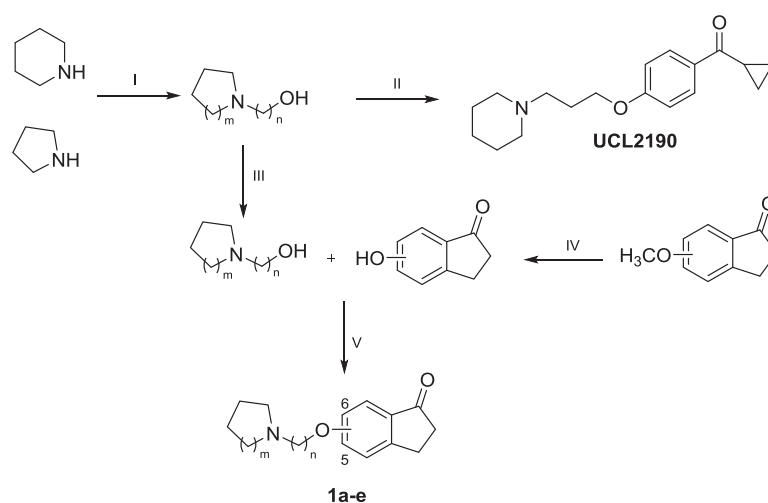
Scheme 1. General procedure for the synthesis of first series of indanone DTLs **1a-e** (m = 1,2; n = 2,3). (I): Piperidine or pyrrolidine, 2-chloroethan-1-ol or 3-chloropropan-1-ol, K_2CO_3, KI, acetone, reflux, 72 h; (II) Cyclopropyl 4-fluorophenyl methanone, acetonitrile, NaH, N_2, r.t.→reflux (III): $SOCl_2$, toluene, N_2, 0 °C→60 °C, 3 h; (IV) $AlCl_3$, toluene, N_2, reflux, 3 h; (V) K_2CO_3, KI, acetone, reflux, 24 h.
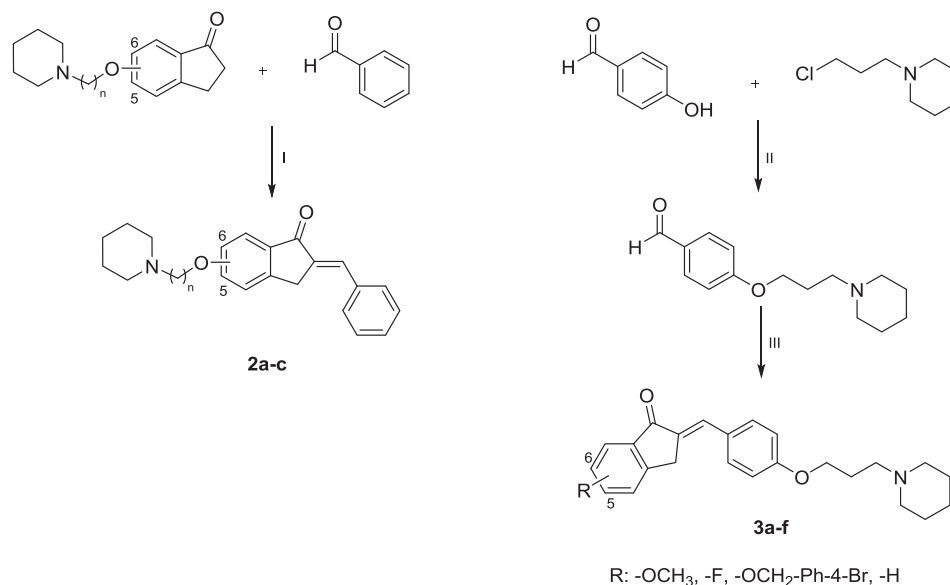
Scheme 2. Synthetic route for the design of second and third series of 2-benzylidene-1-indanone DTLs **2a-c** (n = 2,3) and **3a-f**. Compounds **2a-c**: I) NaOH, ethanol, r.t., 30 min. Compounds **3a-f**: II) K_2CO_3, KI, acetone, reflux, 24 h; III) corresponding indanone, NaOH, ethanol, r.t., 30 min.

analogue UCL2190 bearing a piperidine moiety instead of an imidazole was synthesized and investigated for its MAO inhibition properties. Surprisingly, UCL2190 provides a more favourable selectivity profile for MAO B in addition to an about 30-fold higher hH_3R affinity ($K_i = 11$ nM; 95% CI = [3.5, 33], Fig. 1) compared to ciproxifan, representing an optimized lead structure for synthesis of MAO B/H_3R DTLs. It has been shown previously, that indanone derivatives substituted in C6 and C5 position are potent inhibitors of the human MAO B [18]. Within the first series of indanone DTLs (**1a-e**), most of the compounds exhibit inhibition potency for both MAO isoforms < 50% at 10 μM, with **1b** showing highest MAO B inhibition properties ($72 \pm 4.3\%$) (Table 1). Furthermore, none of these compounds show the desired hH_3R affinity, most probably due to the lack of an additional lipophilic group in the molecule, as frequently observed in the arbitrary region of H_3R antagonists [23].
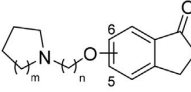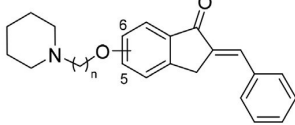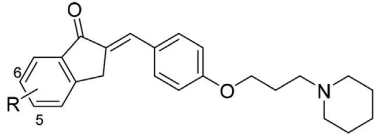
The more lipophilic 2-benzylidene-1-indanone DTLs **2a-c** (Table 1), showed more preferred and improved MAO B inhibition with highest inhibition found for **2a** ($81 \pm 4.5\%$), which still lacks H_3R affinity. Thus, as it could be previously shown, that substitution of the benzylidene moiety in the C4′ position with lipophilic groups (e.g. halogens or alkyl chains) or basic/polar moieties (e.g. tertiary amines) is tolerated by MAO B [19], in the series three DTLs (**3a-f**) the H_3R pharmacophore was attached to the C4′ position of the benzylidene (Table 1). All of these compounds showed inhibition capability for MAO B > 60% and hH_3R affinity in low nanomolar concentration ranges ($K_i < 50$ nM). The DTLs with most potent MAO B inhibition properties **3d** ($94 \pm 8.7\%$), **3e** ($64 \pm 6.5\%$) and **3f** ($87 \pm 3.8\%$) at 10, 2 and 5 μM, respectively, were further evaluated. All three showed IC_{50} values in low micromolar to nanomolar concentration ranges (Table 2), while highest inhibition properties for MAO B with optimized preference (SI > 36) over MAO A was found for DTL **3f** (Fig. 2).

To investigate time dependency and reversibility of inhibition two setups were performed for DTLs **3d-f**: (a) IC_{50} shift experiments after pre-incubation of enzyme and inhibitors (30 min, 37 °C) (Table 2) and (b) 50× dilution experiments after pre-incubation of enzyme and inhibitors (30 min and 60 min, 37 °C)

with excess of substrate (Fig. 3). Interestingly, the IC_{50} values do not show significant difference to non-preincubated ones for **3f**, while a 3.5-fold and 6.3-fold shift of IC_{50} values to nanomolar concentrations was shown for **3d** and **3e**, respectively, suggesting a slow reversible or tight binding inhibition mode within our test conditions. The dilution experiments under saturated substrate conditions, however, revealed a reversible mode of inhibition for all three DTLs, indicated by recovery of enzyme activity after dilution. This would be consistent with findings for structural related (*E*)-3-heteroarylidenechroman-4-ones and (*E*)-3-benzylidenechroman-4-ones showing comparable behaviour and differences within a series of compounds [34,35]. Tight binding inhibitors which do not form covalent bonds with the active site can behave similar to typical covalent binding "suicide inhibitors" like *L*-deprenyl in reversibility studies [17,34]. *In vivo* they might have a safer pharmacological profile with longer duration times than reversible inhibitors, but lacking the suicide inactivation of MAOs. Reversible inhibitors are known to have less severe side effects, such as hypertensive crisis or slow recovery of MAO expression levels after suicide inactivation [17,36] associated with irreversible and non-selective MAO inhibitors. However, since they do not inactivate the enzyme, reversible MAO inhibitors need higher target affinities to compete with the endogenous ligands, which remains a demanding step in MAO B drug design [37].

For early evaluation of drug-likeness of most promising DTLs, ligand efficacy (LE), ligand efficiency dependent lipophilicity (LELP) and ligand-lipophilicity efficiency (LipE) were calculated for hH_3R and MAO B [33] (Supporting Information). The high lipophilic DTLs **3e** and **3f** showed improved MAO B affinity but at the cost of LE due to the high molecular weight (Table 2). Instead, DTL **3d** displays best drug-like physicochemical parameters for both targets representing the most lead-like DTL within this small series. Regarding proposed multi-targeting properties, the overlapping of pharmacophoric elements of H_3R antagonists and AChE/BuChE inhibitors (e.g. piperidinopropyloxy element) most probably result in potential AChE/BuChE inhibition potency for our MAO B/H_3R DTLs. Recently, the multi-target ligand contilisant, combining affinity at

Table 1
H$_3$R and MAO screening data of novel MAO B/H$_3$R dual-targeting ligands.

	Pos.	n	m	R	Inhibition at 10 μM*		K$_i$ [nM] [95% CI]
					MAO A	MAO B	hH$_3$R
1a	6	2	1		−	+	6118 [3129, 11963]
1b	6	3	2		−	++	304 [122, 758]
1c	5	2	1		+	−	345 [103, 1148]
1d	5	2	2		−	+	205 [81, 520]
1e	5	3	2		−	+	159 [37, 678]
2a	6	2			−	+++	696 [302, 1605]
2b	6	3			−	++	39 [8.9, 169]
2c	5	3			−	++	3.9 [0.6, 26]
3a					−	++	2.1 [0.5, 10]
3b	6			-OCH$_3$	++	++	11 [3.5, 38]
3c	5			-OCH$_3$	−	++	33 [12, 89]
3d	5			-F	++[a]	+++[a]	2.2 [0.6, 8.1]
3e	6			-OCH$_2$-Ph-4-Br	+[a]	+ +[a]	32 [13, 81]
3f	5			-OCH$_2$-Ph-4-Br	+[a]	+++[a]	6.5 [1.5, 29]

K$_i$ values for the hH$_3$R are given as mean within the 95% confidence interval (CI). * MAO inhibition was calculated as percentages related to control at a test concentration of 10 μM and given as ≤25% (−), 26–50% (+), 51–75% (++), 76–100% (+++).
[a] Fluorimetric assay with a test concentration of 10, 2 and 5 μM for **3d**, **3e** and **3f**, respectively; Ph = phenyl.

H$_3$Rs, MAOs and cholinesterases *in vitro*, demonstrated a pro-cognitive effect in mice [38]. Additionally, potent antioxidative 2-benzylidene-1-indanones were described previously, combining nanomolar AChE and Aβ aggregation inhibition as possible drugs for Alzheimer's disease (AD) therapy [32]. Finding some additional AChE/BuChE inhibition properties, however, might result in a beneficial multi-targeting ligand (MTL) profile, where several MTLs are already described especially for treatment of cognitive impairments and AD [38–40]. From structural point of view our 2-benzylidene-1-indanone DTLs may act as Michael acceptors, which are able to form adducts with proteins, especially with cysteine residues [41,42]. To address this problem, compound **3d** was incubated with an excess of acetylcysteine at physiological pH and monitored by ESI-MS for up to three days. No thiol adduct was observed, suggesting that formation of adducts with proteins are unlikely for our 2-benzylidene-1-indanone DTLs.

In conclusion, we were able to design hH$_3$R/MAO B DTLs by attaching a generally accepted H$_3$R antagonist pharmacophore in different positions to previously described indanone and 2-benzylidene-1-indanone MAO B inhibitor motifs. Within this study three 2-benzylidene-1-indanone DTLs were obtained, showing promising capabilities with MAO B inhibition properties

(IC$_{50}$ = 232–541 nM after preincubation) and affinity at the human H$_3$R (K$_i$ = 2.2–32 nM). These DTLs (**3d**, **3e** and **3f**) were obtained by attaching the H$_3$R pharmacophore to the C4′ position of the benzylidene ring B, substituted either with fluoride (**3d**) or a bulky, lipophilic element (**3e**, **3f**) on the indanone ring A. Compound **3f** were the most MAO B preferring inhibitor (MAO SI > 36) showing a reversible inhibition mode, while **3d** and **3e** provide interesting, more balanced MAO profiles with presumed tight binding, but still reversible inhibition mode. Thus, we successfully described promising MAO B/H$_3$R DTLs, suitable as a starting point, for further optimization and development of potent DTLs or MTLs for the treatment of Parkinson's disease.
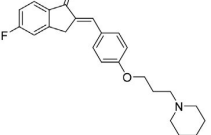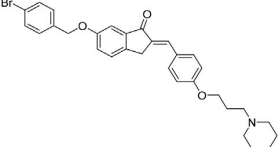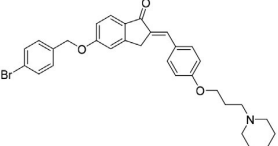
5. Experimental part

5.1. Reagent and instrumentation

Reagents and solvents for synthesis were purchased from Sigma-Aldrich, VWR Chemicals, Fisher Scientific, Panreac Appli-Chem, Alfa Aesar and Chemsolute and were used without further purifications (unless stated otherwise). ^{1}H NMR and ^{13}C NMR were recorded on a Bruker AMX spectrometer (Bruker, Germany) at 300

Table 2
H$_3$R Affinity and MAO IC$_{50}$ values (with and without preincubation) for most potent 2-benzylidene-1-indanone MAO B/H$_3$R dual-targeting ligands.

Compound		Pre-incubation 37 °C [min]	IC$_{50}$ [nM] [95% CI] (n)		MAO SI[a]	
			MAO A	MAO B	MAO B	LE[b]
3d		0	9178 [4169, 20207] (4)	1931 [926, 4025] (4)	4.8	0.28
		30		541 [362, 807] (5)		
3e		0	5514 [3567, 8522] (7)	1455 [840, 2522] (4)	3.7	0.22
		30		232 [70, 769] (5)		0.25
3f		0	>10 000 (3)	276 [197, 385] (6)	>36	0.25
		30		262 [185, 372] (5)		0.25
UCL2190		0	>50 000 (3)	3884 [1816, 8311] (3)	>12	0.35
Safinamide		0	>50 000 (4)	53 [20, 141] (4)	>940	0.45
		30		21 [13, 33] (4)		0.48
L-Deprenyl		0	>30 000 (4)	42 [23, 74] (4)	>710	0.72
		30		3.9 [2.2, 6.8] (5)		0.82

K$_i$ and IC$_{50}$ values for human H$_3$R and MAO A/B, respectively, are given as mean within the 95% confidence interval (CI) of n independent experiments each performed at least in duplicates.
[a] Selectivity index (SI) = IC$_{50}$ MAO A/IC$_{50}$ MAO B.
[b] LE = pIC$_{50}$/HA (heavy atoms), LE $\geq$ 0.3, LE was calculated as previously described [33].
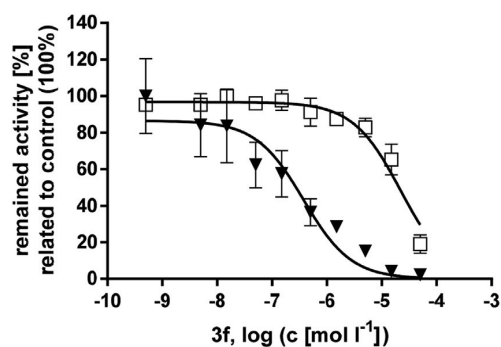
Fig. 2. Monoamine oxidase A ($\square$) and B ($\blacktriangledown$) IC$_{50}$ curves of compound **3f**. Data are given as mean (normalized to control) $\pm$ standard deviation (SD) of one representative experiment performed in duplicates.
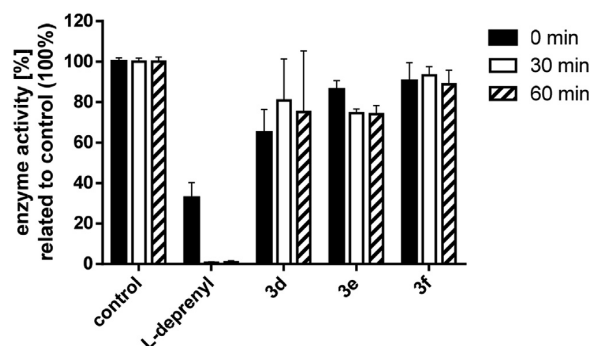
Fig. 3. Reversibility of inhibition after preincubation of MAO B and inhibitors for 0, 30 and 60 min prior to 50$\times$ dilution, measured under saturated substrate assay conditions. Data are given as mean (normalized to each control) $\pm$ standard deviation (SD) of at least two independent experiments, each performed in duplicates (global fit).

and 75 MHz respectively, where CDCl$_3$ or DMSO-d6 were used as a solvent. Tetramethylsilane was used as standard and chemical shifts are reported in parts per million (ppm). Spin multiplicities are given as s (singlet), d (doublet), dd (doublet of doublets), t (triplet), q (quintet) or m (multiplet). Approximate coupling constants (J) in Hertz (Hz). Number and assignment of protons (ax, axial; eq, equatorial; ph, phenyl; ind, indanone; prop, propyl; pip, piperidine; eth, ethyl; cycloprop, cyclopropyl; pyr, pyrrolidine). Elementary analyses (C, H, N) were measured on a CHN-Rapid (Heraeus, Germany) and were within 0.4% of the theoretical values for all final compounds. Electrospray ionization mass spectrometry (ESI-MS) was performed on an amaZon speed (Bruker, Germany) in positive polarity. Data are listed as mass number ([M+H$^+$]) and relative intensity (%). High-resolution mass spectra (HRMS) were run in electrospray ionization (ESI) mode. Melting points (m.p., uncorrected) were determined on a M − 564 Büchi melting point apparatus (Büchi, Germany). Preparative column chromatography was performed on silica gel 60 M, 0.04−0.063 mm (Macherey-Nagel, Germany) and thin-layer chromatography (TLC) was carried out using pre-coated silica gel 60 with fluorescence indicator at UV 254 nm (Macherey-Nagel, Germany).

5.2. Synthesis of precursors

1-(2-Chloroethyl or 3-chloropropyl)piperidine and 1-(2-chloroethyl)pyrrolidine as well as 4-(3-(piperidin-1-yl)propoxy) benzaldehyde were synthetized as described previously [26,43,44]. Demethylation of the 5- or 6-hydroxy-1-indanone was achieved by using well described general methods [25,45]. The precursors were used as starting material for the preparation of the final DTLs (**series 1-3**).

5.3. Synthesis of cyclopropyl(4-(3-(piperidin-1-yl)propoxy)phenyl) methanone hydrochloride (UCL2190) [22,27]

3-(Piperidine-1-yl)propan-1-ol (1 eq) was treated with NaH (5 eq, 60% suspension mineral oil) at room temperature under inert atmosphere for 3 h. The freshly prepared 3-(piperidine-1-yl)propanolate was heated with cyclopropyl-4-fluorophenyl methanone (2 eq) in acetonitrile for 24 h under reflux. The mixture was concentrated under reduced pressure and the residue extracted with dichloromethane and 2N NaOH solution. The organic extract was dried over MgSO$_4$, evaporated and transformed into hydrogen chloride. The white solid was obtained in a yield of 62%: m.p. 174.6 °C.

^{1}H NMR (300 MHz, DMSO-d6) δ 7.99−7.90 (m, 2H, ph-3,7*H*), 7.03−6.94 (m, 2H, ph-4,6*H*), 4.21−4.09 (t, 2H, J = 5.8, prop-1*H$_2$*), 3.62−3.37 (m, 2H, prop-3*H$_2$*), 3.29−3.16 (m, 2H, pip-2,6*H$_{eq}$*), 3.02−2.81 (m, 2H, pip-2,6*H$_{ax}$*), 2.79−2.69 (m, 1H, COCH*CH$_2$*), 2.23−2.10 (m, 2H, prop-2*H$_2$*), 2.01−1.30 (m, 6H, pip-3,5*H$_2$*, pip-4*H$_{eq/ax}$*), 1.14−1.01 (m, 4H, Cycloprop-2,3*H$_2$*); ^{13}C NMR (75 MHz, DMSO-d6) δ 204.6 (C*O*), 162.4 (ph-5*C*), 129.7 (Ph-3,7*C*), 129.4 (ph-6,4*C*), 128.2 (Ph-2*C*), 73.1 (prop-1*C*), 58.5 (prop-3*C*), 57.1 (pip-2,6*C*) 27.7 (prop-2*C*), 25.9 (pip-3,5*C*), 24.5 (pip-4*C*), 18.1 (COCH*CH$_2$*), 12.6 (Cycloprop-2,3(*CH$_2$*)$_2$); ESI-MS *m/z*: calcd for C$_{18}$H$_{25}$NO$_2$ (MH$^+$), 288.1964, found 288.1958.

5.4. Synthesis of the 1-indanone derivatives **1a-e** [26,30]

The appropriately hydroxy phenols (1.2 eq) and chloride precursors (1 eq) were reflux in absolute acetone together with potassium carbonate (3.2 eq) and potassium iodide (1 eq). After 24 h, the reaction was cooled down. The inorganic materials were removed by filtration and the filtrate was concentrated under vacuum. The crude product was taken up in methylene chloride

and 2N NaOH solution. The organic phase was then washed with saturated NaCl-solution and water, dryed over sodium sulfate, and concentrated under vacuum. The resulting oil was purified by column chromatography (CH$_2$Cl$_2$/MeOH, 9/1).

5.4.1. 6-(2-(Pyrrolidin-1-yl)ethoxy)-2,3-dihydro-1H-inden-1-one hydrochloride (**1a**)

Yield: 76%; m.p. 195.2 °C. ^{1}H NMR (300 MHz, D$_2$O) δ 7.48−7.41 (d, 1H, J = 8.5, ph$_{ind}$-7*H*), 7.31−7.25 (dd, 1H, J = 8.5, ph$_{ind}$-5*H*), 7.13−7.08 (d, 1H, J = 2.5, ph$_{ind}$-4*H*), 4.38−4.25 (t, 2H, J = 5.0, eth-1*H$_2$*), 3.72−3.51 (m, 4H, COC*H$_2$*, COCH$_2$C*H$_2$*), 3.20−3.05 (m, 2H, eth-2*H$_2$*), 3.04−2.92 (m, 2H, pyr-2,5*H$_{eq}$*), 2.70−2.57 (m, 2H, pyr-2,5*H$_{ax}$*), 2.21−1.80 (m, 4H, pyr-3,4*H$_2$*); ^{13}C NMR (75 MHz, DMSO-d6) δ 206.4 (C*O*), 157.6 (ph$_{ind}$-6*C*), 148.7 (COCph$_{ind}$-7*C*), 138.4 (COCH$_2$CH$_2$*C*), 128.4 (ph$_{ind}$-7*C*), 123.9 (ph$_{ind}$-6*C*), 106.4 (ph$_{ind}$-4*C*), 64.3 (prop-1*C*), 54.0 (pyr-2,5*C*), 52.1 (prop-2*C*), 37.2 (COC*H$_2$*), 25.3 (COCH$_2$*C*H$_2$), 23.0 (pyr-3,4*C*); ESI-HRMS *m/z*: calcd for C$_{15}$H$_{19}$NO$_2$ (MH$^+$), 246.1494, found 246.1495. Anal. calc.: C, 61.96; H, 7.28; N, 4.82. Found: C, 62.43; H, 7.06; N, 4.98.

5.4.2. 6-(3-(Piperidin-1-yl)propoxy)-2,3-dihydro-1H-inden-1-one (**1b**)

Yield: 81%; m.p. 59.1 °C. ^{1}H NMR (300 MHz, DMSO-d6) δ 7.64−7.57 (d, 1H, J = 8.7, ph$_{ind}$-7*H*), 7.28−7.21 (dd, 1H, J = 8.4, ph$_{ind}$-5*H*), 7.09−7.04 (m, 1H, J = 2.28, ph$_{ind}$-4*H*), 4.07−3.97 (t, 2H, J = 6.4, prop-1*H$_2$*), 3.06−2.94 (t, 2H, J = 5.3, COC*H$_2$*), 2.68−2.59 (m, 2H, COCH$_2$C*H$_2$*), 2.42−2.33 (t, 2H, J = 6.9, prop-3*H$_2$*), 2.32−2.20 (m, 4H, pip-2,6*H$_{eq/ax}$*), 1.93−1.77 (q, 2H, J = 6.7, prop-2*H$_2$*), 1.56−1.43 (m, 4H, pip-3,5*H$_2$*), 1.42−1.30 (m, 2H, pip-4*H$_{eq/ax}$*); ^{13}C NMR (75 MHz, DMSO-d6) δ 208.7 (C*O*), 160.9 (ph$_{ind}$-6*C*), 150.3 (COCph$_{ind}$-7*C*), 140.5 (COCH$_2$CH$_2$*C*), 130.5 (ph$_{ind}$-7*C*), 128.1 (ph$_{ind}$-5*C*), 108.1 (ph$_{ind}$-4*C*), 69.0 (prop-1*C*), 57.7 (prop-3*C*), 56.8 (pip-2,6*C*), 39.3 (COC*H$_2$*), 28.8 (COCH$_2$*C*H$_2$), 28.2 (pip-3,5*C*), 27.3 (prop-2*C*), 26.8 (pip-4*C*); ESI-HRMS *m/z*: calcd for C$_{17}$H$_{23}$NO$_2$ (MH$^+$), 274.1807, found 274.1800. Anal. calc.: C, 74.68; H, 8.48; N, 5.12. Found: C, 74.76; H, 8.68; N, 5.06.

5.4.3. 5-(2-(Pyrrolidin-1-yl)ethoxy)-2,3-dihydro-1H-inden-1-one hydrochloride (**1c**)

Yield: 75%; m.p. 193.8 °C. ^{1}H NMR (300 MHz, D$_2$O) δ 7.59−7.53 (d, 1H, J = 8.6, ph$_{ind}$-7*H*), 7.07−7.01 (m, 1H, ph$_{ind}$-4*H*), 6.99−6.91 (dd, 1H, J = 8.6, ph$_{ind}$-6*H*), 4.43−4.33 (t, 2H, J = 5.0, eth-1*H$_2$*), 3.73−3.58 (m, 4H, COC*H$_2$*, COCH$_2$C*H$_2$*), 3.24−3.07 (m, 2H, eth-2*H$_2$*), 3.06−2.98 (m, 2H, pyr-2,5*H$_{eq}$*), 2.67−2.55 (m, 2H, pyr-2,5*H$_{ax}$*), 2.20−1.86 (m, 4H, pyr-3,4*H$_2$*); ^{13}C NMR (75 MHz, DMSO-d6) δ 204.7 (C*O*), 163.3 (ph$_{ind}$-5*C*), 158.5 (COCph$_{ind}$-7*C*), 130.8 (COCH$_2$CH$_2$*C*), 125.01(ph$_{ind}$-7*C*), 116.1 (ph$_{ind}$-4*C*), 111.4 (ph$_{ind}$-6*C*), 64.1 (prop-1*C*), 54.1 (pyr-2,5*C*), 52.8 (prop-2*C*), 36.4 (COC*H$_2$*), 25.8 (COCH$_2$*C*H$_2$), 22.9 (pyr-3,4*C*); ESI-HRMS *m/z*: calcd for C$_{15}$H$_{19}$NO$_2$ (MH$^+$), 246.1494, found 246.1484. Anal. calc.: C, 62.93; H, 7.22; N, 4.89. Found: C, 62.69; H, 7.09; N, 5.03.

5.4.4. 5-(2-(Piperidin-1-yl)ethoxy)-2,3-dihydro-1H-inden-1-one hydrochloride (**1d**)

Yield: 72%; m.p. 194.4 °C. ^{1}H NMR (300 MHz, D$_2$O) δ 7.51−7.43 (d, 1H, J = 8.6, ph$_{ind}$-7*H*), 7.28−7.21 (m, 1H, ph$_{ind}$-4*H*), 6.96−6.88 (dd, 1H, J = 8.5, ph$_{ind}$-6*H*), 4.43−4.31 (t, 2H, J = 5.0, eth-1*H$_2$*), 3.65−3.42 (m, 4H, COC*H$_2$*, COCH$_2$C*H$_2$*), 3.10−2.88 (m, 4H, pip-2,6*H$_{eq}$*, eth-2*H$_2$*), 2.64−2.50 (m, 2H, pip-*H$_{2,6ax}$*), 2.03−1.30 (m, 6H, pip-3,5*H$_2$*, pip-4*H$_{eq/ax}$*); ^{13}C NMR (75 MHz, DMSO-d6) δ 204.7 (C*O*), 163.3 (ph$_{ind}$-5*C*), 158.5 (COCph$_{ind}$-7*C*), 130.7 (COCH$_2$CH$_2$*C*), 125.1 (ph$_{ind}$-7*C*), 116.1 (ph$_{ind}$-4*C*), 111.4 (ph$_{ind}$-6*C*), 66.1 (prop-1*C*), 54.9 (prop-2*C*), 52.9 (pip-2,6*C*), 36.4 (COC*H$_2$*), 25.8 (COCH$_2$*C*H$_2$), 22.6 (pip-3,5*C*), 21.5 (pip-4*C*); ESI-HRMS *m/z*: calcd for C$_{16}$H$_{21}$NO$_2$ (MH$^+$), 260.1651, found 260.1642. Anal. calc.: C, 64.97; H, 7.50; N, 4.74. Found: C,

64.52; H, 7.55; N, 4.88.

5.4.5. 5-(3-(Piperidin-1-yl)propoxy)-2,3-dihydro-1H-inden-1-one (1e)

Yield: 85%; m.p. 60.1 °C. ^{1}H NMR (300 MHz, DMSO-d6) δ 7.64–7.57 (d, 1H, J = 8.5, ph-7H), 7.18–7.11 (m, 1H, ph-4H), 7.05–6.96 (dd, 1H, J = 8.5, ph-6H), 4.24–4.11 (t, 2H, J = 6.4, prop-1H_2), 3.19–3.04 (t, 2H, J = 6.0, COCH_2), 2.76–2.61 (m, 2H, COCH$_2$CH_2), 2.51–2.40 (t, 2H, J = 7.3, prop-3H_2), 2.40–2.28 (m, 4H, pip-2,6$H_{eq/ax}$), 2.03–1.88 (q, 2H, J = 6.7, prop-2H_2), 1.65–1.51 (m, 4H, pip-3,5H_2), 1.50–1.38 (m, 2H, pip-4$H_{eq/ax}$); ^{13}C NMR (75 MHz, DMSO-d6) δ 204.6 (CO), 164.1 (ph-5C), 158.6 (COCph-7C), 130.4 (COCH$_2$CH$_2$C), 124.9 (ph-7C), 115.9 (ph-4C), 111.1 (ph-6C), 66.3 (prop-1C), 53.4 (prop-3C), 52.2 (pip-2,6C), 36.1 (COCH$_2$), 25.8 (COCH$_2$CH$_2$), 23.5 (prop-2C), 22.7 (pip-3,5C), 21.7 (pip-4C); ESI-HRMS m/z: calcd for C$_{17}$H$_{23}$NO$_2$ (MH$^+$), 274.1807, found 274.1800. Anal. calc.: C, 74.69; H, 8.48; N, 5.12. Found: C, 74,82; H, 8.58; N, 5.01.

5.5. Synthesis of 2-benzylidene-1-indanone derivatives 2a-c [31]

A water solution of sodium hydroxide (1.5 eq) was added at room temperature to an ethanol solution of the appropriately indanone (1 eq) and the commercially available benzaldehyde (1 eq). After 30 min, there was the formation of a precipitate. The solid was filtered off and extracted with ethyl acetate and 2 N NaOH solution. The crude material was dried over sodium sulfate and concentrated under vacuum. The resulting solid was elementary pure without further purification steps.

5.5.1. (E)-2-Benzylidene-6-(2-(piperidin-1-yl)ethoxy)-2,3-dihydro-1H-inden-1-one (2a)

Yield: 90%; m.p. 130.1 °C. ^{1}H NMR (300 MHz, DMSO-d6) δ 7.86–7.72 (m, 2H, ph^1-2,6H), 7.63–7.41 (m, 5H, ph^1-CH, ph$_{ind}$-5,7H, ph^1-3,5H), 7.37–7.20 (m, 2H, ph^1-4H, ph$_{ind}$-4H), 4.20–4.10 (t, 2H, J = 5.5, eth-1H_2), 4.04 (s, 2H, C=CCH_2), 2.76–2.62 (t, 2H, J = 5.2, eth-2H_2), 2.48–2.32 (m, 4H, pip-2,6$H_{eq/ax}$), 1.60–1.44 (m, 4H, pip-3,5H_2), 1.43–1.29 (m, 2H, pip-4$H_{eq/ax}$); ^{13}C NMR (75 MHz, DMSO-d6) δ 193.1 (CO), 158.4 (ph$_{ind}$-6C), 142.6 (COCph$_{ind}$-7C), 138.3 (ph^1-CH), 135.8 (C=CCH$_2$C), 134.8 (COC=C), 132.7 (ph^1-1C), 130.7 (ph^1-2,6C), 129.8 (ph^1-4C), 128.9 (ph^1-3,5C), 127.5 (ph$_{ind}$-7C), 123.9 (ph$_{ind}$-5C), 106.3 (ph$_{ind}$-4C), 66.0 (prop-1C), 57.2 (prop-2C), 54.3 (pip-2,6 C), 31.2 (C=CCH$_2$), 25.5 (pip-3,5C), 25.9 (pip-4C); ESI-HRMS m/z: calcd for C$_{23}$H$_{25}$NO$_2$ (MH$^+$), 348.1964, found 348.1964. Anal. calc.: C, 79.51; H, 7.25; N, 4.03. Found: C, 79.23; H, 7.17; N, 3.88.

5.5.2. (E)-2-Benzylidene-6-(3-(piperidin-1-yl)propoxy)-2,3-dihydro-1H-inden-1-one (2b)

Yield: 80%; m.p. 119.9 °C. ^{1}H NMR (300 MHz, DMSO-d6) δ 7.88–7.80 (m, 2H, ph^1-2,6H), 7.65–7.60 (d, 1H, J = 8.5, ph^1-CH), 7.59–7.47 (m, 4H, ph-5,7H, ph^1-3,5H), 7.38–7.31 (dd, 1H, J = 8.3, ph^1-4H), 7.30–7.27 (d, 1H, J = 2.4, ph$_{ind}$-4H), 4.18–4.10 (t, 2H, J = 6.4, prop-1H_2), 4.09 (s, 2H, C=CCH_2), 2.48–2.40 (t, 2H, J = 7.3, prop-3H_2), 2.40–2.30 (m, 4H, pip-2,6$H_{eq/ax}$), 1.99–1.87 (q, 2H, J = 6.8, prop-2H_2), 1.61–1.48 (m, 4H, pip-3,5H_2), 1.47–1.35 (m, 2H, pip-4$H_{eq/ax}$); ^{13}C NMR (75 MHz, DMSO-d6) δ 193.1 (CO), 158.5 (ph$_{ind}$-6C), 142. (COCph$_{ind}$-7C), 138.3 (ph^1-CH), 135.8 (C=CCH$_2$C), 134.8 (COC=C), 132.6 (ph^1-1C), 130.7 (ph^1-2,6C), 129.8 (ph^1-4C), 128.9 (ph^1-3,5C), 127.5 (ph$_{ind}$-7C), 123.8 (ph$_{ind}$-5C), 106.1 (ph$_{ind}$-4C), 66.4 (prop-1C), 55.0 (prop-3C), 54.1 (pip-2,6C), 31.1 (C=CCH$_2$), 26.1 (prop-2C), 25.5 (pip-3,5C), 24.1 (pip-4C); ESI-HRMS m/z: calcd for C$_{24}$H$_{27}$NO$_2$ (MH$^+$), 362.2120, found 362.2117. Anal. calc.: C, 79.74; H, 7.53; N, 3.87. Found: C, 79.41; H, 7.31; N, 3.78.

5.5.3. (E)-2-Benzylidene-5-(3-(piperidin-1-yl)propoxy)-2,3-dihydro-1H-inden-1-one (2c)

Yield: 86%; m.p. 110.7 °C. ^{1}H NMR (300 MHz, DMSO-d6) δ 7.80–7.74 (m, 2H, ph^1-2,6H), 7.74–7.63 (d, 1H, J = 8.5, ph^1-CH), 7.56–7.41 (m, 4H, ph$_{ind}$-4,7H, ph^1-3,5H), 7.19–7.14 (d, 1H, J = 1.9, ph^1-4H), 7.06–6.98 (dd, 1H, J = 8.5, ph$_{ind}$-6H), 4.18–4.11 (t, 2H, J = 6.4, prop-1H_2), 4.07 (s, 2H, C=CCH_2), 2.45–2.35 (t, 2H, J = 6.9, prop-3H_2), 2.35–2.22 (m, 4H, pip-2,6$H_{eq/ax}$), 1.98–1.82 (q, 2H, J = 6.7, prop-2H_2), 1.55–1.45 (m, 4H, pip-3,5H_2), 1.44–1.31 (m, 2H, pip-4$H_{eq/ax}$); ^{13}C NMR (75 MHz, DMSO-d6) δ 191.5 (CO), 164. (ph$_{ind}$-5C), 152.9 (COCph$_{ind}$-7C), 135.7 (ph^1-CH), 135.0 (C=CCH$_2$C), 131.4 (COC=C), 130.5 (ph^1-2,6C), 130.3 (ph^1-1C), 129.5 (ph^1-4C), 128.9 (ph^1-3,5C), 125.4 (ph$_{ind}$-7C), 115.7 (ph$_{ind}$-4C), 110.6 (ph$_{ind}$-6C), 66.6 (prop-1C), 54.9 (prop-3C), 54.7 (pip-2,6C), 31.9 (C=CCH$_2$), 26.1 (pip-3,5C), 25.6 (prop-2C), 24.1 (pip-4C); ESI-HRMS m/z: calcd for C$_{24}$H$_{27}$NO$_2$ (MH$^+$), 362.2120, found 362.2120. Anal. calc.: C, 79.74; H, 7.53; N, 3.87. Found: C, 79.81; H, 7.33; N, 3.57.

5.6. Synthesis of 2-benzylidene-1-indanone derivatives 3a-f [31]

A water solution of sodium hydroxide (1.5 eq) was added at room temperature to an ethanol solution of th appropriately commercially available indanones (1 eq) and 4-(3-(piperidin-1-yl)-propoxy)-benzaldehyde (1 eq). The work up was performed as described for compounds 2a-c.

5.6.1. (E)-2-(4-(3-(Piperidin-1-yl)propoxy)benzylidene)-2,3-dihydro-1H-inden-1-one (3a)

Yield 81%; m.p. 113.85 °C. ^{1}H NMR (300 MHz, DMSO-d6) δ 7.84–7.80 (d, 1H, J = 7.6, ph^1-CH), 7.61–7.45 (m, 5H, ph^1-2,3,5,6H, ph$_{ind}$-7H), 7.39–7.31 (m, 1H, ph$_{ind}$-6H), 6.94–6.86 (m, 2H, ph$_{ind}$-4,5H), 4.07–3.98 (t, 2H, J = 6.2, prop-1H_2), 3.94 (s, 2H, C=CCH_2), 2.64–2.51 (t, 2H, J = 7.7, prop-3H_2), 2.51–2.31 (m, 4H, pip-2,6$H_{eq/ax}$), 2.10–1.96 (q, 2H, J = 6.7, prop-2H_2), 1.69–1.54 (m, 4H, pip-3,5H_2), 1.49–1.33 (m, 2H, pip-4$H_{eq/ax}$); ^{13}C NMR (75 MHz, CDCl$_3$) δ 193.1 (CO), 158.5 (ph^1-4C), 142.5 (COCph$_{ind}$-7C), 138.4 (ph^1-CH), 135.8 (C=CCH$_2$C), 134.8 (ph^1-2,6C), 132.5 (COC=C), 130.7 (ph^1-1C), 129.7 (ph$_{ind}$-7C), 128.9 (ph$_{ind}$-4C), 127.5 (ph$_{ind}$-6C), 123.8 (ph$_{ind}$-5C), 106.1 (ph^1-3,5C), 66.3 (prop-1C), 55.0 (prop-3C), 54.1 (pip-2,6C), 31.2 (C=CCH$_2$), 26.2 (prop-2C), 25.6 (pip-3,5C), 24.1 (pip-4C); ESI-HRMS m/z: calcd for C$_{24}$H$_{27}$NO$_2$ (MH$^+$), 362.2120, found 362.2116. Anal. calc.: C, 79.74; H, 7.53; N, 3.87. Found: C, 79.72; H, 7.82; N, 3.58.

5.6.2. (E)-6-Methoxy-2-(4-(3-(piperidin-1-yl)propoxy) benzylidene)-2,3-dihydro-1H-inden-1-one (3b)

Yield: 86%; m.p. 118.7 °C. ^{1}H NMR (300 MHz, DMSO-d6) δ 7.79,7.69 (d, 2H, J = 8.6, ph^1-2,6H), 7.62–7.55 (d, 1H, J = 8.3, ph^1-CH), 7.52–7.46 (m, 1H, ph$_{ind}$-7H), 7.33–7.19 (d, 2H, J = 8.3, ph^1-3,5H), 7.11–7.0 (d, 2H, J = 8.5, ph$_{ind}$-4,5H), 4.17–4.03 (t, 2H, J = 6.3, prop-1H_2), 3.99 (s, 2H, C=CCH_2), 3.83 (s, 3H, OCH_3), 2.46–2.34 (t, 2H, J = 6.9, prop-3H_2), 2.34–2.18 (m, 4H, pip-2,6$H_{eq/ax}$), 1.97–1.79 (q, 2H, J = 6.6, prop-2H_2), 1.60–1.43 (m, 4H, pip-3,5H_2), 1.43–1.25 (m, 2H, pip-4$H_{eq/ax}$); ^{13}C NMR (75 MHz, DMSO-d6) δ 193.0 (CO), 160.0 (ph^1-4C), 159.1 (ph$_{ind}$-6C), 142.4 (COCph$_{ind}$-7C), 138.7 (ph^1-CH), 133.2 (C=CCH$_2$C), 132.7 (ph^1-2,6C), 132.7 (COC=C), 127.4 (ph^1-1C), 127.3 (ph$_{ind}$-7C), 123.1 (ph$_{ind}$-4C), 115.0 (ph^1-3,5C), 105.5 (ph$_{ind}$-5C), 66.2 (prop-1C), 55.5 (prop-3C), 55.0 (OCH$_3$), 54.1 (pip-2,6C), 31.2 (C=CCH$_2$), 26.2 (prop-2C), 25.6 (pip-3,5C), 24.1 (pip-4C); ESI-HRMS m/z: calcd for C$_{25}$H$_{29}$NO$_3$ (MH$^+$), 392.2226, found 392.2225. Anal. calc.: C, 76.70; H, 7.47; N, 3.58. Found: C, 76.57; H, 7.47; N, 3.39.

5.6.3. (E)-5-Methoxy-2-(4-(3-(piperidin-1-yl)propoxy) benzylidene)-2,3-dihydro-1H-inden-1-one (3c)

Yield: 81%; m.p. 116.6 °C. ^{1}H NMR (300 MHz, CDCl$_3$) δ 7.81−7.42 (d, 1H, J = 8.4, ph^1-CH), 7.58−7.47 (m, 3H, ph^1-2,6H, ph$_{ind}$-7H), 6.95−6.63 (m, 4H, ph$_{ind}$-4H, ph$_{ind}$-6H, ph^1-3,5H), 4.07−3.97 (t, 2H, J = 6.3, prop-1H_2), 3.88 (s, 2H, C=CCH_2), 3.83 (s, 3H, OCH_3), 2.56−2.47 (t, 2H, J = 7.2, prop-3H_2), 2.46−2.33 (m, 4H, pip-2,6$H_{eq/ax}$), 2.07−1.94 (q, 2H, J = 7.9, prop-2H_2), 1.68−1.52 (m, 4H, pip-3,5H_2), 1.47−1.34 (m, 2H, pip-4$H_{eq/ax}$); ^{13}C NMR (75 MHz, DMSO-d6) δ 191.5 (CO), 164.7 (ph^1-4C), 159.8 (ph$_{ind}$-5C), 152.7 (COCph$_{ind}$-7C), 133.0 (ph^1-CH), 132.4 (ph^1-2,6C), 131.5 (C=CCH_2C), 130.7 (COC=C), 127.5 (ph^1-1C), 125.2 (ph$_{ind}$-7C), 115.2 (ph$_{ind}$-4C), 114.7 (ph^1-3,5C), 110.1 (ph$_{ind}$-6C), 66.1(prop-1C), 55.7 (prop-3C), 55.0 (OCH$_3$), 54.1 (pip-2,6C), 31.9 (C=CCH$_2$), 26.2 (prop-2C), 25.6 (pip-3,5C), 24.1 (pip-4C); ESI-HRMS m/z: calcd for C$_{25}$H$_{29}$NO$_3$ (MH$^+$), 392.2226, found 392.2222. Anal. calc.: C, 76.70; H, 7.47; N, 3.58. Found: C, 76.52; H, 7.61; N, 3.49.

5.6.4. (E)-5-Fluoro-2-(4-(3-(piperidin-1-yl)propoxy)benzylidene)-2,3-dihydro-1H-inden-1-one (3d)

Yield: 80%; m.p. 123.2 °C. ^{1}H NMR (300 MHz, DMSO-d6) δ 7.88−7.79 (m, 1H, ph^1-CH), 7.58−7.50 (m, 3H, ph^1-2,6H, ph$_{ind}$-7H), 7.17−7.10 (dd, 1H, J = 8.4, ph$_{ind}$-4H), 7.09−6.99 (td, 1H, J = 8.9, ph$_{ind}$-6H), 6.96−6.86 (m, 2H, ph^1-3,5H), 4.10−3.96 (t, 2H, J = 6.3, prop-1H_2), 3.93 (s, 2H, C=CCH_2), 2.59−2.46 (t, 2H, J = 7.7, prop-3H_2), 2.46−2.28 (m, 4H, pip-2,6$H_{eq/ax}$), 2.08−1.91 (q, 2H, J = 7.1, prop-2H_2), 1.69−1.51 (m, 4H, pip-3,5H_2), 1.49−1.32 (m, 2H, pip-4$H_{eq/ax}$); ^{13}C NMR (75 MHz, DMSO-d6) δ 192.6 (CO), 165.9 (ph^1-4C), 160.4 (ph$_{ind}$-5C), 152.3 (COCph$_{ind}$-7C), 134.7(ph^1-CH), 133.9 (C=CCH$_2$C), 132.6 (ph^1-2,6C), 131.8 (COC=C), 127.8 (ph^1-1C), 126.5 (ph$_{ind}$-7C), 115.6 (ph$_{ind}$-4C), 115.1 (ph^1-3,5C), 112.8 (ph$_{ind}$-6C), 66.6 (prop-1C), 55.8 (prop-3C), 54.6 (pip-2,6C), 32.4 (C=CCH$_2$), 26.6 (prop-2C), 25.8 (pip-3,5C), 24.3 (pip-4C); ESI-HRMS m/z: calcd for C$_{24}$H$_{26}$FNO$_2$ (MH$^+$), 380.2026, found 380.2017. Anal. calc.: C, 75.96; H, 6.91; N, 3.69. Found: C, 75.90; H, 6.71; N, 3.67.

5.6.5. (E)-6-((4-Bromobenzyl)oxy)-2-(4-(3-(piperidin-1-yl) propoxy)benzylidene)-2,3-dihydro-1H-inden-1-one (3e)

Yield: 87%; m.p. 159.5 °C. ^{1}H NMR (300 MHz, DMSO-d6) δ 7.58−7.51 (m, 3H, ph^1-2,6H, ph^1-CH), 7.47−7.41 (m, 2H, ph^2-3,5H), 7.40−7.35 (d, 1H, J = 8.4, ph$_{ind}$-7H), 7.33−7.30 (d, 1H, J = 2.4, ph$_{ind}$-4H), 7.28−7.21 (m, 2H, ph^2-2,6H), 7.19−7.14 (dd, 1H, J = 8.3, ph$_{ind}$-6H), 6.93−6.85 (m, 2H, ph^1-3,5H), 4.99 (s, 2H, ph^2-CH_2O), 4.09−3.96 (t, 2H, J = 6.2, prop-1H_2), 3.86 (s, 2H, C=CCH_2), 2.65−2.50 (t, 2H, J = 7.7, prop-3H_2), 2.50−2.30 (m, 4H, pip-2,6$H_{eq/ax}$), 2.13−1.94 (q, 2H, J = 6.9, prop-2H_2), 1.73−1.55 (m, 4H, pip-3,5H_2), 1.49−1.33 (m, 2H, pip-4$H_{eq/ax}$); ^{13}C NMR (75 MHz, DMSO-d6) δ 194.1 (CO), 160.2 (ph^1-4C), 158.4 (ph$_{ind}$-6C), 142.7 (C=CCH$_2$C), 139.5 (ph^1-CH), 135.5 (ph^2-1C), 133.8 (COC=C), 133.1 (ph$_{ind}$-7C), 132.6 (ph^1-2,6C), 131.7 (ph^2-3,5C), 129.1 (ph^2-2,6C), 128.1 (COCph$_{ind}$-7C), 127.0 (ph^1-1C), 124.0 (ph$_{ind}$-5C), 122.0 (ph^2-4C), 114.9 (ph^1-3,5C), 104.94 (ph$_{ind}$-4C), 69.5 (prop-1C), 66.3 (ph^2-CH$_2$O), 55.7 (prop-3C), 54.1 (pip-2,6C), 31.8 (C=CCH$_2$), 26.1 (prop-2C), 25.3 (pip-3,5C), 23.9 (pip-4C); ESI-HRMS m/z: calcd for C$_{31}$H$_{32}$BrNO$_3$ (MH$^+$), 546.1644, found 546.1643. Anal. calc.: C, 68.13; H, 5.90; N, 2.56. Found: C, 67.84; H, 5.80; N, 2.36.

5.6.6. (E)-5-((4-Bromobenzyl)oxy)-2-(4-(3-(piperidin-1-yl) propoxy)benzylidene)-2,3-dihydro-1H-inden-1-one (3f)

Yield: 85%; m.p. 133.8 °C. ^{1}H NMR (300 MHz, CDCl$_3$) δ 7.81−7.74 (d, 1H, J = 8.6, ph^1-CH), 7.57−7.47 (m, 4H, ph^2- 3,5H, ph^1-2,6H), 7.44−7.38 (td, 1H, J = 1.3, ph$_{ind}$-7H), 7.33−7.26 (d, 1H, J = 1.1, ph$_{ind}$-4H), 7.23−7.16 (t, 1H, J = 7.6, ph$_{ind}$-6H), 6.98−6.85 (m, 4H, ph^2-2,6H, ph^1-3,5H), 5.05 (s, 2H, ph^2-CH_2O), 4.05−3.95 (t, 2H, J = 6.2, prop-1H_2), 3.87 (s, 2H, C=CCH_2), 2.52−2.42 (t, 2H, J = 7.7, prop-3H_2),

2.41−2.30 (m, 4H, pip-2,6$H_{eq/ax}$), 2.03−1.89 (q, 2H, J = 6.9, prop-2H_2), 1.62−1.51 (m, 4H, pip-3,5H_2), 1.43−1.34 (m, 2H, pip-4$H_{eq/ax}$); ^{13}C NMR (75 MHz, DMSO-d6) δ 191.5 (CO), 163.5 (ph^1-4C), 159.8 (ph$_{ind}$-5C), 152.6 (C=CCH$_2$C), 139.2 (ph^1-CH), 132.9 (ph^2-1C), 132.4 (ph^1-2,6C), 131.6 (ph^2-3C), 131.0 (ph^2-5C), 130.9 (ph^2-2C), 130.7 (ph^2-6C), 130.3 (COC=C), 127.4 (ph$_{ind}$-7C), 126.7 (COCph$_{ind}$-7C), 125.3 (ph^1-1C), 121.7 (ph$_{ind}$-4C), 115.7 (ph^2-4C), 114.9 (ph^1-3,5C), 111.2 (ph$_{ind}$-6C), 68.7 (prop-1C), 66.1 (ph^2-CH$_2$O), 55.0 (prop-3C), 54.0 (pip-2,6C), 31.9 (C=CCH$_2$), 26.2 (prop-2C), 25.5 (pip-3,5C), 24.1 (pip-4C); ESI-HRMS m/z: calcd for C$_{31}$H$_{32}$BrNO$_3$ (MH$^+$), 546.1644, found 546.1632. Anal. calc.: C, 68.13; H, 5.90; N, 2.56. Found: C, 68.06; H, 6.11; N, 2.48.

5.7. Human histamine H$_3$ radioligand depletion assay

Radioligand depletion assay for human histamine H$_3$ receptor were performed as described previously [46] with the following slight modifications. Briefly, HEK-293 cells stably expressing the human histamine H$_3$ receptor were washed and harvested in phosphate buffered saline (PBS) solution. They were centrifuged (3000 × g, 10 min, 4 °C) and homogenized with an ULTRA-TURRAX® T 25 digital (IKA, Germany) in ice-cold binding buffer (12.5 mM MgCl$_2$, 100 mM NaCl and 75 mM Tris/HCl, pH 7.4). The cell membrane homogenate was centrifuged two times at 20 000 × g for 20 min (4 °C). Crude membranes, using 20 μg per well in a final volume of 0.2 mL binding buffer, were incubated with [^{3}H]-N-α-methylhistamine (2 nM, 78.3 Ci mmol^{-1}) purchased from PerkinElmer (MA, USA) and various concentrations of test compounds. Assays were performed at least in duplicates with at least seven appropriate concentrations of test compounds. The incubation was performed for 90 min at room temperature by continuous shaking using 10 μM Pitolisant for determination of non-specific binding. Radioactivity was determined by liquid scintillation counting. Data were analyzed using GraphPad PRISM 6 using implemented non-linear regression fit "one-site competition", where K$_i$ values were calculated according to Cheng-Prusoff equation. Statistical analysis was performed on −log K$_i$ values. Mean values and confidence intervals (95%) were converted to micro- or nanomolar concentrations.

5.8. Monoamine oxidases inhibition assays

For assaying potential monoamine oxidase (MAO) A and B inhibition, compounds were included in one-point screening for both isoforms predominantly using a continuous spectrophotometric method as described previously [20] with the exception of **3d-f**, where a discontinuous fluorimetric assay was used (e.g. described in Ref. [47] with some modifications.

The spectrophotometric one-point measurements were performed in clear, flat-bottom 96 well plates (UV-Star®, No. 655801, greiner bio-one GmbH, Austria), measuring enzyme activity by spectrophotometrical observation of 4-hydroxyquinoline (λ_{max} = 316 nm) formation over time as described previously [20]. Initial velocities of substrate conversion (expressed as milli absorption units per minute) were plotted against log inhibitor concentrations and fitted using the implemented non-linear regression "log inhibitor vs. response (three parameters)". For one-point measurements data were calculated as percentage of control (product formation in absence of inhibitor) and expressed as mean ± standard deviation (%) performing at least two independent experiments, each in duplicates.

The IC$_{50}$ curves were determined in the discontinuous fluorimetric assay, allowing higher assay sensitivity as well as time and cost savings. MAO inhibition assays were carried out using human recombinant membrane-bound MAO A and MAO B purchased from

Sigma-Aldrich (MO, USA). Fluorimetric MAO assays were conducted in a total assay volume of 100 μL (max. 1% DMSO) using black, flat-bottom 96 well plates (No. 655076, greiner bio-one GmbH, Austria), while pipetting was partly automated using a EVO freedom pipetting robot (Tecan Trading AG, Switzerland). IC_{50} values were obtained by measuring enzyme activity (determined as MAO-dependent product formation) with inhibitor concentrations ranging from 0.001 μM to 100 μM in the presence of 2-fold K_M concentrations of kynuramine ($K_M = 30$ μM for MAO A and $K_M = 20$ μM for MAO B). Reactions were started by addition of MAO A (1.25 ng μL^{-1}, 900 units/mL) or MAO B (1.67 ng μL^{-1}, 375 units/mL).

Shift of IC_{50} values were also measured after preincubating inhibitors with enzyme (30 min, 37 °C), while reactions were started by addition of substrate. For optimal enzyme activity conditions, reactions were performed in pre-warmed potassium phosphate buffer (50 mM, pH = 7.4). After incubation (15 or 20 min, 37 °C with and without preincubation IC_{50} setup, respectively) reactions were stopped by manual addition of 35 μL sodium hydroxide (2 N) and enzyme activity was determined by detection of 4-hydroxyquinoline $(\lambda_{Ex} = 320 \pm 20$ nm, $\lambda_{Em} = 405 \pm 20$ nm) using an infinite M1000 Pro microplate reader (Tecan Trading AG, Switzerland). Data were analyzed using GraphPad PRISM 6. Enzyme activity, expressed as relative fluorescence units (RFU), were plotted against log inhibitor concentrations and fitted using the implemented non-linear regression "log inhibitor vs. response (three parameters)". Since few compounds do not reach the lower plateau in IC_{50} curves (e.g. poor soluble compounds **3e** and **3f**), the bottom for non-linear regression was set to zero. Data were obtained from at least three independent experiments, each performed at least in duplicates.

Reversibility of inhibition was assayed by preincubation of MAO B (10 ng μL^{-1}) and inhibitors (10× IC_{50}) for 0, 30 and 60 min at 37 °C prior to 50× dilution in potassium phosphate buffer to give a final concentration of 0.05xIC_{50} of inhibitor. Remained enzyme activity were measured fluorimetrically as described above under substrate saturating (10xK_M) conditions. Data were calculated as percentage of control (without inhibitor for each time point) and expressed as mean ± standard deviation (%) of at least two independent experiments, each performed in duplicates (global fit).

5.9. Michael acceptor capacity determinations

The Michael acceptor capacity of DTL **3d** were evaluated by appearance of probably formed adducts between **3d** and acetylcysteine under physiological conditions (Supporting Information, Figure 37). Accordingly, an aqueous solution containing **3d** (4 μg mL^{-1}) and an excess of acetylcysteine (20 mg mL^{-1}) was prepared. The pH was adjusted to 7.2 using diluted (0.01 M) sodium hydroxide solution. Electron Spray Ionization (ESI) mass spectrometry (MS) was used to observed possible adducts formed at several time points up to three days after mixture. To allow protonation in ESI-Spectra, the samples were diluted with the same amount of water containing 0.1% of formic acid. All the measurements were performed in ESI-MS (+) mode.

Author contributions

AA performed organic synthesis and analysis. SH performed human histamine H_3R radioligand depletion studies and MAO enzyme inhibition studies. AZ, AA and SH performed Michael acceptor capacity studies. AA and SH wrote the main manuscript. HS contributed to compound and experimental design and supervised the project. JMC contributed to experimental design. All authors approved and reviewed the manuscript.

Conflicts of interest

The authors do not declare any conflict of interest.

Appendix A. Supplementary data

Supplementary data related to this article can be found at https://doi.org/10.1016/j.ejmech.2018.02.015.

References

[1] A. Anighoro, J. Bajorath, G. Rastelli, Polypharmacology: challenges and opportunities in drug discovery, J. Med. Chem. 57 (2014) 7874—7887.
[2] M.A. Khanfar, A. Affini, K. Lutsenko, K. Nikolic, S. Butini, H. Stark, Multiple targeting approaches on histamine H3 receptor antagonists, Front. Neurosci. 10 (2016) 1—17.
[3] S. Butini, K. Nikolic, S. Kassel, H. Brückmann, S. Filipic, D. Agbaba, S. Gemma, S. Brogi, M. Brindisi, G. Campiani, H. Stark, Polypharmacology of dopamine receptor ligands, Prog. Neurobiol. 142 (2016) 68—103.
[4] R. Leon, A.G. Garcia, J. Marco-Contelles, Recent advances in the multitarget-directed ligands approach for the treatment of Alzheimer's disease, Med. Res. Rev. 33 (2011) 139—189.
[5] R.R. Ramsay, Monoamine oxidases: the biochemistry of the proteins as targets in medicinal chemistry and drug discovery, Curr. Top. Med. Chem. 12 (2012) 2189—2209.
[6] R.R. Ramsay, Molecular aspects of monoamine oxidase B, Prog. Neuro-Psychopharmacol. Biol. Psychiatry 69 (2016) 81—89.
[7] X. Wang, C. Han, Y. Xu, K. Wu, S. Chen, M. Hu, L. Wang, Y. Ye, Synthesis and evaluation of phenylxanthine derivatives as potential dual A2AR antagonists/MAO-B inhibitors for Parkinson's disease, Molecules 22 (2017) 1010.
[8] M. Berlin, C.W. Boyce, M. de Lera Ruiz, Histamine H3 receptor as a drug discovery target, J. Med. Chem. 54 (2011) 26—53.
[9] K. Sander, T. Kottke, H. Stark, Histamine H3 receptor antagonists go to clinics, Biol. Pharm. Bull. 31 (2008) 2163—2181.
[10] J.C. Schwartz, The histamine H3 receptor: from discovery to clinical trials with pitolisant, Br. J. Pharmacol. 163 (2011) 713—721.
[11] G. Nieto-Alamilla, R. Márquez-Gómez, A.-M. García-Gálvez, G.-E. Morales-Figueroa, J.-A. Arias-Montaño, The histamine H3 receptor: structure, pharmacology and function, Mol. Pharmacol. 3964 (2016) 649—673.
[12] W. Hu, Z. Chen, The roles of histamine and its receptor ligands in central nervous system disorders: an update, Pharmacol. Ther. 175 (2017) 116—132.
[13] C. Ferrada, S. Ferré, V. Casadó, A. Cortés, Z. Justinova, C. Barnes, E.I. Canela, S.R. Goldberg, R. Leurs, C. Lluis, R. Franco, Interactions between histamine H3 and dopamine D2 receptors and the implications for striatal function, Neuropharmacology 55 (2008) 190—197.
[14] D. Masini, C. Lopes-Aguiar, A. Bonito-Oliva, D. Papadia, R. Andersson, A. Fisahn, G. Fisone, The histamine H3 receptor antagonist thioperamide rescues circadian rhythm and memory function in experimental parkinsonism, *Transl.* Psychiatry 7 (2017) e1088.
[15] R. Parmentier, C. Anaclet, C. Guhennec, E. Brousseau, D. Bricout, T. Giboulot, D. Bozyczko-Coyne, K. Spiegel, H. Ohtsu, M. Williams, J.S. Lin, The brain H3-receptor as a novel therapeutic target for vigilance and sleep-wake disorders, Biochem. Pharmacol. 73 (2007) 1157—1171.
[16] J. Lin, O.A. Sergeeva, H.L. Haas, Histamine H3 receptors and sleep-wake regulation, J. Pharmacol. Exp. Therapeut. 336 (2011) 17—23.
[17] S. Carradori, R. Silvestri, New frontiers in selective human MAO-B inhibitors, J. Med. Chem. 58 (2015) 6717—6732.
[18] S. Mostert, A. Petzer, J.P. Petzer, Indanones as high-potency reversible inhibitors of monoamine oxidase, ChemMedChem 10 (2015) 862—873.
[19] M.S. Nel, A. Petzer, J. Petzer, L.J. Legobabe, 2-Benzylidene-1-indanone derivatives as inhibitors of monoamine oxidase, Bioorg. Med. Chem. Lett 26 (2016) 4599—4605.
[20] S. Hagenow, A. Stasiak, R.R. Ramsay, H. Stark, Ciproxifan, a histamine H3 receptor antagonist, reversibly inhibits monoamine oxidase A and B, Sci. Rep. 7 (2017) 40541.
[21] A. Olejarz, U. Cichon, D. Lazewska, T. Karcz, H. Stark, K. Kiec-Kononowicz, Monoamine oxidase B inhibition activity of novel analogs and derivatives of 1-[3-(4-tert-butyl-phenoxy)propyl] piperidine, in: VII Meet. Paul Ehrlich Euro-PhD Network, Book of Abstracts, 2017, p. 26.
[22] G. Meier, J. Apelt, U. Reichert, S. Grassmann, X. Ligneau, S. Elz, F. Leurquin, C.R. Ganellin, J.C. Schwartz, W. Schunack, H. Stark, Influence of imidazole replacement in different structural classes of histamine H(3)-receptor antagonists, Eur. J. Pharmaceut. Sci. 13 (2001) 249—259.
[23] K. Wingen, H. Stark, Scaffold variations in amine warhead of histamine H3

receptor antagonists, Drug Discov, Today Technol 10 (2013) e483–e489.

[24] T. Mikó, X. Ligneau, H.H. Pertz, J.-M. Arrang, C.R. Ganellin, J.-C. Schwartz, W. Schunack, H. Stark, Structural variations of 1-(4-(phenoxymethyl)benzyl) piperidines as nonimidazole histamine H3 receptor antagonists, Bioorg. Med. Chem. 12 (2004) 2727–2736.

[25] S.A. Weissman, D. Zewge, Recent advances in ether dealkylation, Tetrahedron 61 (2005) 7833–7863.

[26] M. Tomasch, J.S. Schwed, L. Weizel, H. Stark, Novel chalcone-based fluorescent human histamine h(3) receptor ligands as pharmacological tools, Front. Syst. Neurosci. 6 (2012) 1–16.

[27] H. Stark, Convenient procedures for synthesis of ciproxifan, a histamine H3-receptor antagonist, Arch. Pharm. Pharm. Med. Chem. 333 (2000) 315–316.

[28] K. Sander, Y. Von Coburg, J.-C Camelin, X. Ligneau, O. Rau, M. Schubert-Zsi-lavecz, J. Schwartz, H. Stark, Acidic elements in histamine H3 receptor an-tagonists, Bioorg. Med. Chem. Lett 20 (2010) 1581–1584.

[29] B. Sadek, J.S. Schwed, D. Subramanian, L. Weizel, M. Walter, A. Adem, H. Stark, Non-imidazole histamine H3 receptor ligands incorporating antiepileptic moieties, Eur. J. Med. Chem. 77 (2014) 269–279.

[30] A. Williamson, About the theory of the formation of ethers, Ann. Chem. 77 (1851) 37–49.

[31] N. Morales-Camilo, C.O. Salas, C. Sanhueza, C. Espinosa-Bustos, S. Sepúlveda-Boza, M. Reyes-Parada, F. Gonzalez-Nilo, M. Caroli-Rezende, A. Fierro, Syn-thesis, biological evaluation, and molecular simulation of chalcones and aurones as selective MAO-B inhibitors, Chem. Biol. Drug Des. 85 (2015) 685–695.

[32] L. Huang, H. Miao, Y. Sun, F. Meng, X. Li, Discovery of indanone derivatives as multi-target-directed ligands against Alzheimer's disease, Eur. J. Med. Chem. 87 (2014) 429–439.

[33] A.L. Hopkins, G.M. Keserü, P.D. Leeson, D.C. Rees, C.H. Reynolds, The role of ligand efficiency metrics in drug discovery, Nat. Rev. Drug Discov. 13 (2014) 105–121.

[34] N. Desideri, A. Bolasco, R. Fioravanti, L. Proietti Monaco, F. Orallo, M. Yáñez, F. Ortuso, S. Alcaro, Homoisoflavonoids: natural scaffolds with potent and selective monoamine oxidase-B inhibition properties, J. Med. Chem. 54 (2011) 2155–2164.

[35] N. Desideri, L. Proietti Monaco, R. Fioravanti, M. Biava, M. Yanez, S. Alcaro, F. Ortuso, (E)-3-Heteroarylidenechroman-4-ones as potent and selective monoamine oxidase-B inhibitors, Eur. J. Med. Chem. 117 (2016) 292–300.

[36] J.P.M. Finberg, Update on the pharmacology of selective inhibitors of MAO-A and MAO-B: focus on modulation of CNS monoamine neurotransmitter

[37] D.S. Johnson, E. Weerapana, B.F. Cravatt, Strategies for discovering and derisking covalent, irreversible enzyme inhibitors, Future Med. Chem. 2 (2010) 949–964.

[38] Ó.M. Bautista-Aguilera, S. Hagenow, A. Palomino-Antolin, V. Farré-Alins, L. Ismaili, P.-L. Joffrin, M.L. Jimeno, O. Soukup, J. Janočková, L. Kalinowsky, E. Proschak, I. Iriepa, I. Moraleda, J.S. Schwed, A. Romero Martínez, F. López-Muñoz, M. Chioua, J. Egea, R.R. Ramsay, J. Marco-Contelles, H. Stark, Multi-target-Directed ligands combining cholinesterase and monoamine oxidase inhibition with histamine H3R antagonism for neurodegenerative diseases, Angew. Chem. Int. Ed. 56 (2017) 12765–12769.

[39] G. Petroianu, K. Arafat, B.C. Sasse, H. Stark, Multiple enzyme inhibitions by histamine H3 receptor antagonists as potential procognitive agents, Phar-mazie 61 (2006) 179–182.

[40] L. Huang, C. Lu, Y. Sun, F. Mao, Z. Luo, T. Su, H. Jiang, W. Shan, X. Li, Multi-target-directed benzylideneindanone derivatives: anti-ß-amyloid (Aß) ag-gregation, antioxidant, metal chelation, and monoamine oxidase B (MAO-B) inhibition properties against Alzheimer's disease, J. Med. Chem. 55 (2012) 8483–8492.

[41] A. Autelitano, A. Minassi, A. Pagani, O. Taglialatela-Scafati, G. Appendino, The reaction of cinnamaldehyde and cinnam(o)yl derivatives with thiols, Acta Pharm. Sin. B. 7 (2017) 523–526.

[42] C. Avonto, O. Taglialatela-Scafati, F. Pollastro, A. Minassi, V. Di-Marzo, L. De-Petrocellis, G. Appendino, An NMR spectroscopic method to identify and classify thiol-trapping agents: revival of michael acceptors for drug discovery? Angew. Chem. Int. Ed. 50 (2011) 467–471.

[43] S. Searles, V.P. Gregory, The reaction of trimethylene oxide with amines, J. Am. Chem. Soc. 76 (1954) 2789–2790.

[44] G. Doherty, T. Burnett, Synthesis of aminoalkylisothiuronium salts and their conversion to mercaptoalkylguanidines, J. Am. Chem. Soc. 3878 (1957) 5–9.

[45] L.W.L. Woo, N.M. Howarth, A. Purohit, H.A.M. Hejaz, M.J. Reed, B.V.L. Potter, Steroidal and nonsteroidal sulfamates as potent inhibitors of steroid sulfatase, J. Med. Chem. 41 (1998) 1068–1083.

[46] T. Kottke, K. Sander, L. Weizel, E.H. Schneider, R. Seifert, H. Stark, Receptor-specific functional efficacies of alkyl imidazoles as dual histamine H3/H4 re-ceptor ligands, Eur. J. Pharmacol. 654 (2011) 200–208.

[47] L. Meiring, J.P. Petzer, A. Petzer, Inhibition of monoamine oxidase by 3,4-dihydro-2(1H)-quinolinone derivatives, Bioorg. Med. Chem. Lett 23 (2013) 5498–5502.

NOVEL INDANONE DERIVATIVES AS MAO B/H₃R DUAL-TARGETING LIGANDS FOR TREATMENT OF PARKINSON´S DISEASES

Anna Affini[a1], Stefanie Hagenow[a1], Aleksandra Zivkovic[a], Jose Marco-Contelles[b], Holger Stark[a*]

[a] Heinrich Heine University Duesseldorf, Institute of Pharmaceutical and Medicinal Chemistry, Universitaetsstr. 1, 40225 Duesseldorf, Germany;

[b] Laboratory of Medicinal Chemistry (IQOG, CSIC), C/ Juan de la Cierva 3, 28006-Madrid, Spain

* Corresponding author: e-mail: stark@hhu.de, Fax +49 211 8113359, phone: +49 211 8110478.

1a
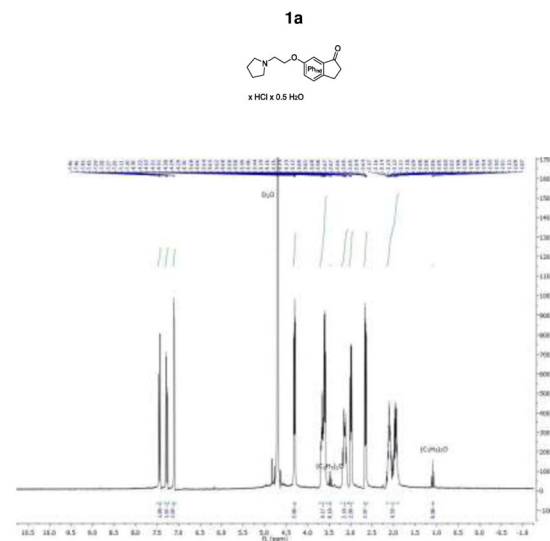
Figure 1. ¹H-NMR (300 MHz, D₂O) of compound **1a**
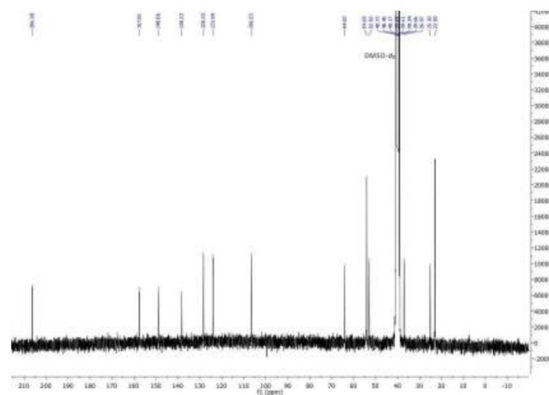
Figure 2. ^{13}C-NMR (75 MHz, DMSO-d_6) of compound **1a**
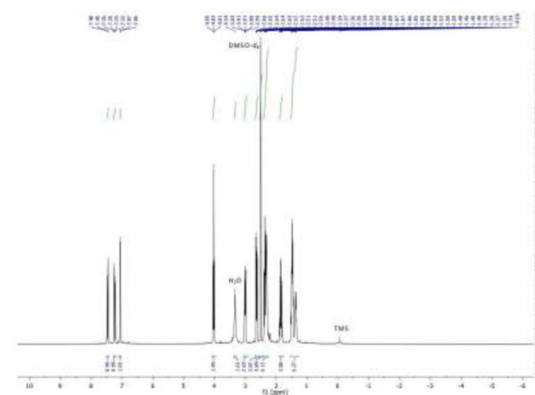
Figure 4. ^{1}H-NMR (300 MHz, DMSO-d_6) of compound **1b**
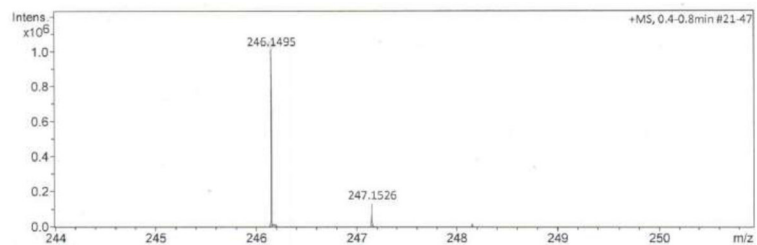
Figure 3. ESI-HRMS of compound **1a**

1b
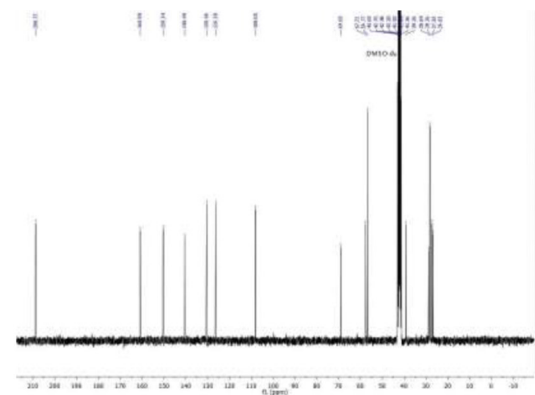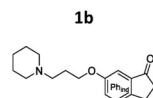
Figure 5. ^{13}C-NMR (75 MHz, DMSO-d_6) of compound **1b**
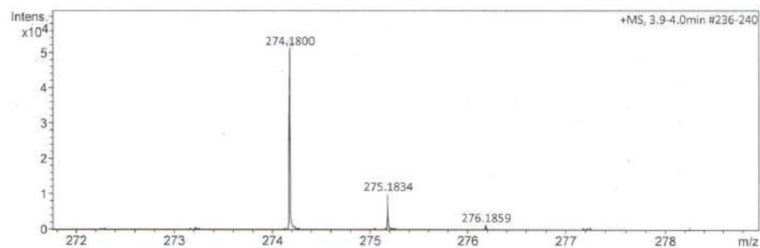
Figure 6. ESI-HRMS of compound 1b

1c

x HCl x 0.25H₂O
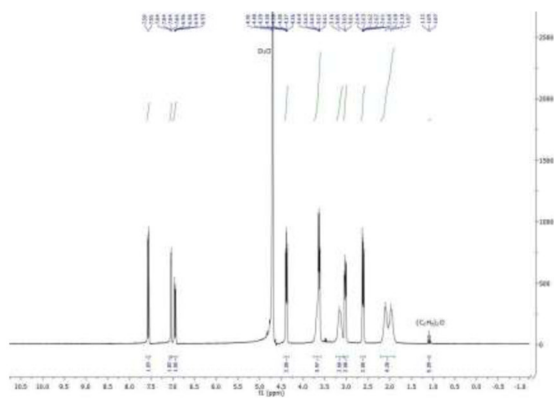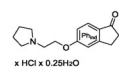
Figure 7. ¹H-NMR (300 MHz, D₂O) of compound 1c
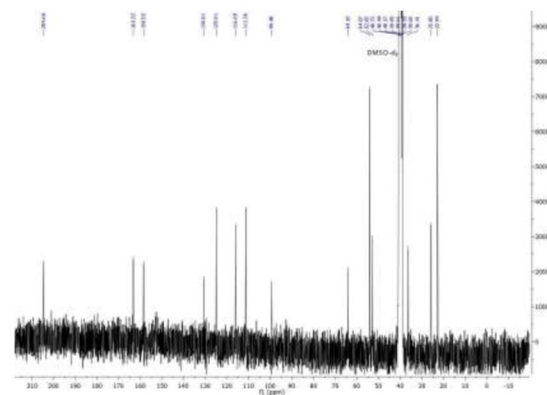
Figure 8. ¹³C-NMR (75 MHz, DMSO-d_6) of compound 1c
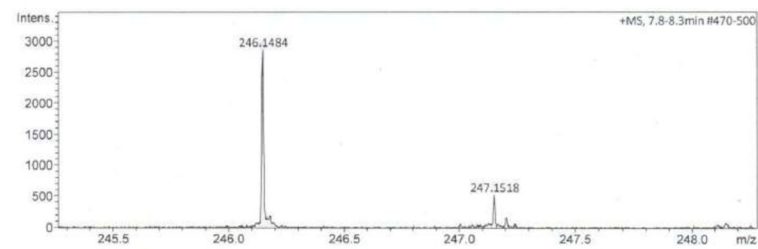
Figure 9. ESI-HRMS of compound 1c

1d

x HCl

:

5

6
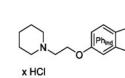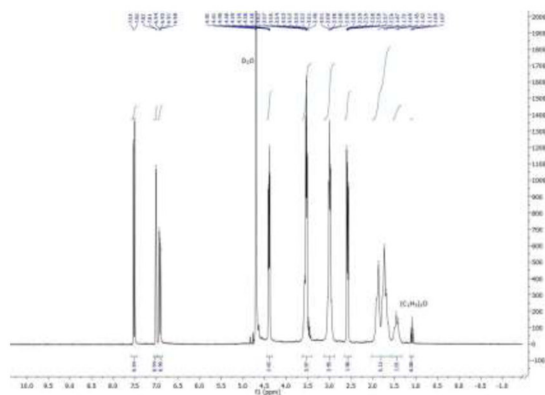
Figure 10. ¹H-NMR (300 MHz, D₂O) of compound **1d**
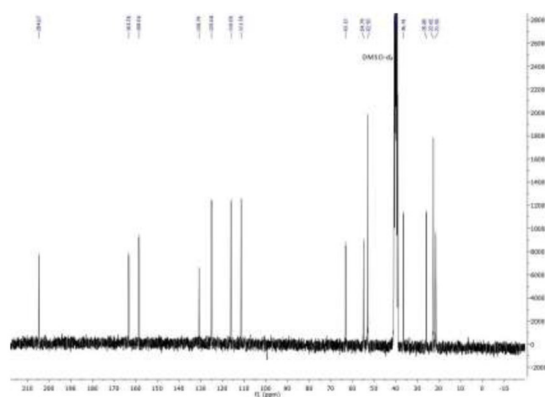
Figure 11. ¹³C-NMR (75 MHz, DMSO-d_6) of compound **1d**

Figure 12. ESI-HRMS of compound **1d**

1e

x HCl x 0.5H₂O
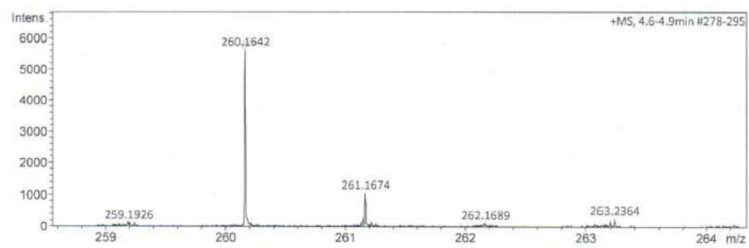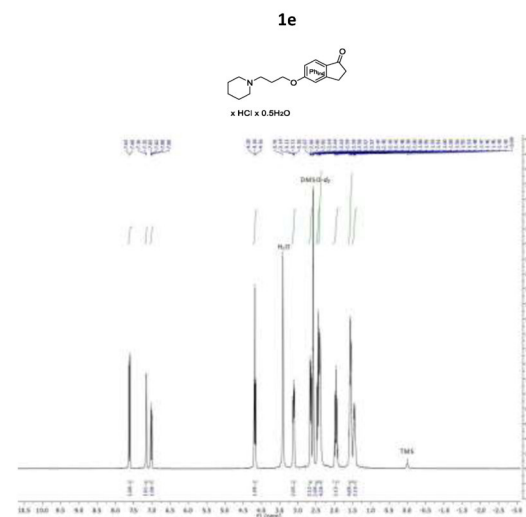
Figure 13. ¹H-NMR (300 MHz, DMSO-d_6) of compound **1e**
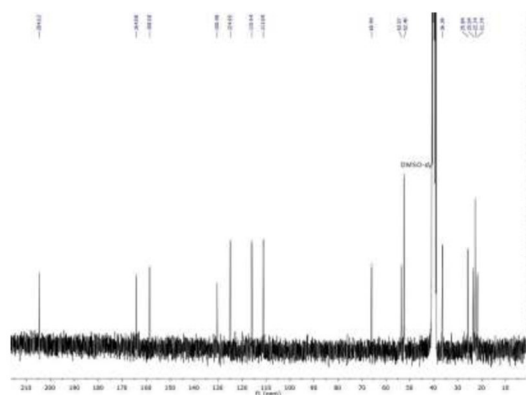
Figure 14. ¹³C-NMR (75 MHz, DMSO-d_6) of compound **1e**
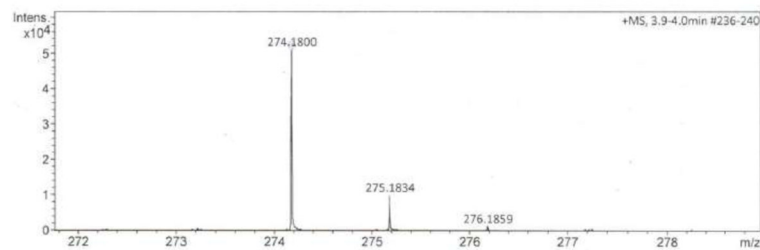
Figure 15. ESI-HRMS of compound **1e**

2a

Figure 16. ¹H-NMR (300 MHz, DMSO-d_6) of compound **2a**

Figure 17. ¹³C-NMR (75 MHz, DMSO-d_6) of compound **2a**
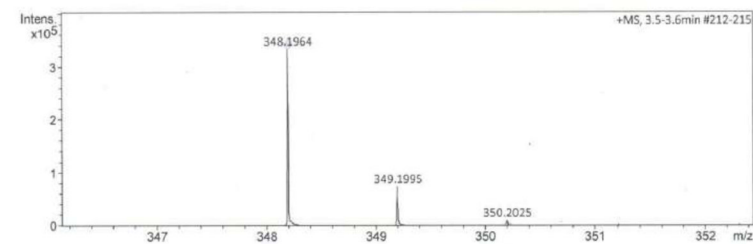
Figure 18. ESI-HRMS of compound **2a**

2b

Figure 19. ¹H-NMR (300 MHz, DMSO-d_6) of compound **2b**

Figure 20. ¹³C-NMR (75 MHz, DMSO-d_6) of compound **2b**

Figure 21. ESI-HRMS of compound **2b**

2c

Figure 22. ¹H-NMR (300 MHz, DMSO-d_6) of compound **2c**
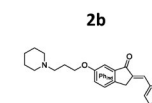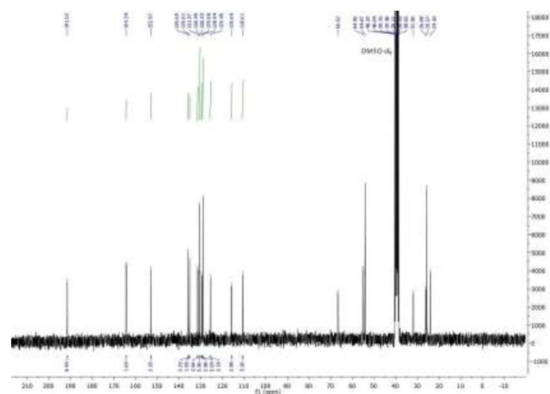
Figure 23. ^{13}C-NMR (75 MHz, DMSO-d_6) of compound **2c**

Figure 24. ESI-HRMS of compound **2c**

3a

Figure 25. ^{1}H-NMR (300 MHz, CDCl$_3$) of compound **3a**
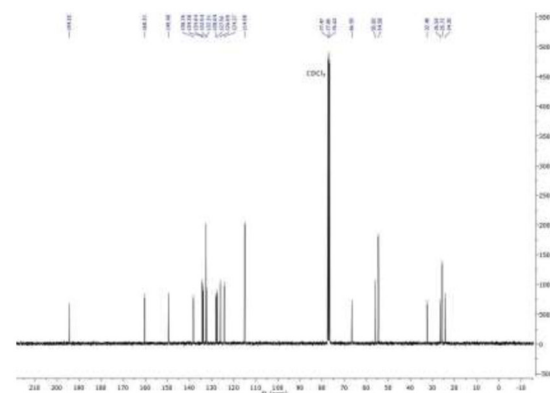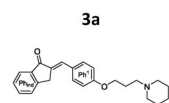
Figure 26. ^{13}C-NMR (75 MHz, CDCl$_3$) of compound **3a**
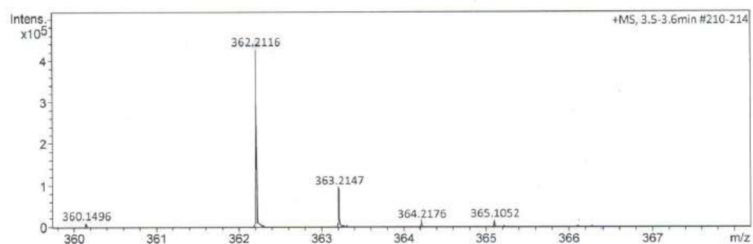
Figure 27. ESI-HRMS of compound **3a**

3b
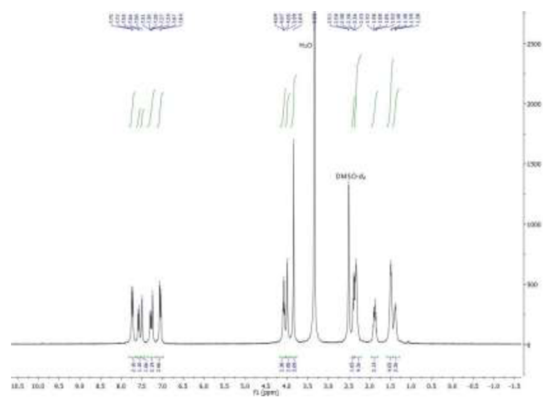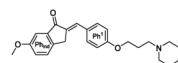
Figure 28. ¹H-NMR (300 MHz, DMSO-d_6) of compound **3b**
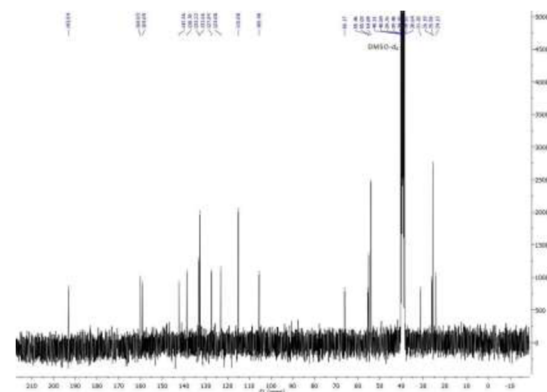
Figure 29. ¹³C-NMR (75 MHz, DMSO-d_6) of compound **3b**
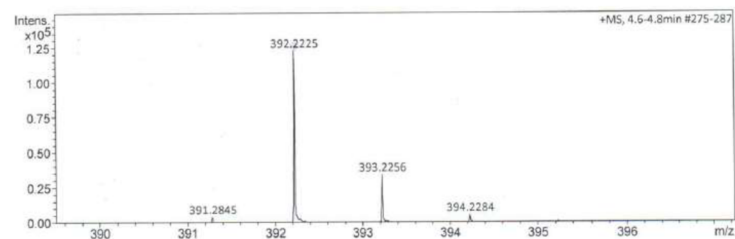
Figure 30. ESI-HRMS of compound **3b**

3c
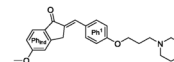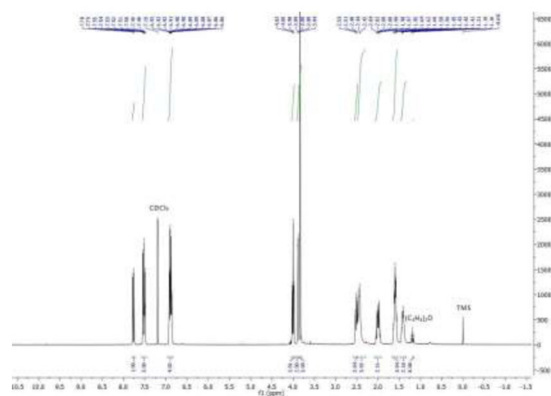
Figure 31. ^{1}H-NMR (300 MHz, CDCl$_3$) of compound **3c**
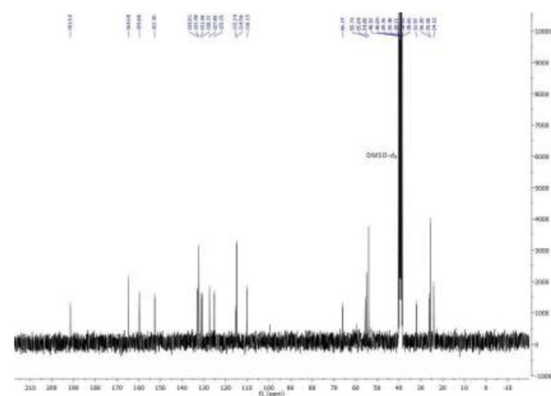
Figure 32. ^{13}C-NMR (75 MHz, DMSO-d_6) of compound **3c**
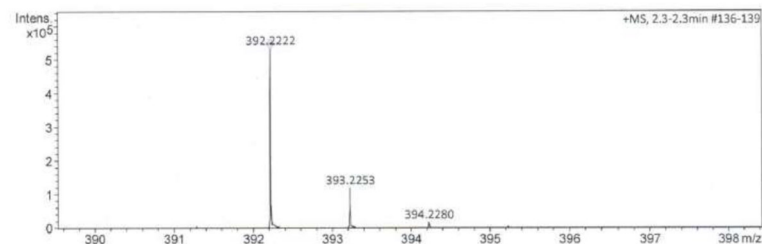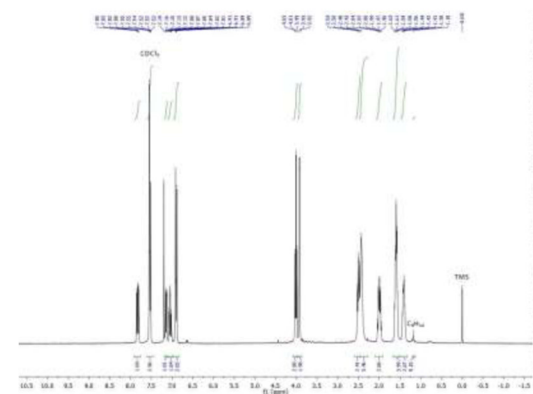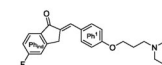

Figure 33. ESI-HRMS of compound **3c**

3d

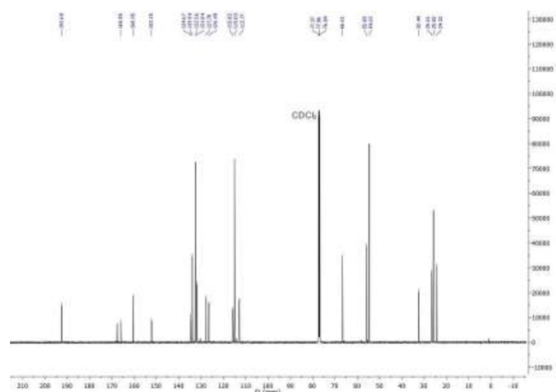**Figure 34.** ^{1}H-NMR (300 MHz, CDCl$_3$) of compound **3d**

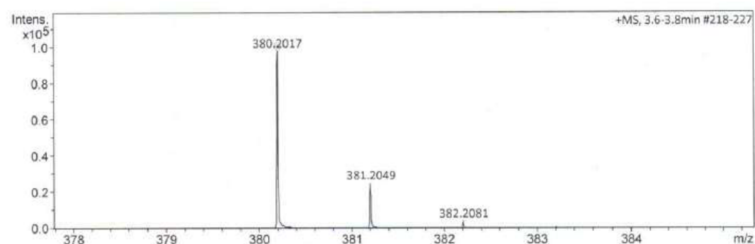**Figure 35.** ^{13}C-NMR (75 MHz, CDCl$_3$) of compound **3d**

Figure 36. ESI-HRMS of compound **3d**

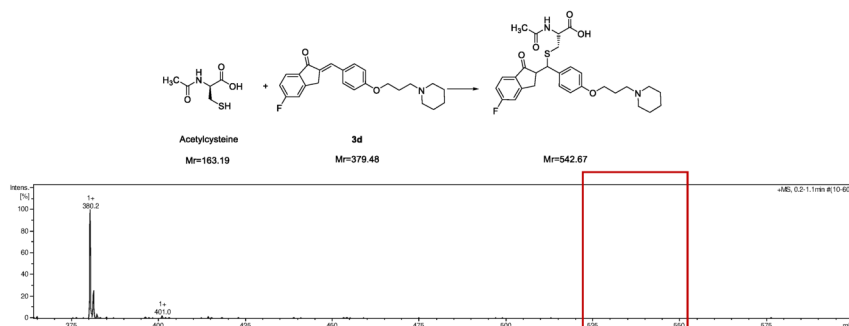**Figure 37.** Suggested adduct formation and exemplified ESI-MS of a mixture of compound **3d** (4 μg mL^{-1}) and acetylcysteine (20 mg mL^{-1}) showing a dominant signal at 380.5 belonging to **3d**, but no signal for the suggested adduct (red box).
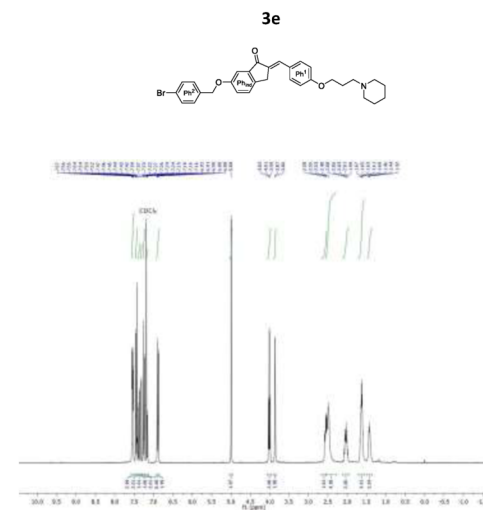
3e

Figure 38. ^{1}H-NMR (300 MHz, CDCl$_3$) of compound **3e**
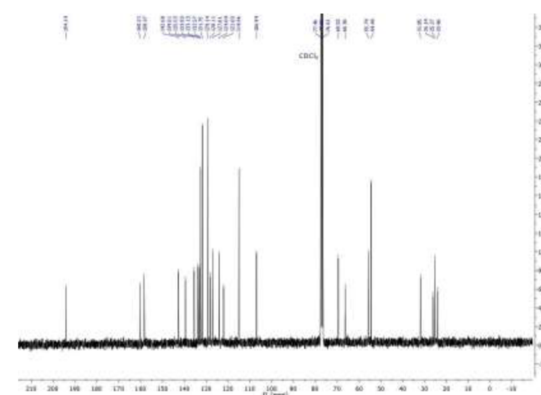

Figure 39. ^{13}C-NMR (75 MHz, CDCl$_3$) of compound **3e**

Figure 40. ESI-HRMS of compound **3e**

3f

Figure 41. ^{1}H-NMR (300 MHz, CDCl$_3$) of compound **3f**

Figure 42. ^{13}C-NMR (75 MHz, DMSO-d_6) of compound **3f**
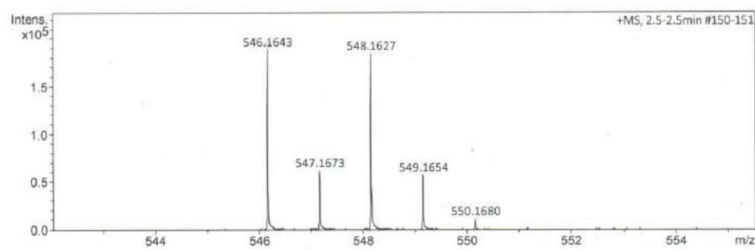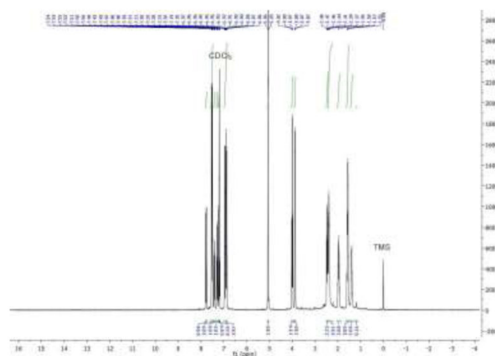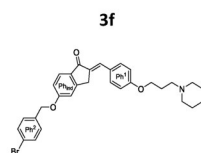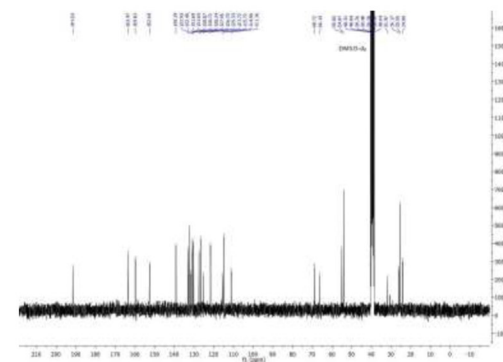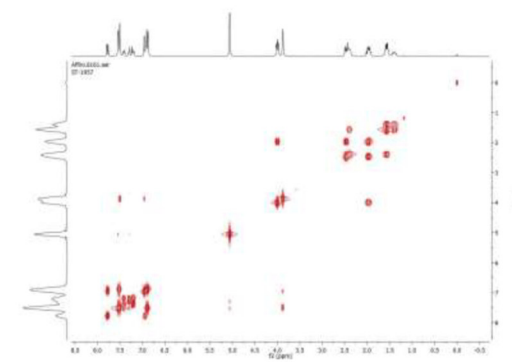
Figure 43. 2D ^{1}H-NMR: NOESY spectra of compound **3f**
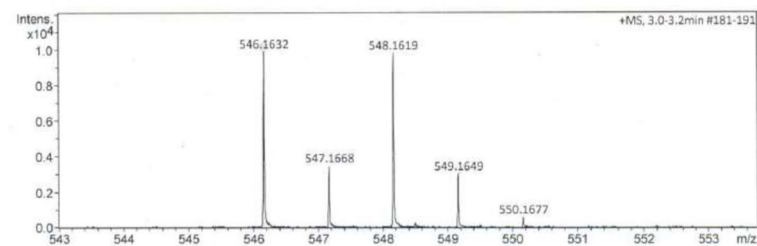
Figure 44. ESI-HRMS of compound **3f**

Table 1. Drug-likeness of synthetized dual MAO B/H₃R ligands **3d-f** and reference compounds.

COMPOUND	clogP[a]	MAO B						hH₃R		
		LE[b]		LELP[c]		LipE[d]		LE[b]	LELP[c]	LipE[d]
3d	6.2	0.28	0.31*	17.16	15.65*	0.90	1.45*	0.42	11.32	3.84
3e	7.1	0.22	0.25*	31.44	27.66*	-1.16	-0.36*	0.28	24.48	0.49
3f	7.1	0.25	0.25*	27.98	27.88*	-0.44	-0.41*	0.31	22.41	1.18
UCL2190	3.77	0.35		10.65			1.64*	0.52	7.24	4.19
L-Deprenyl	2.75	0.72	0.82*	3.80	3.33*	4.63	5.66*			
Safinamide	2.04	0.45	0.48*	4.49	4.26*	5.23	5.64*			

[a] Calculation with Marvin Sketch; [b] MAO B: LE = pIC$_{50}$/HA (heavy atoms), hH₃R: LE = pK$_i$/HA; [c] LELP = clogP/LE; [d] LipE = pIC$_{50}$-cloP, hH₃R: LipE = pK$_i$-clogP, * Values measured after 30 min pre-incubation at 37 °C.

3.3 Publication 3

Multitarget-directed ligands combining cholinesterase and monoamine oxidase inhibition with histamine H₃R antagonism for neurodegenerative diseases

Bautista-Aguilera, O. M.[1*], Hagenow, S.[2*], Palomino-Antolin, A.[3*], Farre-Alins, V.[3*], Ismaili, L.[4], Joffrin, P.-J.[5], Jimeno, M.[1], Soukup, O.[6], Janockova, J.[6], Kalinowsky, L.[7], Proschak, E.[7], Iriepa, I.[8], Moraleda, I.[8], Schwed, J. S.[2], Romero Martinez, A.[9], Lopez-Munoz, F.[10], Chioua, J.[1], Egea, J.[3], Ramsay, R. R.[5], Marco-Contelles, J.[1], Stark, H.[2]

[1] Laboratory of Medicinal Chemistry (IQOG, CSIC), Madrid, Spain. [2] Institute of Pharmaceutical and Medicinal Chemistry, Heinrich Heine University Duesseldorf, Germany. [3] Instituto de Investigación Sanitaria, Universitario de la Princesa, Madrid, Spain. [4] Neurosciences Intégratives et Cliniques EA 481, Université Bourgogne Franche-Comté, Besancon, France. [5] Biomedical Sciences Research Complex, University of St Andrews, UK. [6] Biomedical Research Center, University Hospital Hradec Kralove, Czech Republic. [7] Institute of Pharmaceutical and Medicinal Chemistry, Goethe University Frankfurt, Germany. [8] Department of Organic Chemistry, University of Alcalá, Spain. [9] Departamento de Toxicologia Farmacologia Facultad de Veterinaria, Madrid, Spain. [10] Faculty of Health Sciences, Camilo José Cela University, Madrid, Spain. *These authors have contributed equally to this work.

Abstract

The therapy of complex neurodegenerative diseases requires the development of multi-target-directed drugs (MTDs). Novel indole derivatives with inhibitory activity towards acetyl-/butyrylcholinesterases and monoamine oxidases A/B as well as the histamine H₃ receptor (H₃R) were obtained by optimization of the neuroprotectant ASS234 by incorporating generally accepted H₃R pharmacophore motifs. These small-molecule hits demonstrated balanced activities at the targets, mostly in the nanomolar concentration range. Additional in vitro studies showed antioxidative, neuroprotective effects as well as the ability to penetrate the blood-brain barrier. With this promising in vitro profile, contilisant (at 1 mg kg⁻¹ i.p.) also significantly improved lipopolysaccharide-induced cognitive deficits.

GDCh

Communications

Angewandte
International Edition Chemie

Medicinal Chemistry Hot Paper

Multitarget-Directed Ligands Combining Cholinesterase and Mono-amine Oxidase Inhibition with Histamine H₃R Antagonism for Neurodegenerative Diseases

Óscar M. Bautista-Aguilera⁺, Stefanie Hagenow⁺, Alejandra Palomino-Antolin⁺, Víctor Farré-Alins⁺, Lhassane Ismaili, Pierre-Louis Joffrin, María L. Jimeno, Ondřej Soukup, Jana Janočková, Lena Kalinowsky, Ewgenij Proschak, Isabel Iriepa, Ignacio Moraleda, Johannes S. Schwed, Alejandro Romero Martínez, Francisco López-Muñoz, Mourad Chioua, Javier Egea,* Rona R. Ramsay, José Marco-Contelles,* and Holger Stark*

Abstract: *The therapy of complex neurodegenerative diseases requires the development of multitarget-directed drugs (MTDs). Novel indole derivatives with inhibitory activity towards acetyl/butyrylcholinesterases and monoamine oxidases A/B as well as the histamine H₃ receptor (H3R) were obtained by optimization of the neuroprotectant ASS234 by incorporating generally accepted H3R pharmacophore motifs. These small-molecule hits demonstrated balanced activities at the targets, mostly in the nanomolar concentration range. Additional in vitro studies showed antioxidative neuroprotective effects as well as the ability to penetrate the blood–brain barrier. With this promising in vitro profile, contilisant (at 1 mg kg⁻¹ i.p.) also significantly improved lipopolysaccharide-induced cognitive deficits.*

Alzheimer's disease (AD) and Parkinson's disease (PD) are the most prevalent neurodegenerative diseases, with complex and variable underlying mechanisms. In studies of the causes and in search for more efficient therapies, factors such as mitochondrial dysfunction, neuroinflammation, and especially oxidative stress have been identified as major determinants for the progress and development of these diseases. Consequently, an antioxidant drug development strategy for neurodegenerative diseases, especially AD, has been of paramount importance.[1,2] The recently described multitarget-directed ligand (MDL) ASS234 (Figure 1)[3–5] is able to irreversibly inhibit monoamine oxidases A and B (MAO A/B), and also reduces the production of the secondary product hydrogen peroxide, a reactive oxygen species (ROS).[6] Thus ASS234 prevents the catalytic oxidation of biogenic amines, such as serotonin (5-HT), norepinephrine, and dopamine, all implicated in cognitive processes, as well as the production of ROS, which are associated with neuronal cell death. Additionally, ASS234 reversibly inhibits acetylcholinesterase (AChE), improving memory and cognition similar to marketed AChE inhibitors (e.g., donepezil).[7]

[*] S. Hagenow,[+] J. S. Schwed, Prof. Dr. H. Stark
    Institut für Pharmazeutische und Medizinische Chemie
    Heinrich-Heine-Universität Düsseldorf
    Universitätsstrasse 1, 40225 Düsseldorf (Germany)
    E-mail: stark@hhu.de

    Dr. Ó. M. Bautista-Aguilera,[+] M. L. Jimeno, M. Chioua,
    Prof. Dr. J. Marco-Contelles
    Laboratorio de Química Médica
    Instituto de Química Orgánica General
    CSIC and Centro de Química Orgánica "Lora-Tamayo", CSIC
    C/ Juan de la Cierva 3, 28006 Madrid (Spain)
    E-mail: iqoc21@iqog.csic.es

    A. Palomino-Antolin,[+] V. Farré-Alins,[+] Dr. J. Egea
    Instituto de Investigación Sanitaria
    Servicio de Farmacología Clínica
    Hospital Universitario de la Princesa
    Calle de Diego de León, 62, 28006 Madrid (Spain)
    E-mail: javier.egea@inv.uam.es

    L. Ismaili
    Neurosciences Intégratives et Cliniques EA 481
    Université Bourgogne Franche-Comté
    Rue Ambroise Paré, 25000 Besançon (France)

    P.-L. Joffrin, Dr. R. R. Ramsay
    Biomedical Sciences Research Complex
    University of St Andrews, Biomolecular Sciences Building
    North Haugh, St Andrews KY16 9ST (UK)

    Dr. O. Soukup, Dr. J. Janočková
    Centrum biomedicínského výzkumu
    Fakultní nemocnice Hradec Králové
    Sokolska 581, 50005 Hradec Kralove (Czech Republic)

    L. Kalinowsky, Jun.-Prof. Dr. E. Proschak
    Institut für Pharmazeutische Chemie
    Goethe Universität Frankfurt
    Max-von-Laue-Strasse 9, 60438 Frankfurt (Germany)

    I. Iriepa, I. Moraleda
    Departamento de Química Orgánica y Química Inorgánica
    Universidad de Alcalá
    Ctra. Madrid-Barcelona, Km. 33,6, 28871, Madrid (Spain)

    A. Romero Martínez
    Departamento de Toxicología y Farmacología
    Facultad de Veterinaria, UCM
    Av. Puerta de Hierro, s/n, 28040 Madrid (Spain)

    Dr. F. López-Muñoz
    Universidad Camilo José Cela
    C/ Castillo de Alarcón, 49
    28692 Villanueva de la Cañada, Madrid (Spain)

[+] These authors contributed equally to this work.

    Supporting information (experimental procedures for synthesis, analytics, pharmacological assays, and modeling studies) and the ORCID identification number(s) for the author(s) of this article can be found under:
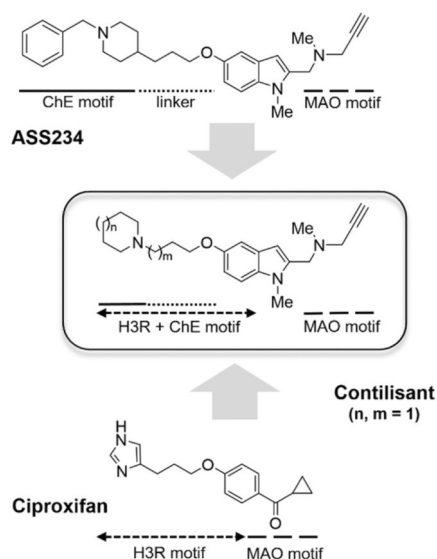   https://doi.org/10.1002/anie.201706072.

Figure 1. General structure of H3R/MAO/ChE MDLs derived from structural elements of the antioxidant ASS234 and the H3R antagonist ciproxifan.

The histamine H_3 receptor (H3R) is involved in the central regulation of histamine and other neurotransmitters,[8,9] and is thus considered as a useful novel pharmacological target. Inhibition of H3R with inverse agonists/antagonists elevates the levels of neurotransmitters, such as acetylcholine (ACh), 5-HT, dopamine, or norepinephrine, in the central nervous system. The first H3R inverse agonist pitolisant (WAKIX) has recently been approved for the treatment of narcolepsy, but it is also under investigation for diverse cognition and sleep impairments.[10] Thus the procognitive use of H3R antagonists/inverse agonists for the treatment of neurodegenerative diseases is being investigated.[11] Although compounds with multipotent profiles, combining H3R affinity with cholinesterase (ChE) inhibition,[12,13] antioxidant capacity,[14] or most recently with MAO inhibition,[15] have been reported,[16] MDLs that are able to simultaneously modulate H3R, MAO, and ChE have not been described to date. Such a multipotent profile might constitute an innovative therapeutic approach for new molecules targeting neurodegenerative diseases with multiple causes.

ASS234 was structurally modified to fit a generally accepted pharmacophore of H3R antagonists (Figure 1). To avoid adverse effects associated with imidazole-containing H3R antagonists (e.g., ciproxifan), cyclic aliphatic amines such as piperidine as the basic center were connected to an arbitrary eastern region via a (propyloxy)phenyl chain. These compounds provide suitable pharmacophores as confirmed by multiple structure–activity relationship (SAR) studies.[17–19] Herein, we report the synthesis and biological evaluation of MDLs **1–7** (Scheme 1) and the identification of compound **4** (contilisant), which combines high antioxidant activity and high affinity at H3R with excellent inhibition of the target

neurotransmitter-catabolizing enzymes. These compounds were evaluated for their affinity at human H3R and H4R and against four neurotransmitter-catabolizing enzymes (AChE and butyrylcholinesterase (BuChE), MAO A/B; for further off-target screening, see the Supporting Information).

All MDLs in this small series inhibited the ChEs at concentrations in the micromolar range (Table 1). Contilisant revealed the best inhibition properties with high nanomolar
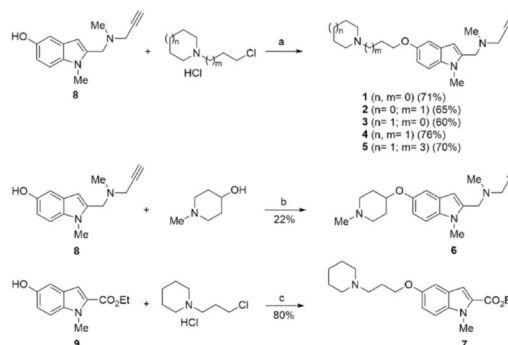
Scheme 1. Synthesis of MDLs **1–7**. Reagents and conditions: a) NaH, DMF, RT; b) PPh$_3$, DIAD, THF, RT; c) K$_2$CO$_3$, DMF, 90°C.

inhibition of AChE. The initial, reversible inhibition of MAO A/B (reflecting binding) and inhibition after 30 min preincubation of the inhibitor with the enzymes (because of irreversible inhibition) were determined (Table 1). Without preincubation, all compounds gave low micromolar IC$_{50}$ values. The spacer length influences the binding to the active sites of MAO A and B, with a two-carbon-atom spacer being optimal for the piperidine derivative. Switching to a pyrrolidine ring has little effect in compounds with a three-carbon-atom spacer (**2** vs. **4**), but decreased the inhibition in compounds with a two-carbon-atom spacer (**1** vs. **3**). After preincubation, the IC$_{50}$ values shifted to nanomolar concentrations for most of the propargylamines. The irreversibility of the MAO inhibition was confirmed for contilisant by 50-fold dilution into excess substrate. The IC$_{50}$ value for compound **6** changed very little with preincubation, suggesting that the propargyl group did not form a covalent adduct with MAO B. Compound **7**, lacking the propargyl group, showed no change with preincubation. MAO activity after 50-fold dilution of **7** was > 95 %, indicating reversible inhibition. Contilisant showed improved irreversible inhibition of MAO B compared to ASS234, which prefers MAO A. The affinities for binding at human H3R as the target and H4R, the structurally most homologous G-protein-coupled receptor, as an off-target were measured (Table 1). None of the compounds bound to H4R, indicating good specificity for H3R. Surprisingly, ASS234 showed remarkable affinity at H3R, but the highest affinity was found for **2** and contilisant, which both contain the propyloxy linker connected to pyrrolidine and piperidine moieties, respectively. Good affinities were also found for **6**, containing a related H3R

GDCh

Communications

Angewandte
International Edition *Chemie*

Table 1: IC$_{50}$ and K_i values for the inhibition of hMAO A/B, hAChE/hBuChE, and hH3R/hH4R, respectively, and ORAC analysis of compounds 1–7, ASS234, ciproxifan, clorgyline, deprenyl, and donepezil.

MTL	Preinc. [min]	hMAO A IC$_{50}$[a] [µM]	hMAO B IC$_{50}$[a] [µM]	SR MAO[b]	hAChE IC$_{50}$[a] [µM]	hBuChE IC$_{50}$[a] [µM]	SR ChE[c]	ORAC[d] (TE)	hH3R K_i[e] [nM]	hH4R K_i [nM]
1	0	3.00±0.34	5.21±0.82	1.7	37.9±1.5	25.1±5.5	1.5	3.11±0.07	178 [44, 716]	>10000
	30	0.095±0.009	0.140±0.008	1.5						
2	0	4.01±0.60	1.80±0.24	0.5	18.8±2.7	7.40±1.41	2.5	4.54±0.08	4.5 [1.8, 11]	>10000
	30	0.073±0.006	0.100±0.020	1.4						
3	0	0.41±0.03	1.32±0.21	3.2	20.6±3.6	8.55±1.48	2.4	1.86±0.06	38.5 [13, 117]	>10000
	30	0.052±0.007	0.017±0.003	0.3						
4 (contilisant)	0	1.85±0.21	1.94±0.15	1.0	0.53±0.05	1.69±0.12	0.3	3.59±0.09	10.8 [4.2, 27]	>100000
	30	0.145±0.010	0.078±0.006	0.5						
5	0	6.52±0.52	41.3±5.5	6.3	8.3±2.4	3.30±0.71	2.5	2.94±0.04	77.7 [19, 311]	>10000
	30	0.166±0.015	4.65±0.06	28						
6	0	1.19±0.15	3.80±0.40	3.2	58.3±11.8	31.1±1.8	1.9		14.7 [3.8, 57]	>10000
	30	0.042±0.004	2.75±0.51	65						
7	0	103±20	12.6±1.0	0.1	20.4±2.0	11.6±1.3	1.8	1.40±0.14	24.4 [12, 50]	>10000
	30	91±1	11.2±0.9	0.1						
ASS234	0	0.033±0.003	3.20±0.41	97	0.81±0.06	1.82±0.14	0.4		84.2 [48, 149]	>10000
	30	0.00027±0.00003	0.12±0.02	444						
ciproxifan	0	11.4±1.2[15]	2.1±0.3[15]	0.2	86.1±20.9	77.3±3.4	1.1		46-180[22–24]	>10000[23]
clorgyline	0	0.042±0.003	3.65±0.39	86	not active[25]	not active[25]				
	30	0.00042±0.00008	3.57±0.36	8500						
deprenyl	0	225±31	0.053±0.005	0.0002	not active[25]	not active[25]				
	30	0.630±0.086	0.0040±0.0009	0.006						
donepezil[4]	0				0.011±0.001	6.22±0.77	0.002			

[a] The error (SE) is indicated for each value. [b] SR = IC$_{50}$(hMAO B)/IC$_{50}$(hMAO A). [c] SR = IC$_{50}$(hAChE)/IC$_{50}$(hBuChE). [d] Oxygen radical absorbance capacity (Trolox equivalents, TE). [e] The confidence interval (95%) is given in square brackets.

pharmacophore, and **7**, which lacks the propargylamine group but features the propyloxy linker. Compounds with ethyloxy or pentyloxy spacers showed moderate H3R affinities. These findings confirmed previously obtained SAR results for H3R antagonists.[17,20,21] As compounds **6** and **7** exhibit comparable H3R affinity, we have demonstrated that the H3R affinity is positively influenced by the introduction of the second basic moiety, the propargylamine motif, which is responsible for MAO inactivation. Compound **6**, albeit less effective against AChE, provides structural variation possibilities as the MAO motif could be combined with various spacers or amine warheads for H3R pharmacophores.

Molecular docking studies on the four targets clearly support the in vitro results as ASS234 and contilisant fit to the various binding cavities of AChE, MAO A/B, and H3R (see the Supporting Information). Among the molecular properties of contilisant obtained with molsoft,[26] its higher hydrophilicity (MolLog$P$ = 3.7) compared to that of ASS234 (MolLog$P$ = 5.5) should be noted, which indicates increased drug likeness. Further indication for central distribution was obtained from a parallel artificial membrane permeability assay (PAMPA), a tool used for predicting blood–brain barrier (BBB) penetration properties (see the Supporting Information). The results clearly indicated the ability of contilisant and ASS234 to pass the BBB by passive diffusion. A complete in silico ADME analysis of the novel hybrids **1–7** has been carried out, suggesting drug suitability, with a special focus on contilisant (see the Supporting Information). The antioxidant capacities of hybrids **1–5** and **7** were measured as the oxygen radical absorbance capacity (ORAC-FL; Table 1),[27] with all MDLs presenting good radical scavenging properties and those for contilisant being close to that of the

positive control ferulic acid (3.74 ± 0.22 TE).[28] The neuroprotection capacities were studied using three different toxic insults involved in neurodegeneration mechanisms in AD:[29] a) a cocktail of mitochondrial respiratory chain blockers, rotenone, and oligomycin A (R/O), a model of ROS generation; b) the protein phosphatase inhibitor okadaic acid (OA), as a model of the hyperphosphorylation of tau protein; and c) β-amyloid peptides (Aβ$_{25–35}$), which are involved in ROS and apoptosis pathways. Overall, the data obtained for compounds **1–7** revealed an interesting neuroprotection profile (see the Supporting Information). At the lowest concentration tested (0.3 µM), contilisant offered significant neuroprotection against the toxic insults assayed (70% vs. R/O, 47% vs. OA, and 65% vs. Aβ$_{25–35}$), comparable to that offered by melatonin (Figure 2).

Memory improvements after ASS234 and contilisant administration were tested in vivo using the novel object recognition test (NOR) in mice (Figure 3)[30] before and after administration of lipopolysaccharide (LPS), which significantly impairs NOR performance. Mice treated with contilisant after LPS impairment showed a significantly improved discrimination index whereas ASS234 (at the same dose) was not able to restore the cognitive deficit.

In conclusion, new MDLs showing inhibitory properties for neurotransmitter-catabolizing enzymes (ChEs and MAOs) alongside H3R affinity have been described for the first time. From this small series, contilisant showed the best overall multitarget properties at nanomolar concentrations, with newly designed and well-balanced properties in terms of permeation as well as the antioxidant and neuroprotective properties. Contilisant displays a pharmacological profile with improved complexity, which might be beneficial for the
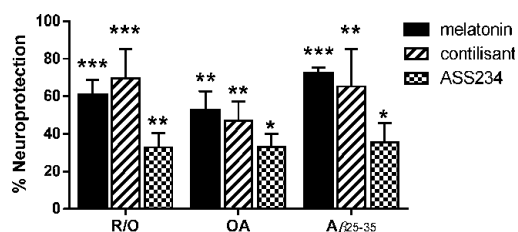
GDCh

Communications

Angewandte
International Edition *Chemie*

Figure 2. Neuroprotective properties of contilisant (0.3 μM), ASS234 (5 μM), and melatonin (0.01 μM) in SH-SY5Y cells following rotenone (30 μM)/oligomycin A (10 μM; R/O), okadaic acid (20 nM; OA), or β-amyloid peptide (30 μM; Aβ$_{25-35}$) intoxications, respectively. Data expressed as % neuroprotection ± SEM of at least four different cultures performed in triplicates (untreated control set to 100%). ***$p \leq 0.001$, **$p \leq 0.01$, *$p \leq 0.05$ compared to control.
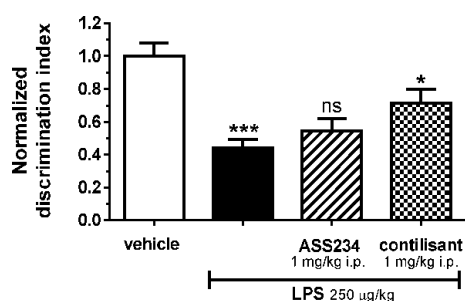

Figure 3. Effect of contilisant and ASS234 on lipopolysaccharide (LPS) induced memory impairment in the novel object recognition test in mice. ***$p \leq 0.001$ vs. vehicle, *$p \leq 0.05$, ns $p > 0.05$ vs. LPS.

treatment of neurodegenerative conditions. Compared to the dual-target H3R/MAO ligand ciproxifan,[15] contilisant is a more potent inhibitor of MAO with irreversible binding. Moreover, contilisant at 1 mg kg^{-1} restored the cognitive deficit of LPS-treated mice.

As intended, all properties of the small-molecule MDL contilisant (**4**) were optimized compared to those of lead compound ASS234, including reduced inhibition of MAO A, and successfully extended by high H3R affinity by taking advantage of the structural blueprint for H3R pharmacophores.[31] The resulting unique pharmacological profile, addressing various targets involved in neurodegenerative processes, may be suitable for the treatment of Alzheimer's or Parkinson's disease.

Acknowledgements

Conflict of interest

S.H., H.S., J.M.C., R.R.R., and F.L.M. declare a conflict of interest based on a related patent application; the other authors declare no conflict of interest.

[1] G. H. Kim, J. E. Kim, S. J. Rhie, S. Yoon, *Exp. Neurobiol.* **2015**, *24*, 325.

[2] E. Niedzielska, I. Smaga, M. Gawlik, A. Moniczewski, P. Stankowicz, J. Pera, M. Filip, *Mol. Neurobiol.* **2016**, *53*, 4094–4125.

[3] O. M. Bautista-Aguilera et al., *J. Med. Chem.* **2014**, *57*, 10455–10463.

[4] G. Esteban, J. Allan, A. Samadi, A. Mattevi, M. Unzeta, J. Marco-Contelles, C. Binda, R. R. Ramsay, *Biochim. Biophys. Acta Proteins Proteomics* **2014**, *1844*, 1104–1110.

[5] I. Bolea, J. Juárez-Jiménez, C. De Los Ríos, M. Chioua, R. Pouplana, F. J. Luque, M. Unzeta, J. Marco-Contelles, A. Samadi, *J. Med. Chem.* **2011**, *54*, 8251–8270.

[6] C. C. Wang, E. Billett, A. Borchert, H. Kuhn, C. Ufer, *Cell. Mol. Life Sci.* **2013**, *70*, 599–630.

[7] M. Racchi, M. Mazzucchelli, E. Porrello, C. Lanni, S. Govoni, *Pharmacol. Res.* **2004**, *50*, 441–451.

[8] M. Walter, H. Stark, *Front. Biosci.* **2012**, *S4*, 461–488.

[9] B. A. Ellenbroek, B. Ghiabi, *Trends Neurosci.* **2014**, *37*, 191–199.

[10] J.-C. Schwartz, *Br. J. Pharmacol.* **2011**, *163*, 713–721.

[11] B. Sadek, A. Saad, A. Sadeq, F. Jalal, H. Stark, *Behav. Brain Res.* **2016**, *312*, 415–430.

[12] W. Huang, L. Tang, Y. Shi, S. Huang, L. Xu, R. Sheng, P. Wu, J. Li, N. Zhou, Y. Hu, *Bioorg. Med. Chem.* **2011**, *19*, 7158–7167.

[13] G. Petroianu, K. Arafat, B. C. Sasse, H. Stark, *Pharmazie* **2006**, *61*, 179–182.

[14] R. Sheng, L. Tang, L. Jiang, L. Hong, Y. Shi, N. Zhou, Y. Hu, *ACS Chem. Neurosci.* **2016**, *7*, 69–81.

[15] S. Hagenow, A. Stasiak, R. R. Ramsay, H. Stark, *Sci. Rep.* **2017**, *7*, 40541.

[16] M. A. Khanfar, A. Affini, K. Lutsenko, K. Nikolic, S. Butini, H. Stark, *Front. Neurosci.* **2016**, *10*, 1–17.

[17] K. Wingen, H. Stark, *Drug Discovery Today Technol.* **2013**, *10*, e483–e489.

[18] S. Celanire, M. Wijtmans, P. Talaga, R. Leurs, I. J. de Esch, *Drug Discovery Today* **2005**, *10*, 1613–1627.

[19] B. Sadek, D. Lazewska, S. Hagenow, K. Kiec-Kononowiczc, H. Stark in *The Receptors. Histamine Receptors* (Eds.: P. Blandina, M. B. Passani), Springer, Cham, **2016**, pp. 109–156.

[20] K. Nikolic, D. Agbaba, H. Stark, *J. Taiwan Inst. Chem. Eng.* **2015**, *46*, 15–29.

[21] K. Nikolic, S. Filipic, D. Agbaba, H. Stark, *CNS Neurosci. Ther.* **2014**, *20*, 613–623.

[22] X. Ligneau, S. Morisset, J. Tardivel-Lacombe, F. Gbahou, C. R. Ganellin, H. Stark, W. Schunack, J. C. Schwartz, J. M. Arrang, *Br. J. Pharmacol.* **2000**, *131*, 1247–1250.

[23] T. Esbenshade, K. Krueger, *J. Pharmacol. Exp. Ther.* **2003**, *305*, 887 – 896.
[24] B. S. Wulff, S. Hastrup, K. Rimvall, *Eur. J. Pharmacol.* **2002**, *453*, 33 – 41.
[25] O. Benek et al., *ChemMedChem* **2016**, *11*, 1264 – 1269.
[26] L. L. C. Molsoft, "http://molsoft.com/mprop/," **2017**.
[27] A. Dávalos, C. Gómez-Cordovés, B. Bartolomé, *J. Agric. Food Chem.* **2004**, *52*, 48 – 54.
[28] M. I. Fernández-Bachiller et al., *ChemMedChem* **2009**, *4*, 828 – 841.

[29] M. Benchekroun et al., *ChemMedChem* **2015**, *10*, 523 – 539.
[30] E. Stragier, V. Martin, E. Davenas, C. Poilbout, R. Mongeau, R. Corradetti, L. Lanfumey, *Transl. Psychiatry* **2015**, *5*, e696.
[31] H. Stark, *Drug Discovery Today* **2004**, *9*, 736 – 737.

SUPPORTING INFORMATION

Angewandte Chemie

Eine Zeitschrift der Gesellschaft Deutscher Chemiker

Supporting Information

Multitarget-Directed Ligands Combining Cholinesterase and Mono-amine Oxidase Inhibition with Histamine H₃R Antagonism for Neurodegenerative Diseases

Óscar M. Bautista-Aguilera⁺, Stefanie Hagenow⁺, Alejandra Palomino-Antolin⁺, Víctor Farré-Alins⁺, Lhassane Ismaili, Pierre-Louis Joffrin, María L. Jimeno, Ondřej Soukup, Jana Janočková, Lena Kalinowsky, Ewgenij Proschak, Isabel Iriepa, Ignacio Moraleda, Johannes S. Schwed, Alejandro Romero Martínez, Francisco López-Muñoz, Mourad Chioua, Javier Egea, Rona R. Ramsay, José Marco-Contelles,* and Holger Stark**

anie_201706072_sm_miscellaneous_information.pdf

Table of Contents

SUPPORTING INFORMATION

SUPPORTING INFORMATION

Synthesis and spectroscopic data
General Synthesis

Reactions were monitored by TLC using precoated silica gel aluminum plates containing a fluorescent indicator (Merck, 5539). Detection was done by UV (254 nm) followed by charring with sulfuric-acetic acid spray, 1% aqueous potassium permanganate solution or 0.5% phosphomolybdic acid in 95% EtOH. Anhydrous Na_2SO_4 was used to dry organic solutions during work-ups and the removal of solvents was carried out under vacuum with a rotary evaporator. Flash column chromatography was performed using silica gel 60 (230-400 mesh, Merck). Melting points were determined on a Kofler block and are uncorrected. IR spectra were obtained on a Perkin-Elmer Spectrum One spectrophotometer. NMR spectra were recorded on a Varian VXR-200 spectrometer (^{1}H 200 MHz, ^{13}C 50MHz) and on a Varian SYSTEM 500 NMR spectrometer (^{1}H 500 MHz, ^{13}C 125 MHz) equipped with a 5-mm HCN cold probe, using tetramethylsilane as internal standard. All the assignments for protons and carbons were in agreement with 2D COSY, HSQC, HMBC, and 1D NOESY spectra. The purity of compounds was checked by elemental analyses, conducted on a Carlo Erba EA 1108 apparatus, and confirmed to be > 95%.

N-Methyl-*N*-((1-methyl-5-(2-(pyrrolidin-1-yl)ethoxy)-1H-indol-2-yl)methyl)prop-2-yn-1-amine (1)

To a solution of compound **8**[1] (120 mg, 0.52 mmol) and commercial 1-(2-chloroethyl)pyrrolidine hydrochloride (89.1 mg, 0.52 mmol) in dry DMF (7 mL), under argon, NaH (38 mg, 1.56 mmol, 60% dispersion in mineral oil) was slowly added. The reaction mixture was stirred at rt overnight. The mixture was evaporated under reduced pressure. Then, a saturated solution of NH_4Cl (50 mL) was added, and the organic layer was extracted with EtOAc (3x200 mL). The combined organic layers were washed with brine and dried over Na_2SO_4, and the solvent evaporated under reduced pressure. The crude was purified by flash column chromatography (hexane/ EtOAc, 10-50%) to yield compound **1** (121 mg, 71%) as a yellow oil: Rf= 0.39 (hexane/AcOEt, 70%); IR (KBr) v 3433, 2955, 2620, 2126, 1724, 1625, 1487, 1405, 1279, 1209 cm^{-1}; ^{1}H NMR (500 MHz, CDCl$_3$) δ 7.16 (d, *J*= 8.8 Hz, 1H), 7.03 (d, *J*= 2.4 Hz, 1H), 6.81 (dd, *J*= 8.8, 2.4 Hz, 1H), 6.32 (s, 1H), 4.49-4.47 (t, *J*= 4.9 Hz, 2H), 3.72 (s, 3H), 3.65 (s, 2H), 3.46 (*J*= 4.9 Hz, 2H), 3.49-3.44 (m, 4H), 3.28 (d, *J*= 2.4 Hz, 2H), 2.32 (s, 3H), 2.28 (t, *J*= 2.4 Hz, 1H), 2.27-2.11 (m, 4H); ^{13}C NMR (126 MHz, CDCl$_3$) δ 151.5, 137.6, 133.9, 127.5, 111.3, 109.8, 104.0, 102.24, 78.30, 73.5, 64.3, 54.1 (2 C), 53.9, 51.7, 44.7, 41.5, 29.9, 23.2 (2 C); MS (ESI) *m/z*: 326.3 (M+1)$^+$. Compound **1** was transformed into its bis-oxalate salt: m.p. 183-5 ºC; ^{1}H NMR (300 MHz, D$_2$O) δ 7.33 (d, *J*= 9.0 Hz, 1H), 7.12 (d, *J*= 2.4 Hz, 1H), 6.94 (dd, *J*= 9.0, 2.2 Hz, 1H), 6.67 (s, 1H), 4.55 (br s, 2H), 4.24 (t, *J*= 4.9 Hz, 2H), 3.93 (d, *J*= 1.9 Hz, 2H), 3.65 (s, 3H), 3.62-3.56 (m, 2H), 3.51 (t, *J*= 4.9 Hz, 2H), 3.09-3.03 (m, 3H), 2.84 (s, 3H), 2.04-2.02 (m, 2H), 1.91-1.87 (m, 2H). Anal. Calcd for C$_{20}$H$_{27}$N$_3$O.2xHCO$_2$CO$_2$H.H$_2$O: C, 55.06; H, 6.35; N, 8.03. Found: C, 54.97; H, 6.15; N, 7.80.

SUPPORTING INFORMATION
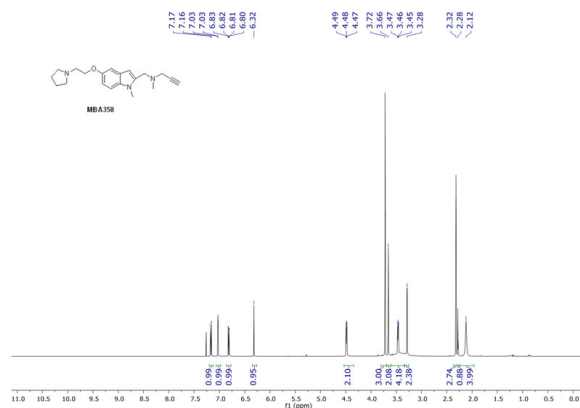
Figure S1. ¹H NMR (500 MHz, CDCl₃) spectrum of compound **1**.

Figure S2. ¹³C NMR (126 MHz, CDCl₃) spectrum of compound **1**.

SUPPORTING INFORMATION
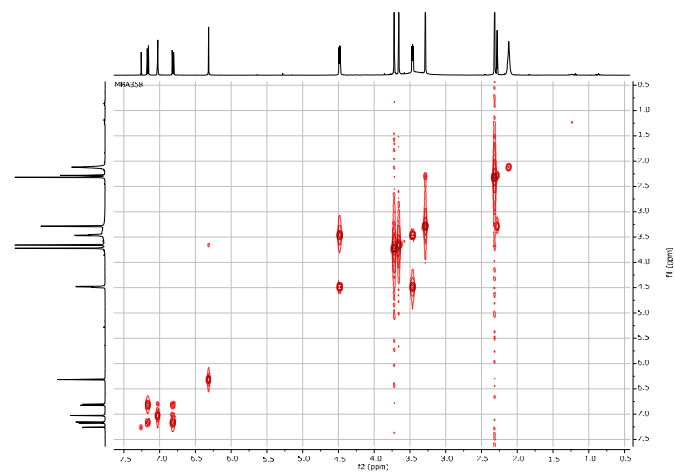
Figure S3. 2D COSY NMR spectrum of compound **1**.
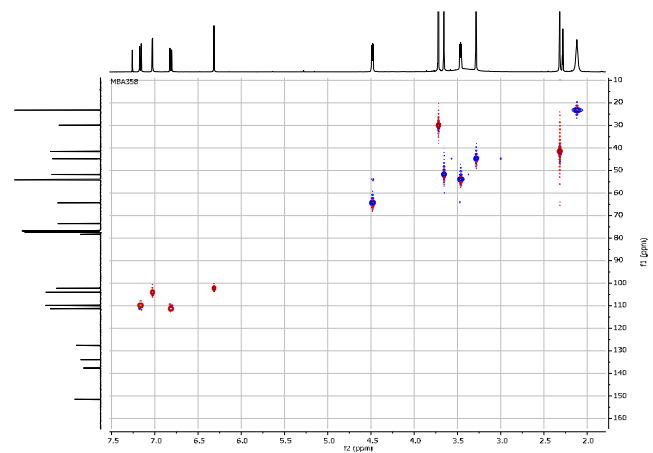
Figure S4. 2D HSQC NMR spectrum of compound **1**.

Figure S5. 2D HSQC NMR spectrum of compound **1**.

N-Methyl-*N*-((1-methyl-5-(3-(pyrrolidin-1-yl)propoxy)-1*H*-indol-2-yl)methyl)prop-2-yn-1-amine (2)

To a solution of compound **8**[1] (150 mg, 0.65 mmol) and commercial 1-(3-chloropropyl)pyrrolidine hydrochloride (121 mg, 0.65 mmol) in dry DMF (10 mL), under argon, NaH (47 mg, 1.95 mmol, 60% dispersion in mineral oil) was slowly added. The reaction mixture was stirred at rt overnight. Then, the solvent was evaporated under reduced pressure, a saturated solution of NH_4Cl (50 mL) was added, and the organic layer was extracted with EtOAc (3x200 mL). The combined organic layers were washed with brine and dried over Na_2SO_4, and the solvents were evaporated under reduced pressure. The crude was purified by flash column chromatography (hexane/ EtOAc, 10-50%) to yield compound **2** (144 mg, 65%) as a yellow oil: Rf= 0.37 (hexane/AcOEt, 70%; ^{1}H NMR (300 MHz, $CDCl_3$) δ 7.19 (d, *J*= 8.8 Hz, 1H), 7.08 (d, *J*= 2.5 Hz, 1H), 6.90 (dd, *J*= 8.8, 2.5 Hz, 1H), 6.36 (s, 1H), 4.09 (t, *J*= 6.4 Hz, 2H), 3.75 (s, 3H), 3.69 (s, 2H), 3.33 (d, *J*= 2.2 Hz, 2H), 2.74-2.71 (m, 2H), 2.69-2.59 (m, 4H), 2.37 (s, 3H), 2.32 (t, *J*= 2.2 Hz, 1H), 2.11-2.08 (m, 2H), 1.85-1.80 (m, 4H); MS (ESI) *m/z* 340.3 (M+1)⁺. Compound **2** has been transformed into its bis-oxalate salt: m.p. 156-9 °C; IR (KBr) v 3432, 3263, 2958, 2618, 2127, 1723, 1624, 1487, 1406, 1279, 1207, 1104, 1058 cm⁻¹; ^{1}H NMR (500 MHz, D_2O) δ 7.31 (d, *J* = 9.3 Hz, 1H), 7.10 (d, *J* = 2.4 Hz, 1H), 6.90 (dd, *J* = 9.3, 2.5 Hz, 1H), 6.65 (s, 1H), 4.52 (br s, 2H), 4.03 (t, *J* = 5.8 Hz, 2H), 3.91 (d, *J* = 2.4 Hz, 2H), 3.63 (s, 3H), 3.57-3.52 (m, 2H), 3.28-3.25 (m, 2H), 3.03 (t, *J* = 2.4 Hz, 1H), 2.95-2.93 (m, 2H), 2.82 (s, 3H), 2.08-2.05 (m, 2H), 2.01-1.94 (m, 2H), 1.90-1.84 (m, 2H); ^{13}C NMR (126 MHz, D_2O) δ 167.8, 154.8, 136.4, 130.8, 129.2, 116.5, 114.0, 106.6, 82.8, 74.0, 68.5, 56.7 (2 C), 55.0, 52.1, 46.8, 41.8, 32.3, 27.8, 25.0 (2 C). Anal. Calcd for $C_{21}H_{29}N_3O_2.2xHCO_2CO_2H$. H_2O: C, 55.86; H, 6.56; N, 7.82. Found: C, 56.15; H, 6.44; N, 7.64.

Figure S6. ^{1}H NMR (500 MHz, D_2O) spectrum of compound **2**.
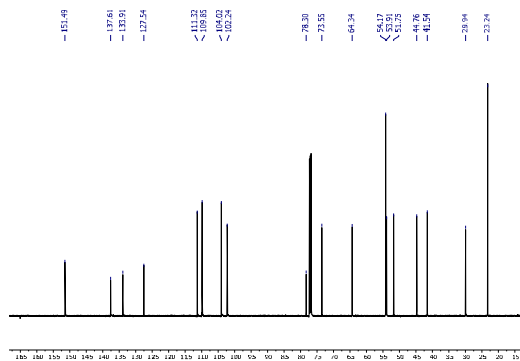

Figure S7. ^{13}C NMR (126 MHz, D_2O) spectrum of compound **2**.

Figure S8. 2D COSY NMR spectrum of compound **2**.

Figure S9. 2D HMBC NMR spectrum of compound **2**
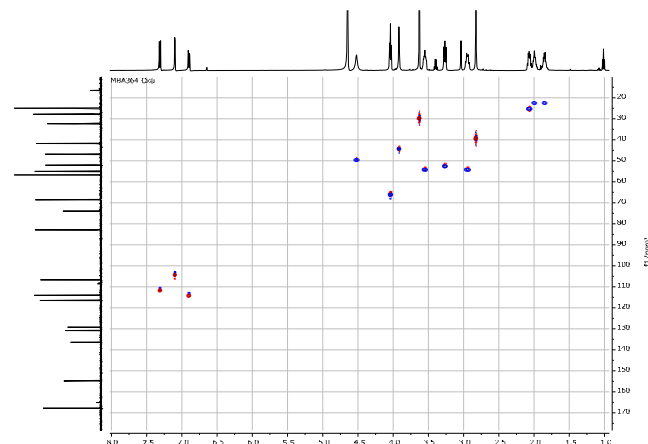
Figure S10. 2D HSQC NMR spectrum of compound **2**.

N-Methyl-N-((1-methyl-5-(2-(piperidin-1-yl)ethoxy)-1H-indol-2-yl)methyl)prop-2-yn-1-amine (3)

To a solution of compound **8**[1] (200 mg, 0.87 mmol) and commercial 1-(2-chloroethyl)piperidine hydrochloride (160 mg, 0.87 mmol) in dry DMF (10 mL), under argon, NaH (63 mg, 2.61 mmol, 60% dispersion in mineral oil) was slowly added. The reaction mixture was stirred at rt overnight. Then, the mixture was evaporated under reduced pressure. Saturated NH_4Cl solution (40 mL) was added, and the organic layer was extracted with EtOAc (3x200 mL). The combined organic layers were washed with brine and dried over Na_2SO_4, and the solvents were evaporated under reduced pressure. The crude product was purified by flash column chromatography (hexane/ EtOAc, 10-50%) to compound **3** (170 mg, 60%) as a yellow solid {Rf= 0.35, hexane/EtOAc, 70%; ^{1}H NMR (300 MHz, $CDCl_3$) δ 7.17 (d, J= 9.0 Hz, 1H), 7.05 (d, J= 2.2 Hz, 1H), 6.87 (dd, J= 9.0, 2.2 Hz, 1H), 6.34 (s, 1H), 4.17 (t, J= 6.1 Hz, 2H), 3.73 (s, 3H), 3.67 (s, 2H), 3.31 (d, J= 2.4 Hz, 2H), 2.83 (t, J= 6.1 Hz, 2H), 2.57 (t, J= 5.0 Hz, 4H), 2.34 (s, 3H), 2.30 (t, J= 2.4 Hz, 1H), 1.67-1.61 (m, 4H), 1.48-1.46 (m, 2H); MS (ESI) m/z 340.4 (M+1)[+]}, which has been transformed into its bis-oxalate salt: m.p. 153-5 ºC; IR (KBr) v 3426, 3276, 2953, 2129, 1728, 1624, 1486, 1407, 1207 cm^{-1}; ^{1}H NMR (500 MHz, D_2O) δ 7.33 (d, J= 8.8 Hz, 1H), 7.11 (d, J= 2.0 Hz, 1H), 6.93 (dd, J= 8.8, 2.0 Hz, 1H), 6.67 (s, 1H), 4.55 (br s, 2H), 4.26 (t, J= 4.8 Hz, 2H), 3.93 (br s, 2H), 3.65 (s, 3H), 3.48 (d, J= 12.2 Hz, 2H), 3.42 (t, J= 4.8 Hz, 2H), 3.05 (m, 1H), 2.91 (t, J= 12.2 Hz, 2H), 2.84 (s, 3H), 1.83-1.80 (m, 2H), 1.69-1.62 (m, 3H), 1.59-1.35 (m, 1H); ^{13}C NMR (126 MHz, D_2O) δ 164.5, 151.9, 133.8, 128.2, 126.5, 113.7, 111.4, 103.6, 80.2, 71.3, 61.9, 55.4, 53.2 (2 C), 49.4, 44.2, 39.1, 29.7, 22.4 (2 C), 20.8 (1 C). Anal. Calcd for $C_{21}H_{29}N_3O \cdot 2xHCO_2CO_2H \cdot 3/2H_2O$: C, 54.94; H, 6.64; N, 7.69. Found: C, 55.14; H, 6.39; N, 7.47.

Figure S11. ¹H NMR (500 MHz, D₂O) spectrum of compound **3**.

Figure S12. ¹³C NMR (126 MHz, D₂O) spectrum of compound **3**.

Figure S13. 2D COSY NMR spectrum of compound **3**.
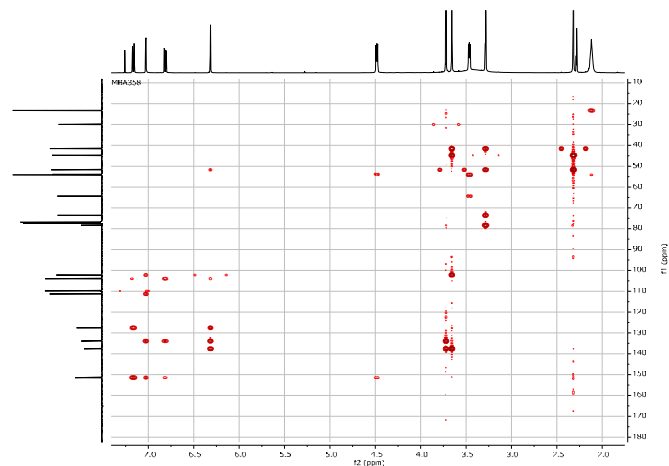

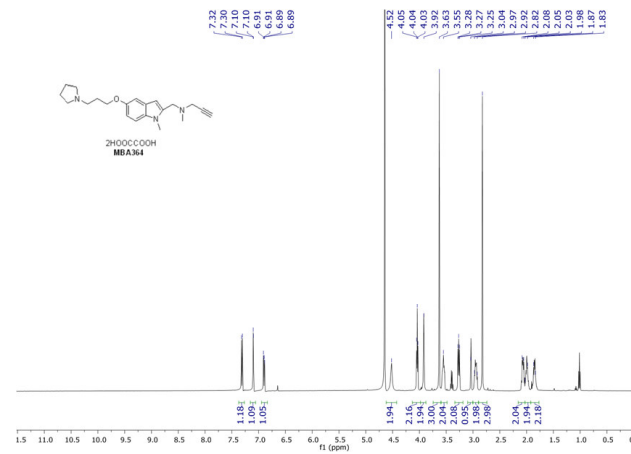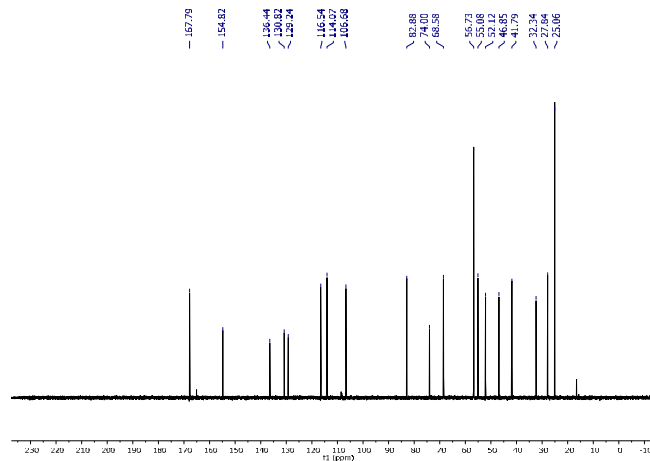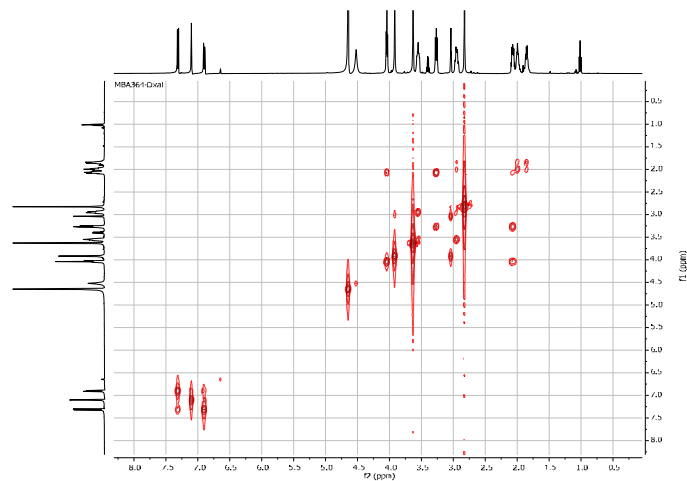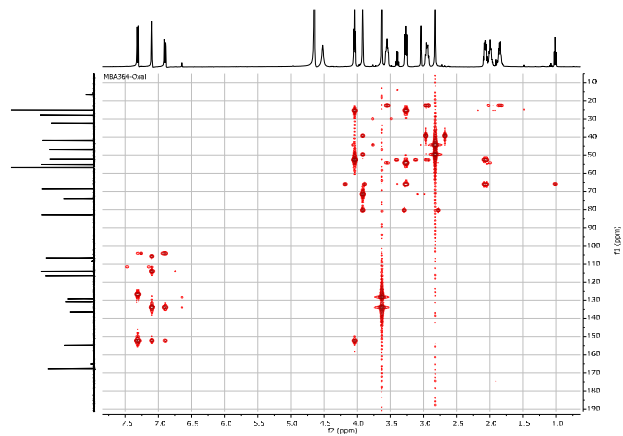Figure S14. 2D HSQC NMR spectrum of compound **3**.

Figure S15. 2D HMBC NMR spectrum of compound **3**.

N-Methyl-N-((1-methyl-5-(3-(piperidin-1-yl)propoxy)-1H-indol-2-yl)methyl)prop-2-yn-1-amine (4=contilisant)

To a solution of compound **8**[1] (390 mg, 1.71 mmol) and commercial 1-(3-chloropropyl)piperidine hydrochloride (338 mg, 1.71 mmol) in dry DMF (4 mL), under argon, NaH (205 mg, 5.13 mmol, 60% dispersion in mineral oil) was added. The mixture reaction was stirred for 24 h at rt. The solvent was evaporated, the reaction cooled at 0 °C, and water (10 mL) and commercial EtOAc (30 mL) were added. The reaction pH was adjusted at 7-8, and the mixture extracted and organic layer was evaporated under reduce pressure, dried, filtered, evaporated to give a residue that was purified for flash column chromatography (DCM/MeOH, 1-5%) to yield compound **4** (400 mg, 76%) as a solid: Rf: 0.32 (DCM/MeOH 10%); m.p. 155-8 °C; IR (KBr) v 3435, 3269, 2942, 2505, 1620, 1489, 1207 cm^{-1}; ^{1}H NMR (500 MHz, CDCl$_3$) δ 7.17 (d, J = 8.8 Hz, 1H), 6.98 (d, J = 2.5 Hz, 1H), 6.78 (dd, J= 8.8, 2.5 Hz, 1H), 6.35 (s, 1H), 4.08 (t, J= 5.3 Hz, 2H), 3.74 (s, 3H), 3.71 (s, 2H), 3.56 (d, J= 11.2 Hz, 2H), 3.33 (s, 2H), 3.18 (m, 2H), 2.66-2.62 (m, 2H), 2.47-2.45 (m, 2H), 2.32 (s, 3H), 2.41-2.27 (m, 2H), 1.92-1.83 (m, 3H), 1.42-1.39 (m, 1H); ^{13}C NMR (126 MHz, CCCl$_3$) δ 165.0, 152.4, 133.6, 127.5, 111.6, 109.8, 103.5, 102.4, 65.7, 55.5, 53.4 (2C), 51.5, 44.6, 41.4, 31.5, 30.0, 24.0, 22.5, 22.1 (2 C), 14.1; MS (ESI) m/z: 354.2 (M+1) $^+$. HRMS. Calcd for C$_{22}$H$_{31}$N$_3$O: 354.2540. Found. 354.2536. Compound **4** was transformed into its bis-hydrochloride salt: m.p. 220-1 °C; ^{1}H NMR (500 MHz, D$_2$O) δ 7.33 (d, J = 9.3 Hz, 1H), 7.12 (d, J = 2.4 Hz, 1H), 6.92 (dd, J= 8.8, 2.4 Hz, 1H), 6.66 (s, 1H), 4.52 (s, 2H), 4.06 (t, J= 5.6 Hz, 2H), 3.92 (d, J= 1.9 Hz, 2H), 3.64 (s, 3H), 3.43 (d, J= 12.3 Hz, 2H), 3.16 (t, J= 7.0 Hz, 2H), 3.06 (t, J= 1.9 Hz, 1H), 2.83 (s, 3H), 2.83-2.77 (m, 2H), 2.10-2.07 (m, 2H), 1.83-1.80 (m, 2H), 1.77-1.55 (m, 1H), 1.60-1.57 (m, 2H), 1.39-1.36 (m, 1H); ^{13}C NMR (126 MHz, CDCl$_3$) δ 152.3, 133.9, 128.4, 126.8, 113.9, 111.5, 105.9, 104.1, 80.3, 71.5, 66.1, 54.5, 53.2 (2 C), 49.6, 44.3, 39.2, 29.8, 23.4, 22.7 (2 C), 21.0. Anal.Calcd for C$_{22}$H$_{31}$N$_3$O.2HCl: C, 74.75; H, 8.84; N, 11.89. Found: C, 74.81; H, 8.62; N, 11.61.

Figure S16. ^{1}H NMR (500 MHz, CDCl$_3$) spectrum of compound **4**.

Figure S17. ^{13}C NMR (126 MHz, CDCl$_3$) spectrum of compound **4**.
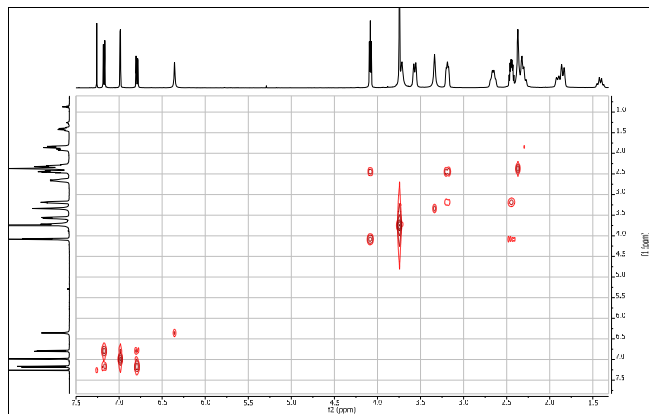
Figure S18. 2D COSY NMR spectrum of compound **4**.
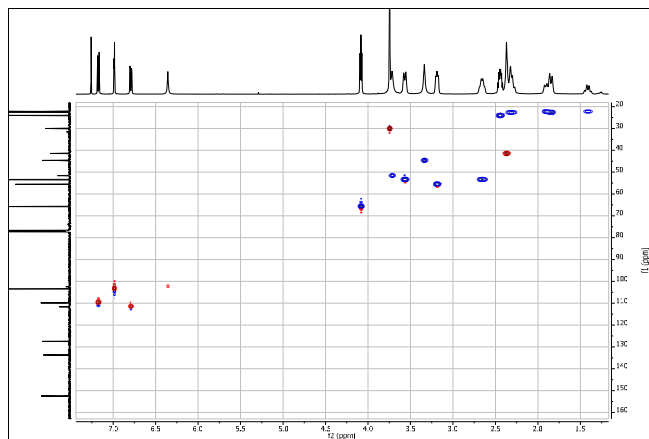
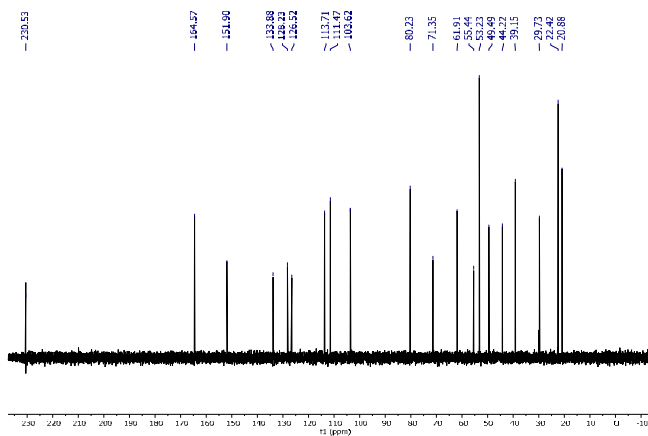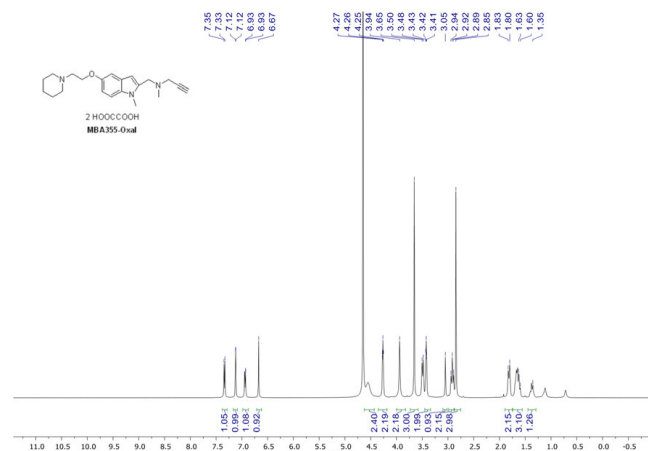Figure S19. 2D HSQC NMR spectrum of compound **4**.
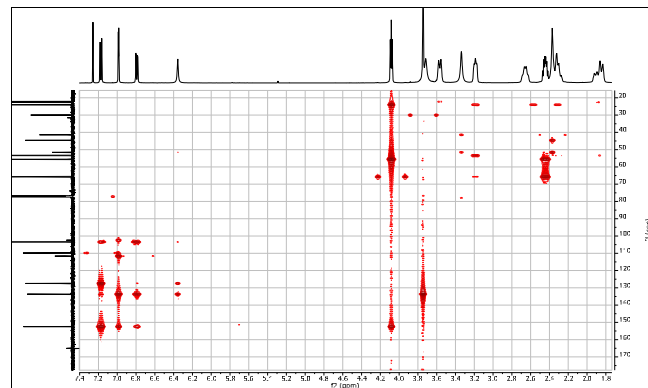
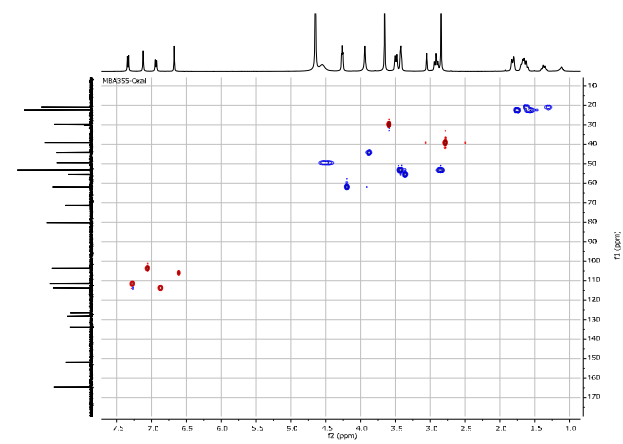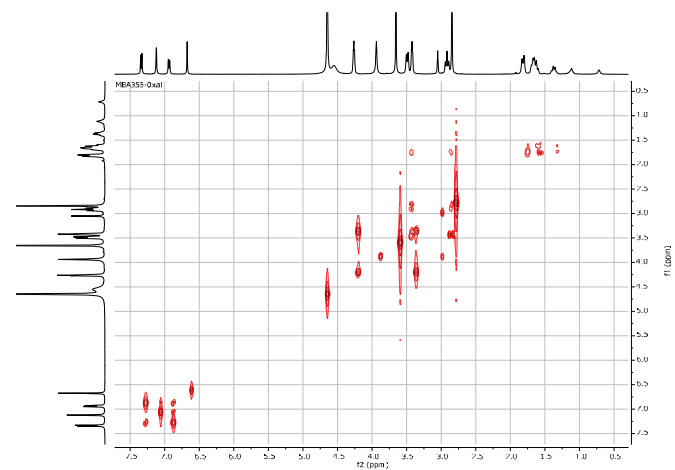Figure S20. 2D HMBC NMR spectrum of compound **4**.

***N*-Methyl-*N*-((1-methyl-5-((5-(piperidin-1-yl)pentyl)oxy)-1*H*-indol-2-yl)methyl)prop-2-yn-1-amine (5)**

To a solution of compound **8**[1] (150 mg, 0.66 mmol) and commercial 1-(5-chloropentyl)piperidine hydrochloride (150 mg, 0.66 mmol) in dry DMF (10 mL), under argon, NaH (48 mg, 1.97 mmol, 60% dispersion in mineral oil) was slowly added. The reaction mixture was stirred at rt overnight. The solvent was evaporated under reduced pressure. Then, a saturated solution of NH_4Cl (35 mL) was added, and the organic layer was extracted with EtOAc (3x200 mL). The combined organic layers were washed with brine and dried over Na_2SO_4, and the solvents were evaporated under reduced pressure. The crude was purified by flash column chromatography (hexane/ EtOAc, 10-50%) to yield compound **5** (175 mg, 70%) as a white solid (Rf= 0.33, hexane/EtOAc 70%): ^{1}H NMR (500 MHz, CDCl₃) δ 7.16 (d, *J*= 8.8 Hz, 1H), 6.99 (*J*= 2.7 1H), 6.81 (dd, *J*= 8.9, 2.7 Hz, 1H), 6.33 (s, 1H), 3.97 (t, *J*= 5.8 Hz, 2H), 3.71 (s, 3H), 3.65 (s, 2H), 3.59-3.37 (m, 2H), 3.29 (d, *J*= 2.1 Hz, 2H), 2.91 (t, *J*= 8.4 Hz, 2H), 2.68-2.53 (m, 2H), 2.32 (s, 3H), 2.28 (t, *J*= 2.1 Hz, 1H), 2.30-2.10 (m, 2H), 2.02-1.89 (m, 4H), 1.82-1.79 (m, 4H), 1.60-1.47 (m, 2H); ^{13}C NMR (126 MHz, CDCl₃) δ 153.0, 137.1, 133.4, 127.5, 111.8, 109.6, 103.4, 102.0, 78.3, 73.5, 68.1, 57.3, 53.1 (2 C), 51.7, 44.7, 41.5, 29.9, 28.8, 23.7, 23.2, 22.5 (2 C), 22.1; MS (ESI) *m/z*: 382.3 (M+1) $^+$. Compound **5** has been transformed into its bis-oxalate salt: m.p. 123-6 ºC; IR (KBr) ν 3431, 3263, 2946, 2868, 2680, 2541, 2124, 1724, 1623, 1537, 1486, 1473, 1405, 1280, 1207 cm^{-1}. Anal. Calcd for $C_{24}H_{35}N_3O.2xHCO_2CO_2H.2H_2O$: C, 56.27; H, 7.25; N, 7.03. Found: C, 56.36; H, 6.97; N, 7.04.
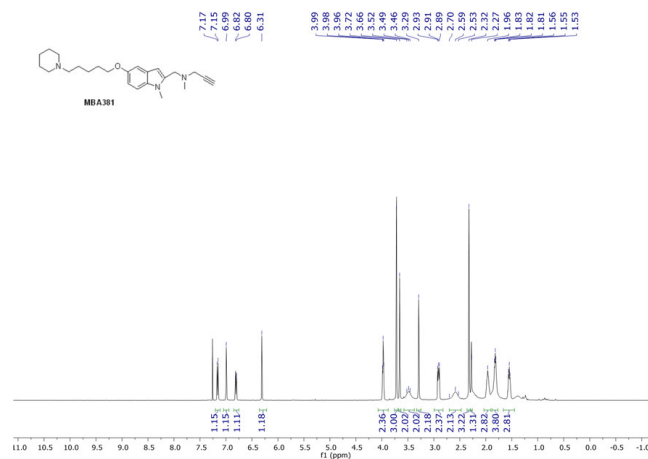
Figure S21. ¹H NMR (500 MHz, CDCl₃) spectrum for compound **5**.

Figure S23. 2D COSY NMR spectrum of compound **5**.

Figure S22. ¹³C NMR (126 MHz, CDCl₃) spectrum for compound **5**.
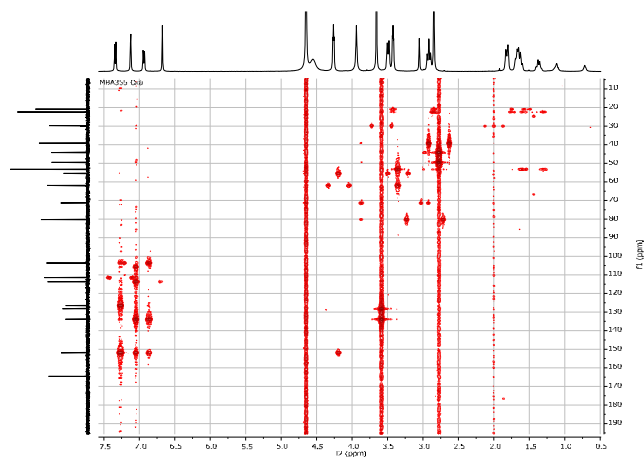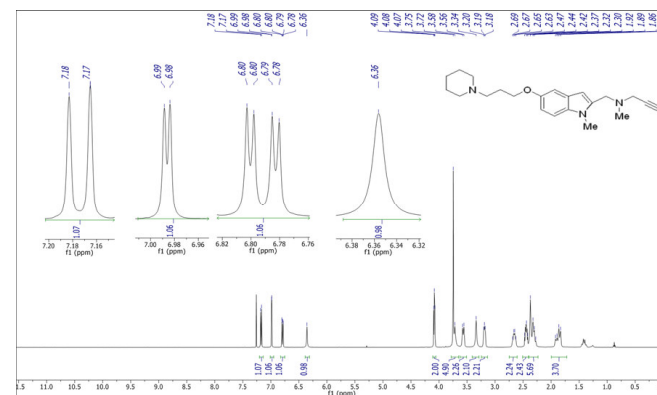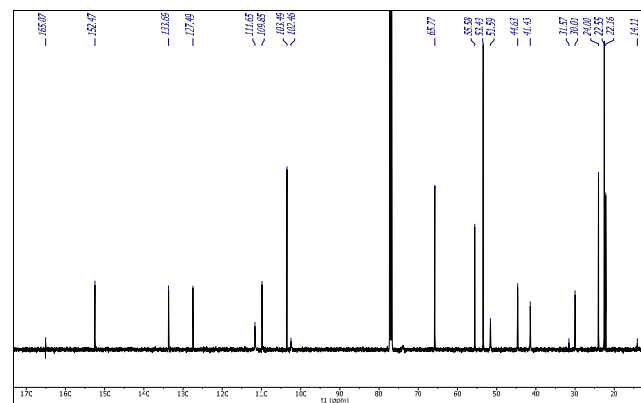

Figure S24. 2D HSQC NMR spectrum of compound **5**.

Figure S25. 2D HMBC NMR spectrum of compound **5**.

N-Methyl-N-((1-methyl-5-((1-methylpiperidin-4-yl)oxy)-1H-indol-2-yl)methyl)prop-2-yn-1-amine (6)

To a solution of PPh₃ (456 mg, 1.74 mmol) in dry THF (5 mL), under argon and at 0 °C, DIAD (0.34 mL, 1.74 mmol) was slowly added, and the mixture was stirred for 1 h; then, compound **8**[1] (200 mg, 0.87 mmol), followed by commercial 1-methylpiperidin-4-ol (100.8 mg, 0.87 mmol) were added, and stirred for 48 h at rt. The solvent was evaporated, and the crude purified by cromatography (hexane/AcOEt, 10-50%) affording compound **6** (62.7 mg, 22%) as an oil (Rf= 0.26, hexane/AcOEt, 60%), that has been transformed into the its bis-hydrochloride salt: m.p. 222-4 °C; IR (KBr) v 3433, 3189, 2955, 2558, 2505, 1619, 1575, 1529, 1481, 1427, 1409, 1344, 1288, 1250, 1241, 1208, 1159 cm⁻¹; ¹H and ¹³C NMR (see subsection, Table S1); MS (ESI) m/z: 326.3 (M+1)⁺. Anal. Calcd for $C_{20}H_{27}N_3O.2xHCl.H_2O$: C, 57.69; H, 7.50; N, 10.09. Found: C, 57.78; H, 7.37; N, 10.31.

NMR study of the bis-hydrochloride salt of compound 6
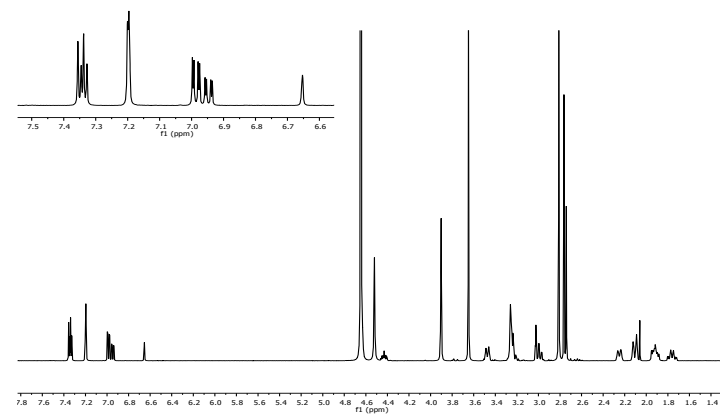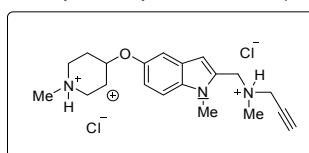
Figure S26. ¹H NMR (500 MHz, D₂O) spectrum of the bis-hydrochloride salt of compound **6**.
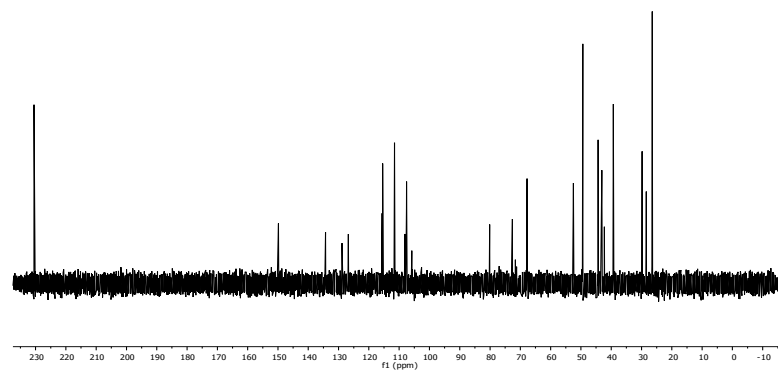
SUPPORTING INFORMATION
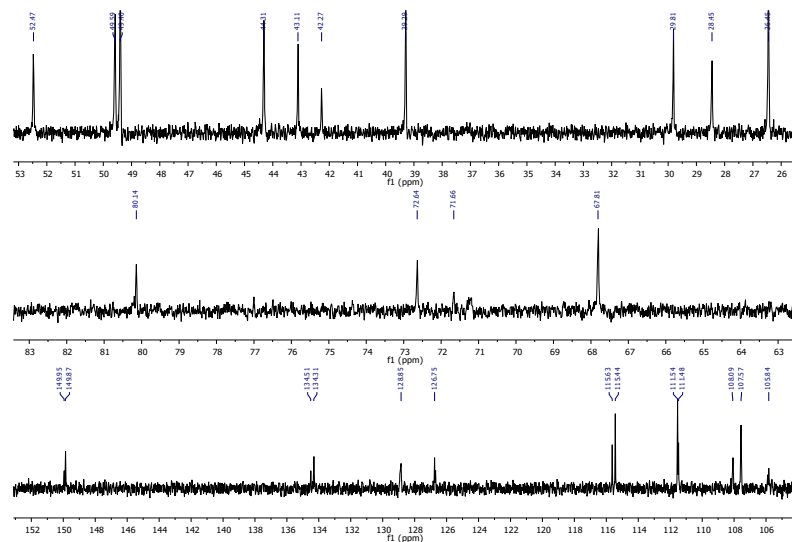
Figure S27. ^{13}C NMR (126 MHz, D$_2$O) spectrum of the bis-hydrochloride salt of compound **6**.

SUPPORTING INFORMATION
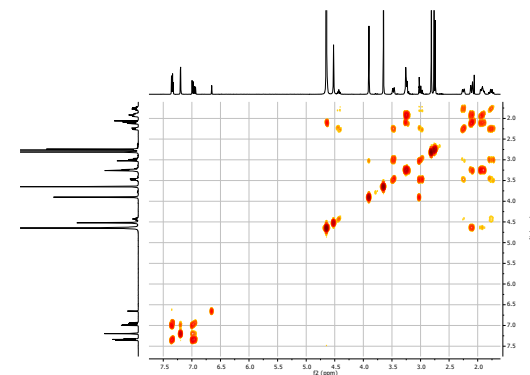
Figure S28. 2D COSY NMR spectrum of bis-hydrochloride salt of compound **6**.

gHSQC   gHMBC
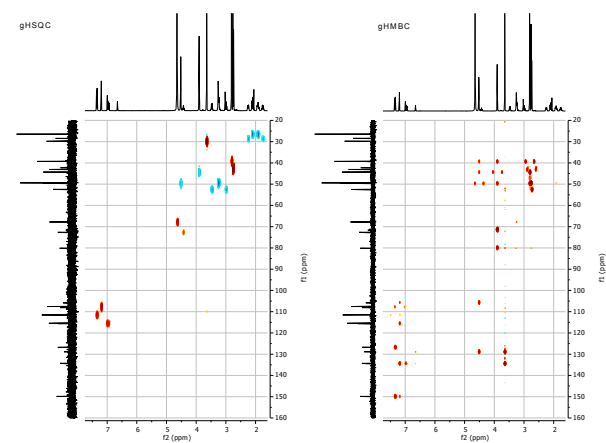
Figure S28. 2D HSQC and HMBC of bis-hydrochloride salt of of compound **6**.

^{1}H and ^{13}C NMR spectra of **6** bis-hydrochloride salt, in D$_2$O at 298 K, showed duplicate NMR signals in 1D ^{1}H and ^{13}C NMR spectra, indicating the presence of two quite different populated isomers at room temperature (ratio of 64:36), probably due to a mixture of *trans* and *cis* forms. Next, a full NMR study of this compound has been carried out. So, structural determination by NMR was performed on both isomers by the combined use of 1D and 2D [^{1}H,^{1}H] and [^{1}H−^{13}C] NMR experiments (gCOSY, NOESY, multiplicity-edited gHSQC and gHMBC). NMR spectra were recorded at 298 K, using D$_2$O as solvent, on a Varian SYSTEM 500 NMR

spectrometer (^{1}H 500 MHz, ^{13}C 126 MHz) equipped with a 5-mm HCN cold probe. Chemical shifts of ^{1}H (δ_H) and ^{13}C (δ_C) in ppm were determined relative to an external standards of sodium [2,2,3,3,3-^{2}H$_4$]-3-(trimethylsilyl)-propanoate in D$_2$O (δ_H 0.00 ppm) and 1, 4-dioxane (δ_C 67.40 ppm) in D$_2$O, respectively. One-dimensional (1D) NMR experiments (^{1}H and ^{13}C) were performed using standard Varian pulse sequences. Two-dimensional (2D) [^{1}H, ^{1}H] gCOSY NMR experiments were carried out with the following parameters: a delay time of 1 s, a spectral width of 1,675.6 Hz in both dimensions, 4,096 complex points in t2 and 4 transients for each of 128 time increments, and linear prediction to 256. The data were zero-filled to 4,096 × 4,096 real points. 2D [^{1}H–^{13}C] NMR experiments (gradient heteronuclear single-quantum coherence [gHSQC] and gradient heteronuclear multiple-bond correlation [gHMBC]) used the same ^{1}H spectral window, a ^{13}C spectral window of 30,165 Hz, 1 s of relaxation delay, 1,024 data points, and 128 time increments, with a linear prediction to 256. The data were zero-filled to 4,096 × 4,096 real points. Typical numbers of transients per increment were 4 and 16, respectively. ^{13}C NMR and ^{1}H NMR chemical shifts for the major and minor isomers of the **6** bis-hydrochloride salt are gathered in the Table S1. Relevant NOESY correlations are shown in figure S29.

Table S1. ^{13}C and ^{1}H chemical shifts (ppm) for the bis-hydrochloride salt of compound **6**.

Fragment	^{1}H		^{13}C	
	Major	Minor	Major	Minor
1	6.99	6.95	115.44	115.63
2	7.34	7.33	111.54	111.48
3	-	-	134.31	134.51
4	-	-	126.75	126.69
5	7.20	7.20	108.09	107.57
6	-	-	149.87	149.95
7	-	-	128.85	128.91
8	6.65	6.65	105.85	105.89
9	4.51	4.51	49.59	49.59
10	3.91	3.91	44.31	44.31
11	-	-	80.14	80.14
12			71.37	71.37
NMe-13	2.81	2.81	39.29	39.29
NMe-14	3.64	3.64	29.81	29.81
NMe-15	2.76	2.74	43.11	42.27
1'	4.64	4.43	67.81	72.64
2'a, 6'a	1.93	1.77	26.45	28.45
2'b, 6'b	2.10	2.24		
3'a, 5'a	3.24	3.47	49.40	52.47
3'b, 5'b	3.25	3.00		
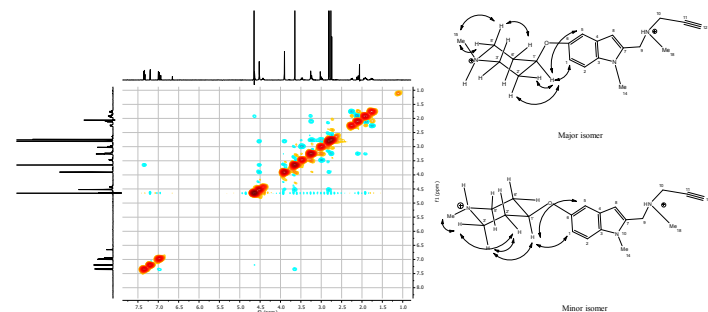
Figure S30. NOESY (500 MHz, D$_2$O) spectrum and NOESY relevant correlations for the bis-hydrochloride salt of compound **6**.

In order to understand and assign those spectra to the different isomers, we carried out a series of variable-temperature ^{1}H NMR experiments. Figure S31 illustrates the dependence on temperature of the ^{1}H NMR spectra, suggesting the existence of dynamic equilibrium. Finally, two EXSY experiments at 25 and 65 °C showed exchange correlation bands between two isomers only at 65 °C (Figure S32). The results showed the existence in solution of both isomers interconverting by a slow exchange on the NMR time-scale (Scheme S1).
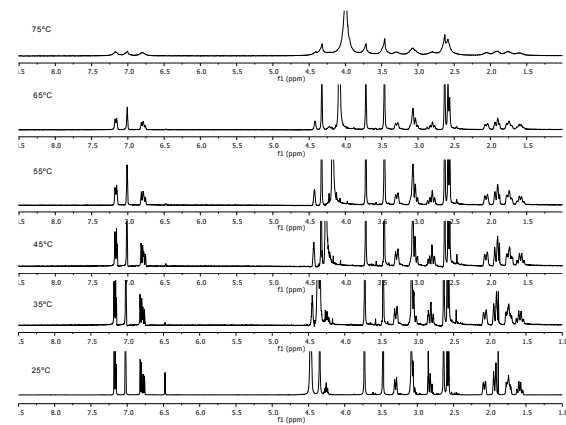
Figure S31. Variable temperature ^{1}H NMR spectra for the bis-hydrochloride salt of compound **6**.

^{13}C NMR (126 MHz, D$_2$O) δ 163.0, 152.2, 135.2, 127.7, 125.2, 116.3, 111.6, 109.4, 103.8, 65.7, 61.5, 54.4, 53.2 (2 C), 31.1, 23.4, 22.7 (2 C), 21.0, 13.3. Anal. Calcd for C$_{20}$H$_{28}$N$_2$O$_3$.2HCl: C, 57.56; H, 7.25; N, 6.71. Found: C, 57.82; H, 7.45; N, 6.51.
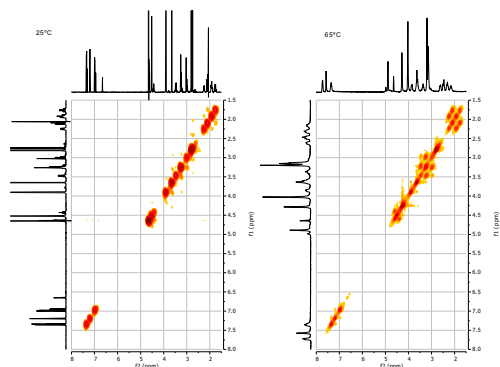
Figure S32. EXSY NMR spectra at 25 and 65 ºC for the bis-hydrochloride salt of compound **6**.
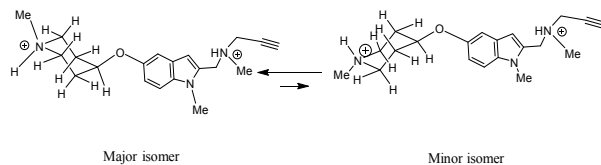
Scheme S1. Dynamic processes for the bis-hydrochloride salt of compound **6**.

Ethyl 1-methyl-5-(3-(piperidin-1-yl)propoxy)-1H-indole-2-carboxylate (7)

To a solution of compound **9**[2] (230 mg, 1.0 mmol) and 1-(3-chloropropyl)piperidine hydrochloride (200 mg, 1.0 mmol) in dry DMF, under argon, K$_2$CO$_3$ (557 mg, 4.0 mmol) was added. The mixture was stirred overnight at 90 ºC. The solvent was evaporated under reduce pressure, and water (10 mL) and commercial EtOAc (50 mL) were added to crude reaction mixture. The reaction pH was adjusted to 7-8, and the mixture was extracted with EtOAc, dried, filtered, evaporated, and purified by flash column chromatography (DCM/MeOH, 1-5%) to yield compound **7** (289, 80%) as a solid: Rf= 0.32, DCM/MeOH 10%); m.p. 200-4 ºC; IR (KBr) v 3427, 2942, 2483, 1710, 1470, 1224, 1089 cm^{-1}; ^{1}H NMR (500 MHz, CDCl$_3$) δ 7.26 (d, *J*= 8.8 Hz, 1H), 7.19 (s, 1H), 7.02 (d, *J* = 2.4 Hz, 1H), 6.95 (dd, *J* = 8.8, 2.4 Hz, 1H), 4.36 (q, *J*= 7.3 Hz, 2H), 4.09 (t, *J* = 5.5 Hz, 2H), 4.04 (s, 3H), 3.64-3.57 (m, 2H), 3.19 (t, *J*= 8.8 Hz, 2H), 2.66-2.64 (m, 2H), 2.49-2.44 (m, 2H), 2.33-2.31 (m, 2H), 1.87-1.85 (m, 3H), 1.41-1.38 (m, 1H), 1.39 (t, *J* = 7.3 Hz, 3H); ^{13}C NMR (126 MHz, CDCl$_3$) δ 162.1, 153.0, 135.3, 128.5, 125.9, 116.2, 111.2, 109.3, 103.7, 65.4, 60.5, 55.5, 53.4 (2 C), 31.7, 23.9, 22.5 (2 C), 22.1, 14.3; MS (ESI) *m/z*: 345.2 (M+1)$^+$. HRMS. Calcd for C$_{20}$H$_{28}$N$_2$O$_3$: 345.2173. Found: 345.2183. Compound **7** has been transformed into its bis-hydrochloride salt: m.p. 210-2 ºC; ^{1}H NMR (500 MHz, D$_2$O) δ 7.04 (d, *J*= 6.3 Hz, 1H), 6.84 (s, 1H), 6.80 (d, *J* = 1.4 Hz, 1H), 6.79 (dd, *J* = 6.3, 1.4 Hz, 1H), 4.06 (q, *J*= 7.3 Hz, 2H), 3.89 (t, *J* = 5.4 Hz, 2H), 3.48 (s, 3H), 3.37-3.34 (m, 2H), 3.08 (t, *J*= 7.8 Hz, 2H), 2.72-2.70 (m, 2H), 2.03-1.99 (m, 2H), 1.77-1.56 (m, 5H), 1.32-1.30 (m, 1H), 1.18 (t, *J* = 7.3 Hz, 3H);
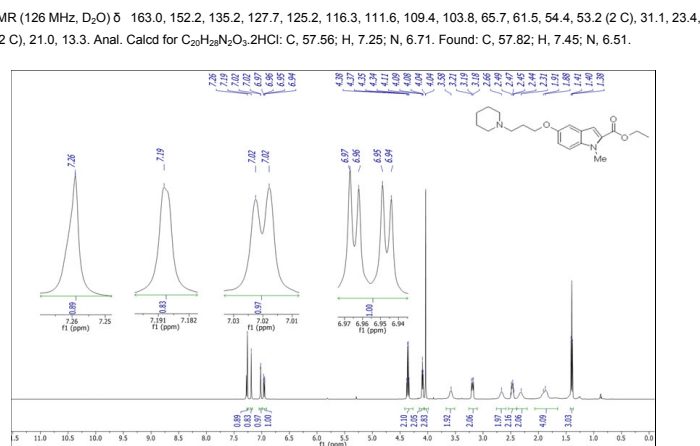
Figure S33. ^{1}H NMR (500 MHz, CDCl$_3$) spectrum of compound **7**.
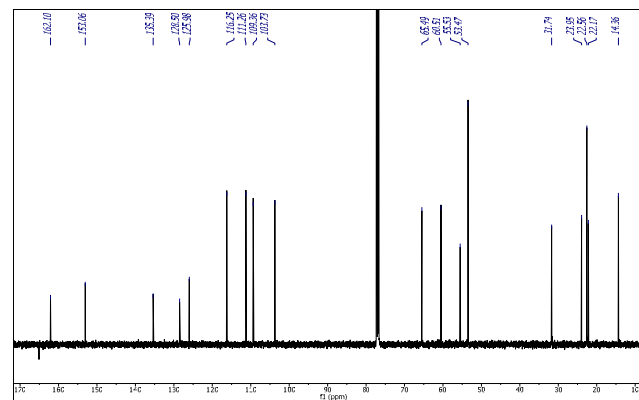
Figure S34. ^{13}C NMR (126 MHz, CDCl$_3$) spectrum of compound **7**.
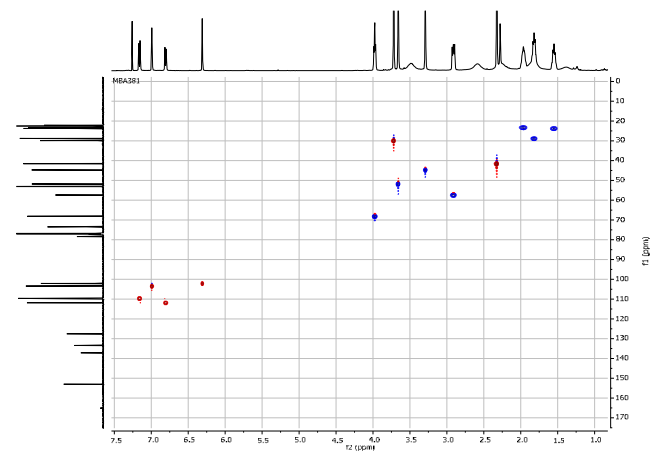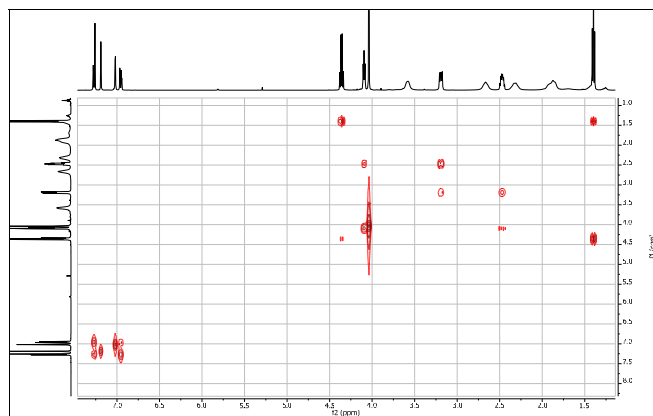
Figure S35. 2D COSY spectrum of compound **7**.
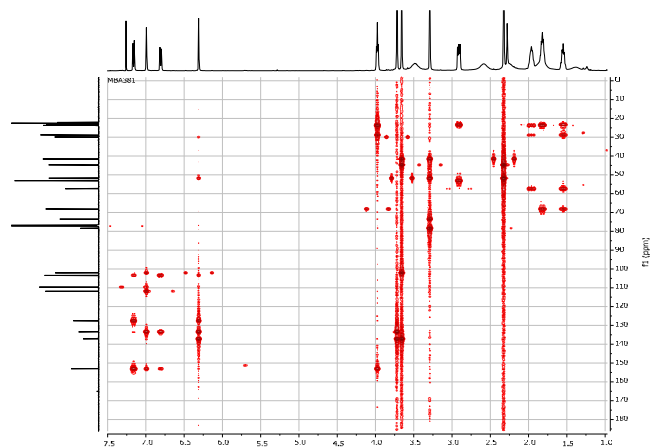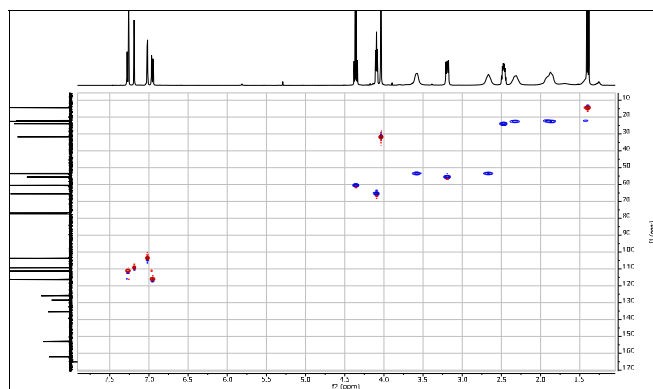

Figure S36. 2D HSQC spectrum of compound **7**.
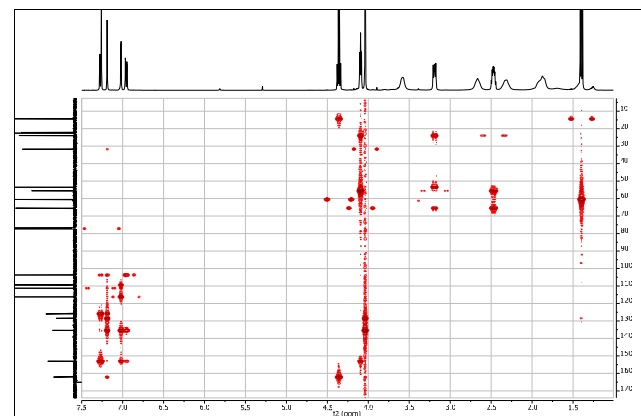
Figure S37. 2D HMBC spectrum of compound **7**.

Pharmacological testing: Experimental procedures

Enzyme inhibition studies

Human MAO A/B

The activity for human recombinant membrane-bound monoamine oxidase A/B (MAO A/B) (Sigma-Aldrich, UK) in 50 mM potassium phosphate buffer pH 7.5 was determined from the production of hydrogen peroxide, coupled to the dye Ampliflu Red (Sigma-Aldrich, UK) at a final concentration of 50 µM via horseradish peroxidase (2.5 U/mL) producing the fluorescent resorufin that was measured in a fluorescence plate-reader (Molecular Devices FilterMax F5) at 30°C.[3–5] Under the conditions used, the K_m for tyramine with MAO A was 0.4 mM and for MAO B was 0.16 mM. The compounds neither quenched the fluorescence of the product, resorufin, nor inhibited the coupling enzyme, horseradish peroxidase.[6] The IC_{50} values for MAO A and B were determined for the compounds (>10 concentrations in duplicate) without and with pre-incubation for 30 min at 30°C. IC_{50} values were determined from the rates with varied inhibitor concentrations in the presence of $2xK_m$ substrate concentration with the enzyme added last for time 0 min, or with the substrate and dye mix added last after pre-incubation of enzyme and inhibitor for 30 min. The data were analysed using the three-parameter equation implemented in GraphPad Prism 4 (San Diego, USA). At least two separate determinations were made for each value reported. The irreversibility of the inactivation by chosen compounds was demonstrated by incubating $10xIC_{50}$ with MAO A or B at 30°C for 30 min or 60 min before diluting the mix 50-fold into assay buffer to give a final concentration of $0.5xIC_{50}$ of inhibitor, 1 mM tyramine substrate, 50 uM Ampliflu Red and horseradish peroxidase as the coupling enzyme.

Human AChE/BuChE

The acetylcholinesterase (AChE; EC 3.1.1.7) and butyrylcholinesterase (BuChE; EC 3.1.1.8) (Sigma-Aldrich, UK) inhibitory activity of the tested drugs was determined using Ellman´s method using human recombinant AChE or human plasma BUChE, with acetylthiocholine iodide as the substrate.[7] Briefly, all the assays, performed in triplicates, were carried out in 0.1 M KH_2PO4/K_2HPO_4, pH 7.5. The activity was determined at 412 nm at 30°C using a multi-mode plate reader (Molecular Devices FilterMax F5). The data obtained from at least two independent experiments were analysed using a three-parameter equation implemented in GraphPad Prism 4 (San Diego, USA).

Radioligand depletion assay

Human H3R

HEK-293 cells stably expressing the hH3R were washed and harvested with PBS buffer. They were centrifuged (3,000 xg, 10 min, 4°C) and homogenized with an Ultraturrax® Homogenizer in ice-cold H3R binding buffer (12.5 mM MgCl2, 100 mM NaCl and 75 mM Tris/HCl, pH 7.4). The cell membrane homogenate was centrifuged (20,000 xg, 20 min, 4°C), the pellet obtained was resuspended in the binding buffer and stored at -80°C until use.[8] Before starting experiments cell membranes were thawed, homogenized by sonication at 4°C and kept in ice-cold binding buffer. Crude membrane extracts (20 µg/well in a final volume of 0.2 ml binding buffer) were incubated with [3H]-N-alpha-methylhistamine (2 nM; 78.3 Ci/mmol) and different concentrations of test ligand. Assays were run at least in duplicates with appropriate concentrations between 0.01 nM and 100 µM of the test compound. Incubations were performed for 90 min at room temperature while shaking continuously. Nonspecific binding was determined in the presence of 10 µM pitolisant. The bound radioligand was separated from free radioligand by filtration through GF/B filters pre-treated with 0.3% (m/v) polyethyleneimine using a cell harvester. Radioactivity was determined by liquid scintillation counting. Data were analyzed by the software GraphPad Prism 6 (San Diego, USA) using non-linear regression fit.

Human H4R

Sf-9 cells were co-infected with baculoviruses containing the hH4R, the G-protein Gα2 and Gβ1γ2 subunits for 48 h. Infected cells were centrifuged (1,000 xg, 10 min, 4°C) and washed with H4R binding buffer (12.5 mM MgCl2, 1 mM EDTA and 75 mM Tris/HCl, pH 7.4). For cell lysis cells were resuspended in ice-cold lysis buffer (10 mM Tris/HCl (pH 7.4), EDTA 1 mM, phenylmethylsulfonyl fluoride 0.2 mM, benzamidine 10 µg/mL and leupeptin 10 µg/mL) and homogenized in a hand potter. The cell membrane homogenate was centrifuged (18,000 xg, 20 min, 4°C), the pellet obtained was resuspended in the binding buffer and stored at -80°C until use.[8,9] Before starting experiments cell membranes were thawed, homogenized by sonication at 4°C and kept in ice-cold binding buffer. Membranes (40 µg/well in a final volume of 0.2 ml binding buffer) were incubated with [3H]-Histamine (10 nM; 10.6 Ci/mmol) and different concentrations of test ligand. Assays were run in triplicates with appropriate concentrations between 100 nM and 100 µM for in case of compound **7** and **4** (contilisant). All other compounds were run as one-point measurements in triplicates with a test concentration of 100 µM, calculating percent inhibition relative to total radioligand binding. Incubations were performed for 60 min at room temperature. Nonspecific binding was determined in the presence of 100 µM JNJ7777120. Following steps were performed as described above for hH3R.

Human H1R

CHO cells stably expressing the human histamine H1 receptor were washed and harvested with PBS buffer. Cells were centrifuged homogenized by sonication (3x15 sec) in ice-cold HEPES-H1R binding buffer (20 mM HEPES, 10 mM MgCl2, 100 mM NaCl). The cell homogenate was centrifuged (20,000 xg, 30 min, 4°C), the pellet obtained was resuspended in the binding buffer, homogenized using a handpotter and stored at -80°C until use. Before starting experiments cell membranes were thawed, homogenized by sonication at 4°C and kept in ice-cold binding buffer. Membranes (40 µg/well in a final volume of 0.2 ml binding buffer) were incubated with [3H]-Pyrilamine (1 nM; 27 Ci/mmol) and different concentrations of test ligand. Assays were run at least in duplicates with appropriate concentrations between 1 nM and 100 µM of the test compound. Incubations were performed for 120 min at room temperature. Nonspecific binding was determined in the presence of 10 µM Chlorpheniramine. Following steps were performed as described above for hH3R.

Human D2SR and D3R

CHO cells stably expressing the human dopamine D3 and D2short receptor were washed and collected with PBS buffer. Crude membrane extracts were obtained as described for human H3R expressing HEK cells by using ice-cold D2R/D3R binding buffer (10 mM MgCl2, 10 mM CaCl2, 5 mM KCl, 120 mM NaCl and 50 mM Tris, pH 7.4). Before starting experiments cell membranes were thawed, homogenized by sonication at 4°C and kept in ice-cold binding buffer. Crude membrane extracts (25 and 20 µg/well in a final volume of 0.2 ml binding buffer for D2SR and D3R, respectively) were incubated with [3H]-Spiperone (0.2 nM; 15.2 Ci/mmol) and different concentrations of test ligand for 120 min. Assays were run at least in duplicates with appropriate concentrations

between 1 nM and 100 µM of the test compound. Nonspecific binding was determined in the presence of 10 µM Haloperidol. Following steps were performed as described above for human H3R.

Human D1R and D5R

CHO cells stably expressing the human dopamine D1 and D5 receptor were washed and collected with PBS buffer. Crude membrane extracts were obtained as described for human D2SR and D3R. Crude membrane extracts (20 and 10 µg/well in a final volume of 0.2 ml binding buffer for D1R and D5R, respectively) were incubated with [3H]-SCH23390 (0.3 nM; 82.9 Ci/mmol) and different concentrations of test ligand. Assays were run at least in duplicates with appropriate concentrations between 1 nM and 100 µM of the test compound. Nonspecific binding was determined in the presence of 100 µM Fluphenazin. Following steps were performed as described above for hH3R.

Antioxidant analysis

The antioxidant activity of the selected compounds was determined by the oxygen radical absorbance capacity-fluorescein (ORAC-FL) method[10,11] using 2,2'-azobis-(amidinopropane) dihydrochloride (AAPH) as generator of peroxyl radicals at 37 °C. The reaction was carried out at 37 °C in 75 mM phosphate buffer (pH 7.4). Firstly, a solution of antioxidant (20 µL) and fluorescein (FL, 120 µL, final concentration of 70 nM) were incubated in a black 96-well microplate (Nunc) for 15 min at 37 °C into a Varioskan Flash plate reader with built-in injectors (Thermo Scientific). Then, 2,2'-azobis(amidinopropane) dihydrochloride (AAPH, 60 µL, final concentration of 12 mM) solution was added quickly using the built-in injector and the fluorescence was measured every minute for 60 min at λ_{ex}= 485 nm and λ_{em}= 535 nm. The blank composed of 120 µL of FL, 60 µL of AAPH and 20 µL of phosphate buffer (pH 7.4) was carried out in each assay. The Trolox was used as standard with 1–8 µM as final concentration and the samples measured at different concentrations 0.1–1 µM. All assays were tested in triplicate and at least three different assays were conducted for each sample. Fluorescence measurement was first normalized to the curve of the blank (without antioxidant and the area under the fluorescence decay curve (AUC) was calculated as:

$$AUC= 1 + sum(f_i/f_0),$$

where f_0 is the initial fluorescence at 0 min and f_i is the fluorescence at time i. The netAUC for each the sample was calculated as follows:

$$netAUC= AUC_{antioxidant} − AUC_{blank}.$$

The regression equations were extrapolated by plotting the netAUC against the concentration of the antioxidant. The ORAC values corresponds to the ratio of slopes of the latter curve and Trolox in the same assay. Final ORAC values were expressed as Trolox equivalents (TE) and data are expressed as means ± standard deviation (SD), with ferulic acid (3.74±0.22 TE) used as positive control.[12]

PAMPA analysis

In order to predict passive blood-brain penetration of novel compounds modification of the parallel artificial membrane permeation assay (PAMPA) has been used based on reported protocol.[13,14] The filter membrane of the donor plate was coated with PBL (Polar Brain Lipid, Avanti, USA) in dodecane (4 µl of 20 mg/ml PBL in dodecane) and the acceptor well was filled with 300 µl of PBS pH 7.4 buffer (V_D). Tested compounds were dissolved first in DMSO and diluted with PBS pH 7.4 to reach the final concentration 100 µM in the donor well. Concentration of DMSO did not exceed 0.5% (V/V) in the donor solution. Next, 300 µl of the donor solution was added to the donor wells (V_A) and the donor filter plate was carefully put on the acceptor plate so that coated membrane was "in touch" with both donor solution and acceptor buffer. Test compound diffused from the donor well through the lipid membrane (Area=0.28cm2) to the acceptor well. The concentration of the drug in both donor and the acceptor wells was assessed after 3, 4, 5 and 6 h of incubation in quadruplicate using the UV plate reader Synergy HT (Biotek, USA) at the maximum absorption wavelength

of each compound. Concentration of the compounds was calculated from the standard curve and expressed as the permeability (Pe) according the equation (1):[15,16]

$$\log P_e = \log \left\{ C \times -ln \left(1 - \frac{n_{acceptor}}{n_{total}}\right) \right\} \ where \ C = \left(\frac{V_D \times V_A}{(V_D + V_A) \times Area \times time} \right)(1)$$

Molecular modelling

Docking analysis on AChE/BuChE, MAO A/B and H3R of ASS234 and contilisant

For a complete picture of the multi-target compound ASS234 and the new identified contilisant (**4**) a binding mode prediction was carried out. For four targets, histamine H3 receptor (H3R), acetylcholinesterase (AChE), monoamine oxidase A (MAO A) and monoamine oxidase B (MAO B), the binding mode for ASS234 and contilisant was predicted using the software MOE 2015.[17] All energy minimization steps were conducted using the default force field settings Amber10:EHT, if not defined differently.

The crystal structure 4EY7 was used as the complex structure of AChE. This structure was chosen due to the same scaffold benzylpiperidine of the crystalized ligand (donepezil) and compound ASS234. The structure of 4EY7 was loaded into MOE and complex preparation steps were performed using the "QuickPrep" function. These steps include a protonation step as well as an energy minimization step for the ligand and receptor atoms in an 8 Å surrounding. The binding modes of ASS234 and contilisant were predicted using the docking function in MOE. Since the benzylpiperidine moiety was identified as key for the inhibition of AChE, a pharmacophore driven approach for binding mode prediction was used. A pharmacophore point (cationic and hydrogen donor properties) was placed on the positively charged nitrogen atom in the piperidine moiety. Docking was carried out using default settings leading to the proposed binding modes.

The crystal structure 4CRT was used as the complex structure of MAO B. This structure was chosen since the crystalized ligand is ASS234. Although the resolution of 1.8 Å is pleasing the benzylpiperidine moiety was only partly resolved.[5] Therefore, the benzylpiperidine group for ASS234 was manually added using the "Build" tool in MOE. For contilisant the piperidine group was added using the same tool. In dependence on the MAO A procedure minimization was carried out. For the energy minimization steps the ligand was constrained from the ether bridge to the cofactor FAD well as the rest of the receptor atoms and solvent atoms not included in the ligand surrounding (9 Å). Only the added ligand parts for ASS234 and contilisant as well as the surrounding receptor atoms were energy minimized leading to the proposed binding modes.

The crystal structure 2BXR was used as the complex structure of MAO A. This structure was chosen due to the same scaffold methylpropargyl amine of the crystalized ligand (clorgyline) and ASS234 as well as contilisant. The structure of 2BXR was loaded into MOE and complex preparation steps were performed using the "QuickPrep" function according to AChE. Since the two compounds of interest are going to bind covalently to the cofactor FAD in the MAO A structure (due to the alkyne moiety) a conventional docking procedure was not possible. Due to the fact of the same methylpropargy lamine scaffold a simple modification of the crystalized ligand structure to the desired compounds (ASS234 and contilisant) was carried out. This modification was achieved using the "Builder" tool in MOE. Followed by a ligand energy minimization step where the receptor, solvent, cofactor as well as the covalently bond methylpropylamine moiety was constrained. In the next energy minimization, the ligand and its surrounding receptor atoms and solvent atoms (9 Å) were unfixed to allow this part of the complex to relax (OH bond length fixed, rigid water molecules, planar systems were considered rigid bodies). The compound composition and the two minimization steps were used for the predicted binding mode of ASS234 and contilisant to MAO A.

The structure of the human histamine H3 receptor has not been determined yet. Therefore, a homology model had to be built for binding mode prediction of ASS234 and contilisant. The crystal structure of histamine H1 receptor (3RZE) was chosen as a template for the homology model. The H3R amino acid sequence was taken from www.uniprot.org (identifier: Q9Y5N1-1) in fasta format. Using the template structure 3RZE and the H3R sequence a series of homology models (10) were build using the standard MOE workflow and the "Homology Model" tool in MOE. Different force fields were tested to obtain an optimal homology model for H3R. The Amber99 force field led to best agreement with the template structure H1R. An overall RMSD of 1.51 Å was achieved. Only

taking the seven transmembrane helices into account an RMSD of 0.68 Å was obtained. Based on the generally accepted tertiary basic amine key motive a pharmacophore driven approach for binding mode prediction was used. A pharmacophore point (cationic and hydrogen donor properties) was placed on the positively charged nitrogen atom of the crystalized ligand doxepin. Docking was carried out using pharmacophore placement and induced fit refinement leading to the proposed binding modes.

The structure of the murine histamine H3 receptor (mH3R) has not been determined jet. As described for the human H3 receptor, a homology model was built using the crystal structure of histamine H1 receptor (3RZE). The murine H3R amino acid sequence was taken from www.uniprot.org (identifier: P58406) in fasta format. Using the template structure 3RZE and the H3R sequence a series of 5 homology models were build using the default MOE workflow and the "Homology Model" tool in MOE. Different force fields were tested to obtain an optimal homology model for mH3R. The Amber99 force field led to best agreement with the template structure H1R. Taking the seven transmembrane helices into account an RMSD of 0.85 Å was obtained. The binding mode of contilisant in the human H3R homology model was used as a starting binding mode. Sequence identity between human and mouse H3R is 94%. The same amino acids are involved in binding. After placing contilisant in the binding pocket, energy minimization was carried out solely on contilisant (fixed receptor atoms).

Docking analysis on human BuChE of contilisant

Protonated contilisant was assembled within Discovery Studio, version 2.1, software package, using standard bond lengths and bond angles. With the CHARMm force field[18] and partial atomic charges, the molecular geometry of contilisant (**4**) was energy-minimized using the adopted-based Newton-Raphson algorithm. Structure was considered fully optimized when the energy changes between iterations were less than 0.01 kcal mol⁻¹.[19] The coordinates of hBuChE (PDB ID: 4BDS), were obtained from the Protein Data Bank (PDB). For docking studies, initial protein was prepared by removing all water molecules, heteroatoms, any co-crystallized solvent and the ligand. Proper bonds, bond orders, hybridization and charges were assigned using protein model tool in Discovery Studio, version 2.1, software package. CHARMm force field was applied using the receptor-ligand interactions tool in Discovery Studio, version 2.1, software package. Docking calculations were performed with the program Autodock Vina.[20] AutoDockTools (ADT; version 1.5.4) was used to add hydrogens and partial charges for proteins and ligands using Gasteiger charges. The box center was defined and the docking box was displayed using ADT. The docking procedure was applied to the whole protein target, without imposing the binding site ("blind docking"). A grid box of 66 x 66 x 70 with grid points separated 1 Å, was positioned at the middle of the protein (x=136.0; y=123.59; z=38.56). Default parameters were used except num_modes, which was set to 40. The lowest docking-energy conformation was considered as the most stable orientation. Finally, the docking results generated were directly loaded into Discovery Studio, version 2.1. Two dimensional figures of the contilisant-enzyme interactions were groomed using DS 2.1.

Neuroprotection analysis

SH-SY5Y cell culture

Human dopaminergic neuroblastoma SH-SY5Y cell line was obtained from Sigma-Aldrich (Madrid, Spain). The cells were maintained in a 1:1 mixture of Nutrient Mixture F-12 and Eagle´s minimum essential medium (EMEM) supplemented with 15 nonessential amino acids, 1 mM sodium pyruvate, 10% heat-inactivated FBS, 100 units/ml penicillin, and 100 µg/ml streptomycin. Cultures were seeded into flasks containing supplemented medium and maintained at 37 °C in a humidified atmosphere of 5% CO₂ and 95% air. For assays, SH-SY5Y cells were sub-cultured in 96-well plates at a seeding density of 5x10⁴ cells per well for two days. The cells were then incubated with 30 µM Rotenone and 10 µM Oligomycin-A (R/O), Okadaic Acid (20 nM), or Aβ₂₅₋₃₅ peptide (30 µM) (Sigma-Aldrich, Spain) with or without compounds at different concentrations for 24 h. In this study, all cells were used at a low passage number (<14).

MTT assay and cell viability

Cell viability was measured by quantitative colorimetric assay with 3-[4,5 dimethylthiazol-2-yl]-2,5-diphenyl-tetrazolium bromide (MTT) (Sigma Aldrich, Spain), as described previously (PMID: 3486233). Briefly, 10 µL of the MTT labeling reagent, at a final concentration of 0.5 mg/mL, was added to each well at the end of the incubation period and the plate was placed in a humidified

SUPPORTING INFORMATION

incubator at 37 °C with 5% CO_2 and 95% air (v/v) for an additional 1 h period. Then, the medium was replaced and the insoluble formazan was dissolved with dimethylsulfoxide (DMSO). Colorimetric determination of MTT reduction was measured at 540 nm. Control cells treated with MEM/F12 were taken as 100% viability.

Statistical analysis

Statistically significant differences between groups were determined by a one-way analysis of variance (ANOVA) followed by a Tukey post hoc analysis. The level of statistical significance was taken at $P< 0.05$.

In vivo studies of ASS234 and contilisant

Novel object recognition test

Novel object recognition (NOR) test was used as a benchmark task for assessing recognition memory. Animals were placed for 10 min on a field (40×40×40 cm made up of polyvinyl chloride) during three consecutive days. On the 1st day (**T0**), mice explored the empty box. On the 2nd day (**T1**), animals were placed on the field with two identical objects (cylindrical glass bottles, heavy enough to prevent mice from moving; height, 22 cm; diameter, 9 cm) and they were allowed to explore them for 10 min. On the 3rd day (**T2**), a new object (novel) was placed on the site of the old object (familiar). Exploration of the objects was timed with stopwatches when subjects sniffed at, whisked at, or looked at the objects from no more than 2 cm away. All locations for the objects were counterbalanced among groups, and objects and field were washed with 0.1% acetic acid between trials to equate olfactory cues. The amount of time spent investigating the novel or familiar object was video recorded for 10 min and evaluated by a blinded observer. Discrimination index in the **T2** were estimated as follows: Discrimination Index (DI) = [Time exploring novel object - Time exploring familiar object) / (Time exploring novel object + Time exploring familiar object)].[21] Hence, if DI is 1, the animals spent all time on the novel object. A DI value of 0 is achieved when animals spent the same time on the two objects (no discrimination). A negative value could be obtained if animals spent more time on the familiar object, with a maximum value of -1 for spending the whole time on the familiar object. Data were normalized to vehicle control (vehicle discrimination index for this C57/B16J mice cohort (0.54) was normalized to 1.00) (Table S2). LPS (250 μg/kg) alone or in the presence of compound contilisant or ASS234 (1 mg/kg) were injected intraperitoneally just after the end of **T1** phase.

Table S2. Discrimination indices (DI) for ASS234 and contilisant of novel object recognition test in lipopolysaccharide (LPS)-treated mice.

	Treatment	Discrimination index	Normalized Discrimination index[a]
		x̄ ± SD	x̄ ± SD
	Vehicle control	0.54 ± 0.10	1.00 ± 0.18
LPS 250 μg/kg	-	0.24 ± 0.07	0.44 ± 0.12
	ASS234 1 mg/kg i.p.	0.30 ± 0.09	0.54 ± 0.16
	Contilisant 1 mg/kg i.p.	0.39 ± 0.12	0.71 ± 0.23

[a] No discrimination between novel and familiar object (DI = 0) was set to 0, while vehicle control (=0.54) was set to 1.00 for normalization; SD, standard deviation.

SUPPORTING INFORMATION

Statistical analysis

Statistically significant differences between groups (compared to LPS-treated) were determined by a one-way analysis of variance (ANOVA) followed by a Dunnett´s multiple comparison analysis. The level of statistical significance was taken at $P< 0.05$.

ADME prediction of compounds 1-7

The druggability of compounds **1-7** has been investigated by calculating their absorption, distribution, metabolism and elimination (ADME) properties, using the QikProp module of Schrodinger suite (QikProp, version 3.8, Schrodinger, LLC, New York, NY, 2013). About 45 physically significant descriptors and pharmacologically relevant properties of compounds **1-7** were predicted and some of the important properties were analyzed.

Pharmacological testing: Results and Discussion

Irreversibility of MAO inactivation

The irreversibility of the inactivation by the propargylamines ASS234 and compound **4** (contilisant) was demonstrated by incubating $10xIC_{50}$ with MAO A or B for 30 or 60 min before diluting the mix 50-fold into assay buffer (Figure S38). As expected, compound **7**, lacking the propargyl group, show complete recovery of MAO activity after 50x dilution suggesting a total reversible inhibition behavior (Figure S38).
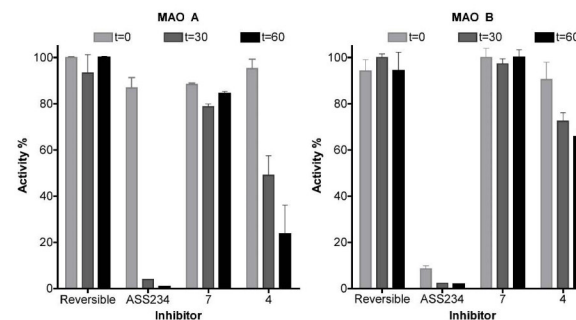
Figure S38. Activity of MAO after preincubation with reversible and irreversible inhibitors.

Additional in vitro characterization of ciproxifan and contilisant

As most promising multitarget-directed ligand within these small series of compounds, contilisants (**4**) selectivity for the human H3R over other GPCRs were determined in radioligand binding studies (Table S3). Contilisant shows no affinity for other histamine and dopamine receptor subtypes tested (K_i > 1000 nM).

Table S3. Additional binding affinities of contilisant and ciproxifan at different human histamine (hH1R/hH2R) and dopamine receptor subtypes (hD1R/hD5R/hD2R/hD3R).

MTDL	H H1R K_i (nM)	hH2R K_i (nM)	hD1R K_i (nM)	hD5R K_i (nM)	hD2SR K_i (nM)	hD3R K_i (nM)
Contilisant	>1000		>1000	>1000	>1000	>1000
Ciproxifan	>10 000[22]	>10 000[22]				

PAMPA analysis

Penetration across the blood brain barrier (BBB) is an essential property for compounds targeting the central nervous system (CNS). Prediction of BBB penetration for selected compounds is summarized in Table S4. Based on the obtained data, ASS234, contilisant (**4**) and compound **2** all show high probability for crossing the BBB via passive diffusion. Data obtained (Pe values) for the new compounds are correlated to those from standard CNS drugs available. Our data show high resemblance with previously reported penetrations of standard drugs as well as with a general knowledge about the availability in the CNS in vivo [13,14].

Table S4. Prediction of blood-brain barrier penetration of drugs expressed as Pe ± SEM (n=3).

Compound	BBB penetration estimation	
	Pe ± SEM (*10^{-6} cm s^{-1})	CNS (+/-)
ASS234	7.85 ± 0.73	CNS (+)
Contilisant (**4**)	8.50 ± 0.32	CNS (+)
2	7.67 ± 0.31	CNS (+)
Donepezil	7.3 ± 0.9	CNS (+)
Rivastigmine	6.6 ± 0.5	CNS (+)
Testosterone	11.3 ± 1.6	CNS (+)
Chlorpromazine	5.1 ± 0.3	CNS (+)
Cefuroxim	2.7 ± 0.1	CNS (-)
Piroxicam	2.2 ± 0.15	CNS (-)
Obidoxime	0.46 ± 0.2	CNS (-)
Atenolol	1.02 ± 0.37	CNS (-)

Molecular Modelling

Docking analysis on AChE/BuChE, MAO A/B and H3R

The molecular docking studies support the in vitro binding studies for hAChE/hBuChE, hMAO A/B and hH3R, since both ASS234 and contilisant sufficiently fit all binding pockets (Figure S39). The higher efficacy of ASS234 for MAO A inhibition could be explained by occupying more energetically favorable-site occupancy compared to that of contilisant, due to its enlarged western part with additional aromatic bindings (Figure S39, E and F). We could also demonstrate that contilisant fits not only the hH3R binding pocket (Figure S39, G and H), but also the binding pocket of the murine H3R (Figure S40). Human and rodent H3Rs share about 94% identical residues, while all binding site residues are identical (Figure S40). Residues 119 and 122 in transmembrane region III differ between human and rodent H3Rs, being critically involved in H3R ligand species-specificity, but are more than 4Å away from the binding site.[23–25] Direct comparison of contilisant fitting these two binding sites most probably suggest comparable binding properties at rodent H3R and the hH3R. The higher human H3R affinity of contilisant might be a result of the more accessible basic amine, involved in ionic interactions with the conserved aspartate (Asp114). Due to the lack of a hH3R crystal structure, a homology model was build based on doxepin-docked H1R crystal structure by taking advantage of the general accepted non-imidazole H3R antagonist/inverse agonist pharmacophore. Thus, contilisant fitting the designed binding pocket might indicate rather antagonistic properties. Early studies on H3R agonists already showed, that the 4-imidazolyl residue is mandatory for H3R agonism, confirming that the non-imidazole compounds contilisant and ASS234 most probably act as antagonists/inverse agonists.
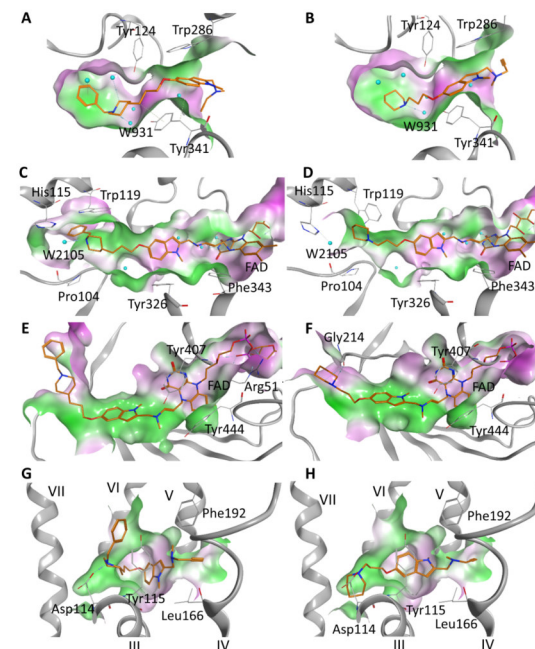
Figure S39. Binding modes of ASS234 (A, C, E, G) and contilisant (B, D, F, H) proposed by molecular modelling. A,B: AChE; C,D: MAO B; E,F: MAO A; G,H: H3R. Ligands are displayed as orange sticks, amino acid residues as gray lines, water molecules as cyan spheres, protein backbone as gray tubes. Molecular surface of the binding site is colored by lipophilicity (green: lipophilic; magenta: hydrophilic).
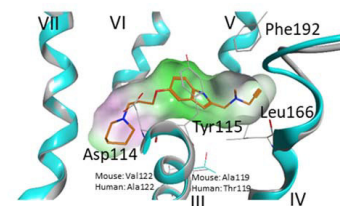
Figure S40. Binding mode of contilisant proposed by molecular modelling. Comparison between human (cyan) and mouse (grey) H3R. Ligands are displayed as orange sticks, amino acid residues as gray lines, protein backbone as gray tubes. Molecular surface of the binding site is colored by lipophilicity (green: lipophilic; magenta: hydrophilic).

SUPPORTING INFORMATION

Docking analysis on human BuChE of contilisant

Contilisant protonated in the nitrogen atom of the piperidine moiety was modeled into the structure of hBuChE (PDB: 4BDS) and all the experiments were performed as blind dockings. The blind docking technique was used for the detection of possible binding sites and modes of peptide ligands, by scanning the entire surface of protein targets, so that a location with the highest binding affinity on the proteins may be found. Docking simulations were carried out using AutoDock Vina.[20]

Analysis of the binding modes revealed that compound contilisant could bind to hBuChE in two modes (Mode I and Mode II) (Figure S41 and S42). In both modes the ligand is accommodated inside the binding pocket interacting with the catalytic triad residue His438 and with the amino acids in the middle of the active-site gorge. In both cases, the ligand occupies the same spatial region of the active site, and interact with BuChE amino acid residues primarily through hydrophobic interactions, however the orientation of the ligand appeared different.

In Mode I (-7.8 kcal mol^{-1}), the piperidine moiety is pointed toward the catalytic triad residue His438. This protonated ring established π-cation and π-alkyl interactions with Trp82. Alkyne moiety is situated in the acyl binding pocket of the enzyme and makes interactions with Phe329, Phe398, Leu286 and Trp231. Moreover, the positive charged nitrogen atom can find an π-cation intramolecular interaction with the indole ring (Figures S42).
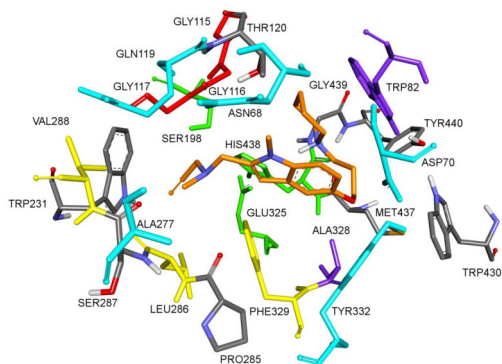
Figure S41. Proposed binding mode for contilisant inside gorge cavity of hBuChE. Mode I: Contilisant is colored orange. Different subsites of the active site were colored: catalytically anionic site (CAS) in green, oxyanion hole (OH) in red, choline binding site (CBS) in violet, acyl binding pocket (ABP) in yellow, and peripheral site (PAS) in blue.

SUPPORTING INFORMATION
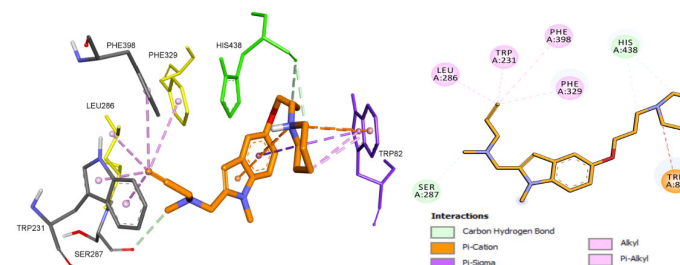
Figure S42. Mode I. Docking pose of contilisant into hBuChE highlighting the protein residues that establish the main interactions with the ligand (left). Schematic representation of different interactions of compound contilisant with hBuChE (right).

Slightly different binding features were revealed in analysis of the results obtained for the Mode I relative Mode II. In Mode II (-7.8 kcal mol^{-1}), contilisant is turned by 180º with respect to the position adopted in Mode I (Figure S43). The alkyne moiety is pointed toward the catalytic triad residue His438 and it also establishes interaction with Trp82. The protonated piperidine ring is pointed toward the acyl binding pocket establishing interactions with Trp231 and Leu286. The intramolecular Pi-cation interaction between the indole ring and the protonated piperidine nitrogen is also proposed (Figures S44).
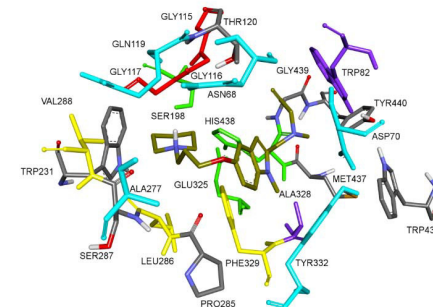
Figure S43. Proposed binding mode for contilisant inside gorge cavity of hBuChE. Mode II: Contilisant is colored olive green. Different subsites of the active site were colored: catalytically anionic site (CAS) in green, oxyanion hole (OH) in red, choline binding site (CBS) in violet, acyl binding pocket (ABP) in yellow, and peripheral site (PAS) in blue.
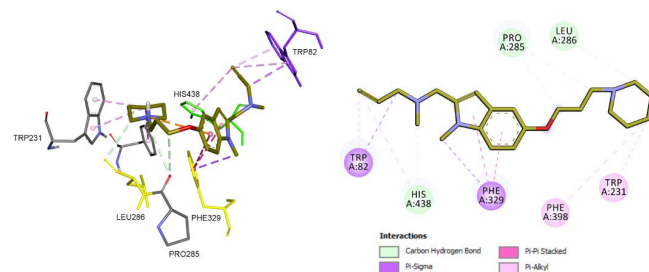
Figure S44. Mode II. Docking pose of contilisant into hBuChE highlighting the protein residues that establish the main interactions with the ligand (left). Schematic representation of different interactions of contilisant with hBuChE (right).

ADME prediction of compounds 1-7

Drugs that used for neurological disorder treatment are generally CNS acting agents. At first, factors that are relevant to the success of CNS drugs were analyzed. Usually, CNS drugs show values of MW < 450, HB donor < 3, HB acceptors < 7, QPlogPo/w < 5, PSA < 90, number of rotatable bonds < 8 and hydrogen bonds < 8. Thus, based on the values shown in table S4, compounds **1-7** satisfied the characteristics of CNS acting drugs. These results suggest that for all the compounds do not exist any important violations of Lipinski's rule (0-1), as all calculated descriptors and properties are within the expected thresholds. The solubility of organic molecules in water has a significant impact on many ADME-related properties. The seven compounds showed solubility values within the limits. The partition coefficient (QPlogPo/w), critical for estimation of absorption within the body, ranged between 3.80 and 5.42 (Table S5). The BBB must be crossed for the effect of compounds to be executed. Then, the hydrophilicity (logS) and logBB are the most important descriptors for CNS penetration. Experimental values of log BB cover the range from about 0.17 to 0.97. Within this range, compounds with log BB > 0.30 cross BBB

Table S5. Physicochemical properties for compounds **1-7** (**4**, contilisant).

	MW	SASA	volume	donorHB	accptHB	QPlogPo/w	QPlogS
1	325.453	661.476	1.165.727	0.500	4.750	3.801	-2.415
2	339.480	684.669	1.217.704	0.500	4.750	4.126	-2.703
3	339.480	709.993	1.264.606	0.500	4.750	4.434	-2.986
4	353.506	703.979	1.263.743	0.500	4.750	4.432	-2.986
5	381.560	800.650	1.414.287	0.500	4.750	5.416	-3.565
6	325.453	669.700	1.171.190	0.500	4.750	3.843	-2.410
7	344.453	693.319	1.201.190	0.000	4.750	4.231	-3.712

|	QPPCaco	PSA	QPlogBB	metab	QPlogKhsa	% HOA	ROF	ROT
1	588.482	16.079	0.857	5	0.520	100.000	0	0
2	583.235	18.378	0.792	5	0.621	100.000	0	0
3	590.520	17.416	0.798	5	0.749	100.000	0	0
4	605.742	17.372	0.810	5	0.748	100.000	0	0
5	609.544	15.493	0.692	5	1.076	95.542	1	0
6	581.791	16.917	0.972	4	0.618	100.000	0	0
7	1.165.654	43.329	0.171	2	0.537	100.000	0	0

MW: Molecular weight of the molecule (130.0-725.0). SASA: Total Solvent Accessible Surface Area, in square angstroms, using a probe with a 1.4Å radius (limits 300.0-1000.0). volume: Total solvent-accessible volume, in cubic angstroms, using a probe with a 1.4 Å radius (limits 500.0-2000.0). donorHB: Estimated number of hydrogen bonds that would be accepted by the solute (limits: 2.0-20.0). accptHB: Estimated number of hydrogen bonds that would be donated by the solute (limits: 0.0-6.0). QPlogPo/w: Predicted octanol/water partition coefficient (limits -2.0-6.5). QPlogS: Predicted aqueous solubility. S, in mol/dm³, is the concentration of the solute's saturated solution that is in equilibrium with crystalline solid (limits -6.5-0.5). QPPCaco: Predicted apparent Caco-2 cell permeability in nm/sec. Caco-2 cells is a model for the gut-blood barrier. QikProp predictions are for non-active transport. (< 25 poor, > 500 great). PSA: Van der Waals surface area of polar nitrogen and oxygen atoms (limits 7.0-200.0). QPlog BB: Predicted brain/blood partition coefficient (limits -3.0–1.2). metab: Number of likely metabolic reactions (limits 1-8). QPlogKhsa: Prediction of binding to human serum albumin (limits -1.5-1.5). HOA: Predicted qualitative Human Oral Absorption on 0 to 100% scale. ROF: Number of violations of Lipinski's Rule Of Five (Lipinski, C. A., Lombardo, F., Dominy, B. W., Feeney, P. J., "Experimental and computational approaches to estimate solubility and permeability in drug discovery and development settings", *Adv. Drug Delivery rev.* **2001**, 46, 3-26). (molecular weight < 500, QPlogPo/w < 5, number of hydrogen bond donor ≤ 5, number of hydrogen bond acceptors HB ≤ 10). ROT: Number of violations of Jorgensen's rule of three [(a) Duffy, E. M., Jorgensen, W. L., "Prediction of Properties from Simulations: Free Energies of Solvation in Hexadecane, Octanol, and Water", *J. Am. Chem. Soc.* 2000, 122, 2878-2888; (b) Jorgensen, W. L., Duffy, E. M., "Prediction of Drug Solubility from Monte Carlo Simulations", *Bioorg. Med. Chem. Lett.* **2000**, 10, 1155-1158] (QPlogS> -5.7, QPCaco> 22 nm/s, number of primary metabolites < 7).

readily, while compounds with a log BB < -1.00 are poorly distributed into the brain. The logBB values for compounds **1-6** (Table S5) were greater than 0.30, indicating excellent potential for BBB penetration. Literature survey suggests that Polar Surface Area (PSA) is a measure of a molecule's hydrogen bonding capacity and its value should not exceed a certain limit if the compound is intended to be CNS active. The most active CNS drugs have PSA lower than 70 A². The values of PSA for compounds **1-7** are in the range from 15.49 to 43.33 A² confirming good penetration to the BBB. Similarly, the percentage human oral absorption for the compounds is 100% except for compound **5** (95.5%) (Table S5). Other physicochemical descriptors obtained by QikProp (Table S5) are within the acceptable range for human use, thereby indicating their potential as drug-like molecules and possible CNS drug. In particular, for contilisant, the more significant observed data were thus: total Solvent Accessible Surface Area, in square angstroms, using a probe with a 1.4 Å radius (SASA = 703.979; limits 300.0-1000.0); estimated number of hydrogen bonds that would be accepted by the solute (donorHB = 0.50; limits: 2.0-20.0); estimated number of hydrogen bonds that would be donated by the solute (accptHB = 4.750; limits: 0.0-6.0); predicted octanol/water partition coefficient (QPlogPo/w = 4.432; limits -2.0-6.5); predicted aqueous solubility. S, in mol/dm³, is the concentration of the solute's saturated solution that is in equilibrium with crystalline solid (QPlogS = -2.986; limits -6.5-0.5); Van der Waals surface area of polar nitrogen and oxygen atoms (PSA = 17.372; limits 7.0-200.0); predicted brain/blood partition coefficient (QPlog BB = 0.810; limits -3.0–1.2); number of violations of Lipinski's Rule Of Five (molecular weight < 500, QPlogPo/w < 5, number of hydrogen bond donor ≤ 5, number of hydrogen bond acceptors HB ≤ 10; ROF= 0); number of violations of Jorgensen's rule of three (QPlogS> -5.7, QPCaco> 22 nm/s, number of primary metabolites < 7; ROT= 0).

Neuroprotection analysis

As shown, the overall data obtained for compounds **1-7** revealed an interesting neuroprotection profile, being compound **4** the best of the series (Table S6). At concentrations of 0.3 and 1 μM, multitarget-directed ligand (MDL) **4** offered significant neuroprotection against the three toxic insults assayed (69.7% vs R/O, 47.0% vs OA and 65.2% vs $A\beta_{25-35}$ at 0.3 μM). Note also that compound **7**, at 0.3 μM, afforded the best neuroprotective profile against OA insult (60.7%), but showed poor and less neuroprotection against and R/O and $A\beta_{25-35}$ than compound **4**. Similarly, compound **2**, at 0.3 μM showed an interesting neuroprotective effect against R/O (49.3%) and OA (43.5%), and less but significant neuroprotection against $A\beta_{25-35}$ (28.4%) compared with compound **5**. In all cases, when we increased the concentration of compounds to 3 μM, the protective capacity decreased against all toxic stimuli. Moreover, we assayed the toxicity of the compounds applied alone to SH-SY5Y cells at all concentrations tested and we did not observed any toxic effect (data not shown).

Table S6. Quantitative data of the effect of MTDLs **1-7**, ASS234 and melatonin on SH-SY5Y cell death induced by rotenone (R, 30 μM) plus oligomycin A (O, 10 μM) (R/O), okadaic acid (OA, 20 nM) and β-Amyloid peptide 25-35 ($A\beta_{25-35}$, 30 μM).

MTDL	μM	R/O	OA	$A\beta_{25-35}$
	0.3	34.0 ± 25.8^{ns}	44.8 ± 11.7^{ns}	26.6 ± 13.2
1	1	27.4 ± 16.6^{ns}	$49.8 \pm 7.9^{*}$	$53.5 \pm 12.0^{**}$
	3	24.8 ± 7.2^{ns}	42.8 ± 12.4^{ns}	nd
	0.3	$49.3 \pm 16.8^{*}$	$43.5 \pm 8.5^{*}$	$28.4 \pm 12.3^{**}$
2	1	38.8 ± 14.9^{ns}	38.5 ± 12.1^{ns}	$27.3 \pm 10.7^{*}$
	3	15.1 ± 11.9^{ns}	nd	nd
	0.3	27.6 ± 9.3^{ns}	44.0 ± 13.4^{ns}	24.2 ± 21.0^{ns}
3	1	30.9 ± 19.9^{ns}	$54.2 \pm 9.9^{**}$	20.2 ± 20.1^{ns}
	3	30.9 ± 8.6^{ns}	$46.4 \pm 8.5^{*}$	nd
4	0.3	$69.7 \pm 15.6^{***}$	$47.0 \pm 10.2^{*}$	$65.2 \pm 20.1^{*}$
(contilisant)	1	37.3 ± 10.8^{ns}	$48.5 \pm 10.1^{*}$	$69.5 \pm 16.2^{*}$
	3	25.5 ± 16.8^{ns}	$44.8 \pm 14.8^{*}$	nd
	0.3	$39.2 \pm 16.2^{*}$	$52.0 \pm 13.8^{**}$	$57.9 \pm 16.7^{*}$
5	1	17.3 ± 11.0^{ns}	28.1 ± 13.4^{ns}	33.1 ± 2.1
	3	18.4 ± 8.9^{ns}	35.8 ± 12.9^{ns}	nd
	0.3	22.2 ± 13.5^{ns}	40.0 ± 7.8^{ns}	$47.4 \pm 12.0^{*}$
6	1	21.6 ± 12.3^{ns}	43.7 ± 12.4^{ns}	$42.3 \pm 12.6^{*}$
	3	20.1 ± 10.5^{ns}	$47.0 \pm 7.1^{*}$	nd
	0.3	15.1 ± 7.9^{ns}	$60.7 \pm 10.7^{***}$	$30.9 \pm 15.7^{*}$
7	1	48.8 ± 12.1^{ns}	44.4 ± 10.7^{ns}	23.6 ± 13.7
	3	25.5 ± 16.8^{ns}	42.1 ± 14.7^{ns}	nd
ASS234	5	$32.8 \pm 7.6^{**}$	$33.0 \pm 7.1^{*}$	$35.5 \pm 10.1^{*}$
Melatonin	0.01	$60.8 \pm 8.0^{***}$	$52.5 \pm 10.2^{**}$	$72.1 \pm 3.1^{***}$

Data are expressed as % neuroprotection ± s.e.m. of triplicate of at least four different cultures. All compounds were assayed at 0.3, 1 and 3 μM. ***$P \leq 0.001$ **$P \leq 0.01$, *$P \leq 0.05$, ns: not significant with respect to control. nd; Not determined

In vivo studies of ASS234 and contilisant

Novel object recognition test

It could be shown that contilisant (1 mg/kg i.p.), but not ASS234, is able to restore cognition of LPS-impaired mice by about 30% in novel object recognition test. We assume that contilisants H3R antagonistic properties together with its AChE inhibition are mandatory for the pro-cognitive effects in LPS-induced mice, as described previously for H3R antagonists/inverse agonists.[26] Thus, contilisants performance in the novel recognition test as functional assay proves its H3R antagonist/inverse agonist potency.

References

[1] M. A. Cruces, C. Elorriaga, E. Fernandez-Alvarez, *Eur J Med Chem* **1991**, *26*, 33–41.

[2] P. C. Unangst, D. T. Connor, S. R. Miller, *J. Heterocycl. Chem.* **1996**, *33*, 1627–1630.

[3] M. Zhou, N. Panchuk-Voloshina, *Anal. Biochem.* **1997**, *253*, 169–174.

[4] A. Holt, M. M. Palcic, *Nat. Protoc.* **2006**, *1*, 2498–2505.

[5] G. Esteban, J. Allan, A. Samadi, M. Mattevi, M. Unzeta, J. Marco-Contelles, C. Binda, R. R. Ramsay, *Biochim. Biophys. Acta - Proteins Proteomics* **2014**, *1844*, 1104–1110.

[6] O. Benek, O. Soukup, M. Pasdiorova, L. Hroch, V. Sepsova, P. Jost, M. Hrabinova, D. Jun, K. Kuca, D. Zala, et al., *ChemMedChem* **2016**, *11*, 1264–1269.

[7] G. L. Ellman, K. D. Courtney, V. Andres, R. M. Featherstone, *Biochem. Pharmacol.* **1961**, *7*, 88–95.

[8] T. Kottke, K. Sander, L. Weizel, E. H. Schneider, R. Seifert, H. Stark, *Eur. J. Pharmacol.* **2011**, *654*, 200–208.

[9] E. H. Schneider, R. Seifert, *Pharmacol. Ther.* **2010**, *128*, 387–418.

[10] B. Ou, M. Hampsch-Woodill, R. L. Prior, *J. Agric. Food Chem.* **2001**, *49*, 4619–4626.

[11] A. Dávalos, C. Gómez-Cordovés, B. Bartolomé, *J. Agric. Food Chem.* **2004**, *52*, 48–54.

[12] M. I. Fernández-Bachiller, C. Pérez, N. E. Campillo, J. A. Páez, G. C. González-Muñoz, P. Usán, E. García-Palomero, M. G. López, M. Villarroya, A. G. García, et al., *ChemMedChem* **2009**, *4*, 828–841.

[13] L. F. N. Lemes, G. De Andrade Ramos, A. S. De Oliveira, F. M. R. Da Silva, G. De Castro Couto, M. Da Silva Boni, M. J. R. Guimaraes, I. N. O. Souza, M. Bartolini, V. Andrisano, et al., *Eur. J. Med. Chem.* **2016**, *108*, 687–700.

[14] L. Di, E. H. Kerns, K. Fan, O. J. McConnell, G. T. Carter, *Eur. J. Med. Chem.* **2003**, *38*, 223–232.

[15] K. Sugano, H. Hamada, M. Machida, H. Ushio, *J. Biomol. Screen.* **2001**, *6*, 189–196.

[16] F. Wohnsland, B. Faller, *J. Med. Chem.* **2001**, *44*, 923–930.

[17] "Chemical Computing Group Inc. Molecular Operating Environment (MOE). 2015.10," **2016**.

[18] B. R. Brooks, R. E. Bruccoleri, B. D. Olafson, D. J. States, S. Swaminathan, M. Karplus, *J. Comput. Chem.* **1983**, *4*, 187–217.

[19] A. Morreale, F. Maseras, I. Iriepa, E. Gálvez, *J. Mol. Graph. Model.* **2002**, *21*, 111–118.

[20] O. Trott, A. J. Olson, *J. Comput. Chem.* **2009**, *31*, 456–461.

[21] M. Antunes, G. Biala, *Cogn. Process.* **2012**, *13*, 93–110.

[22] T. Esbenshade, K. Krueger, *J. Pharmacol. Exp. Ther.* **2003**, *305*, 887–896.

[23] X. Ligneau, S. Morisset, J. Tardivel-Lacombe, F. Gbahou, C. R. Ganellin, H. Stark, W. Schunack, J. C. Schwartz, J. M. Arrang, *Br. J. Pharmacol.* **2000**, *131*, 1247–1250.

[24] H. Stark, W. Sippl, X. Ligneau, J. M. Arrang, C. R. Ganellin, J. C. Schwartz, W. Schunack, *Bioorg. Med. Chem. Lett.* **2001**, *11*, 951–4.

[25] D. Schnell, A. Strasser, R. Seifert, *Biochem. Pharmacol.* **2010**, *80*, 1437–1449.

[26] D. G. Brown, P. R. Bernstein, A. Griffin, S. Wesolowski, D. Labrecque, M. C. Tremblay, M. Sylvester, R. Mauger, P. D. Edwards, S. R. Throner, et al., *J. Med. Chem.* **2014**, *57*, 733–758.

Zuschriften

Medizinische Chemie **Hot Paper**

Multipotente Liganden mit kombinierter Cholinesterase- und Monoaminooxidase-Inhibition sowie Histamin-H3R-Antagonismus bei neurodegenerativen Erkrankungen

Óscar M. Bautista-Aguilera⁺, Stefanie Hagenow⁺, Alejandra Palomino-Antolin⁺, Víctor Farré-Alins⁺, Lhassane Ismaili, Pierre-Louis Joffrin, María L. Jimeno, Ondřej Soukup, Jana Janočková, Lena Kalinowsky, Ewgenij Proschak, Isabel Iriepa, Ignacio Moraleda, Johannes S. Schwed, Alejandro Romero Martínez, Francisco López-Muñoz, Mourad Chioua, Javier Egea,* Rona R. Ramsay, José Marco-Contelles* und Holger Stark*

Abstract: *Die Therapie von komplexen neurodegenerativen Erkrankungen erfordert eine Entwicklung von Multitarget-orientierten Wirkstoffen. Durch strukturelle Optimierung des neuroprotektiven Liganden ASS234 mittels Integration etablierter Pharmakophore des Histamin-H3-Rezeptors (H3R) konnten neuartige Indolderivate mit inhibitorischer Aktivität an Acetylcholin-/Butyrylcholinesterasen und Monoaminooxidasen A und B sowie am H3R erzielt werden. Diese zeigten ein ausbalanciertes Wirkprofil an den gewünschten Targets in zumeist nanomolaren Konzentrationsbereichen. Weiterführende In-vitro-Untersuchungen zeigten antioxidative und neuroprotektive Fähigkeiten sowie die Überwindung der Blut-Hirn-Schranke. Mit diesem vielversprechenden Wirkprofil zeigte Contilisant (bei 1 mg kg⁻¹ i.p.) eine signifikante Verbesserung von Lipopolysaccharid-induzierten kognitiven Defiziten.*

Morbus Alzheimer und Morbus Parkinson zählen zu den häufigsten neurodegenerativen Erkrankungen, welche durch komplexe und vielfältige Mechanismen gekennzeichnet sind. Bei der Suche nach möglichen Krankheitsursachen sowie effizienteren Therapieoptionen stellten sich mitochondriale Dysfunktionen, Neuroinflammation und oxidativer Stress als Schlüsselfaktoren bei der Entstehung und dem Fortschreiten dieser Erkrankungen heraus. Folglich ist die Entwicklung von antioxidativen Wirkstoffstrategien für diese Erkrankungen, insbesondere für Morbus Alzheimer, von großer Bedeutung.[1,2] Der kürzlich beschriebene Multitarget-orientierten Ligand (MTL) ASS234 (Abbildung 1)[3–5] zeigt eine irreversible Hemmung der Monoaminooxidasen A und B (MAO A/ B) und reduziert die Entstehung des Sekundärproduktes Wasserstoffperoxid, eine reaktive Sauerstoffspezies (ROS).[6] Dies führt zum einen zur Verminderung der katalytischen Oxidation von biogenen Aminen, wie Serotonin (5-HT), Norepinephrin und Dopamin, die an kognitiven Prozessen beteiligt sind, und zum anderen zur verminderten Erzeugung von ROS, die zum neuronalen Zelltod führen können. ASS234 zeigt zusätzlich eine reversible Inhibition von Ace-

[*] S. Hagenow,[+] J. S. Schwed, Prof. Dr. H. Stark
Institut für Pharmazeutische und Medizinische Chemie
Heinrich-Heine-Universität Düsseldorf
Universitätsstrasse 1, 40225 Düsseldorf (Deutschland)
E-Mail: stark@hhu.de

Dr. Ó. M. Bautista-Aguilera,[+] M. L. Jimeno, M. Chioua,
Prof. Dr. J. Marco-Contelles
Laboratorio de Química Médica
Instituto de Química Orgánica General
CSIC and Centro de Química Orgánica „Lora-Tamayo", CSIC
C/ Juan de la Cierva 3, 28006 Madrid (Spanien)
E-Mail: iqoc21@iqog.csic.es

A. Palomino-Antolin,[+] V. Farré-Alins,[+] Dr. J. Egea
Instituto de Investigación Sanitaria, Servicio de Farmacología Clínica
Hospital Universitario de la Princesa
Calle de Diego de León, 62, 28006 Madrid (Spanien)
E-Mail: javier.egea@inv.uam.es

L. Ismaili
Neurosciences Intégratives et Cliniques EA 481
Université Bourgogne Franche-Comté
Rue Ambroise Paré, 25000 Besançon (Frankreich)

P.-L. Joffrin, Dr. R. R. Ramsay
Biomedical Sciences Research Complex
University of St Andrews, Biomolecular Sciences Building
North Haugh, St Andrews KY16 9ST (Großbritannien)

Dr. O. Soukup, Dr. J. Janočková
Centrum biomedicínského výzkumu
Fakultní nemocnice Hradec Králové
Sokolska 581, 50005 Hradec Kralove (Tschechische Republik)

L. Kalinowsky, Jun.-Prof. Dr. E. Proschak
Institut für Pharmazeutische Chemie, Goethe Universität Frankfurt
Max-von-Laue-Strasse 9, 60438 Frankfurt (Deutschland)

I. Iriepa, I. Moraleda
Departamento de Química Orgánica y Química Inorgánica
Universidad de Alcalá
Ctra. Madrid-Barcelona, Km. 33,6, 28871, Madrid (Spanien)

A. Romero Martínez
Departamento de Toxicología y Farmacología
Facultad de Veterinaria, UCM
Av. Puerta de Hierro, s/n, 28040 Madrid (Spanien)

Dr. F. López-Muñoz
Universidad Camilo José Cela, C/ Castillo de Alarcón, 49
28692 Villanueva de la Cañada, Madrid (Spanien)

[+] Diese Autoren haben zu gleichen Teilen zu der Arbeit beigetragen.

Hintergrundinformationen (zu Synthese, Analytik, pharmakologischer Testung und molekularen Bindungsstudien) und die Identifikationsnummern (ORCID) mehrerer Autoren sind unter:
https://doi.org/10.1002/ange.201706072 zu finden.
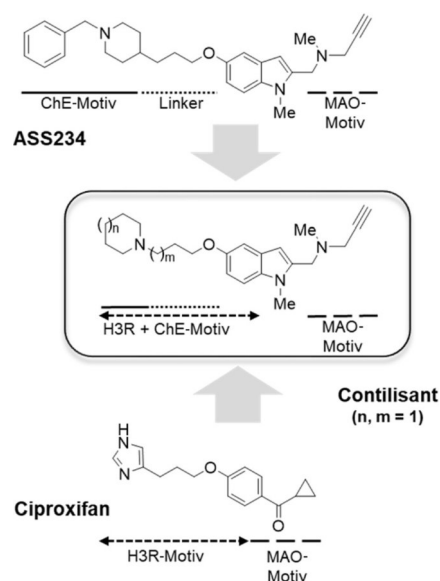
Abbildung 1. Allgemeine Strukturmotive von H3R/MAO/ChE-MTLs, abgeleitet von Elementen des Antioxidans ASS234 und des H3R-Antagonisten Ciproxifan.

sche aliphatische Amine wir Piperidin als basisches Zentrum über einen (Propyloxy)phenyl-Linker an eine variable Region im östlichen Teil des Moleküls gekuppelt. Diese Verbindungen bieten ein geeignetes Pharmakophor, was bereits durch mehrere Studien zu Struktur-Wirkungs-Beziehungen verifiziert wurde.[17–19] Hier beschreiben wir die Synthese und biologische Evaluierung von MTL **1–7** (Schema 1),

Schema 1. Synthese von MTL **1–7**. Reagenzien und Bedingungen: a) NaH, DMF, RT; b) PPh$_3$, DIAD, THF, RT; c) K$_2$CO$_3$, DMF, 90°C.

tylcholinesterasen (AChE) vergleichbar mit kommerziellen AChE-Inhibitoren (z.B. Donepizil),[7] zur Steigerung von Lern- und Erinnerungsfähigkeit.

Der Histamin-H$_3$-Rezeptor (H3R) ist involviert in die zentralen Regulation von Histamin sowie anderen Neurotransmittern[8,9] und gilt daher als nützlicher neuartiger pharmakologischer Angriffspunkt. Die Inhibierung von H3R durch inverse Agonisten/Antagonisten führt zum Anstieg verschiedener Neurotransmitter wie Acetylcholin (ACh), 5-HT, Dopamin oder Norepinephrin im zentralen Nervensystem. Erst kürzlich wurde der erste inverse H3R-Agonist, Pitolisant (WAKIX), für die Therapie von Narkolepsie zugelassen; die Verbindung wird aktuell in Hinblick auf diverse kognitive Dysfunktionen und Schlafstörungen diskutiert.[10] Folglich wird das prokognitive Potenzial von verschiedenen inversen H3R-Agonisten/Antagonisten für neurodegenerative Erkrankungen breit untersucht.[11] Obwohl Substanzen mit multipotenten Wirkprofilen wie H3R-Affinität kombiniert mit Cholinesterase(ChE)-Inhibition[12,13] und antioxidativer Kapazität[14] oder, erst kürzlich, MAO-Inhibition[15] bereits beschrieben wurden (siehe die Übersicht in Lit. [16]), wurde bisher nicht über Verbindungen berichtet, die H3R, MAO und ChE simultan adressieren. Dieses multipotente Profil stellt einen innovativen therapeutischen Ansatz für neue Wirkstoffe gegen neurodegenerative Erkrankungen unterschiedlichen Ursprungs dar.

ASS234 wurde strukturell so modifiziert, dass es das generell akzeptierte Pharmakophor von H3R-Antagonisten beinhaltet (Abbildung 1). Um unerwünschte Begleiteffekt zu minimieren, die durch Imidazol-haltige H3R Antagonisten (z.B. Ciproxifan) verursacht werden könnten, wurden cycli-

sowie die Identifizierung von Verbindung **4** (Contilisant), die eine gute antioxidative Kapazität mit hoher H3R-Affinität und exzellenter Inhibition von Neurotransmitter-abbauenden Enzymen aufweist. Diese Verbindungen wurden in Hinblick auf ihre Affinität zum humanen H3R, H4R und vier verschiedenen Neurotransmitter-abbauenden Enzymen (AChE, Butyrylcholinesterase (BuChE), MAO A/B) untersucht (für weiterführende Off-Target-Screenings, siehe die Hintergrundinformation).

Innerhalb dieser kleinen Serie inhibierten alle MTLs die ChEs in mindestens mikromolaren Konzentrationsbereichen (Tabelle 1). Contilisant zeigte die besten Inhibitionseigenschaften mit nanomolarer Inhibition von AChE. Die initiale reversible Inhibition von MAO A/B (initiale Bindung) und die Inhibition nach 30 Minuten Präinkubation von Inhibitor und Enzym (aufgrund irreversibler Bindung) wurde bestimmt (Tabelle 1). Ohne Präinkubation zeigten alle Substanzen IC$_{50}$-Werte im niedrigen mikromolaren Bereich. Die unterschiedlichen Linker-Längen beeinflussen die Bindung an das aktive Zentrum von MAO A und B, wobei der Dimethylen-Linker bei den Piperidin-Derivaten optimal ist. Der Wechsel zum Pyrrolidin-Ring als basisches Zentrum zeigt nur geringen Einfluss bei den Verbindungen mit Trimethylen-Linker (**2** und **4**), führt aber zu verminderter Inhibition bei den Verbindungen mit Dimethylen-Linker (**1** und **3**). Für die meisten Propargylamine ergibt sich nach Präinkubation eine Verschiebung der IC$_{50}$-Werte in den nanomolaren Konzentrationsbereich. Die Irreversibilität der MAO-Inhibition von Contilisant wurde durch eine 50-fache Verdünnung mit Überschuss an Substrat bestätigt. Der IC$_{50}$-Wert für Verbindung **6** ändert sich nur geringfügig nach Präinkubation, was dafür spricht, dass die Propargyl-Funktion keine kovalente Bindung mit MAO B eingeht. Verbindung **7**, die keine Pro-

GDCh   *Zuschriften*   **Angewandte** Chemie

Tabelle 1: IC$_{50}$- und K_i-Werte für die Inhibition von hMAO/B, hAChE/hBuChE bzw. hH3R/hH4R sowie ORAC-Bestimmungen der Verbindungen **1–7**, ASS234, Ciproxifan, Clorgylin, Deprenyl und Donepezil.

MTL	Präink. [min]	hMAO A IC$_{50}$[a] [µM]	hMAO B IC$_{50}$[a] [µM]	SR MAO[b]	hAChE IC$_{50}$[a] [µM]	hBuChE IC$_{50}$[a] [µM]	SR ChE[c]	ORAC[d] (TE)	hH3R K_i[e] [nM]	hH4R K_i [nM]
1	0	3.00 ± 0.34	5.21 ± 0.82	1.7	37.9 ± 1.5	25.1 ± 5.5	1.5	3.11 ± 0.07	178	> 10000
	30	0.095 ± 0.009	0.140 ± 0.008	1.5					[44, 716]	
2	0	4.01 ± 0.60	1.80 ± 0.24	0.5	18.8 ± 2.7	7.40 ± 1.41	2.5	4.54 ± 0.08	4.5	> 10000
	30	0.073 ± 0.006	0.100 ± 0.020	1.4					[1.8, 11]	
3	0	0.41 ± 0.03	1.32 ± 0.21	3.2	20.6 ± 3.6	8.55 ± 1.48	2.4	1.86 ± 0.06	38.5	> 10000
	30	0.052 ± 0.007	0.017 ± 0.003	0.3					[13, 117]	
4 (Contilisant)	0	1.85 ± 0.21	1.94 ± 0.15	1.0	0.53 ± 0.05	1.69 ± 0.12	0.3	3.59 ± 0.09	10.8	> 100000
	30	0.145 ± 0.010	0.078 ± 0.006	0.5					[4.2, 27]	
5	0	6.52 ± 0.52	41.3 ± 5.5	6.3	8.3 ± 2.4	3.30 ± 0.71	2.5	2.94 ± 0.04	77.7	> 10000
	30	0.166 ± 0.015	4.65 ± 0.06	28					[19, 311]	
6	0	1.19 ± 0.15	3.80 ± 0.40	3.2	58.3 ± 11.8	31.1 ± 1.8	1.9		14.7	> 10000
	30	0.042 ± 0.004	2.75 ± 0.51	65					[3.8, 57]	
7	0	103 ± 20	12.6 ± 1.0	0.1	20.4 ± 2.0	11.6 ± 1.3	1.8	1.40 ± 0.14	24.4	> 10000
	30	91 ± 1	11.2 ± 0.9	0.1					[12, 50]	
ASS234	0	0.033 ± 0.003	3.20 ± 0.41	97	0.81 ± 0.06	1.82 ± 0.14	0.4		84.2	> 10000
	30	0.00027 ± 0.00003	0.12 ± 0.02	444					[48, 149]	
Ciproxifan	0	11.4 ± 1.2[15]	2.1 ± 0.3[15]	0.2	86.1 ± 20.9	77.3 ± 3.4	1.1		46–180[22–24]	> 10000[23]
Clorgylin	0	0.042 ± 0.003	3.65 ± 0.39	86	nicht aktiv[25]	nicht aktiv[25]				
	30	0.00042 ± 0.00008	3.57 ± 0.36	8500						
Deprenyl	0	225 ± 31	0.053 ± 0.005	0.0002	nicht aktiv[25]	nicht aktiv[25]				
	30	0.630 ± 0.086	0.0040 ± 0.0009	0.006						
Donepezil[4]	0				0.011 ± 0.001	6.22 ± 0.77	0.002			

[a] Der Standardfehler (SE) für jeden Wert ist angegeben. [b] SR = IC$_{50}$(hMAO B)/IC$_{50}$(hMAO A). [c] SR = IC$_{50}$(hAChE)/IC$_{50}$(hBuChE). [d] Oxygen Radical Absorbance Capacity [Trolox-Äquivalente (TE)]. [e] Das 95 %-Konfidenzintervall ist in eckigen Klammern angegeben.

pargyl-Funktion enthält, zeigt ebenfalls keine Änderung nach Präinkubation. Die MAO-Aktivität nach 50-facher Verdünnung für **7** betrug mehr als 95 % was für eine reversible Inhibition spricht. Contilisant zeigte im Vergleich zur MAO-A-präferierenden ASS234 eine verbesserte MAO-B-Inhibition. Die Bindungsaffinität am humanen H3R sowie am H4R („Off-Target"), als G-Protein-gekoppelter Rezeptor mit der höchsten Homologie, wurde bestimmt (Tabelle 1). Keine der Verbindungen zeigte eine Affinität an H4R und somit eine gute H3R-Selektivität. Überraschenderweise zeigte ASS234 bereits eine nennenswerte H3R-Affinität, wobei die höchsten Affinitäten für Verbindung **2** und Contilisant gefunden wurden – beide mit Propyloxy-Linker gekoppelt an eine Pyrrolidino- bzw. Piperidino-Gruppe. Hohe Affinitäten zeigten ebenfalls die beiden Propyloxy-Verbindungen **6**, mit variierten H3R-Pharmakophor, und **7**, ohne Propargyl-Gruppe. Die Verbindungen mit Ethyloxy- oder Pentyloxy-Linker zeigten nur moderate H3R-Affinität. Diese Untersuchungen sind in Übereinstimmung mit bereits zuvor gezeigten Struktur-Wirkungs-Beziehungen für H3R-Antagonisten.[17,20,21] Da die Verbindungen **6** und **7** eine vergleichbare H3R-Affinität haben, konnte gezeigt werden, dass die H3R-Affinität durch Einführung einer zweiten basischen Funktionalität, der Propargyl-Funktion als MAO-Funktionalität, positiv beeinflusst wird. Verbindung **6**, obwohl weniger effektiv bezüglich AChE, bietet strukturelle Variationsmöglichkeiten, da die MAO-Funktionalität mit verschiedenen Linkern oder Amin-Bausteinen als H3R-Pharmakophor kombiniert werden kann.

Molekulare Bindungsstudien für die vier Targets bestätigen die In-vitro-Daten, da ASS234 und Contilisant eine gute Einpassung für die unterschiedlichen Bindungsstellen von AChE, MAO A/B und H3R aufweisen (siehe die Hintergrundinformationen). Erwähnenswert bezüglich der molekularen Eigenschaften von Contilisant, erhoben mit molsoft,[26] ist die höhere Hydrophilie (MolLogP = 3.7) im Vergleich zu ASS234 (MolLogP = 5.5), was einen verbesserten Wirkstoff-Ähnlichkeitsfaktor bestätigt. Weitere Indizien für die zentrale Verteilung wurde mittels „Parallel-Artificial-Membrane-Permeability"-Assay (PAMPA) nachgewiesen, einem Vorhersageverfahren für die Überwindung der Blut-Hirn-Schranke (siehe die Hintergrundinformationen). Die Ergebnisse zeigen die Fähigkeit von Contilisant und ASS234, die Blut-Hirn-Schranke mittels passiver Diffusion zu überwinden. Eine komplette theoretische ADME-Analyse der neuen Hybride **1–7**, mit speziellen Fokus auf Contilisant, wurde durchgeführt, um Arzneimitteleignung nachzuweisen (siehe die Hintergrundinformationen). Die antioxidative Kapazität der Hybride **1–5** und **7** wurde mittels „Oxygen-Radical-Absorbance-Capacity"(ORAC-FL)-Test gemessen (Tabelle 1),[27] wobei alle MTLs gute Radikalfänger-Eigenschaften zeigten und Contilisant ähnliche Werte erzielte wie die Positivkontrolle Ferulasäure (3.74 ± 0.22 TE).[28] Die neuroprotektiven Fähigkeiten wurden anhand dreier unterschiedlicher Toxizitätsmechanismen untersucht, die bei Morbus Alzheimer an neurodegenerativen Prozessen beteiligt sind:[29] (a) eine Mischung von Rotenon und Oligomycin A (R/O), welche die mitochondriale Atmungsketten blockieren, als Modell für oxidativen Stress; (b) Okadinsäure (OA), ein Proteinphosphatase-Hemmer, als Modell der Tau-Protein-Hyperphosphorylierung; (c) β-Amyloidpeptide (Aβ$_{25-35}$), welche an ROS und Apoptose-Signalwegen betei-

ligt sind. Insgesamt lieferten diese Daten für MTL **1–7** ein interessantes neuroprotektives Profil (siehe die Hintergrundinformationen). Bei der niedrigsten Testkonzentration (0.3 μm) zeigte Contilisant eine signifikante Neuroprotektion gegen alle Neurotoxine (70 % gegen R/O, 47 % gegen OA und 65 % gegen Aβ$_{25-35}$), vergleichbar zur Referenzverbindung Melatonin (Abbildung 2).
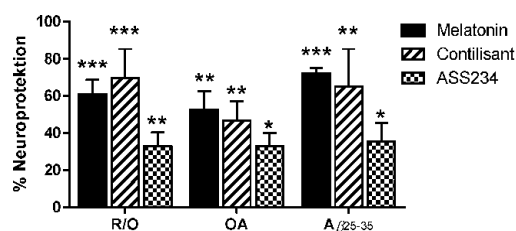
Abbildung 2. Neuroprotektive Fähigkeiten von Contilisant (0.3 μm), ASS234 (5 μm) und Melatonin (0.01 μm) in SH-SY5Y-Zellen nach Rotenon 30 μm/Oligomycin A 10 μm (R/O), Okadainsäure 20 nm (OA) bzw. β-Amyloidpeptide 30 μm (Aβ$_{25-35}$) Intoxikation. Daten angegeben in % Neuroprotektion ± SEM von mindestens vier unterschiedlichen Kulturen jeweils in Triplikaten (Kontrolle entspricht 100 %). ***$p \leq 0.001$, **$p \leq 0.01$, *$p \leq 0.05$ im Vergleich zur Kontrolle.

Eine potenzielle Verbesserung der Erinnerungs- und Lernfähigkeit in vivo durch ASS234 und Contilisant wurde mittels „Novel-Object-Recognition"(NOR)-Test in Mäusen (Abbildung 3) untersucht,[30] vor und nach Gabe von Lipopolysaccharid (LPS), das eine signifikante Reduktion der NOR-Leistung verursacht. Mäuse, die nach LPS-Schädigung mit Contilisant behandelt wurden, zeigten einen verbesserten Differenzierungsindex, wobei ASS234 (bei gleicher Dosis) keine Verbesserung der kognitiven Defizite erzielte.
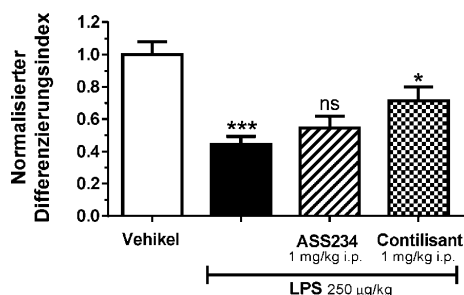
Abbildung 3. Einflüsse von Contilisant und ASS234 auf LPS-induzierte Gedächtnisstörungen im NOR-Test in Mäusen. ***$p \leq 0.001$ vs. Vehikel, *$p \leq 0.05$, ns $p > 0.05$ vs. LPS.

Zusammenfassend wurden erstmals neue MTLs mit inhibitorischen Eigenschaften an Neurotransmitter-abbauenden Enzymen (ChEs und MAOs) mit kombinierter H3R-Affinität beschrieben. Von dieser kleinen Substanzserie zeigte Contilisant insgesamt die besten Multitarget-Eigenschaften in nanomolaren Konzentrationsbereichen mit zu-

sätzlichen und ausgeglichenen Eigenschaften bezüglich Permeation, antioxidativer und neuroprotektiver Kapazität. Contilisant bietet damit ein pharmakologisches Profil mit erhöhter Komplexität, das potenziell vorteilhaft für die Behandlung von neurodegenerativen Erkrankungen ist. Im Vergleich zum dualpotenten H3R/MAO-Liganden Ciproxifan[15] ist Contilisant ein verbesserter MAO-Inhibitor mit irreversiblen Bindungsmodus. Zusätzlich zeigt Contilisant (1 mg kg^{-1}) eine Verbesserung der kognitiven Eigenschaften in LPS-geschädigten Mäusen.

Wie beabsichtigt, wurden alle Eigenschaften des niedermolekularen MTL Contilisant (**4**) im Vergleich zur Leitstruktur ASS234 optimiert, insbesondere die Verminderung der Inhibition von MAO A, sowie erfolgreich basierend auf der strukturellen Integration von H3R-Pharmakophoren um eine hohe H3R-Affinität erweitert.[31] Dieses einzigartige pharmakologische Profil, gerichtet gegen verschiedene Targets innerhalb neurodegenerativer Prozesse, könnte hilfreich sein bei der Therapie von Morbus Alzheimer oder Morbus Parkinson.

Interessenkonflikt

S.H., H.S., J.M.C., R.R.R. und F.L.M. haben ein thematisch verwandtes Patent angemeldet. Die übrigen Autoren haben keine Interessenkonflikte.

Stichwörter: Antioxidantien · Inhibitoren · Multitarget-Wirkstoffe · Neurologische Wirkstoffe · Wirkstoffentwicklung

[1] G. H. Kim, J. E. Kim, S. J. Rhie, S. Yoon, *Exp. Neurobiol.* **2015**, *24*, 325.

[2] E. Niedzielska, I. Smaga, M. Gawlik, A. Moniczewski, P. Stankowicz, J. Pera, M. Filip, *Mol. Neurobiol.* **2016**, *53*, 4094–4125.

[3] O. M. Bautista-Aguilera, A. Samadi, M. Chioua, K. Nikolic, S. Filipic, D. Agbaba, E. Soriano, L. de Andrés, M. I. Rodríguez-Franco, S. Alcaro, et al., *J. Med. Chem.* **2014**, *57*, 10455–10463.

[4] G. Esteban, J. Allan, A. Samadi, A. Mattevi, M. Unzeta, J. Marco-Contelles, C. Binda, R. R. Ramsay, *Biochim. Biophys. Acta Proteins Proteomics* **2014**, *1844*, 1104 – 1110.

[5] I. Bolea, J. Juárez-Jiménez, C. De Los Ríos, M. Chioua, R. Pouplana, F. J. Luque, M. Unzeta, J. Marco-Contelles, A. Samadi, *J. Med. Chem.* **2011**, *54*, 8251 – 8270.

[6] C. C. Wang, E. Billett, A. Borchert, H. Kuhn, C. Ufer, *Cell. Mol. Life Sci.* **2013**, *70*, 599 – 630.

[7] M. Racchi, M. Mazzucchelli, E. Porrello, C. Lanni, S. Govoni, *Pharmacol. Res.* **2004**, *50*, 441 – 451.

[8] M. Walter, H. Stark, *Front. Biosci.* **2012**, *4*, 461 – 488.

[9] B. A. Ellenbroek, B. Ghiabi, *Trends Neurosci.* **2014**, *37*, 191 – 199.

[10] J.-C. Schwartz, *Br. J. Pharmacol.* **2011**, *163*, 713 – 721.

[11] B. Sadek, A. Saad, A. Sadeq, F. Jalal, H. Stark, *Behav. Brain Res.* **2016**, *312*, 415 – 430.

[12] W. Huang, L. Tang, Y. Shi, S. Huang, L. Xu, R. Sheng, P. Wu, J. Li, N. Zhou, Y. Hu, *Bioorg. Med. Chem.* **2011**, *19*, 7158 – 7167.

[13] G. Petroianu, K. Arafat, B. C. Sasse, H. Stark, *Pharmazie* **2006**, *61*, 179 – 182.

[14] R. Sheng, L. Tang, L. Jiang, L. Hong, Y. Shi, N. Zhou, Y. Hu, *ACS Chem. Neurosci.* **2016**, *7*, 69 – 81.

[15] S. Hagenow, A. Stasiak, R. R. Ramsay, H. Stark, *Sci. Rep.* **2017**, *7*, 40541.

[16] M. A. Khanfar, A. Affini, K. Lutsenko, K. Nikolic, S. Butini, H. Stark, *Front. Neurosci.* **2016**, *10*, 1 – 17.

[17] K. Wingen, H. Stark, *Drug Discovery Today Technol.* **2013**, *10*, e483 – e489.

[18] S. Celanire, M. Wijtmans, P. Talaga, R. Leurs, I. J. de Esch, *Drug Discovery Today* **2005**, *10*, 1613 – 1627.

[19] B. Sadek, D. Lazewska, S. Hagenow, K. Kiec-Kononowiczc, H. Stark in *The Receptors. Histamine Receptors.* (Hrsg.: P. Blandina, M. B. Passani), Springer, Cham, **2016**, S. 109 – 156.

[20] K. Nikolic, D. Agbaba, H. Stark, *J. Taiwan Inst. Chem. Eng.* **2015**, *46*, 15 – 29.

[21] K. Nikolic, S. Filipic, D. Agbaba, H. Stark, *CNS Neurosci. Ther.* **2014**, *20*, 613 – 623.

[22] X. Ligneau, S. Morisset, J. Tardivel-Lacombe, F. Gbahou, C. R. Ganellin, H. Stark, W. Schunack, J. C. Schwartz, J. M. Arrang, *Br. J. Pharmacol.* **2000**, *131*, 1247 – 1250.

[23] T. Esbenshade, K. Krueger, *J. Pharmacol. Exp. Ther.* **2003**, *305*, 887 – 896.

[24] B. S. Wulff, S. Hastrup, K. Rimvall, *Eur. J. Pharmacol.* **2002**, *453*, 33 – 41.

[25] O. Benek, O. Soukup, M. Pasdiorova, L. Hroch, V. Sepsova, P. Jost, M. Hrabinova, D. Jun, K. Kuca, D. Zala, et al., *Chem-MedChem* **2016**, *11*, 1264 – 1269.

[26] L. L. C. Molsoft, „http://molsoft.com/mprop/", **2017**.

[27] A. Dávalos, C. Gómez-Cordovés, B. Bartolomé, *J. Agric. Food Chem.* **2004**, *52*, 48 – 54.

[28] M. I. Fernández-Bachiller, C. Pérez, N. E. Campillo, J. A. Páez, G. C. González-Muñoz, P. Usán, E. García-Palomero, M. G. López, M. Villarroya, A. G. García, et al., *ChemMedChem* **2009**, *4*, 828 – 841.

[29] M. Benchekroun, M. Bartolini, J. Egea, A. Romero, E. Soriano, M. Pudlo, V. Luzet, V. Andrisano, M. L. Jimeno, M. G. López, et al., *ChemMedChem* **2015**, *10*, 523 – 539.

[30] E. Stragier, V. Martin, E. Davenas, C. Poilbout, R. Mongeau, R. Corradetti, L. Lanfumey, *Transl. Psychiatry* **2015**, *5*, e696.

[31] H. Stark, *Drug Discovery Today* **2004**, *9*, 736 – 737.

3.4 Publication 4

Systematic data mining reveals synergistic H$_3$R/MCHR1 ligands

Schaller, D.[1], Hagenow, S.[2], Alpert, G.[2], Naß, A.[1], Schulz, R.[1], Bermudez, M.[1], Stark, H.[2], Wolber, G.[1]

[1] Pharmaceutical and Medicinal Chemistry, Freie Universitaet Berlin, Koenigin-Luise-Str. 2+4, 14195 Berlin, Germany. [2] Pharmaceutical and Medicinal Chemistry, Heinrich Heine University Duesseldorf, Universitaetsstr. 1, 40225 Duesseldorf, Germany.

Abstract

In this study, we report a ligand-centric data mining approach that guided the identification of suitable target profiles for treating obesity. The newly developed method is based on identifying target pairs for synergistic positive effects and also encompasses the exclusion of compounds showing a detrimental effect on obesity treatment (off-targets). Ligands with known activity against obesity-relevant targets were compared using fingerprint representations. Similar compounds with activities to different targets were evaluated for the mechanism of action since activation or deactivation of drug targets determines the pharmacological effect. In vitro validation of the modeling results revealed that three known modulators of melanin-concentrating hormone receptor 1 (MCHR1) show a previously unknown submicromolar affinity to the histamine H$_3$ receptor (H$_3$R). This synergistic activity may present a novel therapeutic option against obesity.

Systematic Data Mining Reveals Synergistic H3R/MCHR1 Ligands

David Schaller,[†] Stefanie Hagenow,[‡] Gina Alpert,[‡] Alexandra Naß,[†] Robert Schulz,[†] Marcel Bermudez,[†] Holger Stark,[‡] and Gerhard Wolber*[,†]

[†]Pharmaceutical and Medicinal Chemistry, Freie Universität Berlin, Königin-Luise-Str. 2+4, 14195 Berlin, Germany

[‡]Pharmaceutical and Medicinal Chemistry, Heinrich-Heine-Universität Düsseldorf, Universitätsstr. 1, 40225 Düsseldorf, Germany

ⓢ Supporting Information

ABSTRACT: In this study, we report a ligand-centric data mining approach that guided the identification of suitable target profiles for treating obesity. The newly developed method is based on identifying target pairs for synergistic positive effects and also encompasses the exclusion of compounds showing a detrimental effect on obesity treatment (off-targets). Ligands with known activity against obesity-relevant targets were compared using fingerprint representations. Similar compounds with activities to different targets were evaluated for the mechanism of action since activation or deactivation of drug targets determines the pharmacological effect. *In vitro* validation of the modeling results revealed that three known modulators of melanin-concentrating hormone receptor 1 (MCHR1) show a previously unknown submicromolar affinity to the histamine H3 receptor (H₃R). This synergistic activity may present a novel therapeutic option against obesity.

KEYWORDS: *Multitarget drugs, fingerprints, histamine H3 receptor, melanin-concentrating hormone receptor 1, obesity*
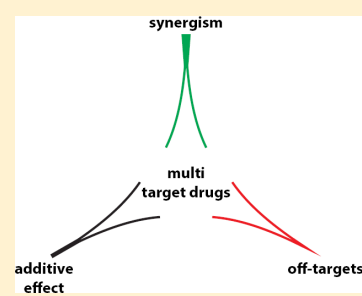
Rational drug design has traditionally focused on the discovery of selective ligands for specific molecular targets. It was assumed that by increasing the selectivity of a ligand for the desired target, undesired side effects arisen from binding to off-targets would be minimized. In recent years, multitarget approaches (often termed "polypharmacology") challenged this dogma proposing that the modulation of multiple targets in the biological network simultaneously may be required to effectively modify a phenotype.[1] Particularly diseases with a complex etiology gained attention for development of multitarget drugs.[2] For instance, several anticancer agents were designed to inhibit certain kinases involved in different aspects of apoptosis and angiogenesis.[3] Also the most effective medications for central nervous system disorders modulate various neurotransmitter levels by targeting several GPCRs or enzymes involved.[4]

Research on databases for ligand activity data indicates that most drugs bind to multiple targets.[5] Furthermore, these drug-target networks are far from being complete since testing each drug against each possible target is economically not favorable. Computational approaches present a suitable option to close this gap and can support the rational multitarget drug design process.[6−9] Analyzing chemical similarities of already known drug-like molecules proved to be particularly successful. Keiser and colleagues were the pioneers in this research field using fingerprint representations of small molecules to predict potential off-targets of approved drugs.[10] Later, Besnard and colleagues calculated Bayesian models for 784 proteins and were able to optimize ligands to a wide array of targets and potential off-targets.[11] Continuously growing public databases for ligand activity data (e.g., ChEMBL[12]) support these ligand-centric approaches.

In this study, we focused on the first step of rational multitarget drug design, the identification of target pairs that can be modulated by the same ligand. Obesity was chosen as model disease since it is known to bear a complex etiology and single-target medications still lack efficacy and safety.[13] To achieve our goal, we implemented a data mining workflow in KNIME that clusters obesity-relevant targets based on the chemical similarity of ligands from the ChEMBL database.[12,14] Despite its significance for the pharmacological effect, the mechanism of action is still missing for the majority of compounds in public bioactivity databases. For instance, when antagonism of a certain receptor is discussed for obesity treatment, agonism will be ineffective or even induce obesity. Thus, special emphasis was placed on evaluating the mechanism of action of ligand data in terms of activation or deactivation. This strategy led to the identification of several potential target pairs and off-targets that should be considered in obesity treatment. The most promising target pair comprising histamine H3 receptor (H₃R) and melanin-concentrating hormone receptor 1 (MCHR1) could be confirmed *in vitro*.

A literature research yielded 39 obesity-relevant targets with associated activity data stored in the ChEMBL 21 database.[12] These targets can be classified into 25 receptors (24 GPCRs, 1 nuclear receptor), 11 enzymes of the lipid metabolism, and
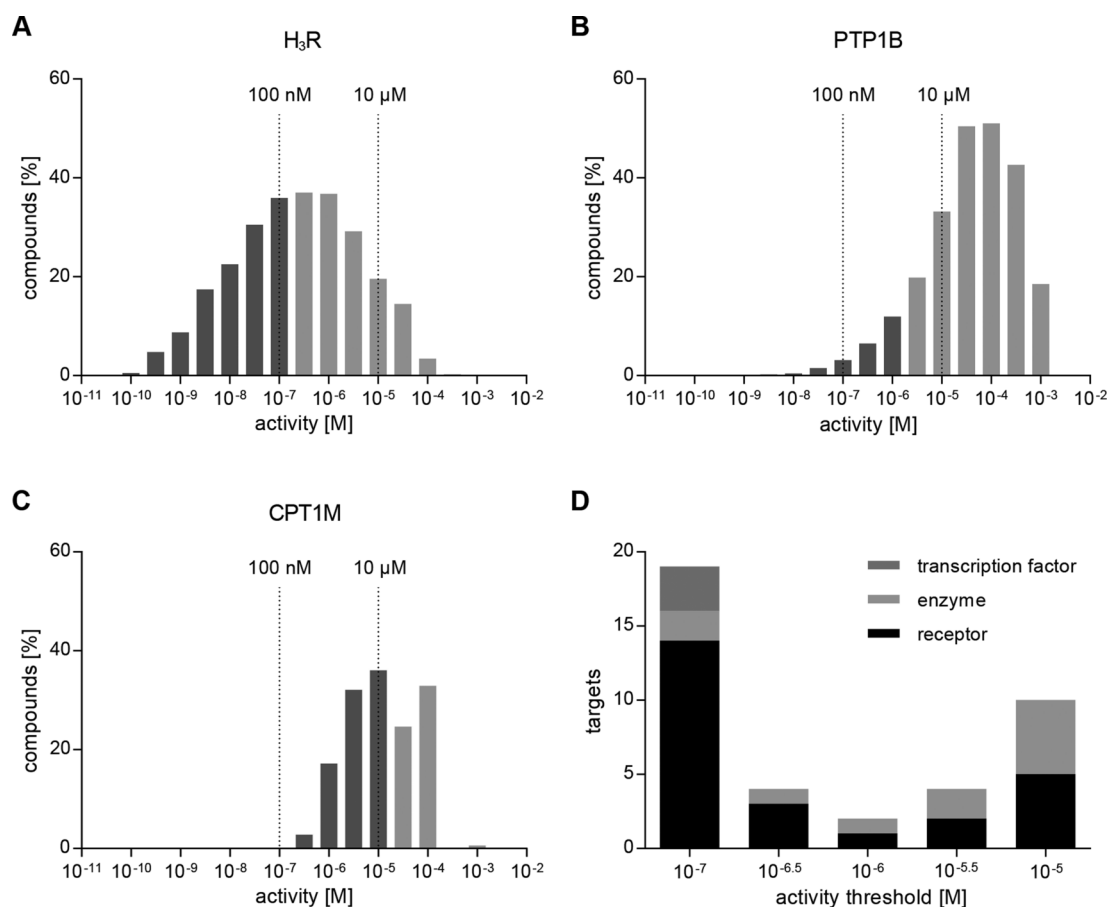
Figure 1. Assignment of activity thresholds for each target separately based on activity data stored in the ChEMBL database. Activity ranges for ligands of (A) histamine H3 receptor, (B) protein-tyrosine phosphatase 1B, and (C) carnitine palmitoyltransferase 1 (muscle isoform). Activity threshold is set three orders of magnitude above the most active compound and limited to a minimum of 100 nM and a maximum of 10 μM. Compounds satisfying the activity threshold are highlighted in dark gray. (D) Distribution of activity thresholds for targets included in this study.

three transcription factors. The multitude of targets discussed in literature underlines the complex etiology of obesity and the necessity to address several targets in the signaling network. A complete list can be found in the Supporting Information (Table S3).

The activity range of ligands in the ChEMBL database can be dramatically different for each target (Figure 1A–C). Thus, a single threshold (e.g., 1 μM) for all targets may not present the most suitable option to extract and focus on the most interesting and active ligands. For instance, a well explored GPCR may require a lower activity threshold than a less well explored protein–protein interaction. Consequently, a protocol has been implemented setting the activity threshold three orders of magnitude above the most active compound. In certain cases, this procedure would result in activity thresholds below 100 nM and subsequently would exclude potentially interesting compounds. Thus, we decided to limit the thresholds to a minimum of 100 nM. Furthermore, a maximum was introduced at 10 μM to exclude poorly active compounds. Targets with a lower activity threshold include several well explored GPCRs, like serotonin receptors, histamine H3 receptor (H3R), and melanin-concentrating hormone receptor

1 (MCHR1), whereas higher thresholds were commonly assigned to enzymes like carnitine palmitoyltransferase 1 (muscle isoform) and less well explored GPCRs like amylin receptor 1 (Figure 1D). Applying these thresholds to our data set resulted in the selection of 20841 compounds for similarity analysis.

Multitarget action can frequently be observed within a target family since target subtypes bind the same endogenous ligand or substrate and thus share similarities in the binding pocket.[2] Therefore, target subtypes were grouped into target families to allow the identification of more distant relations (structure file activity_data.sdf with assigned target families is provided as Supporting Information).

Subsequently, chemical similarities between compounds of different target families were investigated using Morgan Feature circular fingerprints as implemented in RDKit.[15,16] Compounds were considered similar if they belong to different target families and if the Tanimoto score is 0.7 or higher.

From the initial data set (20841 compounds) only 204 compounds with 233 activities against 19 obesity-relevant targets fulfilled the similarity criteria (Tanimoto score $\geq$ 0.7) to a compound of a different target family.
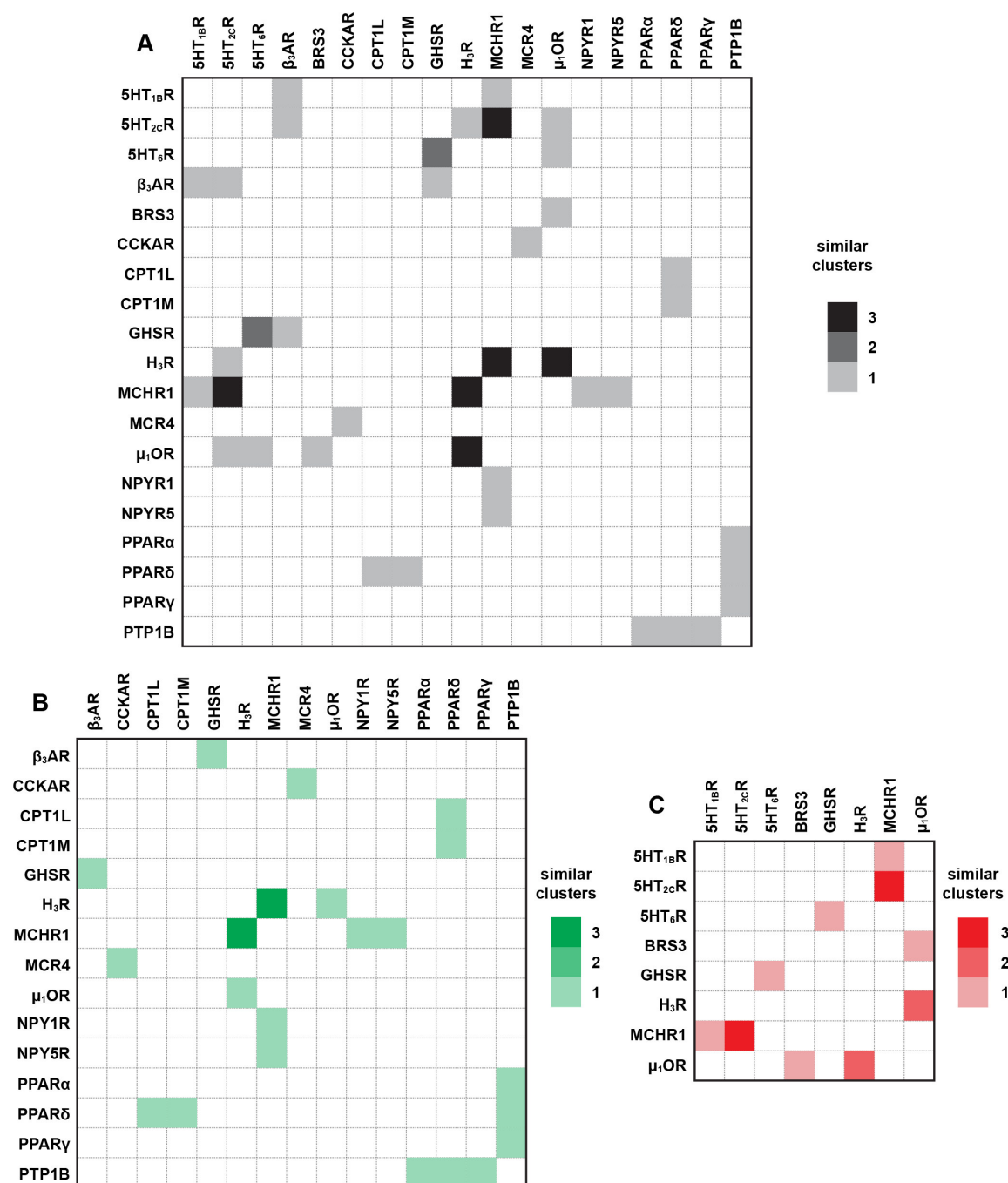
Figure 2. Similarity matrices for obesity-relevant targets based on the chemical similarity of known ligands. Only target pairs are considered that belong to different target families. Ligands were clustered to allow a quality assessment of the target pairs. (A) Similarity matrix without validation of mechanism of action. (B) Similarity matrix with the desired antiobese mechanism of action for both elements of the target pair. (C) Similarity matrix for target pairs, whereas one of the elements of a target pair has a conflictive mechanism of action and thus presents a potential off-target in obesity treatment.

For each target pair, similar compounds were analyzed for diversity by using an in-house implementation of the Taylor–Butina clustering algorithm.[17] This step allows a quality assessment since a higher number of shared similar clusters indicates an increased probability to identify multitarget drugs against this target pair. The identified target pairs are gathered
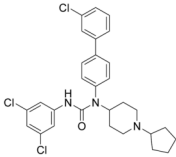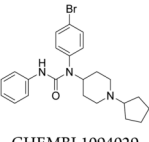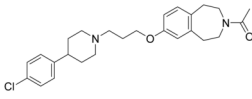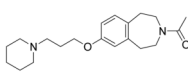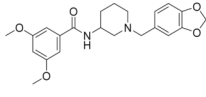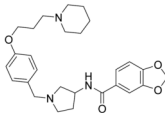
in a similarity matrix, whereas each target pair is rated based on the number of similar clusters (Figure 2A). The target pairs MCHR1/5HT$_{2C}$R, $_{\mu 1}$OR/H$_3$R, and H$_3$R/MCHR1 are rated the best sharing three similar clusters.

Next, the mechanism of action for each cluster was retrieved from literature. This evaluation resulted in the generation of two similarity matrices (Figure 2B,C). One holds information about possible synergistic effects with the desired antiobese mechanism of action for both elements of the target pair (Figure 2B). The target pair comprising H$_3$R and MCHR1 is the only one with more than one similar cluster. The second similarity matrix shows potential off-targets (Figure 2C). For instance, MCHR1 antagonists (desired mechanism of action) show similarities to serotonin receptor 2C (5HT$_{2C}$R) antagonists (conflictive mechanism of action). Noteworthy, several screening campaigns against MCHR1 have reported 5HT$_{2C}$R as off-target.[18] A full list of clusters with associated mechanism of action can be found in the Supporting Information (Table S4).
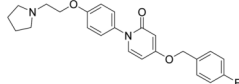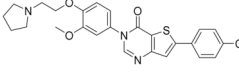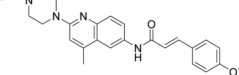
The identified similar clusters for H$_3$R/MCHR1 (Table 1) share a positively charged amine function that is known to be involved in Coulomb interactions with a conserved aspartate for many aminergic GPCRs but also for MCHR1.[18,19]

Table 1. Cluster Pairs Binding to H$_3$R and MCHR1, Respectively

MCHR1	H$_3$R
A CHEMBL433591	CHEMBL1094029
B CHEMBL1914860	CHEMBL210291
C CHEMBL187916	CHEMBL3094128

Considering the high Morgan Feature fingerprint similarity of known ligands, H$_3$R and MCHR1 were chosen for further validation. A shape-based screening campaign using ROCS led to the selection of three known MCHR1 antagonists for a radioligand displacement assay at H$_3$R.[20] All three tested compounds show submicromolar activity against both receptors (Table 2). Compounds **1** and **2** were already described to have antiobesity effects in rodents.[21−24] To our knowledge, compound **3** with the most balanced activity against both receptors (K_i/IC$_{50}$ < 20 nM) has not yet been tested *in vivo*. The ligand efficiency (LE) for compound **3** of 0.34 lies above the limit for drug-like molecules (LE > 0.3) and thus indicates a good starting point for further development.[25] The lip-

Table 2. Activity Table of Known MCHR1 Antagonists

structure	H$_3$R[a] K_i [nM]	MCHR1[b] IC$_{50}$ [nM]
1	516.7	5.6
2	208.0	89.1
3	10.6	16.0

[a]Mean of at least three independent experiments, each performed at least in duplicates in a radioligand displacement assay at H$_3$R. [b]Data for compounds **1**,[24] **2**,[23] and **3**[26] are taken from the literature.

ophilicity-corrected ligand efficiency (LELP) includes lipophilicity for quality assessment as this property has been shown to accompany with promiscuity.[25] The LELP of 12.40 for compound **3** points to potential promiscuity issues. Indeed, closely related compounds of this series show moderate affinity at 5HT$_{2C}$R, emphasizing the consideration of this receptor as off-target.[26]

Only two studies were found describing compounds with a multitarget character against H$_3$R and MCHR1.[27,28] However, the authors did not aim at developing compounds with balanced activity against both receptors. Screening campaigns for selective antagonists of H$_3$R or MCHR1 did not yet result in development of an effective antiobesity treatment. Though, there is evidence for a possible synergistic effect. A recent study revealed that activation of H$_3$R leads to the inhibition of MCH expression.[29] This inhibition could be avoided through administration of a H$_3$R antagonist resulting in expression of MCH. A concurrent expression of the appetite stimulant MCH might explain why the ongoing effort in designing H$_3$R antagonists for obesity treatment did not lead to an effective therapy yet. Although this study focused on sleep and arousal, translating these results into obesity research indicates a promising synergistic effect of dual antagonism of H$_3$R and MCHR1.

In this study, we have successfully applied a ligand-centric data mining approach to identify target pairs that have the potential to drive future multitarget drug research for obesity treatment. The most promising target pair comprising H$_3$R and MCHR1 was validated *in vitro*. Three compounds have been confirmed to hold a multitarget character in the submicromolar activity range. Evaluating the mechanism of action not only allowed the identification of potential target pairs but additionally pointed to several off-targets that should be considered in antiobesity drug development.

■ ASSOCIATED CONTENT

Ⓢ Supporting Information

The Supporting Information is available free of charge on the ACS Publications website at DOI: 10.1021/acsmedchem-lett.7b00118.

Experimental procedures as well as tables of included targets and identified similarities (PDF)
Structures in sdf format (ZIP)

■ AUTHOR INFORMATION

Corresponding Author
*E-mail: gerhard.wolber@fu-berlin.de.
ORCID ⊙
David Schaller: 0000-0002-1881-4518
Gerhard Wolber: 0000-0002-5344-0048

Author Contributions
D.S. conducted analysis, designed and performed experiments, and wrote the manuscript. S.H. and G.A. designed and performed experiments. A.N., R.S., M.B., H.S., and G.W. designed experiments. H.S. and G.W. directed the studies. All authors reviewed the manuscript.

Notes
The authors declare no competing financial interest.

■ ABBREVIATIONS

$5HT_{1B}R$, serotonin receptor 1B; $5HT_{2C}R$, serotonin receptor 2C; $5HT_6R$, serotonin receptor 6; $\beta 3AR$, beta 3 adrenergic receptor; BRS3, bombesin receptor subtype 3; CCKAR, cholecystokinin A receptor; CPT1L, carnitine O-palmitoyl-transferase 1 (liver isoform); CPT1M, carnitine O-palmitoyl-transferase 1 (muscle isoform); GHSR, growth hormone secretory receptor; H_3R, histamine H3 receptor; MCR4, melanocortin receptor 4; MCHR1, melanin-concentrating hormone receptor 1; μ_1OR, mu 1 opioid receptor; NPYR1, neuropeptide Y receptor 1; NPYR5, neuropeptide Y receptor 5; PPARα, peroxisome proliferator-activated receptor alpha; PPARδ, peroxisome proliferator-activated receptor delta; PPARγ, peroxisome proliferator-activated receptor gamma; PTP1B, protein-tyrosine phosphatase 1B

■ REFERENCES

(1) Anighoro, A.; Bajorath, J.; Rastelli, G. Polypharmacology: Challenges and Opportunities in Drug Discovery. *J. Med. Chem.* **2014**, *57* (19), 7874−7887.

(2) Peters, J.-U. Polypharmacology - Foe or Friend? *J. Med. Chem.* **2013**, *56* (22), 8955−8971.

(3) Faivre, S.; Demetri, G.; Sargent, W.; Raymond, E. Molecular Basis for Sunitinib Efficacy and Future Clinical Development. *Nat. Rev. Drug Discovery* **2007**, *6* (9), 734−745.

(4) Roth, B. L.; Sheffler, D. J.; Kroeze, W. K. Magic Shotguns versus Magic Bullets: Selectively Non-Selective Drugs for Mood Disorders and Schizophrenia. *Nat. Rev. Drug Discovery* **2004**, *3* (4), 353−359.

(5) Mestres, J.; Gregori-Puigjané, E.; Valverde, S.; Solé, R. V. The Topology of Drug-Target Interaction Networks: Implicit Dependence on Drug Properties and Target Families. *Mol. BioSyst.* **2009**, *5* (9), 1051−1057.

(6) Lavecchia, A.; Cerchia, C. In Silico Methods to Address Polypharmacology: Current Status, Applications and Future Perspectives. *Drug Discovery Today* **2016**, *21* (2), 288−298.

(7) Nikolic, K.; Filipic, S.; Agbaba, D.; Stark, H. Procognitive Properties of Drugs with Single and Multitargeting H 3 Receptor Antagonist Activities. *CNS Neurosci. Ther.* **2014**, *20*, 613−623.

(8) Nikolic, K.; Agbaba, D.; Stark, H. Pharmacophore Modeling, Drug Design and Virtual Screening on Multi-Targeting Procognitive Agents Approaching Histaminergic Pathways. *J. Taiwan Inst. Chem. Eng.* **2015**, *46*, 15−29.

(9) Khanfar, M. A.; Affini, A.; Lutsenko, K.; Nikolic, K.; Butini, S.; Stark, H. Multiple Targeting Approaches on Histamine H3 Receptor Antagonists. *Front. Neurosci.* **2016**, *10* (MAY), 1−17.

(10) Keiser, M. J.; Roth, B. L.; Armbruster, B. N.; Ernsberger, P.; Irwin, J. J.; Shoichet, B. K. Relating Protein Pharmacology by Ligand Chemistry. *Nat. Biotechnol.* **2007**, *25* (2), 197−206.

(11) Besnard, J.; Ruda, G. F.; Setola, V.; Abecassis, K.; Rodriguiz, R. M.; Huang, X.-P.; Norval, S.; Sassano, M. F.; Shin, A. I.; Webster, L. A.; Simeons, F. R. C.; Stojanovski, L.; Prat, A.; Seidah, N. G.; Constam, D. B.; Bickerton, G. R.; Read, K. D.; Wetsel, W. C.; Gilbert, I. H.; Roth, B. L.; Hopkins, A. L. Automated Design of Ligands to Polypharmacological Profiles. *Nature* **2012**, *492* (7428), 215−220.

(12) Bento, A. P.; Gaulton, A.; Hersey, A.; Bellis, L. J.; Chambers, J.; Davies, M.; Krüger, F. A.; Light, Y.; Mak, L.; McGlinchey, S.; Nowotka, M.; Papadatos, G.; Santos, R.; Overington, J. P. The ChEMBL Bioactivity Database: An Update. *Nucleic Acids Res.* **2014**, *42*, D1083.

(13) Saltiel, A. R. New Therapeutic Approaches for the Treatment of Obesity. *Sci. Transl. Med.* **2016**, *8* (323), 323rv2.

(14) Berthold, M. R.; Cebron, N.; Dill, F.; Gabriel, T. R.; Kötter, T.; Meinl, T.; Ohl, P.; Sieb, C.; Thiel, K.; Wiswedel, B. KNIME: The Konstanz Information Miner. *Data Analysis, Machine Learning and Applications* **2008**, 319−326.

(15) Rogers, D.; Hahn, M. Extended-Connectivity Fingerprints. *J. Chem. Inf. Model.* **2010**, *50* (5), 742−754.

(16) RDKit: Open-Source Cheminformatics. http://www.rdkit.org.

(17) Butina, D. Unsupervised Data Base Clustering Based on Daylight's Fingerprint and Tanimoto Similarity: A Fast and Automated Way To Cluster Small and Large Data Sets. *J. Chem. Inf. Comput. Sci.* **1999**, *39* (4), 747−750.

(18) Högberg, T.; Frimurer, T. M.; Sasmal, P. K. Melanin Concentrating Hormone Receptor 1 (MCHR1) Antagonists - Still a Viable Approach for Obesity Treatment? *Bioorg. Med. Chem. Lett.* **2012**, *22* (19), 6039−6047.

(19) Katritch, V.; Cherezov, V.; Stevens, R. C. Structure-Function of the G Protein−Coupled Receptor Superfamily. *Annu. Rev. Pharmacol. Toxicol.* **2013**, *53* (1), 531−556.

(20) Hawkins, P. C. D.; Skillman, A. G.; Nicholls, A. Comparison of Shape-Matching and Docking as Virtual Screening Tools. *J. Med. Chem.* **2007**, *50* (1), 74−82.

(21) Hertzog, D. L.; Al-Barazanji, K. A.; Bigham, E. C.; Bishop, M. J.; Britt, C. S.; Carlton, D. L.; Cooper, J. P.; Daniels, A. J.; Garrido, D. M.; Goetz, A. S.; Grizzle, M. K.; Guo, Y. C.; Handlon, A. L.; Ignar, D. M.; Morgan, R. O.; Peat, A. J.; Tavares, F. X.; Zhou, H. The Discovery and Optimization of Pyrimidinone-Containing MCH R1 Antagonists. *Bioorg. Med. Chem. Lett.* **2006**, *16* (18), 4723−4727.

(22) Ito, M.; Ishihara, A.; Gomori, A.; Egashira, S.; Matsushita, H.; Mashiko, S.; Ito, J.; Ito, M.; Nakase, K.; Haga, Y.; Iwaasa, H.; Suzuki, T.; Ohtake, N.; Moriya, M.; Sato, N.; MacNeil, D. J.; Takenaga, N.; Tokita, S.; Kanatani, A. Melanin-Concentrating Hormone 1-Receptor Antagonist Suppresses Body Weight Gain Correlated with High Receptor Occupancy Levels in Diet-Induced Obesity Mice. *Eur. J. Pharmacol.* **2009**, *624* (1−3), 77−83.

(23) Oyarzabal, J.; Howe, T.; Alcazar, J.; Andrés, J. I.; Alvarez, R. M.; Dautzenberg, F.; Iturrino, L.; Martínez, S.; Van der Linden, I. Novel Approach for Chemotype Hopping Based on Annotated Databases of Chemically Feasible Fragments and a Prospective Case Study: New Melanin Concentrating Hormone Antagonists. *J. Med. Chem.* **2009**, *52* (7), 2076−2089.

(24) Haga, Y.; Mizutani, S.; Naya, A.; Kishino, H.; Iwaasa, H.; Ito, M.; Ito, J.; Moriya, M.; Sato, N.; Takenaga, N.; Ishihara, A.; Tokita, S.; Kanatani, A.; Ohtake, N. Discovery of Novel Phenylpyridone

Derivatives as Potent and Selective MCH1R Antagonists. *Bioorg. Med. Chem.* **2011**, *19* (2), 883−893.

(25) Hopkins, A. L.; Keserü, G. M.; Leeson, P. D.; Rees, D. C.; Reynolds, C. H. The Role of Ligand Efficiency Metrics in Drug Discovery. *Nat. Rev. Drug Discovery* **2014**, *13*, 105.

(26) Ulven, T.; Frimurer, T. M.; Receveur, J.-M.; Little, P. B.; Rist, O.; Nørregaard, P. K.; Högberg, T. 6-Acylamino-2-Aminoquinolines as Potent Melanin-Concentrating Hormone 1 Receptor Antagonists. Identification, Structure-Activity Relationship, and Investigation of Binding Mode. *J. Med. Chem.* **2005**, *48* (18), 5684−5697.

(27) Cirauqui, N.; Schrey, A. K.; Galiano, S.; Ceras, J.; Pérez-Silanes, S.; Aldana, I.; Monge, A.; Kühne, R. Building a MCHR1 Homology Model Provides Insight into the Receptor-Antagonist Contacts That Are Important for the Development of New Anti-Obesity Agents. *Bioorg. Med. Chem.* **2010**, *18* (21), 7365−7379.

(28) Johansson, A.; Löfberg, C.; Antonsson, M.; Von Unge, S.; Hayes, M. A.; Judkins, R.; Ploj, K.; Benthem, L.; Lindén, D.; Brodin, P.; Wennerberg, M.; Fredenwall, M.; Li, L.; Persson, J.; Bergman, R.; Pettersen, A.; Gennemark, P.; Hogner, A. Discovery of (3-(4-(2-Oxa-6-azaspiro[3.3]heptan-6-Ylmethyl)phenoxy)azetidin-1-yl)(5-(4-Methoxyphenyl)-1,3,4-Oxadiazol-2-Yl)methanone (AZD1979), a Melanin Concentrating Hormone Receptor 1 (MCHr1) Antagonist with Favorable Physicochemical Properties. *J. Med. Chem.* **2016**, *59* (6), 2497−2511.

(29) Parks, G. S.; Olivas, N. D.; Ikrar, T.; Sanathara, N. M.; Wang, L.; Wang, Z.; Civelli, O.; Xu, X. Histamine Inhibits the Melanin-Concentrating Hormone System: Implications for Sleep and Arousal. *J. Physiol.* **2014**, *592* (Pt 10), 2183−2196.

Supporting Information

Systematic data mining reveals synergistic H3R/MCHR1 ligands

David Schaller, Stefanie Hagenow, Gina Alpert, Alexandra Naß, Robert Schulz, Marcel

Bermudez, Holger Stark and Gerhard Wolber[*]

Table of contents

Experimental Procedures

Data mining

The PubMed database was searched for reviews that contain the keywords "obesity" and "treatment" in the title or abstract.[1] Discussed targets were further reviewed and checked for available activity data in the ChEMBL 21 database.[2] This procedure yielded 39 obesity-relevant targets (Tab. S3).

The following workflow was conducted in KNIME if not specified else.[3] The activity data of studied targets was extracted from the ChEMBL 21 database.[2] Several criteria were applied to exclude ambiguous data. Compounds were filtered for confidence score ($\geq$7), organism (homo sapiens), activity type (K_i, K_D, IC_{50} or EC_{50}), standard units (nM) and operator (=). Additionally, a molecular weight cutoff was set to 700 Da. In total 36626 compounds with 56740 activity data points were included in this study. If multiple data points were available for one compound against the same target, binding data (K_i, K_D) was preferred over functional data (IC_{50}, EC_{50}) and more recent published data was preferred over older data. This procedure condensed the activity data to 41545 activities.

Activity thresholds were set for each target separately based on the available data in the ChEMBL 21 database.[2] The threshold was set three orders of magnitude above the most active compound. However, if a threshold would fall below 100 nM or above 10 µM, this threshold is set to 100 nM or 10 µM respectively (Fig. 2). 20841 compounds with 22018 activities against 38 targets remained for further analysis. The pancreatic lipase was excluded because the compounds did not match the filtering criteria.

38 target subtypes were grouped into 26 target families to focus on more distant relations. For instance, $5HT_{2C}R$, $5HT_{1B}R$ and $5HT_6R$ are part of 5HTR.

Compounds were protonated and fragments removed by using the database wash application in MOE (structure file activity_data.sdf is provided as supporting information).[4] MorganFeat fingerprints (diameter = 4) were generated using the RDKit.[5,6] Compounds were considered similar if the Tanimoto score was at least 0.7 and if they belong to different target families. This procedure resulted in the retrieval of 204 compounds with 233 activities.

To allow quality assessment, similar molecules for each target pair were clustered using an in-house implementation of the Taylor-Butina algorithm with a Tanimoto cutoff at 0.5.[7] First, the number of neighbors (similar molecules with a Tanimoto score of at least 0.5) is calculated for each molecule. Next, the molecule with the most neighbors and all its neighbors are used to define the first cluster. Then, the prior steps are run a second time without the molecules of the first cluster to define the second cluster. These steps are repeated until all molecules are assigned to a cluster. Cluster pairs are defined in each cluster separately by identifying those molecules that show activity against different targets and are the most similar for the investigated cluster. Finally, each element of the cluster pairs was evaluated for their mechanism of action in terms of activation or deactivation (e.g. agonist or antagonist, Tab. S4). Furthermore, target pairs were investigated for potential synergistic effects.
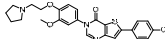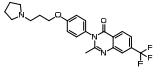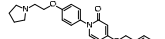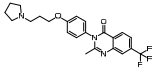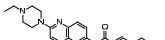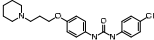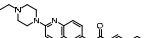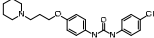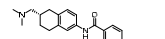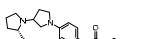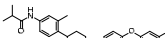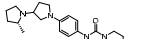
Virtual Screening

Based on our results MCHR1 and H$_3$R presented the most promising target pair and were chosen for further investigation. Scientific literature has been screened for publications to compile manually curated databases of known H$_3$R and MCHR1 antagonists. Structures were downloaded from ChEMBL or if not available using the Sdf-Export tool from Scifinder.[2,8] Six known MCHR1 antagonists (K$_i$/IC$_{50}$ <= 100 nM) were found in the ZINC database to be purchasable from different vendors (structure file ZINC_MCHR1.sdf is provided as supporting information).[9] These compounds were used as query in a shape-based screening campaign against 342 known

H$_3$R antagonists (K$_i$/IC$_{50}$ <= 1 nM, structure file H3R_1nM.sdf is provided as supporting information). First, MCHR1 and H$_3$R antagonists were protonated and energy minimized with the MMFF94 forcefield in MOE.[4,10] Next, conformations of the H$_3$R antagonists were generated using OMEGA with default settings.[11] Finally, each purchasable MCHR1 antagonist was screened against H$_3$R antagonist conformations using ROCS with default settings.[12] Results were analyzed using the TanimotoCombo score as implemented in ROCS (Tab. S1).
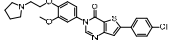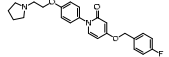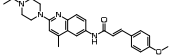
Compound **1 – 5** possess a TanimotoCombo score higher than 1.0 and were considered for *in-vitro* validation. Compound **3** and **4** are nearly identical. Thus, compound **4** with the lower score was excluded. Compound **5** turned out to be not in stock and was not purchased. Compound **6** had a score below 1.0 and hence was not considered for *in-vitro* validation.

Table S1: Purchasable MCHR1 antagonists (K$_i$/IC$_{50}$ <= 100 nM) and the most similar H$_3$R antagonist (K$_i$/IC$_{50}$ <= 1 nM) according to the TanimotoCombo score.

	MCHR1	TanimotoCombo	H$_3$R
1		1.441	
2		1.295	
3		1.165	
4		1.099	
5		1.386	
6		0.979	

Ordered compounds were analyzed with LC-MS and possess a purity of at least 95 % (Tab. S2).

Table S2. Purity and activity of tested compounds analyzed with LC-MS and radioligand depletion experiment, respectively.

	structure	purity	MW [g/mol]	m/z [M+H]$^+$	$pK_i \pm$ SEM
1		> 95 %	408.2	409.0	6.34 ± 0.14
2		> 95 %	481.1	481.8	6.70 ± 0.07
3		> 95 %	430.2	431.0	7.97 ± 0.64

Ligand efficiency calculations

Ligand efficiency (LE) and lipophilicity-corrected ligand efficiency (LELP) were calculated as published previously.[13] The clogP of 4.217 for compound **3** used for LELP was calculated using MOE.[4]

Histamine H$_3$ receptor *in-vitro* assay

For preparation of crude hH$_3$R membrane extracts HEK-293 cells stably expressing the hH$_3$R were cultivated, harvested and processed as described previously.[14]

For the radioligand depletion experiments cell membranes were thawed and homogenized by sonication in ice-cold binding buffer (12.5mM MgCl2,1mM EDTA and 75mM Tris/HCl, pH 7.4). Crude membrane extracts (20 µg/well; final volume of 0.2 ml) were incubated (90 min; room temperature) with various concentrations of test ligands (between 0.01 nM and 100 µM) and [^{3}H]-N-alpha-methylhistamine (2 nM final concentration; 78.3 Ci/mmol). Nonspecific binding was obtained by using pitolisant (10 µM final concentration). Membrane extracts were separated from unbound components by filtration through GF/B filters pre-treated with 0.3% (m/v) polyethyleneimine using an Inotech cell harvester. Liquid scintillation counting was used

for measuring bound radioligand. Data analysis were performed with GraphPad Prism 6 using non-linear regression. The Ki values for each experiment were obtained by using an incorporated equation of GraphPad Prism according to Cheng-Prusoff. Statistical analysis was conducted on pK_i values. Mean values were calculated from at least three independent experiments, each performed at least in duplicates (Tab. S1). Confidence intervals (95%) were calculated and converted to nanomolar concentrations.

Obesity-relevant targets

Table S3. Obesity-relevant targets included in this study categorized by the desired mechanism of action to induce an anti-obese effect.

Agonists/activators

Target	Full name	CHEMBLID	Target family
5HT$_{1B}$R[15]	Serotonin 1B receptor	1898	5HTR
5HT$_{2C}$R[15]	Serotonin 2C receptor	225	5HTR
AMY1[16]	Amylin receptor 1	2111189	AMY
AMY3[16]	Amylin receptor 3	2111190	AMY
β$_3$AR	Beta 3 adrenergic receptor	246	β3AR
BRS3[17]	Bombesin receptor subtype 3	4080	BRS3
CCKAR[18]	Cholecystokinin A receptor	1901	CCKAR
GLP1R[18]	Glucagon-like peptide 1 receptor	1784	GLP1R
MCR3[19]	Melanocortin receptor 3	4644	MCR
MCR4[19]	Melanocortin receptor 4	259	MCR
NPYR2[20]	Neuropeptide Y receptor 2	4018	NPYR
NPYR4[20]	Neuropeptide Y receptor 4	4877	NPYR
OXR1[21]	Orexin receptor 1	5113	OXR
OXR2[21]	Orexin receptor 2	4792	OXR
PPARα[22]	Peroxisome proliferator-activated receptor alpha	239	PPAR
PPARδ[22]	Peroxisome proliferator-activated receptor delta	3979	PPAR
PPARγ[22]	Peroxisome proliferator-activated receptor gamma	235	PPAR
SIRT1[23]	Sirtuin 1	4506	SIRT1
THRβ[24]	Thyroid hormone receptor beta	1947	THRβ

Antagonists/inverse agonists/inhibitors

Target	Full name	CHEMBLID	Target family
11βHD1[25]	11-beta hydroxysteroid dehydrogenase 1	4235	11βHD1
5HT$_6$R[26]	Serotonin 6 receptor	3371	5HTR
ACC1[27]	Acetyl-CoA carboxylase 1	3351	ACC
ACC2[27]	Acetyl-CoA carboxylase 2	4829	ACC
SCD1[28]	Stearoyl-CoA desaturase 1	5555	SCD1
CB1[29]	Cannabinoid receptor 1	218	CB1
CPT1L[30]	Carnitine O-palmitoyltransferase 1, liver isoform	1293194	CPT1
CPT1M[30]	Carnitine O-palmitoyltransferase 1, muscle isoform	2216739	CPT1
CRHR2[31]	Corticotropin releasing hormone receptor 2	4096	CRHR2
DGAT1[32]	Diacylglycerol O-acyltransferase	6009	DGAT1
FAS[33]	Fatty acid synthase	4158	FAS
GALR1[34]	Galanin receptor 1	4894	GAL1R
GHSR[18]	Growth hormone secretory receptor	4616	GHSR
H$_3$R[35]	Histamine H3 receptor	264	H3R
MCHR1[36]	Melanin-concentrating hormone receptor 1	344	MCHR1
μ$_1$OR[37]	Mu 1 opioid receptor	233	MOR
NPYR1[20]	Neuropeptide Y receptor 1	4777	NPYR
NPYR5[20]	Neuropeptide Y receptor 5	4561	NPYR
PLIP[38]	Pancreatic lipase	1812	PLIP
PTP1B[39]	Protein-tyrosine phosphatase 1B	335	PTP1B

Cluster pairs with mode of action

Table S4. Similar cluster pairs with mechanism of action (MOA) and activity to different obesity-relevant targets. n/a – mode of action not available in literature.

target	CHEMBL ID	MOA	tanimoto	MOA	CHEMBL ID	target
$5HT_{1B}R$	3126382	n/a	0.82	agonist	1814275	β_3AR
$5HT_{1B}R$	194837	antagonist	1.00	antagonist	194837	MCHR1
$5HT_{2C}R$	723	n/a	1.00	antagonist	723	β_3AR
$5HT_{2C}R$	127307	agonist	1.00	n/a	127307	H_3R
$5HT_{2C}R$	1818901	antagonist	1.00	antagonist	1818800	MCHR1
$5HT_{2C}R$	216280	antagonist	1.00	antagonist	216280	MCHR1
$5HT_{2C}R$	383800	antagonist	0.71	antagonist	215508	MCHR1
$5HT_{2C}R$	482496	agonist	1.00	n/a	482496	μ_1OR
$5HT_6R$	431298	antagonist	0.83	agonist	2364345	GHSR1a
$5HT_6R$	1079311	n/a	1.00	agonist	1079311	GHSR1a
$5HT_6R$	482496	agonist	1.00	n/a	482496	μ_1OR
β_3AR	1814275	agonist	0.82	n/a	3126382	$5HT_{1B}R$
β_3AR	723	antagonist	1.00	n/a	723	$5HT_{2C}R$
β_3AR	12998	agonist	0.87	antagonist	1077617	GHSR1a
BRS3	3144501	agonist	0.81	agonist	2178733	μ_1OR
CCKAR	327815	agonist	0.77	agonist	591041	MCR4
CPT1L	3431630	inhibitor	0.85	agonist	522575	PPARδ
CPT1M	3431628	inhibitor	0.76	agonist	496116	PPARδ
GHSR	2364345	agonist	0.83	antagonist	431298	$5HT_6R$
GHSR	1079311	agonist	1.00	n/a	1079311	$5HT_6R$
GHSR	1077617	antagonist	0.87	agonist	12998	β_3AR
H_3R	127307	n/a	1.00	agonist	127307	$5HT_{2C}R$
H_3R	1094029	antagonist	0.88	antagonist	433591	MCHR1
H_3R	210291	antagonist	0.73	antagonist	1914860	MCHR1
H_3R	3094128	antagonist	0.76	antagonist	187916	MCHR1
H_3R	3092839	antagonist	0.83	antagonist	237294	μ_1OR
H_3R	441705	antagonist	0.75	agonist	101454	μ_1OR
H_3R	1627	antagonist	1.00	agonist	1627	μ_1OR
MCR4	591041	agonist	0.77	agonist	327815	CCKAR
MCHR1	194837	antagonist	1.00	antagonist	194837	$5HT_{1B}R$
MCHR1	1818800	antagonist	1.00	antagonist	1818901	$5HT_{2C}R$
MCHR1	216280	antagonist	1.00	antagonist	216280	$5HT_{2C}R$
MCHR1	215508	antagonist	0.71	antagonist	383800	$5HT_{2C}R$
MCHR1	433591	antagonist	0.88	antagonist	1094029	H_3R
MCHR1	1914860	antagonist	0.73	antagonist	210291	H_3R
MCHR1	187916	antagonist	0.76	antagonist	3094128	H_3R
MCHR1	217171	antagonist	0.72	antagonist	41457	NPYR1
MCHR1	180003	antagonist	1.00	antagonist	193771	NPYR5
μ_1OR	482496	n/a	1.00	agonist	482496	$5HT_{2C}R$
μ_1OR	482496	n/a	1.00	agonist	482496	$5HT_6R$
μ_1OR	2178733	agonist	0.81	agonist	3144501	BRS3
μ_1OR	237294	antagonist	0.83	antagonist	3092839	H_3R
μ_1OR	101454	agonist	0.75	antagonist	441705	H_3R
μ_1OR	1627	agonist	1.00	antagonist	1627	H_3R
NPYR1	41457	antagonist	0.72	antagonist	217171	MCHR1
NPYR5	193771	antagonist	1.00	antagonist	180003	MCHR1
PPARα	1935608	agonist	1.00	inhibitor	1935608	PTP1B
PPARδ	522575	agonist	0.85	inhibitor	3431630	CPT1L
PPARδ	496116	agonist	0.76	inhibitor	3431628	CPT1M
PPARδ	37495	agonist	0.74	inhibitor	282113	PTP1B
PPARγ	1933093	agonist	1.00	inhibitor	1933093	PTP1B
PTP1B	1935608	inhibitor	1.00	agonist	1935608	PPARα
PTP1B	282113	inhibitor	0.74	agonist	37495	PPARδ
PTP1B	1933093	inhibitor	1.00	agonist	1933093	PPARγ

References

(1) PubMed: US National Library of Medicine, https://www.ncbi.nlm.nih.gov/pubmed/.

(2) Bento, A. P.; Gaulton, A.; Hersey, A.; Bellis, L. J.; Chambers, J.; Davies, M.; Krüger, F. A.; Light, Y.; Mak, L.; McGlinchey, S.; Nowotka, M.; Papadatos, G.; Santos, R.; Overington, J. P. The ChEMBL Bioactivity Database: An Update. *Nucleic Acids Res.* **2014**, *42*.

(3) Berthold, M. R.; Cebron, N.; Dill, F.; Gabriel, T. R.; Kötter, T.; Meinl, T.; Ohl, P.; Sieb, C.; Thiel, K.; Wiswedel, B. KNIME: The Konstanz Information Miner; 2008; pp 319–326.

(4) Chemical Computing Group Inc. Molecular Operating Environment (MOE). Montreal, QC, Canada 2015, p 1010 Sherbooke St. West, Suite #910.

(5) Rogers, D.; Hahn, M. Extended-Connectivity Fingerprints. *J. Chem. Inf. Model.* **2010**, *50* (5), 742–754.

(6) RDKit: Open-Source Cheminformatics; Http://www.rdkit.org.

(7) Butina, D. Unsupervised Data Base Clustering Based on Daylight's Fingerprint and Tanimoto Similarity: A Fast and Automated Way To Cluster Small and Large Data Sets. *J. Chem. Inf. Comput. Sci.* **1999**, *39* (4), 747–750.

(8) Scifinder - A CAS Solution; Http://scifinder.cas.org/scifinder.

(9) Irwin, J. J.; Shoichet, B. K. ZINC--a Free Database of Commercially Available Compounds for Virtual Screening. *J. Chem. Inf. Model. 45* (1), 177–182.

(10) Halgren, T. A. Merck Molecular Force Field. I. Basis, Form, Scope, Parameterization, and Performance of MMFF94. *J. Comput. Chem.* **1996**, *17* (5–6), 490–519.

(11) OMEGA 2.5.1.4: OpenEye Scientific Software, Santa Fe, NM; Http://www.eyesopen.com.

(12) ROCS 3.2.0.4: OpenEye Scientific Software, Santa Fe, NM; Http://www.eyesopen.com.

(13) Hopkins, A. L.; Keserü, G. M.; Leeson, P. D.; Rees, D. C.; Reynolds, C. H. The Role of Ligand Efficiency Metrics in Drug Discovery. *Nat. Publ. Gr.* **2014**, *13*.

(14) Kottke, T.; Sander, K.; Weizel, L.; Schneider, E. H.; Seifert, R.; Stark, H. Receptor-Specific Functional Efficacies of Alkyl Imidazoles as Dual Histamine H3/H4 Receptor Ligands. *Eur. J. Pharmacol.* **2011**, *654* (3), 200–208.

(15) Heisler, L. K.; Jobst, E. E.; Sutton, G. M.; Zhou, L.; Borok, E.; Thornton-Jones, Z.; Liu, H. Y.; Zigman, J. M.; Balthasar, N.; Kishi, T.; Lee, C. E.; Aschkenasi, C. J.; Zhang, C.-Y.; Yu, J.; Boss, O.; Mountjoy, K. G.; Clifton, P. G.; Lowell, B. B.; Friedman, J. M.; Horvath, T.; Butler, A. a; Elmquist, J. K.; Cowley, M. a. Serotonin Reciprocally Regulates Melanocortin Neurons to Modulate Food Intake. *Neuron* **2006**, *51* (2), 239–249.

(16) Roth, J. D. Amylin and the Regulation of Appetite and Adiposity: Recent Advances in Receptor Signaling, Neurobiology and Pharmacology. *Curr. Opin. Endocrinol. Diabetes. Obes.* **2013**, *20* (1), 8–13.

(17) Ramos-Álvarez, I.; Martín-Duce, A.; Moreno-Villegas, Z.; Sanz, R.; Aparicio, C.; Portal-Núñez, S.; Mantey, S. A.; Jensen, R. T.; González, N. Bombesin Receptor Subtype-3 (BRS-3), a Novel Candidate as Therapeutic Molecular Target in Obesity and Diabetes. *Mol. Cell. Endocrinol.* **2013**, *367*, 109–115.

(18) Perry, B.; Wang, Y. Appetite Regulation and Weight Control: The Role of Gut Hormones. *Nutr. Diabetes* **2012**, *2* (1), e26.

(19) Warne, J. P.; Xu, A. W. Metabolic Transceivers: In Tune with the Central Melanocortin

System. *Trends Endocrinol. Metab.* **2013**, *24* (2), 68–75.

(20) Ishihara PhD, A.; Moriya PhD, M.; MacNeil PhD, D. J.; Fukami PhD, T.; Kanatani PhD, A. Neuropeptide Y Receptors as Targets of Obesity Treatment. *Expert Opin. Ther. Pat.* **2006**, *16* (12), 1701–1712.

(21) Xu, T.-R.; Yang, Y.; Ward, R.; Gao, L.; Liu, Y. Orexin Receptors: Multi-Functional Therapeutic Targets for Sleeping Disorders, Eating Disorders, Drug Addiction, Cancers and Other Physiological Disorders. *Cell. Signal.* **2013**, *25* (12), 2413–2423.

(22) Grygiel-Górniak, B. Peroxisome Proliferator-Activated Receptors and Their Ligands: Nutritional and Clinical Implications--a Review. *Nutr. J.* **2014**, *13*, 17.

(23) Boutant, M.; Joffraud, M.; Kulkarni, S. S.; García-Casarrubios, E.; García-Roves, P. M.; Ratajczak, J.; Fernández-Marcos, P. J.; Valverde, A. M.; Serrano, M.; Cantó, C. SIRT1 Enhances Glucose Tolerance by Potentiating Brown Adipose Tissue Function. *Mol. Metab.* **2015**, *4* (2), 118–131.

(24) Grover, G. J.; Mellström, K.; Malm, J. Therapeutic Potential for Thyroid Hormone Receptor-Beta Selective Agonists for Treating Obesity, Hyperlipidemia and Diabetes. *Curr. Vasc. Pharmacol.* **2007**, *5* (2), 141–154.

(25) Chapman, K.; Holmes, M.; Seckl, J. 11B-Hydroxysteroid Dehydrogenases: Intracellular Gate-Keepers of Tissue Glucocorticoid Action. *Physiol. Rev.* **2013**, *93*, 1139–1206.

(26) Heal, D. J.; Smith, S. L.; Fisas, A.; Codony, X.; Buschmann, H. Selective 5-HT6 Receptor Ligands: Progress in the Development of a Novel Pharmacological Approach to the Treatment of Obesity and Related Metabolic Disorders. *Pharmacol. Ther.* **2008**, *117* (2), 207–231.

(27) Strable, M. S.; Ntambi, J. M. Genetic Control of de Novo Lipogenesis: Role in Diet-Induced Obesity. *Crit. Rev. Biochem. Mol. Biol.* **2010**, *45* (3), 199–214.

(28) Sampath, H.; Ntambi, J. M. Role of Stearoyl-CoA Desaturase-1 in Skin Integrity and Whole Body Energy Balance. *Journal of Biological Chemistry*. 2014, pp 2482–2488.

(29) Watkins, B. A.; Kim, J. The Endocannabinoid System: Directing Eating Behavior and Macronutrient Metabolism. *Front. Psychol.* **2014**, *5*, 1506.

(30) Bruce, C. R.; Hoy, A. J.; Turner, N.; Watt, M. J.; Allen, T. L.; Carpenter, K.; Cooney, G. J.; Febbraio, M. a; Kraegen, E. W. Overexpression of Carnitine Palmitoyltransferase-1 in Skeletal Muscle Is Sufficient to Enhance Fatty Acid Oxidation and Improve High-Fat Diet-Induced Insulin Resistance. *Diabetes* **2009**, *58* (3), 550–558.

(31) Mastorakos, G.; Zapanti, E. The Hypothalamic-Pituitary-Adrenal Axis in the Neuroendocrine Regulation of Food Intake and Obesity: The Role of Corticotropin Releasing Hormone. *Nutr. Neurosci.* *7* (5–6), 271–280.

(32) Yen, C.-L. E.; Stone, S. J.; Koliwad, S.; Harris, C.; Farese, R. V. Thematic Review Series: Glycerolipids. DGAT Enzymes and Triacylglycerol Biosynthesis. *J. Lipid Res.* **2008**, *49* (11), 2283–2301.

(33) Lodhi, I. J.; Yin, L.; Jensen-Urstad, A. P. L.; Funai, K.; Coleman, T.; Baird, J. H.; El Ramahi, M. K.; Razani, B.; Song, H.; Fu-Hsu, F.; Turk, J.; Semenkovich, C. F. Inhibiting Adipose Tissue Lipogenesis Reprograms Thermogenesis and PPARγ Activation to Decrease Diet-Induced Obesity. *Cell Metab.* **2012**, *16* (2), 189–201.

(34) Fang, P.; Yu, M.; Guo, L.; Bo, P.; Zhang, Z.; Shi, M. Galanin and Its Receptors: A Novel Strategy for Appetite Control and Obesity Therapy. *Peptides*. 2012, pp 331–339.

(35)   Masaki, T.; Yoshimatsu, H. Therapeutic Approach of Histamine H3 Receptors in Obesity. *Recent Pat. CNS Drug Discov.* **2007**, *2* (3), 238–240.

(36)   Borowsky, B.; Durkin, M. M.; Ogozalek, K.; Marzabadi, M. R.; DeLeon, J.; Lagu, B.; Heurich, R.; Lichtblau, H.; Shaposhnik, Z.; Daniewska, I.; Blackburn, T. P.; Branchek, T. a; Gerald, C.; Vaysse, P. J.; Forray, C. Antidepressant, Anxiolytic and Anorectic Effects of a Melanin-Concentrating Hormone-1 Receptor Antagonist. *Nat. Med.* **2002**, *8* (8), 825–830.

(37)   Karlsson, H. K.; Tuominen, L.; Tuulari, J. J.; Hirvonen, J.; Parkkola, R.; Helin, S.; Salminen, P.; Nuutila, P.; Nummenmaa, L. Obesity Is Associated with Decreased -Opioid But Unaltered Dopamine D2 Receptor Availability in the Brain. *J. Neurosci.* **2015**, *35*, 3959–3965.

(38)   Hvizdos, K. M.; Markham, A. Orlistat: A Review of Its Use in the Management of Obesity. *Drugs* **1999**, *58* (4), 743–760.

(39)   Allison, M. B.; Myers, M. G. 20 YEARS OF LEPTIN: Connecting Leptin Signaling to Biological Function. *J. Endocrinol.* **2014**, *223* (1), T25–T35.

4 Concluding Discussion and Perspectives

The steadily growing awareness about the high complexity defining neurological diseases forced researchers to develop novel approaches for pharmacotherapeutic treatment with a similar complexity. This need is fulfilled by design of multitargeting ligands (MTLs) interacting simultaneously with several targets or mechanisms involved. We hypothesize that histamine H_3 receptor (H_3R) antagonist effects to be introduced in MTLs result in suitable pharmacotherapeutic tools to address a number of symptoms and conditions accompanying these diseases, in particular neurodegenerative diseases. To date, numerous H_3R MTLs, predominantly H_3R antagonists, have been successfully developed for treatment of central nervous system (CNS) disorders, showing additional interaction with other G-protein coupled receptors (GPCRs) such as dopamine or serotonin receptors, enzymes, transporters or signalling molecules.[78]

Within the scope of this thesis, promising MTLs were designed showing H_3R antagonism/inverse agonism combined with either blockade of neurotransmitter-catabolizing enzymes, i.e. monoamine oxidases (MAOs) and cholinesterases (ChEs), or GPCRs such as melanin-concentrating hormone receptors 1 (MCHRs). Most promising lead compounds are presented in Figure 11, showing the aimed design-in of H_3R affinity into MTLs with overall promising pharmacological efficacy and drug-likeness.

Proposed as novel therapeutics for the treatment of neurodegenerative diseases, H_3R MTLs showing reversible or irreversible inhibition of MAO A/B were successfully developed. While a number of H_3R MTLs demonstrating inhibition of ChEs as well as histamine N-methyltransferases (HNMT) were previously published,[78] no H_3R MTLs showing additional MAO inhibition were described to that time. Identified during an initial screening of established H_3R ligands for potential MAO inhibition properties, we could demonstrate ciproxifan's ability to reversibly inhibit preferential MAO B in a low micromolar concentration range in two species (human and rat), presenting the first dualtargeting H_3R/MAO B ligand (Publication 1). Considering ciproxifan's frequent use as reference ligand in rodent models for numerous neurological diseases, our findings suggest, that its MAO inhibition capacity may partially contribute to its in vivo efficacy when applied at high doses. However, only moderate human H_3R affinity and unfavourable pharmacological properties such as cytochrome P450 inhibition, a common drawback of the imidazoles,[251] forced us to enlarge these approach on non-imidazole H_3R antagonists in order to enhance drug-likeness. With ciproxifan's non-imidazole analogue UCL2190, demonstrating improved dualtargeting properties with higher preference for MAO B over MAO A, an optimized lead structure was identified for knowledge-based design of reversible H_3R/MAO B MTLs. Our subsequent ob-
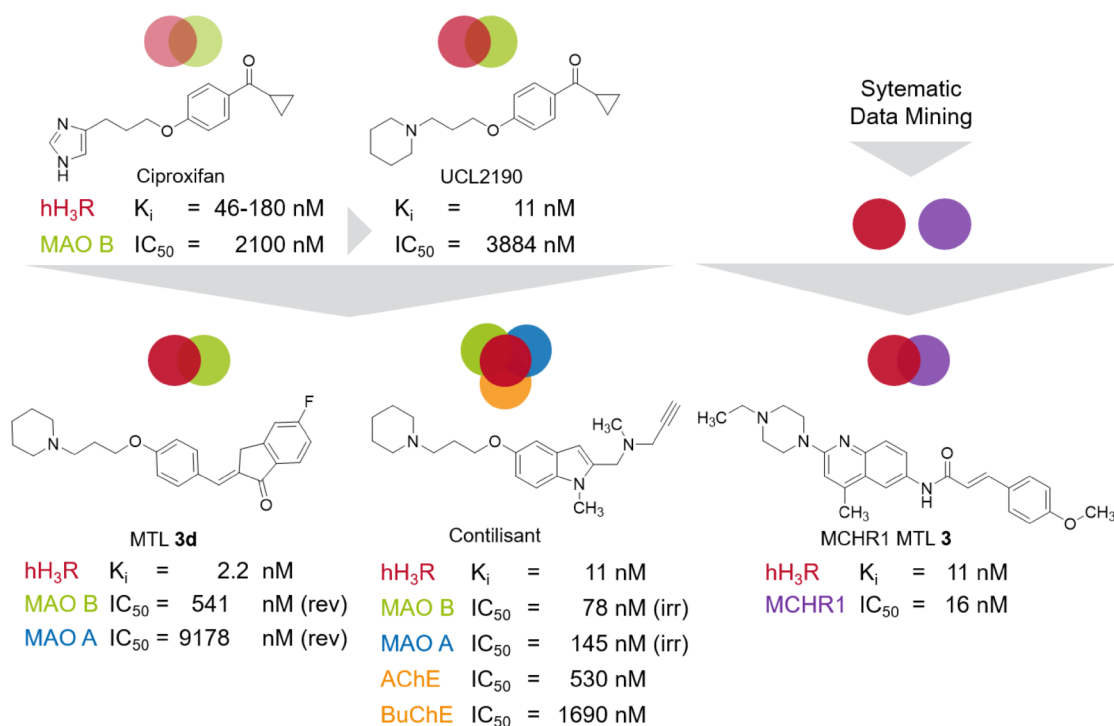
Figure 11 – Most promising histamine H_3 receptor (H_3R) mulitargeting ligands described in this thesis showing either additional reversible/irreversible (rev/irr) monoamine oxidase (MAO) A/B, acetyl-/butyrylcholinesterase (AChE/BuChE) and melanin-concentration hormone receptor (MCHR) 1 inhibition, respectively.

tained small series of 2-benzylidene-1-indanones showed target affinities in nanomolar concentrations ranges with an interesting tight binding or slow reversible behaviour at MAO B without showing Michael acceptor properties (Publication 2). Introduction of large lipophilic residues (i.e. a 4-bromobenzyloxy substituent) led to improvement of MAO B inhibition and/or selectivity, but at the cost of reduced drug-likeness. Compound **3d** (substituted with fluoride) present nanomolar MAO B inhibition with the most drug-like physicochemical properties within this series. Compared to safinamide, the only marketed reversible MAO B inhibitor, these MTLs show about 10-fold less MAO B affinity. Therefore, as primarily developed for the treatment of Parkinson's disease (PD), particularly improvement or balancing of drug-likeness scores and MAO B affinity remain to be addressed prior to in vivo testing.

In parallel, a knowledge-based MTL strategy was pursued with investigation of indole derivatives as irreversible H_3R/MAO inhibitors, whereas a propargyl amine moiety, used as pharmacophoric element, should ensure the covalent binding to the MAO active site as well as neuroprotective features. With the design of contilisant as advancement of the previously in vivo characterized ChE/MAO inhibitor ASS234,[136] an interesting ChE/MAO/H_3R MTL with an optimized, unique phar-

macological profile for neurodegenerative diseases was discovered (Publication 3). As part of a propargyl amine series, proposed as novel drugs for the treatment of Alzheimer's disease (AD), contilisant demonstrated nanomolar affinities at the desired targets, as well as antioxidative and neuroprotective abilities in human neuroblastoma cells. In vivo, contilisant (1 mg kg^{-1}) showed pro-cognitive abilities in mice, while ASS234 at the same dose failed to restore cognitive performance. These proven therapeutic efficacy is most probably due to contilisant's designed-in H$_3$R affinity and more balanced inhibition potency at both MAO isoforms (MAO B/MAO A selevtivity index (SI) = 0.5). With more pronounced MAO B inhibition properties compared to that of ASS234 (SI = 444), contilisant arouses an additional interest for therapy of PD, where predominantly MAO B selective inhibitors are approved.[157] Overall, contilisant might be considered as proof-of-concept MTL, highlighting the therapeutic value for the target combination of H$_3$R with two different types of neurotransmitter-catabolizing enzymes (ChEs, MAOs) involved in neurodegenerative diseases. More comprehensive in vitro validation, e.g. in terms of neurorestorative and -protective capacities, as well as further PD-related in vivo investigations are mandatory, while an antiparkinsonian efficacy of contilisant might be conceivable and similar to that of the irreversible MAO/ChE inhibitor ladostigil.

For the treatment of PD, both strategies of knowledge-based H$_3$R/MAO B multitargeting drug design, comprising either reversible (Publication 2) or irreversible type of MAO (A)/B inhibition (Publication 3), can be considered as pioneering. Based on propargyl amines like contilisant, demonstrating anti-AD properties, general refinement and potential balancing of target affinities may lead to PD-relevant multitargeting candidates. Notably, an optimal, disease-oriented target affinity balance of "on-cell" targets (H$_3$Rs) and "in-cell" targets (ChEs, MAOs) has to be determined. Furthermore, the most sufficient MAO isoform selectivity profile for neurodegenerative diseases as well as the potential utility of combined H$_3$R/ChE inhibition for PD therapy regarding cognitive impairment should be evaluated. Lacking any screening results on antiparkinsonian efficacy so far, we can only hypothesize that H$_3$R/MAO B MTLs are able to maintain antiparkinsonian potency comparable to that of approved MAO B inhibitors but advantageously supported by amelioration of comorbid symptoms like cognitive or sleep impairment. With pitolisant currently in late clinical stages for treatment of excessive daytime sleepiness (EDS) in PD, positive influences of such MTLs on sleep disruptions, either by disease or drug-induced, are most likely, while also pro-cognitive efficiency might be expected via H$_3$R antagonism/inverse agonism, presumably synergistically combined with AChE inhibition. Prospectively, in any case the H$_3$R-based MTL principle might be enlarged to direct dopaminergic targets in PD treatment, i.e. dopa-

mine receptors, as direct interactions between H_3Rs and dopamine receptors are assumed.[17]

Even though the contribution of brain histamine in food intake is undisputed, the preclinically demonstrated anti-obese potential of selective H_3R antagonists remain controversial, especially due to a lack of clinical efficacy but with investigations are still ongoing. However, considering the anti-obese effects of the dual-acting H_1R/H_3R ligand betahistine in schizophrenic patients,[243] the design of H_3R MTLs also including non-histaminergic targets may possess therapeutic relevance, since H_3Rs evidently interact with multiple endocrine systems involved in feeding behaviour such as the melanin-concentrating hormone (MCH) system. Activation of postsynaptic H_3Rs, expressed on MCH neurons, was found to decrease expression of MCH acting via melanin-concentrating hormone receptors, i.a. MCHR1, to induce appetite and food intake. This implies that H_3R antagonists may have an appetising/orexigenic rather than an appetite-suppressing effect, at least within the MCH endocrine system. This once more demonstrate that potential anti-obese effects of H_3R ligands might not only be achieved by presynaptic H_3R autoreceptors, regulating the histaminergic system itself, but also by postsynaptic receptors,[35] probably with opposing mechanisms of action regarding food intake. It might also explain the contradictory clinical observations for selective H_3R antagonists so far, but at the same time suggest the utility of synergistically acting $H_3R/MCHR1$ antagonists as potential appetite-suppressants (Publication 4), which has to be further verified in the future.

Despite the straightforward MTL drug design presented here, realized by combination of target-specific pharmacophoric motifs, further MTL development remain a challenging task in medicinal chemistry due to the need for more extensive pharmacological evaluation as well as reduced flexibility in terms of lead optimization to obtain the desired "selected promiscuity". Issues like selective functional efficacy, design-out of off-target affinities as well as favourable pharmacokinetics i.e. sufficient blood-brain barrier penetration and subsequent brain/plasma distribution, has to be considered like for any other CNS drug. Clearly welcoming in this respect is the tolerance of H_3Rs for structural variability when preserving simple aforementioned pharmacophoric elements, once more endorsing its qualification for multitargeting drug design. However, the pharmacological multiplicity of H_3R modulation on the molecular and therapeutic level, which enables various therapeutic options, may also blur or complicate the estimation of in vivo potency for H_3R MTLs using classical initial disease-relevant models. Preclinical H_3R MTLs should be comprehensively evaluated using distinct animal models, in particular, when temporary or unselective drug-induced behavioural models are used, such as haloperidol-induced catalepsy or reserpine-induced akinesia models.[252] These mod-

els may be less reliable due to possible interference of H_3R ligands with several neurotransmitter systems involved.

As concluding remark, the highly explorative character of the herein described H_3R MTL approach might be noticed. Despite the limited information on therapeutic efficacy for described H_3R MTLs so far, we considered the work presented here as initial evidence for a promising perspective of H_3R antagonists in multitargeting drug design. Thus, we still feel encouraged to further promote H_3R MTL design especially for neurodegenerative diseases, awaiting the development of multitargeting drug candidates.

5 References

1. Gribkoff, V. K. & Kaczmarek, L. K. The need for new approaches in CNS drug discovery: Why drugs have failed, and what can be done to improve outcomes. *Neuropharmacology* **120**, 11–19 (**2017**).

2. Anighoro, A., Bajorath, J. & Rastelli, G. Polypharmacology: Challenges and opportunities in drug discovery. *J. Med. Chem.* **57**, 7874–7887 (**2014**).

3. Ramsay, R. R., Popovic-Nikolic, M. R., Nikolic, K., Uliassi, E. & Bolognesi, M. L. A perspective on multi-target drug discovery and design for complex diseases. *Clin. Transl. Med.* **7**, 1–14 (**2018**).

4. Butini, S., Nikolic, K., Kassel, S., Brückmann, H., Filipic, S., Agbaba, D., Gemma, S., Brogi, S., Brindisi, M., Campiani, G. & Stark, H. Polypharmacology of dopamine receptor ligands. *Prog. Neurobiol.* **142**, 68–103 (**2016**).

5. Morphy, R. & Rankovic, Z. Designed multiple ligands. An emerging drug discovery paradigm. *J. Med. Chem.* **48**, 6523–6543 (**2005**).

6. Millan, M. J. On 'polypharmacy' and multi-target agents, complementary strategies for improving the treatment of depression: a comparative appraisal. *Int. J. Neuropsychopharmacol.* **17**, 1009–1037 (**2014**).

7. Casey, A. B. & Canal, C. E. Classics in Chemical Neuroscience: Aripiprazole. *ACS Chem. Neurosci.* **8**, 1135–1146 (**2017**).

8. Talevi, A. Multi-target pharmacology: Possibilities and limitations of the "skeleton key approach" from a medicinal chemist perspective. *Front. Pharmacol.* **6**, 1–7 (**2015**).

9. Bolognesi, M. L. Polypharmacology in a single drug: multitarget drugs. *Curr. Med. Chem.* **20**, 1639–1645 (**2013**).

10. Morphy, R. & Rankovic, Z. The physicochemical challenges of designing multiple ligands. *J. Med. Chem.* **49**, 4961–4970 (**2006**).

11. Morphy, R., Kay, C. & Rankovic, Z. From magic bullets to designed multiple ligands. *Drug Discov. Today* **9**, 641–651 (**2004**).

12. Wermuth, C., Ganellin, C., Lindberg, P & Mitscher, L. Glossary of Terms Used in Medicinal Chemistry. *Pure Appl. Chem.* **70**, 1129–1143 (**1998**).

13. Fuxe, K., O. Borroto-Escuela, D., Marcellino, D., Romero-Fernandez, W., Frankowska, M., Guidolin, D., Filip, M., Ferraro, L., Woods, A., Tarakanov, A., Ciruela, F., F. Agnati, L. & Tanganelli, S. GPCR Heteromers and their allosteric receptor-receptor interactions. *Curr. Med. Chem.* **19**, 356–363 (**2012**).

14. Hiller, C., Kling, R. C., Heinemann, F. W., Meyer, K., Hübner, H. & Gmeiner, P. Functionally selective dopamine D2/D3 receptor agonists comprising an enyne moiety. *J. Med. Chem.* **56**, 5130–5141 (**2013**).

15. Ferré, S., Casadó, V., Devi, L. A., Filizola, M., Jockers, R., Lohse, M. J., Milligan, G., Pin, J.-P. & Guitart, X. G protein-coupled receptor oligomerization revisited: functional and pharmacological perspectives. *Pharmacol. Rev.* **66**, 413–434 (**2014**).

16. Prati, F., Cavalli, A. & Bolognesi, M. Navigating the chemical space of multitarget-directed ligands: from hybrids to fragments in Alzheimer's disease. *Molecules* **21,** 466 (**2016**).

17. Panula, P. & Nuutinen, S. The histaminergic network in the brain: basic organization and role in disease. *Nat. Rev. Neurosci.* **14,** 472–487 (**2013**).

18. Schwartz, J. C., Pollard, H. & Quach, T. T. Histamine as a neurotransmitter in mammalian brain: neurochemical evidence. *J. Neurochem.* **35,** 26–33 (**1980**).

19. Panula, P., Yang, H.-Y. T & Costa, E. Histamine-containing neurons in the rat hypothalamus. *Proc. Natl. Acad. Sci. USA* **81,** 2572–2576 (**1984**).

20. Watanabe, T., Taguchi, Y., Shiosaka, S., Tanaka, J., Kubota, H., Terano, Y., Tohyama, M. & Wada, H. Distribution of the histaminergic neuron system in the central nervous system of rats; a fluorescent immunohistochemical analysis with histidine decarboxylase as a marker. *Brain Res.* **295,** 13–25 (**1984**).

21. Haas, H. & Panula, P. The role of histamine and the tuberomamillary nucleus in the nervous system. *Nat. Rev. Neurosci.* **4,** 121–130 (**2003**).

22. Sadek, B. S., Saad, A., Latacz, G., Kuder, K., Olejarz, A., Karcz, T., Stark, H. & Kiec-Kononowicz, K. Non-imidazole-based histamine H3 receptor antagonists with anticonvulsant activity in different seizure models in male adult rats. *Drug Des. Devel. Ther.* **10,** 3879–3898 (**2016**).

23. Brown, R. E., Stevens, D. R. & Haas, H. L. The physiology of brain histamine. *Prog. Neurobiol.* **63,** 637–672 (**2001**).

24. Maldonado, M. & Maeyama, K. The metabolism of histamine in rat hypothalamus and cortex after reserpine treatment. *Neurochem. Int.* **85-86,** 31–39 (**2015**).

25. Lim, H. D., van Rijn, R. M., Ling, P., Bakker, R. A., Thurmond, R. L. & Leurs, R. Evaluation of histamine H1-, H2-, and H3-receptor ligands at the human histamine H4 receptor: identification of 4-methylhistamine as the first potent and selective H4 receptor agonist. *J. Pharmacol. Exp. Ther.* **314,** 1310–1321 (**2005**).

26. Panula, P., Chazot, P. L., Cowart, M. D., Gutzmer, R., Leurs, R., Liu, W. L., Stark, H., Thurmond, R. L. & Haas, H. L. International Union of Basic and Clinical Pharmacology. XCVIII. Histamine Receptors. *Pharmacol. Rev.* **67,** 601–655 (**2015**).

27. Mocking, T. A. M., Bosma, R., Rahman, S. N., Verweij, E. W. E., McNaught-Flores, D. A., Vischer, H. F. & Leurs, R. Molecular Aspects of Histamine Receptors. in *Histamine Receptors: Preclinical and Clinical Aspects* (eds Blandina, P. & Passani, M. B.) 28th ed., 1–49 (Humana Press, Cham, Switzerland, **2016**).

28. Arrang, J. M., Garbarg, M. & Schwartz, J. C. Auto-inhibition of brain histamine-release mediated by a novel class H3 of histamine receptor. *Nature* **302,** 832–837 (**1983**).

29. Passani, M. B. & Blandina, P. Histamine receptors in the CNS as targets for therapeutic intervention. *Trends Pharmacol. Sci.* **32,** 242–249 (**2011**).

30. Bongers, G., Bakker, R. A. & Leurs, R. Molecular aspects of the histamine H3 receptor. *Biochem. Pharmacol.* **73,** 1195–1204 (**2007**).

31. Lai, X., Ye, L., Liao, Y., Jin, L., Ma, Q., Lu, B., Sun, Y., Shi, Y. & Zhou, N. Agonist-induced activation of histamine H3 receptor signals to extracellular signal-regulated kinases 1 and 2 through PKC-, PLD-, and EGFR-dependent mechanisms. *J. Neurochem.* **137**, 200–215 (**2016**).

32. Rapanelli, M., Frick, L. R., Horn, K. D., Schwarcz, R. C., Pogorelov, V., Nairn, A. C. & Pittenger, C. The histamine H3 receptor differentially modulates mitogen-activated protein kinase (MAPK) and Akt signaling in striatonigral and striatopallidal neurons. *J. Biol. Chem.* **291**, 21042–21052 (**2016**).

33. Farooqui, A. A. & Horrocks, L. A. Phospholipase A2-generated lipid mediators in the brain: The good, the bad, and the ugly. *Neuroscientist.* **12**, 245–260 (**2006**).

34. Nieto-Alamilla, G., Márquez-Gómez, R., García-Gálvez, A.-M., Morales-Figueroa, G.-E. & Arias-Montaño, J.-A. The histamine H3 receptor: structure, pharmacology and function. *Mol. Pharmacol.* **3964**, 649–673 (**2016**).

35. Parks, G. S., Olivas, N. D., Ikrar, T., Sanathara, N. M., Wang, L., Wang, Z., Civelli, O. & Xu, X. Histamine inhibits the melanin-concentrating hormone system: Implications for sleep and arousal. *J. Physiol.* **592**, 2183–2196 (**2014**).

36. Schwartz, J.-C., Morisset, S., Rouleau, A., Ligneau, X., Gbahou, F., Tardivel-Lacombe, J., Stark, H., Schunack, W., Ganellin, C. R. & Arrang, J.-M. Therapeutic implications of constitutive activity of receptors: the example of the histamine H3 receptor. *J. Neural. Transm. Suppl.* 1–16 (**2003**).

37. Kenakin, T. & Williams, M. Defining and characterizing drug/compound function. *Biochem. Pharmacol.* **87**, 40–63 (**2014**).

38. Lovenberg, T. W., Roland, B. L., Wilson, S. J., Jiang, X, Pyati, J, Huvar, A, Jackson, M. R. & Erlander, M. G. Cloning and functional expression of the human histamine H3 receptor. *Mol. Pharmacol.* **55**, 1101–1107 (**1999**).

39. Nguyen, T., Shapiro, D. A., George, S. R., Setola, V., Lee, D. H., Cheng, R., Rauser, L., Lee, S. P., Lynch, K., Roth, B. L. & O'Dowd, B. F. Discovery of a novel member of the histamine receptor family. *Mol. Pharmacol.* **59**, 427–433 (**2001**).

40. Tardivel-Lacombe, J., Rouleau, A., Héron, A., Morisset, S., Pillot, C., Cochois, V., Schwartz, J. C. & Arrang, J. M. Cloning and cerebral expression of the guinea pig histamine H3 receptor: Evidence for two isoforms. *Neuroreport.* **11**, 755–759 (**2000**).

41. Yao, B., Hutchins, C., Carr, T., Cassar, S, Masters, J., Bennani, Y., Esbenshade, T. & Hancock, A. Molecular modeling and pharmacological analysis of species-related histamine H3 receptor heterogeneity. *Neuropharmacology* **44**, 773–786 (**2003**).

42. Chen, J., Liu, C. & Lovenberg, T. W. Molecular and pharmacological characterization of the mouse histamine H3 receptor. *Eur. J. Pharmacol.* **467**, 57–65 (**2003**).

43. Ireland-Denny, L., Parihar, A. S., Miller, T. R., Kang, C. H., Krueger, K. M., Esbenshade, T. A. & Hancock, A. A. Species-related pharmacological heterogeneity of histamine H3 receptors. *Eur. J. Pharmacol.* **433**, 141–150 (**2001**).

44. Yao, B. B., Sharma, R., Cassar, S., Esbenshade, T. A. & Hancock, A. A. Cloning and pharmacological characterization of the monkey histamine H3 receptor. *Eur. J. Pharmacol.* **482**, 49–60 (**2003**).

45. Peitsaro, N., Sundvik, M., Anichtchik, O. V., Kaslin, J. & Panula, P. Identification of zebrafish histamine H1, H2 and H3 receptors and effects of histaminergic ligands on behavior. *Biochem. Pharmacol.* **73,** 1205–1214 (**2007**).

46. Leurs, R., Bakker, R. A., Timmerman, H. & de Esch, I. J. P. The histamine H3 receptor: from gene cloning to H3 receptor drugs. *Nat. Rev. Drug Discov.* **4,** 107–120 (**2005**).

47. Rouleau, A., Héron, A., Cochois, V., Pillot, C., Schwartz, J.-C. & Arrang, J.-M. Cloning and expression of the mouse histamine H3 receptor: Evidence for multiple isoforms. *J. Neurochem.* **90,** 1331–1338 (**2004**).

48. Esbenshade, T. A., Browman, K. E., Bitner, R. S., Strakhova, M, Cowart, M. D. & Brioni, J. D. The histamine H3 receptor: A attractive target for the treatment of cognitive disorders. eng. *Br. J. Pharmacol.* **154,** 1166–1181 (**2008**).

49. Lovenberg, T. W., Pyati, J., Chang, H., Wilson, S. J., Erlander, M. G., Pharmaceutical, R. W. J. & Diego, S. Cloning of rat histamine H3 receptor reveals distinct species pharmacological profiles. *J. Pharmacol. Exp. Ther.* **293,** 771–778 (**2000**).

50. Micallef, S., Stark, H. & Sasse, A. Polymorphisms and genetic linkage of histamine receptors. *Life Sci.* **93,** 487–494 (**2013**).

51. Arrang, J. M., Garbarg, M. & Schwartz, J. C. Auto-inhibition of brain histamine release mediated by a novel class H3 of histamine receptor. *Nature* **302,** 832–837 (**1983**).

52. Arrang, J. M., Garbarg, M. & Schwartz, J. C. Autoregulation of histamine release in brain by presynaptic H3-receptors. *Neuroscience* **15,** 553–562 (**1985**).

53. Schlicker, E., Schunack, W. & Göthert, M. Histamine H3 receptor-mediated inhibition of noradrenaline release in pig retina discs. *Naunyn Schmiedeberg's Arch. Pharmacol.* **342,** 497–501 (**1990**).

54. Schlicker, E., Fink, K., Detzner, M. & Göthert, M. Histamine inhibits dopamine release in the mouse striatum via presynaptic H3 receptors. *J. Neural. Transm.* **93,** 1–10 (**1993**).

55. Clapham, J. & Kilpatrick, G. J. Histamine H3 receptors modulate the release of [3H]-acetylcholine from slices of rat entorhinal cortex: evidence for the possible existence of H3 receptor subtypes. *Br. J. Pharmacol.* **107,** 919–923 (**1992**).

56. Blandina, P., Giorgetti, M., Bartolini, L., Cecchi, M., Timmerman, H., Leurs, R., Pepeu, G. & Giovannini, M. G. Inhibition of cortical acetylcholine release and cognitive performance by histamine H3 receptor activation in rats. *Br. J. Pharmacol.* **119,** 1656–1664 (**1996**).

57. Ellenbroek, B. A. & Ghiabi, B. The other side of the histamine H3 receptor. *Trends Neurosci.* **37,** 191–199 (**2014**).

58. Martinez-Mir, M. I., Pollard, H., Moreau, J., Arrang, J. M., Ruat, M., Traiffort, E., Schwartz, J. C. & Palacios, J. M. Three histamine receptors (H1, H2 and H3) visualized in the brain of human and non-human primates. *Brain Res.* **526,** 322–327 (**1990**).

59. Goodchild, R. E., Court, J. A., Hobson, I, Piggott, M. A., Perry, R. H., Ince, P, Jaros, E & Perry, E. K. Distribution of histamine H3-receptor binding in the normal human basal ganglia: comparison with Huntington's and Parkinson's disease cases. *Eur. J. Neurosci.* **11,** 449–456 (**1999**).

60. Anichtchik, O. V., Peitsaro, N., Rinne, J. O., Kalimo, H. & Panula, P. Distribution and modulation of histamine H3 receptors in basal ganglia and frontal cortex of healthy controls and patients with Parkinson's disease. *Neurobiol. Dis.* **8**, 707–716 (**2001**).

61. Wijtmans, M., Leurs, R. & de Esch, I. Histamine H3 receptor ligands break ground in a remarkable plethora of therapeutic areas. *Expert Opin. Investig. Drugs* **16**, 967–985 (**2007**).

62. Kenakin, T. Principles: receptor theory in pharmacology. *Trends Pharmacol. Sci.* **25**, 186–192 (**2004**).

63. Arrang, J.-M., Morisset, S. & Gbahou, F. Constitutive activity of the histamine H3 receptor. *Trends Pharmacol. Sci.* **28**, 350–357 (**2007**).

64. Berlin, M., Boyce, C. W. & de Lera Ruiz, M. Histamine H3 Receptor as a Drug Discovery Target. *J. Med. Chem.* **54**, 26–53 (**2011**).

65. Cowart, M., Altenbach, R., Black, L., Faghih, R., Zhao, C. & Hancock, A. A. Medicinal chemistry and biological properties of non-imidazole histamine H3 antagonists. *Mini Rev. Med. Chem.* **4**, 979–992 (**2004**).

66. Ganellin, C. R., Leurquin, F., Piripitsi, A., Arrang, J. M., Garbarg, M., Ligneau, X., Schunack, W. & Schwartz, J. C. Synthesis of potent non-imidazole histamine H3 receptor antagonists. *Arch. Pharm. Pharm. Med. Chem.* **331**, 395–404 (**1998**).

67. Meier, G., Apelt, J., Reichert, U., Grassmann, S, Ligneau, X., Elz, S., Leurquin, F., Ganellin, C. R., Schwartz, J. C., Schunack, W., Stark, H., Graßmann, S., Ligneau, X., Elz, S., Leurquin, F., Ganellin, C. R., Schwartz, J. C., Schunack, W. & Stark, H. Influence of imidazole replacement in different structural classes of histamine H3-receptor antagonists. *Eur. J. Pharm. Sci.* **13**, 249–259 (**2001**).

68. Kalindjan, S. B., Buck, I. M., Linney, I. D., Watt, G. F., Harper, E. A. & Shankley, N. P. Histamine H3 receptor ligands (WO 1999042458 A1). *Patent* (**1999**).

69. Tozer, M. J. & Kalindjian, S. B. Histamine H3 receptor antagonists. *Expert Opin. Ther. Pat.* **10**, 1045–1055 (**2000**).

70. Wingen, K. & Stark, H. Scaffold variations in amine warhead of histamine H3 receptor antagonists. *Drug Discov. Today Technol.* **10**, e483–e489 (**2013**).

71. Sander, K., Kottke, T. & Stark, H. Histamine H3 receptor antagonists go to clinics. eng. *Biol. Pharm. Bull.* **31**, 2163–2181 (**2008**).

72. Schwartzbach, C. J., Grove, R. A., Brown, R., Tompson, D., Then Bergh, F. & Arnold, D. L. Lesion remyelinating activity of GSK239512 versus placebo in patients with relapsing-remitting multiple sclerosis: a randomised, single-blind, phase II study. *J. Neurol.* **264**, 304–315 (**2017**).

73. Kasteleijn-Nolst Trenite, D., Parain, D., Genton, P., Masnou, P., Schwartz, J. C. & Hirsch, E. Efficacy of the histamine 3 receptor (H3R) antagonist pitolisant (formerly known as tiprolisant; BF2.649) in epilepsy: dose-dependent effects in the human photosensitivity model. *Epilepsy Behav.* **28**, 66–70 (**2013**).

74. Dutilleul, P. C., Ryvlin, P., Kahane, P., Vercueil, L., Semah, F., Biraben, A., Schwartz, J. C., De Seze, J., Hirsch, E. & Collongues, N. Exploratory Phase II trial to evaluate the safety and the antiepileptic effect of pitolisant (BF2.649) in refractory partial seizures, given as adjunctive treatment during 3 months. *Clin. Neuropharmacol.* **39**, 188–193 (**2016**).

75. Abad, V. C. & Guilleminault, C. New developments in the management of narcolepsy. *Nat. Sci. Sleep* **9**, 39–57 (**2017**).

76. Provensi, G., Blandina, P. & Passani, M. B. The histaminergic system as a target for the prevention of obesity and metabolic syndrome. *Neuropharmacology* **106**, 3–12 (**2016**).

77. Constantino, L. & Barlocco, D. New perspectives on the development of antiobesity drugs. *Future Med. Chem.* **7**, 315–336 (**2015**).

78. Khanfar, M. A., Affini, A., Lutsenko, K., Nikolic, K., Butini, S. & Stark, H. Multiple targeting approaches on histamine H3 receptor antagonists. *Front. Neurosci.* **10**, 1–17 (**2016**).

79. Querfurth, H. W. & Laferla, F. M. Alzheimer's Disease. *N. Engl. J. Med.* **4**, 329–344 (**2010**).

80. Guzior, N., Wiickowska, A., Panek, D. & Malawska, B. Recent development of multifunctional agents as potential drug candidates for the treatment of Alzheimer's disease. *Curr. Med. Chem.* **22**, 373–404 (**2015**).

81. Selkoe, D. J. & Hardy, J. The amyloid hypothesis of Alzheimer's disease at 25 years. *EMBO Mol. Med.* **8**, 595–608 (**2016**).

82. Sengupta, U., Nilson, A. N. & Kayed, R. The Role of Amyloid-β Oligomers in Toxicity, Propagation, and Immunotherapy. *EBioMedicine* **6**, 42–49 (**2016**).

83. Brioni, J. & Esbenshade, T. Discovery of histamine H3 antagonists for the treatment of cognitive disorders and Alzheimer's disease. *J. Pharmacol. Exp. Ther.* **336**, 38–46 (**2011**).

84. Grill, J. & J.Cummings. Novel targets for Alzheimer's disease treatment. *Expert Rev. Neurother.* **10**, 711–728 (**2010**).

85. Cummings, J., Lee, G., Mortsdorf, T., Ritter, A. & Zhong, K. Alzheimer's disease drug development pipeline: 2017. *Alzheimer's Dement. Transl. Res. Clin. Interv.* **3**, 367–384 (**2017**).

86. Youdim, M. B. H. Multi target neuroprotective and neurorestorative anti-Parkinson and anti-Alzheimer drugs ladostigil and M30 derived from rasagiline. *Exp. Neurobiol.* **22**, 1–10 (**2013**).

87. Emre, M., Poewe, W., De Deyn, P. P., Barone, P., Kulisevsky, J., Pourcher, E., Van Laar, T., Storch, A., Micheli, F., Burn, D., Durif, F., Pahwa, R., Callegari, F., Tenenbaum, N. & Strohmaier, C. Long-term safety of rivastigmine in Parkinson disease dementia: An open-label, randomized study. *Clin. Neuropharmacol.* **37**, 9–16 (**2014**).

88. Riederer, P. & Laux, G. MAO-inhibitors in Parkinson's Disease. *Exp. Neurobiol.* **20**, 1–17 (**2011**).

89. Ramsay, R. R. Molecular aspects of monoamine oxidase B. *Prog. Neuropsychopharmacol. Biol. Psychiatry* **69**, 81–89 (**2016**).

90. Ramsay, R. R., Majekova, M., Medina, M. & Valoti, M. Key targets for multitarget ligands designed to combat neurodegeneration. *Front. Neurosci.* **10**, 1–24 (**2016**).

91. Nakamura, S., Takemura, M., Ohnishi, K., Suenaga, T., Nishimura, M., Akiguchi, I., Kimura, J. & Kimura, T. Loss of large neurons and occurrence of neurofibrillary tangles in the tuberomammillary nucleus of patients with Alzheimer's disease. *Neurosci. Lett.* **151**, 196–199 (**1993**).

92. Vohora, D. & Bhowmik, M. Histamine H3 receptor antagonists/inverse agonists on cognitive and motor processes: relevance to Alzheimer's disease, ADHD, schizophrenia, and drug abuse. *Front. Syst. Neurosci.* **6**, 1–10 (**2012**).

93. Shan, L., Swaab, D. F. & Bao, A. M. Neuronal histaminergic system in aging and age-related neurodegenerative disorders. *Exp. Gerontol.* **48**, 603–607 (**2013**).

94. Medhurst, A. D., Roberts, J. C., Lee, J., Chen, C. P., Brown, S. H., Roman, S. & Lai, M. K. Characterization of histamine H3 receptors in Alzheimer's disease brain and amyloid over-expressing TASTPM mice. *Br. J. Pharmacol.* **157**, 130–138 (**2009**).

95. Fox, G. B., Pan, J. B., Lewis, A. M., Browman, K. E., Komater, V. A., Buckley, M. J., Curzon, P, Radek, R. J., Faghih, R, Esbenshade, T. A., Cowart, M. D., Decker, M. W. & Hancock, A. A. Cognition enhancing effects of novel H3 receptor (H3R) antagonists in several animal models. *Inflamm. Res.* **53**, S49–S50 (**2004**).

96. Nikolic, K., Mavridis, L., Bautista-Aguilera, O. M., Marco-Contelles, J., Stark, H., do Carmo Carreiras, M., Rossi, I., Massarelli, P., Agbaba, D., Ramsay, R. R. & Mitchell, J. B. O. Predicting targets of compounds against neurological diseases using cheminformatic methodology. *J. Comput. Aided. Mol. Des.* **29**, 183–198 (**2015**).

97. Sadek, B., Saad, A., Schwed, J. S., Weizel, L., Walter, M. & Stark, H. Anticonvulsant effects of isomeric nonimidazole histamine H3 receptor antagonists. *Drug Des. Devel. Ther.* **10**, 3633–3651 (**2016**).

98. Toyota, H., Dugovic, C., Koehl, M., Laposky, A. D., Weber, C., Ngo, K., Wu, Y., Lee, D. H., Yanai, K., Sakurai, E., Watanabe, T., Liu, C., Chen, J., Barbier, A. J., Turek, F. W., Fung-Leung, W.-P. & Lovenberg, T. W. Behavioral characterization of mice lacking histamine H3 receptors. *Mol. Pharmacol.* **62**, 389–397 (**2002**).

99. Komater, V. A., Browman, K. E., Curzon, P, Hancock, A. A., Decker, M. W. & Fox, G. B. H3 receptor blockade by thioperamide enhances cognition in rats without inducing locomotor sensitization. *Psychopharmacology (Berl)* **167**, 363–372 (**2003**).

100. Cowart, M, Faghih, R, Gfesser, G, Curtis, M, Sun, M, Zhao, C, Bennani, Y, Wetter, J, Marsh, K, Miller, T. R., Krueger, K, Pan, J. B., Drescher, K, Fox, G. B., Esbenshade, T. A. & Hancock, A. A. Achievement of behavioral efficacy and improved potency in new heterocyclic analogs of benzofuran H3 antagonists. eng. *Inflamm. Res.* **54**, S25–S26 (**2005**).

101. Fox, G. B., Esbenshade, T. A., Pan, J. B., Radek, R. J., Krueger, K. M., Yao, B. B., Browman, K. E., Buckley, M. J., Ballard, M. E., Komater, V. A., Miner, H., Zhang, M., Faghih, R., Rueter, L. E., Bitner, R. S., Drescher, K. U., Wetter, J, Marsh, K., Lemaire, M., Porsolt, R. D., Bennani, Y. L., Sullivan, J. P., Cowart, M. D., Decker, M. W. & Hancock, A. A. Pharmacological properties of ABT-239 [4-(2-{2-[(2R)-2-Methylpyrrolidinyl]ethyl}-benzo furan-5-yl)benzonitrile]: II. Neurophysiological characterization and broad preclinical efficacy in cognition and schizophrenia of a potent and selective histamine H3 r. *J. Pharmacol. Exp. Ther.* **313**, 176–190 (**2005**).

102. Ligneau, X., Perrin, D., Landais, L., Camelin, J. C., Calmels, T. P., Berrebi-Bertrand, I, Lecomte, J. M., Parmentier, R., Anaclet, C., Lin, J. S., Bertaina-Anglade, V., la Rochelle, C. D., D'Aniello, F., Rouleau, A., Gbahou, F., Arrang, J. M., Ganellin, C. R., Stark, H., Schunack, W. & Schwartz, J. C. BF2.649 [1-{3-[3-(4-Chlorophenyl)propoxy]propyl}piperidine, hydro chloride], a nonimidazole inverse agonist/antagonist at the human histamine H3 receptor: Preclinical pharmacology. *J. Pharmacol. Exp. Ther.* **320**, 365–375 (**2007**).

103. Bardgett, M. E., Davis, N. N., Schultheis, P. J. & Griffith, M. S. Ciproxifan, an H3 receptor antagonist, alleviates hyperactivity and cognitive deficits in the APPTg2576 mouse model of Alzheimer's disease. eng. *Neurobiol. Learn. Mem.* **95**, 64–72 (**2011**).

104. Grove, R., Harrington, C., Mahler, A, Beresford, I, Maruff, P, Lowy, M., Nicholls, A., Boardley, R., Berges, A., Nathan, P. & Horrigan, J. A randomized, double-blind, placebo-controlled, 16-week study of the H3 receptor antagonist, GSK239512 as a monotherapy in subjects with mild-to-moderate Alzheimer's disease. *Curr. Alzheimer Res.* **11**, 47–58 (**2014**).

105. Egan, M., Zhao, X., Gottwald, R., Harper-Mozley, L., Zhang, Y., Snavely, D., Lines, C. & Michelson, D. Randomized crossover study of the histamine H3 inverse agonist MK-0249 for the treatment of cognitive impairment in patients with schizophrenia. *Schizophr. Res.* **146**, 224–230 (**2013**).

106. Haig, G. M., Pritchett, Y., Meier, A., Othman, A. A., Hall, C., Gault, L. M. & Lenz, R. A. A randomized study of H3 antagonist ABT-288 in mild-to-moderate Alzheimer's dementia. *J. Alzheimer's Dis.* **42**, 959–971 (**2014**).

107. Sadek, B., Łażewska, D., Hagenow, S., Kieć-Kononowicz, K. & Stark, H. Histamine H3R Antagonists: From Scaffold Hopping to Clinical Candidates. in *Histamine Receptors: Preclinical and Clinical Aspects* (eds Blandina, P. & Passani, M. B.) 28th ed., 109–155 (Humana Press, Cham, Switzerland, **2016**).

108. Kubo, M., Kishi, T., Matsunaga, S. & Iwata, N. Histamine H3 receptor antagonists for Alzheimer's disease: A systematic review and meta-analysis of randomized placebo-controlled trials. *J. Alzheimer's Dis.* **48**, 667–671 (**2015**).

109. Rosini, M., Simoni, E., Minarini, A. & Melchiorre, C. Multi-target design strategies in the context of Alzheimers disease: Acetylcholinesterase inhibition and NMDA receptor antagonism as the driving forces. *Neurochem. Res.* **39**, 1914–1923 (**2014**).

110. Bitner, R. S., Markosyan, S., Nikkel, A. L. & Brioni, J. D. In-vivo histamine H3 receptor antagonism activates cellular signaling suggestive of symptomatic and disease modifying efficacy in Alzheimer's disease. *Neuropharmacology* **60**, 460–466 (**2011**).

111. Fu, Q., Dai, H., He, P., Hu, W., Fan, Y., Zhang, W. & Chen, Z. The H3 receptor antagonist clobenpropit protects against Aß42-induced neurotoxicity in differentiated rat PC12 cells. *Pharmazie* **65**, 257–260 (**2010**).

112. Hancock, A. A. The challenge of drug discovery of a GPCR target: analysis of preclinical pharmacology of histamine H3 antagonists/inverse agonists. *Biochem. Pharmacol.* **71**, 1103–1113 (**2006**).

113. Delay-Goyet, P., Blanchard, V., Schussler, N., Lopez-Grancha, M., Ménager, J., Mary, V., Sultan, E., Buzy, A., Guillemot, J. C., Stemmelin, J., Bertrand, P., Rooney, T., Pradier, L. & Barnéoud, P. SAR110894, a potent histamine H3-receptor antagonist, displays disease-modifying activity in a transgenic mouse model of tauopathy. *Alzheimer's Dement. Transl. Res. Clin. Interv.* **2**, 267–280 (**2016**).

114. Howlett, D. R., George, A. R., Owen, D. E., Ward, R. V. & Markwell, R. E. Common structural features determine the effectiveness of carvedilol, daunomycin and rolitetracycline as inhibitors of Alzheimer β-amyloid fibril formation. *Biochem. J.* **343**, 419–423 (**1999**).

115. Rosini, M., Simoni, E., Bartolini, M., Cavalli, A., Ceccarini, L., Pascu, N., McClymont, D. W., Tarozzi, A., Bolognesi, M. L., Minarini, A., Tumiatti, V., Andrisano, V., Mellor, I. R. & Melchiorre, C. Inhibition of acetylcholinesterase, β-amyloid aggregation, and NMDA receptors in Alzheimer's disease: A promising direction for the multi-target-directed ligands gold rush. *J. Med. Chem.* **51**, 4381–4384 (**2008**).

116. Doody, R. S., Gavrilova, S. I., Sano, M., Thomas, R. G., Aisen, P. S., Bachurin, S. O., Seely, L. & Hung, D. Effect of dimebon on cognition, activities of daily living, behaviour, and global function in patients with mild-to-moderate Alzheimer's disease: a randomised, double-blind, placebo-controlled study. *Lancet* **372**, 207–215 (**2008**).

117. Mohamed, T., Yeung, J. C., Vasefi, M. S., Beazely, M. A. & Rao, P. P. Development and evaluation of multifunctional agents for potential treatment of Alzheimer's disease: Application to a pyrimidine-2,4-diamine template. *Bioorg. Med. Chem. Lett.* **22**, 4707–4712 (**2012**).

118. Mohamed, T. & Rao, P. P. 2,4-Disubstituted quinazolines as amyloid-β aggregation inhibitors with dual cholinesterase inhibition and antioxidant properties: Development and structure-activity relationship (SAR) studies. *Eur. J. Med. Chem.* **126**, 823–843 (**2017**).

119. Fernández-Bachiller, M. I., Pérez, C., Campillo, N. E., Páez, J. A., González-Muñoz, G. C., Usán, P., García-Palomero, E., López, M. G., Villarroya, M., García, A. G., Martínez, A. & Rodríguez-Franco, M. I. Tacrine-melatonin hybrids as multifunctional agents for Alzheimer's disease, with cholinergic, antioxidant, and neuroprotective properties. *ChemMedChem* **4**, 828–841 (**2009**).

120. Peng, X. & Frohman, M. Mammalian phospholipase D physiological and pathological roles. *Acta Physiol.* **204**, 219–226 (**2012**).

121. Zhao, X.-J., Gong, D.-M., Jiang, Y.-R., Guo, D., Zhu, Y. & Deng, Y.-C. Multipotent AChE and BACE-1 inhibitors for the treatment of Alzheimer's disease: Design, synthesis and bio-analysis of 7-amino-1,4-dihydro-2H-isoquilin- 3-one derivates. *Eur. J. Med. Chem.* **138**, 738–747 (**2017**).

122. Panek, D., Więckowska, A., Pasieka, A., Godyń, J., Jończyk, J., Bajda, M., Knez, D., Gobec, S. & Malawska, B. Design, synthesis, and biological evaluation of 2-(benzylamino-2-hydroxyalkyl)isoindoline-1,3-diones derivatives as potential disease-modifying multifunctional anti-Alzheimer agents. *Molecules* **23**, 347 (**2018**).

123. Sterling, J., Herzig, Y., Goren, T., Finkelstein, N., Lerner, D., Goldenberg, W., Miskolczi, I., Molnar, S., Rantal, F., Tamas, T., Toth, G., Zagyva, A., Zekany, A., Lavian, G., Gross, A., Friedman, R., Razin, M., Huang, W., Krais, B., Chorev, M., Youdim, M. B. & Weinstock, M. Novel dual inhibitors of AChE and MAO derived from hydroxy aminoindan and phenethylamine as potential treatment for Alzheimer's disease. *J. Med. Chem.* **45**, 5260–5279 (**2002**).

124. Bolea, I., Juárez-Jiménez, J., De Los Ríos, C., Chioua, M., Pouplana, R., Luque, F. J., Unzeta, M., Marco-Contelles, J. & Samadi, A. Synthesis, biological evaluation, and molecular modeling of donepezil and N-[(5-(Benzyloxy)-1 -methyl-1H-indol-2-yl)methyl]-N-methylprop-2-yn-1-amine hybrids as new multipotent cholinesterase/monoamine oxidase inhibitors for the treatment of Alzheimer's d. *J. Med. Chem.* **54**, 8251–8270 (**2011**).

125. Sun, H., Zhu, L., Yang, H., Qian, W., Guo, L., Zhou, S., Gao, B., Li, Z., Zhou, Y., Jiang, H., Chen, K., Zhen, X. & Liu, H. Asymmetric total synthesis and identification of tetrahydroprotoberberine derivatives as new antipsychotic agents possessing a dopamine D1, D2 and serotonin 5-HT1A multi-action profile. *Bioorg. Med. Chem.* **21**, 856–868 (**2013**).

126. Khan, N. A., Khan, I., Abid, S. M., Zaib, S., Ibrar, A., Andleeb, H., Hameed, S. & Iqbal, J. Quinolinic carboxylic acid derivatives as potential multi-target compounds for neurodegeneration: Monoamine oxidase and cholinesterase inhibition. *Med. Chem.* **14**, 74–85 (**2018**).

127. Lecoutey, C., Hedou, D., Freret, T., Giannoni, P., Gaven, F., Since, M., Bouet, V., Ballandonne, C., Corvaisier, S., Malzert Fréon, A., Mignani, S., Cresteil, T., Boulouard, M., Claeysen, S., Rochais, C. & Dallemagne, P. Design of donecopride, a dual serotonin subtype 4 receptor agonist/acetylcholin esterase inhibitor with potential interest for Alzheimer's disease treatment. *Proc. Natl. Acad. Sci. USA* **111**, 3825–3830 (**2014**).

128. Rochais, C., Lecoutey, C., Gaven, F., Giannoni, P., Hamidouche, K., Hedou, D., Dubost, E., Genest, D., Yahiaoui, S., Freret, T., Bouet, V., Dauphin, F., De Oliveira Santos, J. S., Ballandonne, C., Corvaisier, S., Malzert-Fréon, A., Legay, R., Boulouard, M., Claeysen, S. & Dallemagne, P. Novel multitarget-directed ligands (MTDLs) with acetylcholinesterase (AChE) inhibitory and serotonergic subtype 4 receptor (5-HT4R) agonist activities as potential agents against Alzheimer's disease: The design of donecopride. *J. Med. Chem.* **58**, 3172–3187 (**2015**).

129. Zhou, L.-Y., Zhu, Y., Jiang, Y.-R., Zhao, X.-J. & Guo, D. Design, synthesis and biological evaluation of dual acetylcholinesterase and phosphodiesterase 5A inhibitors in treatment for Alzheimer's disease. *Bioorg. Med. Chem. Lett.* **27**, 4180–4184 (**2017**).

130. Mao, F., Wang, H., Ni, W., Zheng, X., Wang, M., Bao, K., Ling, D., Li, X., Xu, Y., Zhang, H. & Li, J. Design, synthesis, and biological evaluation of orally available first-generation dual-target selective inhibitors of acetylcholinesterase (AChE) and phosphodiesterase 5 (PDE5) for the treatment of Alzheimer's disease. *ACS Chem. Neurosci.* **9**, 328–345 (**2018**).

131. Shaik, J. B., Palaka, B. K., Penumala, M., Kotapati, K. V., Devineni, S. R., Eadlapalli, S., Darla, M. M., Ampasala, D. R., Vadde, R. & Amooru, G. D. Synthesis, pharmacological assessment, molecular modeling and in silico studies of fused tricyclic coumarin derivatives as a new family of multifunctional anti-Alzheimer agents. *Eur. J. Med. Chem.* **107,** 219–232 (**2015**).

132. Blandini, F., Armentero, M. T., Fancellu, R., Blaugrund, E. & Nappi, G. Neuroprotective effect of rasagiline in a rodent model of Parkinson's disease. *Exp. Neurol.* **187,** 455–459 (**2004**).

133. Weinreb, O., Amit, T., Bar-Am, O. & B.H. Youdim, M. Ladostigil: A novel multimodal neuroprotective drug with cholinesterase and brain-selective monoamine oxidase inhibitory activities for Alzheimer's disease treatment. *Curr. Drug Targets* **13,** 483–494 (**2012**).

134. Esteban, G., Allan, J., Samadi, A., Mattevi, A., Unzeta, M., Marco-Contelles, J., Binda, C. & Ramsay, R. R. Kinetic and structural analysis of the irreversible inhibition of human monoamine oxidases by ASS234, a multi-target compound designed for use in Alzheimer's disease. *Biochim. Biophys. Acta* **1844,** 1104–1110 (**2014**).

135. Stasiak, A., Mussur, M., Unzeta, M., Samadi, A., Marco-Contelles, J. & Fogel, W. Effects of novel monoamine oxidases and cholinesterases targeting compounds on brain neurotransmitters and behavior in rat model of vascular dementia. *Curr. Pharm. Des.* **20,** 161–171 (**2014**).

136. Marco-Contelles, J., Unzeta, M., Bolea, I., Esteban, G., Ramsay, R. R., Romero, A., Martínez-Murillo, R., Carreiras, M. C. & Ismaili, L. ASS234, as a new multitarget directed propargylamine for Alzheimer's disease therapy. *Front. Neurosci.* **10,** 1–7 (**2016**).

137. Serrano, M. P., Herrero-Labrador, R., Futch, H. S., Serrano, J., Romero, A., Fernandez, A. P., Samadi, A., Unzeta, M., Marco-Contelles, J. & Martínez-Murillo, R. The proof-of-concept of ASS234: Peripherally administered ASS234 enters the central nervous system and reduces pathology in a male mouse model of Alzheimer disease. *J. Psychiatry Neurosci.* **42,** 59–69 (**2017**).

138. Huang, L., Lu, C., Sun, Y., Mao, F., Luo, Z., Su, T., Jiang, H., Shan, W. & Li, X. Multitarget-directed benzylideneindanone derivatives: Anti-ß-amyloid (Aß) aggregation, antioxidant, metal chelation, and monoamine oxidase B (MAO-B) inhibition properties against Alzheimer's disease. *J. Med. Chem.* **55,** 8483–8492 (**2012**).

139. Wang, Z.-M., Li, X.-M., Xu, W., Li, F., Wang, J., Kong, L.-Y. & Wang, X.-B. Acetophenone derivatives: novel and potent small molecule inhibitors of monoamine oxidase B. *Med. Chem. Commun.* **6,** 2146–2157 (**2015**).

140. Xie, S., Chen, J., Li, X., Su, T., Wang, Y., Wang, Z., Huang, L. & Li, X. Synthesis and evaluation of selegiline derivatives as monoamine oxidase inhibitor, antioxidant and metal chelator against Alzheimer's disease. *Bioorg. Med. Chem.* **23,** 3722–3729 (**2015**).

141. Hegde, M. L., Bharathi, P, Suram, A., Venugopal, C. & Jagannathan, R. Challenges associated with metal chelation Therapy in Alzheimer's disease. *J. Alzheimer's Dis.* **17,** 457–468 (**2009**).

142. Bautista-Aguilera, Ó. M., Hagenow, S., Palomino-Antolin, A., Farré-Alins, V., Ismaili, L., Joffrin, P. L., Jimeno, M. L., Soukup, O., Janočková, J., Kalinowsky, L., Proschak, E., Iriepa, I., Moraleda, I., Schwed, J. S., RomeroMartínez, A., López-Muñoz, F., Chioua, M., Egea, J., Ramsay, R. R., Marco-Contelles, J. & Stark, H. Multitarget-directed ligands combining cholinesterase and monoamine oxidase inhibition with histamine H3R antagonism for neurodegenerative diseases. *Angew. Chem. Int. Ed.* **56**, 12765–12769 (**2017**).

143. Apelt, J., Ligneau, X., Pertz, H. H., Arrang, J.-M., Ganellin, C. R., Schwartz, J.-C., Schunack, W. & Stark, H. Development of a new class of nonimidazole histamine H3 receptor ligands with combined inhibitory histamine N- methyltransferase activity. *J. Med. Chem.* **45**, 1128–1141 (**2002**).

144. Petroianu, G., Arafat, K., Sasse, B. C. & Stark, H. Multiple enzyme inhibitions by histamine H3 receptor antagonists as potential procognitive agents. *Pharmazie* **61**, 179–182 (**2006**).

145. Bembenek, S. D., Keith, J. M., Letavic, M. A., Apodaca, R., Barbier, A. J., Dvorak, L., Aluisio, L., Miller, K. L., Lovenberg, T. W. & Carruthers, N. I. Lead identification of acetylcholinesterase inhibitors-histamine H3 receptor antagonists from molecular modeling. *Bioorg. Med. Chem.* **16**, 2968–2973 (**2008**).

146. Darras, F. H., Pockes, S., Huang, G., Wehle, S., Strasser, A., Wittmann, H. J., Nimczick, M., Sotriffer, C. A. & Decker, M. Synthesis, biological evaluation, and computational studies of tri- and tetracyclic nitrogen-bridgehead compounds as potent dual-acting AChE inhibitors and hH3 receptor antagonists. *ACS Chem. Neurosci.* **5**, 225–242 (**2014**).

147. Khan, N., Saad, A., Nurulain, S. M., Darras, F. H., Decker, M. & Sadek, B. The dual-acting H3 receptor antagonist and AChE inhibitor UW-MD-71 dose-dependently enhances memory retrieval and reverses dizocilpine-induced memory impairment in rats. *Behav. Brain Res.* **297**, 155–164 (**2016**).

148. Huang, W., Tang, L., Shi, Y., Huang, S., Xu, L., Sheng, R., Wu, P., Li, J., Zhou, N. & Hu, Y. Searching for the multi-target-directed ligands against Alzheimer's disease: Discovery of quinoxaline-based hybrid compounds with AChE, H3R and BACE 1 inhibitory activities. *Bioorg. Med. Chem.* **19**, 7158–7167 (**2011**).

149. Claeysen, S., Bockaert, J. & Giannoni, P. Serotonin: A new hope in Alzheimer's disease? *ACS Chem. Neurosci.* **6**, 940–943 (**2015**).

150. Lepailleur, A., Freret, T., Lemaître, S., Boulouard, M., Dauphin, F., Hinschberger, A., Dulin, F., Lesnard, A., Bureau, R. & Rault, S. Dual histamine H3R/serotonin 5-HT4R ligands with antiamnesic properties: pharmacophore-based virtual screening and polypharmacology. *J. Chem. Inf. Model.* **54**, 1773–1784 (**2014**).

151. Smith, H. S., Cox, L. R. & Smith, B. R. Dopamine receptor antagonists. *Ann. Palliat. Med.* **1**, 137–142 (**2012**).

152. Maiti, P., Manna, J. & Dunbar, G. L. Current understanding of the molecular mechanisms in Parkinson's disease: Targets for potential treatments. *Transl. Neurodegener.* **6**, 5–35 (**2017**).

153. Obeso, J. A., Stamelou, M., Goetz, C. G., Poewe, W., Lang, A. E., Weintraub, D., Burn, D., Halliday, G. M., Bezard, E., Przedborski, S., Lehericy, S., Brooks, D. J., Rothwell, J. C., Hallett, M., DeLong, M. R., Marras, C., Tanner, C. M., Ross, G. W., Langston, J. W., Klein, C., Bonifati, V., Jankovic, J., Lozano, A. M., Deuschl, G., Bergman, H., Tolosa, E., Rodriguez-Violante, M., Fahn, S., Postuma, R. B., Berg, D., Marek, K., Standaert, D. G., Surmeier, D. J., Olanow, C. W., Kordower, J. H., Calabresi, P., Schapira, A. H. & Stoessl, A. J. Past, present, and future of Parkinson's disease: A special essay on the 200th Anniversary of the Shaking Palsy. *Mov. Disord.* **32,** 1264–1310 (**2017**).

154. Cazorla, M., Kang, U. J. & Kellendonk, C. Balancing the basal ganglia circuitry: A possible new role for dopamine D2 receptors in health and disease. *Mov. Disord.* **30,** 895–903 (**2015**).

155. Galvan, A., Devergnas, A. & Wichmann, T. Alterations in neuronal activity in basal ganglia-thalamocortical circuits in the parkinsonian state. *Front. Neuroanat.* **9,** 1–21 (**2015**).

156. Beaulieu, J.-M., Espinoza, S. & Gainetdinov, R. R. Dopamine receptors - IUPHAR Review 13. *Br. J. Pharmacol.* **172,** 1–23 (**2015**).

157. DeMaagd, G. & Philip, A. Parkinson's disease and its management: part 3: Non-dopaminergic and nonpharmacological treatment options. *P T* **40,** 668–679 (**2015**).

158. Heikkinen, H., Varhe, A., Laine, T., Puttonen, J., Kela, M., Kaakkola, S. & Reinikainen, K. Entacapone improves the availability of L-dopa in plasma by decreasing its peripheral metabolism independent of L-dopa/carbidopa dose. *Br. J. Clin. Pharmacol.* **54,** 363–371 (**2002**).

159. Stocchi, F. The levodopa wearing-off phenomenon in Parkinson's disease: pharmacokinetic considerations. *Expert Opin. Pharmacother.* **7,** 1399–1407 (**2006**).

160. Meissner, W. G., Frasier, M., Gasser, T., Goetz, C. G., Lozano, A., Piccini, P., Obeso, J. a., Rascol, O., Schapira, A., Voon, V., Weiner, D. M., Tison, F. & Bezard, E. Priorities in Parkinson's disease research. *Nat. Rev. Drug Discov.* **10,** 377–393 (**2011**).

161. Espinoza, S., Managò, F., Leo, D., Sotnikova, T. D. & Gainetdinov, R. R. Role of catechol-O-methyltransferase (COMT)-dependent processes in Parkinson's disease and L-DOPA treatment. *CNS Neurol. Disord. - Drug Targets* **11,** 251–263 (**2012**).

162. Foley, P., Gerlach, M., Double, K. L. & Riederer, P. Dopamine receptor agonists in the therapy of Parkinson's disease. *J. Neural. Transm.* **111,** 1375–446 (**2004**).

163. DeMaagd, G. & Philip, A. Parkinson's disease and its management part 2: Introduction to the pharmacotherapy of Parkinson's disease, with a focus on the use of dopaminergic agents. *P T* **40,** 590–600 (**2015**).

164. Blandini, F. & Armentero, M.-T. Dopamine receptor agonists for Parkinson's disease. *Expert Opin. Investig. Drugs* **23,** 387–410 (**2014**).

165. Millan, M. J., Maiofiss, L. & Cussac, D. Differential actions of antiparkinson agents at multiple classes of monoaminergic receptor. I. A multivariate analysis of the binding profiles of 14 drugs at 21 native and cloned human receptor subtypes. *J. Pharmacol. Exp. Ther.* **303,** 791–804 (**2002**).

166. Newman-Tancredi, A., Cussac, D., Erie, V. A. L., Nicolas, J.-p. & Ed, F. R. Differential actions of antiparkinson agents at multiple classes of monoaminergic receptor. II . Agonist and antagonist properties at subtypes of dopamine D2 - like receptor and a1/a2 adrenoceptors. *J. Pharmacol. Exp. Ther.* **303**, 805–814 (**2002**).

167. Eisenreich, W., Sommer, B., Hartter, S. & Jost, W. H. Pramipexole extended release: A novel treatment option in Parkinson's disease. *Parkinson's. Dis.* **2010**, 1–7 (**2010**).

168. Ramsay, R. R. Monoamine oxidases: The biochemistry of the proteins as targets in medicinal chemistry and drug discovery. *Curr. Top. Med. Chem.* **12**, 2189–2209 (**2012**).

169. Ramsay, R. R. & Di Giovanni, G. Editorial: Structure-based drug design for diagnosis and treatment of neurological diseases. *Front. Pharmacol.* **8**, 1–2 (**2017**).

170. Mandemakers, W., Morais, V. A. & De Strooper, B. A cell biological perspective on mitochondrial dysfunction in Parkinson disease and other neurodegenerative diseases. *J. Cell Sci.* **120**, 1707–1716 (**2007**).

171. Lezi, E & Swerdlow, R. H. Mitochondria in Neurodegeneration. *Adv. Exp. Med. Biol.* **942**, 269–286 (**2012**).

172. Perier, C. & Vila, M. Mitochondrial biology and Parkinson's disease. *Cold Spring Harb. Perspect. Med.* **4**, 1–19 (**2012**).

173. Rizzi, G. & Tan, K. R. Dopamine and acetylcholine, a circuit point of view in Parkinson's disease. *Front. Neural Circuits* **11**, 1–14 (**2017**).

174. Poewe, W. Non-motor symptoms in Parkinson's disease. *Eur. J. Neurol.* **15**, 14–20 (**2008**).

175. DeMaagd, G. & Philip, A. Parkinson's disease and its management: Part 5: Treatment of nonmotor complications. *P T* **40**, 838–846 (**2015**).

176. Wilby, K. J., Johnson, E. G., Johnson, H. E. & Ensom, M. H. Evidence-based review of pharmacotherapy used for Parkinson's disease psychosis. *Ann. Pharmacother.* **51**, 682–695 (**2017**).

177. Anichtchik, O. V., Rinne, J. O., Kalimo, H. & Panula, P. An altered histaminergic innervation of the substantia nigra in Parkinson's disease. *Exp. Neurol.* **163**, 20–30 (**2000**).

178. Rinne, J. O., Anichtchik, O. V., Eriksson, K. S., Kaslin, J., Tuomisto, L., Kalimo, H., Röyttä, M. & Panula, P. Increased brain histamine levels in Parkinson's disease but not in multiple system atrophy. *J. Neurochem.* **81**, 954–960 (**2002**).

179. Shan, L., Liu, C. Q., Balesar, R., Hofman, M. A., Bao, A. M. & Swaab, D. F. Neuronal histamine production remains unaltered in Parkinson's disease despite the accumulation of Lewy bodies and Lewy neurites in the tuberomamillary nucleus. *Neurobiol. Aging* **33**, 1343–1344 (**2012**).

180. Nowak, P., Noras, Ł., Jochem, J., Szkilnik, R., Brus, H., Körossy, E., Drab, J., Kostrzewa, R. M. & Brus, R. Histaminergic activity in a rodent model of Parkinson's disease. *Neurotox. Res.* **15**, 246–251 (**2009**).

181. Liu, C. Q., Chen, Z., Liu, F. X., Hu, D. N. & Luo, J. H. Involvement of brain endogenous histamine in the degeneration of dopaminergic neurons in 6-hydroxydopamine-lesioned rats. *Neuropharmacology* **53**, 832–841 (**2007**).

182. Ryu, J. H., Yanai, K., Iwata, R., Ido, T. & Watanabe, T. Heterogeneous distributions of histamine H3, dopamine D1 and D2 receptors in rat brain. *Neuroreport* **5**, 621–624 (**1994**).

183. Garcia, M., Floran, B., Arias-Montaño, J. A., Young, J. M. & Aceves, J. Histamine H3 receptor activation selectively inhibits dopamine D1 receptor-dependent [3H] GABA release from depolarization-stimulated slices of rat substantia nigra pars reticulata. *Neuroscience* **80**, 241–249 (**1997**).

184. Molina-Hernández, A., Nuñez, A., Sierra, J. & Arias-Montaño, J. Histamine H3 receptor activation inhibits glutamate release from rat striatal synaptosomes. *Neuropharmacology* **41**, 928–934 (**2001**).

185. González-Sepúlveda, M., Rosell, S., Hoffmann, H. M., Castillo-Ruiz, M. d. M., Mignon, V., Moreno-Delgado, D., Vignes, M., Díaz, J., Sabriá, J. & Ortiz, J. Cellular distribution of the histamine H3 receptor in the basal ganglia: Functional modulation of dopamine and glutamate neurotransmission. *Basal Ganglia* **3**, 109–121 (**2013**).

186. Aquino-Miranda, G., Escamilla-Sánchez, J., González-Pantoja, R., Bueno-Nava, A. & Arias-Montaño, J.-A. Histamine H3 receptor activation inhibits dopamine synthesis but not release or uptake in rat nucleus accumbens. *Neuropharmacology* **106**, 91–101 (**2016**).

187. Ferrada, C., Ferré, S., Casadó, V., Cortés, A., Justinova, Z., Barnes, C., Canela, E. I., Goldberg, S. R., Leurs, R., Lluis, C. & Franco, R. Interactions between histamine H3 and dopamine D2 receptors and the implications for striatal function. *Neuropharmacology* **55**, 190–197 (**2008**).

188. Ferrada, C., Moreno, E., Casadó, V., Bongers, G., Cortés, A., Mallol, J., Canela, E. I., Leurs, R., Ferré, S., Lluís, C. & Franco, R. Marked changes in signal transduction upon heteromerization of dopamine D1 and histamine H3 receptors. *Br. J. Pharmacol.* **157**, 64–75 (**2009**).

189. Hu, W. & Chen, Z. The roles of histamine and its receptor ligands in central nervous system disorders: An update. *Pharmacol. Ther.* **175**, 116–132 (**2017**).

190. Liu, Z., Chen, X., Sun, P., Yu, L., Zhen, X. & Zhang, A. N-Propylnoraporphin-11-O-yl carboxylic esters as potent dopamine D(2) and serotonin 5-HT(1A) receptor dual ligands. *Bioorg. Med. Chem.* **16**, 8335–8338 (**2008**).

191. Morisset, S., Pilon, C., Tardivel-Lacombe, J., Weinstein, D., Rostene, W., Betancur, C., Sokoloff, P., Schwartz, J. C. & Arrang, J. M. Acute and chronic effects of methamphetamine on tele-methylhistamine levels in mouse brain: selective involvement of the D2 and not D3 receptor. *J. Pharmacol. Exp. Ther.* **300**, 621–628 (**2002**).

192. Pillot, C., Ortiz, J., Heron, A., Ridray, S., Schwartz, J. C. & Arrang, J. M. Ciproxifan, a histamine H3-receptor antagonist/inverse agonist, potentiates neurochemical and behavioral effects of haloperidol in the rat. *J. Neurosci.* **22**, 7272–7280 (**2002**).

193. Bardgett, M. E., Points, M., Kleier, J., Blankenship, M. & Griffith, M. S. The H3 antagonist, ciproxifan, alleviates the memory impairment but enhances the motor effects of MK-801 (dizocilpine) in rats. *Neuropharmacology* **59**, 492–502 (**2010**).

194. Vanhanen, J., Kinnunen, M., Nuutinen, S. & Panula, P. Histamine H3 receptor antagonist JNJ-39220675 modulates locomotor responses but not place conditioning by dopaminergic drugs. *Psychopharmacology* **232,** 1143–1153 (**2015**).

195. Clapham, J. & Kilpatrick, G. J. Thioperamide, the selective histamine H3 receptor antagonist, attenuates stimulant-induced locomotor activity in the mouse. *Eur. J. Pharmacol.* **259,** 107–114 (**1994**).

196. Gomez-Ramirez, J., Johnston, T. H., Visanji, N. P., Fox, S. H. & Brotchie, J. M. Histamine H3 receptor agonists reduce L-dopa-induced chorea, but not dystonia, in the MPTP-lesioned nonhuman primate model of Parkinson's disease. *Mov. Disord.* **21,** 839–846 (**2006**).

197. Lin, J. S. Brain structures and mechanisms involved in the control of cortical activation and wakefulness, with emphasis on the posterior hypothalamus and histaminergic neurons. *Sleep Med. Rev.* **4,** 471–503 (**2000**).

198. Barbier, A. J. & Bradbury, M. J. Histaminergic control of sleep-wake cycles: recent therapeutic advances for sleep and wake disorders. eng. *CNS Neurol. Disord. - Drug Targets* **6,** 31–43 (**2007**).

199. Lin, J.-S., Sergeeva, O. A. & Haas, H. L. Histamine H3 receptors and sleep-wake regulation. *J. Pharmacol. Exp. Ther.* **336,** 17–23 (**2011**).

200. Gondard, E., Anaclet, C., Akaoka, H., Guo, R.-X., Zhang, M., Buda, C., Franco, P., Kotani, H. & Lin, J.-S. Enhanced histaminergic neurotransmission and sleep-wake alterations, a study in histamine H3-receptor knock-out mice. *Neuropsychopharmacology* **38,** 1015–1031 (**2013**).

201. Ligneau, X., Lin, J.-S., Vanni-Mercier, G., Jouvet, M., Muir, J. L., Ganellin, C. R., Stark, H., Elz, S., Schunack, W. & Schwartz, J.-C. Neurochemical and behavioral effects of ciproxifan, a potent histamine H3-receptor antagonist. *J. Pharmacol. Exp. Ther.* **287,** 658–666 (**1998**).

202. Le, S., Gruner, J. A., Mathiasen, J. R., Marino, M. J. & Schaffhauser, H. Correlation between ex vivo receptor occupancy and wake-promoting activity of selective H3 receptor antagonists. *J. Pharmacol. Exp. Ther.* **325,** 902–909 (**2008**).

203. Masini, D., Lopes-Aguiar, C., Bonito-Oliva, A., Papadia, D., Andersson, R., Fisahn, A. & Fisone, G. The histamine H3 receptor antagonist thioperamide rescues circadian rhythm and memory function in experimental parkinsonism. *Transl. Psychiatry* **7,** 1–9 (**2017**).

204. Youdim, M. B. H., Kupershmidt, L., Amit, T. & Weinreb, O. Promises of novel multi-target neuroprotective and neurorestorative drugs for Parkinson's disease. *Parkinsonism Relat. Disord.* **20,** S132–S136 (**2014**).

205. Youdim, M. B. H. M30, a brain permeable multi target neurorestorative drug in post nigrostriatal dopamine neuron lesion of parkinsonism animal models. *Parkinsonism Relat. Disord.* **18,** S151–S154 (**2012**).

206. Jörg, M., May, L., Mak, F. S., Lee, K. C. K., Miller, N. D., Scammells, P. J. & Capuano, B. Synthesis and pharmacological evaluation of dual acting ligands targeting the adenosine A2A and dopamine D2 receptors for the potential treatment of Parkinson's disease. *J. Med. Chem.* **58,** 718–738 (**2015**).

207. Shao, Y.-M., Ma, X, Paira, P, Tan, A, Herr, D. R., Lim, K. L., Ng, C. H., Venkatesan, G, Klotz, K.-N., Frederico, S, Spalluto, G, Cheong, S. L., Chen, Y. Z. & Pastorin, G. Discovery of indolylpiperazinylpyrimidines with dual-target profiles at adenosine A2A and dopamine D2 receptors for Parkinson's disease treatment. *PLoS One* **13,** 1–27 (**2018**).

208. Stößel, A., Schlenk, M., Hinz, S., Küppers, P., Heer, J., Gütschow, M. & Müller, C. E. Dual targeting of adenosine A2A receptors and monoamine oxidase B by 4H-3,1-benzothiazin-4-ones. *J. Med. Chem.* **56,** 4580–4596 (**2013**).

209. Van der Walt, M. M., Terre'Blanche, G., Petzer, A. & Petzer, J. P. The adenosine receptor affinities and monoamine oxidase B inhibitory properties of sulfanylphthalimide analogues. *Bioorg. Chem.* **59,** 117–123 (**2015**).

210. Wang, X., Han, C., Xu, Y., Wu, K., Chen, S., Hu, M., Wang, L. & Ye, Y. Synthesis and evaluation of phenylxanthine derivatives as potential dual A2AR antagonists/MAO-B inhibitors for Parkinson's disease. *Molecules* **22,** 1010 (**2017**).

211. Shook, B. C., Rassnick, S., Wallace, N., Crooke, J., Ault, M., Chakravarty, D., Barbay, J. K., Wang, A., Powell, M. T., Leonard, K., Alford, V., Scannevin, R. H., Carroll, K., Lampron, L., Westover, L., Lim, H.-K., Russell, R., Branum, S., Wells, K. M., Damon, S., Youells, S., Li, X., Beauchamp, D. A., Rhodes, K. & Jackson, P. F. Design and characterization of optimized adenosine A2A /A1 receptor antagonists for the treatment of Parkinson's disease. *J. Med. Chem.* **55,** 1402–1417 (**2012**).

212. Pinna, A. Adenosine A2A receptor antagonists in Parkinson's disease: Progress in clinical trials from the newly approved istradefylline to drugs in early development and those already discontinued. *CNS Drugs* **28,** 455–474 (**2014**).

213. Pinna, A., Ko, W. K. D., Costa, G., Tronci, E., Fidalgo, C., Simola, N., Li, Q., Tabrizi, M. A., Bezard, E., Carta, M. & Morelli, M. Antidyskinetic effect of A2A and 5-HT1A/1B receptor ligands in two animal models of Parkinson's disease. *Mov. Disord.* **31,** 501–511 (**2016**).

214. Pinna, A., Serra, M., Morelli, M. & Simola, N. Role of adenosine A2A receptors in motor control: relevance to Parkinson's disease and dyskinesia. *J. Neural. Transm.* **in press** (**2018**).

215. Suzuki, K., Miyamoto, T., Miyamoto, M., Uchiyama, T. & Hirata, K. Could istradefylline be a treatment option for postural abnormalities in mid-stage Parkinson's disease? *J. Neurol. Sci.* **385,** 131–133 (**2018**).

216. Morales-Figueroa, G. E., Márquez-Gómez, R., González-Pantoja, R., Escamilla-Sánchez, J. & Arias-Montaño, J. A. Histamine H3 receptor activation counteracts adenosine A2A receptor-mediated enhancement of depolarization-evoked [3H]-GABA release from rat globus pallidus synaptosomes. *ACS Chem. Neurosci.* **5,** 637–645 (**2014**).

217. Grover, S. A., Kaouache, M., Rempel, P., Joseph, L., Dawes, M., Lau, D. C. & Lowensteyn, I. Years of life lost and healthy life-years lost from diabetes and cardiovascular disease in overweight and obese people: A modelling study. *Lancet Diabetes Endocrinol.* **3,** 114–123 (**2015**).

218. Omran, Z. Obesity: Current Treatment and Future Horizons. *Mini Rev. Med. Chem.* **17,** 51–61 (**2017**).

219. Marsh, D. J., Weingarth, D. T., Novi, D. E., Chen, H. Y., Trumbauer, M. E., Chen, A. S., Guan, X.-M., Jiang, M. M., Feng, Y., Camacho, R. E., Shen, Z., Frazier, E. G., Yu, H., Metzger, J. M., Kuca, S. J., Shearman, L. P., Gopal-Truter, S., MacNeil, D. J., Strack, A. M., MacIntyre, D. E., Van der Ploeg, L. H. T. & Qian, S. Melanin-concentrating hormone 1 receptor-deficient mice are lean, hyperactive, and hyperphagic and have altered metabolism. *Proc. Natl. Acad. Sci. USA* **99**, 3240–3245 (**2002**).

220. Borowsky, B., Durkin, M. M., Ogozalek, K., Marzabadi, M. R., DeLeon, J., Heurich, R., Lichtblau, H., Shaposhnik, Z., Daniewska, I., Blackburn, T. P., Branchek, T. A., Gerald, C., Vaysse, P. J. & Forray, C. Antidepressant, anxiolytic and anorectic effects of a melanin-concentrating hormone-1 receptor antagonist. *Nat. Med.* **8**, 825–830 (**2002**).

221. Takekawa, S., Asami, A., Ishihara, Y., Terauchi, J., Kato, K., Shimomura, Y., Mori, M., Murakoshi, H., Kato, K., Suzuki, N., Nishimura, O. & Fujino, M. T-226296: A novel, orally active and selective melanin-concentrating hormone receptor antagonist. *Eur. J. Pharmacol.* **438**, 129–135 (**2002**).

222. Lecklin, A. & Tuomisto, L. The blockade of H1 receptors attenuates the suppression of feeding and diuresis induced by inhibition of histamine catabolism. *Pharmacol. Biochem. Behav.* **59**, 753–758 (**1998**).

223. Fülöp, A. K., Földes, A., Buzás, E., Hegyi, K., Miklós, I. H., Romics, L., Kleiber, M., Nagy, A., Falus, A. & Kovács, K. J. Hyperleptinemia, visceral adiposity, and decreased glucose tolerance in mice with a targeted disruption of the histidine decarboxylase gene. *Endocrinology* **144**, 4306–4314 (**2003**).

224. Jørgensen, E. A., Knigge, U., Watanabe, T., Warberg, J. & Kjaer, A. Histaminergic neurons are involved in the orexigenic effect of orexin-A. *Neuroendocrinology* **82**, 70–77 (**2005**).

225. Inzunza, O., Serón-Ferré, M. J., Bravo, H. & Torrealba, F. Tuberomammillary nucleus activation anticipates feeding under a restricted schedule in rats. *Neurosci. Lett.* **293**, 139–142 (**2000**).

226. Valdés, J. L., Sánchez, C., Riveros, M. E., Blandina, P., Contreras, M., Farías, P. & Torrealba, F. The histaminergic tuberomammillary nucleus is critical for motivated arousal. *Eur. J. Neurosci.* **31**, 2073–2085 (**2010**).

227. Umehara, H., Mizuguchi, H., Mizukawa, N., Matsumoto, M., Takeda, N., Senba, E. & Fukui, H. Deprivation of anticipated food under scheduled feeding induces c-Fos expression in the caudal part of the arcuate nucleus of hypothalamus through histamine H1 receptors in rats: Potential involvement of E3 subgroup of histaminergic neurons in tuberomammi. *Brain Res.* **1387**, 61–70 (**2011**).

228. Hancock, A. A. & Brune, M. E. Assessment of pharmacology and potential anti-obesity properties of H3 receptor antagonists/inverse agonists. *Expert Opin. Investig. Drugs* **14**, 223–241 (**2005**).

229. Masaki, T., Chiba, S., Yasuda, T., Noguchi, H., Kakuma, T., Watanabe, T., Sakata, T. & Yoshimatsu, H. Involvement of hypothalamic histamine H1 receptor in the regulation of feeding rhythm and obesity. *Diabetes* **53**, 2250–2260 (**2004**).

230. Takahashi, K., Suwa, H., Ishikawa, T. & Kotani, H. Targeted disruption of H3 receptors results in changes in brain histamine tone leading to an obese phenotype. *J. Clin. Invest.* **110**, 1791–1799 (**2002**).

231. Baptista, T., Zarate, J., Joober, R., Colasante, C., Beaulieu, S., Paez, X. & Hernandez, L. Drug induced weight gain, an impediment to successful pharmacotherapy: Focus on antipsychotics. *Curr. Drug Targets* **5**, 279–299 (**2004**).

232. Kroeze, W. K., Hufeisen, S. J., Popadak, B. A., Renock, S. M., Steinberg, S., Ernsberger, P., Jayathilake, K., Meltzer, H. Y. & Roth, B. L. H1-Histamine receptor affinity predicts short-term weight gain for typical and atypical antipsychotic drugs. *Neuropsychopharmacology* **28**, 519–526 (**2003**).

233. Wirshing, D. A., Spellberg, B. J., Erhart, S. M., Marder, S. R. & Wirshing, W. C. Novel antipsychotics and new onset diabetes. *Biol. Psychiatry* **44**, 778–783 (**1998**).

234. Yoshimoto, R., Kanatani, A. & Tokita, S. Distinctive role of central histamine H3 receptor in various orexigenic pathways. *Eur. J. Pharmacol.* **579**, 229–232 (**2008**).

235. Itoh, E., Fujimiya, M. & Inui, A. Thioperamide, a histamine H3 receptor antagonist, suppresses NPY-but not Dynorphin A-induced feeding in rats. *Regul. Pept.* **75-76**, 373–376 (**1998**).

236. Davoodi, N., Kalinichev, M. & Clifton, P. G. Comparative effects of olanzapine and ziprasidone on hypophagia induced by enhanced histamine neurotransmission in the rat. *Behav. Pharmacol.* **19**, 121–128 (**2008**).

237. Kotańska, M., Kuder, K., Szczepańska, K., Sapa, J. & Kieć-Kononowicz, K. The histamine H3 receptor inverse agonist pitolisant reduces body weight in obese mice. *Naunyn Schmiedeberg's Arch. Pharmacol.* (**2018**).

238. Dudek, M., Kuder, K., Kołaczkowski, M., Olczyk, A., Żmudzka, E., Rak, A., Bednarski, M., Pytka, K., Sapa, J. & Kieć-Kononowicz, K. H3 histamine receptor antagonist pitolisant reverses some subchronic disturbances induced by olanzapine in mice. *Metab. Brain Dis.* **31**, 1023–1029 (**2016**).

239. Malmlöf, K., Zaragoza, F., Golozoubova, V., Refsgaard, H. H., Cremers, T., Raun, K., Wulff, B. S., Johansen, P. B., Westerink, B. & Rimvall, K. Influence of a selective histamine H3 receptor antagonist on hypothalamic neural activity, food intake and body weight. *Int. J. Obes.* **29**, 1402–1412 (**2005**).

240. Malmlöf, K., Hastrup, S., Wulff, B. S., Hansen, B. C., Peschke, B., Jeppesen, C. B., Hohlweg, R. & Rimvall, K. Antagonistic targeting of the histamine H3 receptor decreases caloric intake in higher mammalian species. *Biochem. Pharmacol.* **73**, 1237–1242 (**2007**).

241. Peschke, B., Bak, S., Hohlweg, R., Pettersson, I., Frølund Refsgaard, H. H., Viuff, D. & Rimvall, K. Cinnamic amides of (S)-2-(aminomethyl)pyrrolidines are potent H3 antagonists. *Bioorg. Med. Chem.* **12**, 2603–2616 (**2004**).

242. Lau, J. F., Jeppesen, C. B., Rimvall, K. & Hohlweg, R. Ureas with histamine H3-antagonist receptor activity - A new scaffold discovered by lead-hopping from cinnamic acid amides. *Bioorg. Med. Chem. Lett.* **16**, 5303–5308 (**2006**).

243. Gbahou, F., Davenas, E., Morisset, S. & Arrang, J.-M. Effects of betahistine at histamine H3 receptors: mixed inverse agonism/agonism in vitro and partial inverse agonism in vivo. *J. Pharmacol. Exp. Ther.* **334**, 945–954 (**2010**).

244. Fossati, A., Barone, D. & Benvenuti, C. Binding affinity profile of betahistine and its metabolites for central histamine receptors of rodents. *Pharmacol. Res.* **43**, 389–392 (**2001**).

245. Barak, N., Greenway, F. L., Fujioka, K., Aronne, L. J. & Kushner, R. F. Effect of histaminergic manipulation on weight in obese adults: a randomized placebo controlled trial. *Int. J. Obes.* **32**, 1559–1565 (**2008**).

246. Ali, A. H., Yanoff, L. B., Stern, E. A., Akomeah, A., Courville, A., Kozlosky, M., Brady, S. M., Calis, K. A., Reynolds, J. C., Crocker, M. K., Barak, N. & Yanovski, J. A. Acute effects of betahistine hydrochloride on food intake and appetite in obese women: a randomized, placebo-controlled trial. *Am. J. Clin. Nutr.* **92**, 1290–1297 (**2010**).

247. Poyurovsky, M., Pashinian, A., Levi, A., Weizman, R. & Weizman, A. The effect of betahistine, a histamine H1 agonist/H3 antagonist, on olanzapine-induced weight gain in first-episode schizophrenia patients. *Int. Clin. Psychopharmacol.* **20**, 101–103 (**2005**).

248. Poyurovsky, M., Fuchs, C., Pashinian, A., Levi, A., Weizman, R. & Weizman, A. Reducing antipsychotic-induced weight gain in schizophrenia: A double-blind placebo-controlled study of reboxetine-betahistine combination. *Psychopharmacology* **226**, 615–622 (**2013**).

249. Van Ruitenbeek, P. & Mehta, M. A. Potential enhancing effects of histamine H1 agonism/H3 antagonism on working memory assessed by performance and bold response in healthy volunteers. *Br. J. Pharmacol.* **170**, 144–155 (**2013**).

250. Jin, C. Y., Anichtchik, O. & Panula, P. Altered histamine H3 receptor radioligand binding in post-mortem brain samples from subjects with psychiatric diseases. *Br. J. Pharmacol.* **157**, 118–129 (**2009**).

251. Zhang, M., Ballard, M. E., Pan, L., Roberts, S., Faghih, R., Cowart, M., Esbenshade, T. A., Fox, G. B., Decker, M. W., Hancock, A. A. & Rueter, L. E. Lack of cataleptogenic potentiation with non-imidazole H3 receptor antagonists reveals potential drug-drug interactions between imidazole-based H3 receptor antagonists and antipsychotic drugs. *Brain Res.* **1045**, 142–149 (**2005**).

252. Duty, S. & Jenner, P. Animal models of Parkinson's disease: A source of novel treatments and clues to the cause of the disease. *Br. J. Pharmacol.* **164**, 1357–1391 (**2011**).

Curriculum Vitae

Personal Information	
Name	Stefanie Hagenow (née Kaßel)
Address (academic)	Heinrich Heine University, Institute of Pharmaceutical and Medicinal Chemistry, Universitaetsstr. 1, 40225 Duesseldorf
E-Mail	Stefanie.hagenow@hhu.de, steffi.kassel@gmx.net
Phone (academic)	+49 (0) 211 81 13831
Birth date	07.09.1989
Nationality	German

Education	
2014 - 2018	PhD graduation
	Heinrich Heine University Duesseldorf, Germany
2011 - 2014	M. Sc. Toxicology
	Heinrich Heine University Duesseldorf, Germany
2008 - 2011	B. Sc. Chemistry
	Georg August University Goettingen, Germany

Memberships & Awards	
2018	Young Investigator Award, 1st Prize (received from the EHRS)
2018	European Histamine Research Society (EHRS)
2015	German Pharmaceutical Society (DPhG)

Work Experience	
2014 - 2018	Supervisor in biochemical & molecular biological education
	Heinrich Heine University Duesseldorf, Germany
2013 - 2014	Scientific assistant, Institute of Toxicology
	University Hospital Duesseldorf, Germany
2011	Student assistant
	Poison Center GIZ Nord Goettingen, Germany

Internships	
2017	St Andrews, Scotland
	Short-termed scientific mission, COST Action CA15135
2015	St Andrews, Scotland
	Short-termed scientific mission, COST Action CM1103

Skills & Qualifications	
Languages	German (native language), English (fluent)
Practical Skills	Biosafety level 1 tasks, radionucleotide handling, enzymology, biochemistry, toxicology, molecular biology
Certifications	Certification for laboratory animal science
	General Knowledge of Chemicals (5§ChemVerbotsV)

List of Publications

<table>
<tr>
<td>Original Publications
in this thesis</td>
<td>A. Affini[*], <u>S. Hagenow</u>[*], A. Zivkovic, J. Marco-Contelles, H. Stark, Novel indanone derivatives as MAO B/H3R dual targeting ligands for treatment of Parkinson's disease, Eur. J. Med. Chem., 148, 487-497, 2018. (IF, 4.861, 2017)
[*] equal contribution</td>
</tr>
</table>

Ó.M. Bautista-Aguilera[*], <u>S. Hagenow</u>[*], A. Palomino-Antolin[*], V. Farré-Alins[*], L. Ismaili, P.L. Joffrin, M.L. Jimeno, O. Soukup, J. Janockova, L. Kalinowsky, E. Proschak, I. Iriepa, I. Moraleda, J.S. Schwed, A. Romero Martínez, F. López-Munoz, M. Chioua, J. Egea, R.R. Ramsay, J. Marco-Contelles, H. Stark, Multitarget-Directed Ligands Combining Cholinesterase and Monoamine Oxidase Inhibition with Histamine H_3R Antagonism for Neurodegenerative Diseases, *Angew. Chem. Int. Ed.*, 56, 12765-12769, 2017. (IF, 12.102, 2017)
[*] equal contribution

AND

Multipotente Liganden mit kombinierter Cholinesterase- und Monoaminooxidase-Inhibition sowie Histamin-H_3R-Antagonismus bei neurodegenerativen Erkrankungen, *Angew. Chem.*, 129, 12939-12943, 2017. (German Version)

<u>S. Hagenow</u>, A. Stasiak, R. R. Ramsay, and H. Stark, Ciproxifan, a histamine H_3 receptor antagonist, reversibly inhibits monoamine oxidase A and B, *Sci. Rep.*, 7, 40541, 2017. (IF, 4.609, 5-year, 2017)

D. Schaller, <u>S. Hagenow</u>, G. Alpert, A. Naß, R. Schulz, M. Bermudez, H. Stark, G. Wolber, Systematic Data Mining Reveals Synergistic H_3R/MCHR1 Ligands, *ACS Med. Chem. Lett.*, 8, 648-653, 2017. (IF, 3.794, 2017)

<table>
<tr>
<td>Original Publications
& Reviews</td>
<td>M A. Khanfar, D. Reiner, <u>S. Hagenow</u>, H. Stark, Design, synthesis, and biological evaluation of novel oxadiazole- and thiazole-based histamine H_3R ligands, Bioorg. Med. Chem., in press, doi: 10.1016/j.bmc.2018.06.028, 2018. (IF, 2.881, 2017)</td>
</tr>
</table>

H. Elshaflu, T. R. Todorovic, M. Nikolic, A. Lolic, A. Visnjevac, <u>S. Hagenow</u>, J. M. Padron, A. T. Garcia-Sosa, I. S. Djordjevic, S. Grubisic, H. Stark, N. R. Filipovic, Selenazolyl-hydrazones as novel class of selective MAO inhibitors with antiproliferative and antioxidant activities, *Front. Chem.*, 6(247), 1-18, 2018. (IF, 3.994, 2017)

K. Szczepańska, T. Karcz, S. Mogilski, A. Siwek, K. J. Kuder, G. Latacz, <u>S. Hagenow</u>, A. Lubelska, A. Olejarz, M. Kotańska, B. Sadek, H. Stark, K. Kieć-Kononowicz, Synthesis and biological activity of novel tert-butyl and tert-pentylphenoxyalkyl piperazine derivatives as histamine H_3R ligands, *Eur. J. Med. Chem.*, 152, 223-234, 2018. (IF, 4.861, 2017)

D. Lazewska, M. Kaleta, S. Hagenow, S. Mogilski, G. Latacz, T. Karcz, B. Filipek, H. Stark, K. Kieć-Kononowicz, Novel naphthyloxy derivatives - potent histamine H_3 receptor ligands. Synthesis and pharmacological evaluation, *Bioorg. Med. Chem.*, 26(9), 2573-2585, 2018. (IF, 2.881, 2017)

B. Sadek, D. Lazewska, S. Hagenow, K. Kiec-Kononowiczc, H. Stark, Histamine H_3R Antagonists: From Scaffold Hopping to Clinical Candidates, in *Histamine Receptors: Clinical and Preclinical Apsects*, vol. 28, P. Blandina and M. B. Passani, Eds. Cham, Switzerland: Springer, 109-156, 2016.

S. Butini, K. Nikolic, S. Kassel, H. Brückmann, S. Filipic, D. Agbaba, S. Gemma, S. Brogi, M. Brindisi, G. Campiani, H. Stark, Polypharmacology of dopamine receptor ligands, *Prog. Neurobiol.*, 142, 68-103, 2016. (IF, 14.163, 2017)

S. Kaßel, J. Hagenow, H. Stark, H_1-Antihistimanika - Neue Aspekte einer alten Wirkstoffklasse [H_1 Antihistamines - Current aspects of an old class of drugs], *Pharmakon*, 2, 96-108, 2015.

S. Kassel, J. S. Schwed, H. Stark, Dopamine D_3 receptor agonists as pharmacological tools, *Eur. Neuropsychopharmacol.*, 25(9), 1480-1499, 2015. (IF, 4.129, 2017)

F. Stuhldreier, S. Kassel, L. Schumacher, S. Wesselborg, P. Proksch, G. Fritz, Pleiotropic effects of spongean alkaloids on mechanisms of cell death, cell cycle progression and DNA damage response (DDR) of acute myeloid leukemia (AML) cells, *Cancer Lett.*, 361(1), 39-48, 2015. (IF, 6.491, 2017)

Patent application
F. López-Munoz, J. Marco Contelles, H. Stark, S. Hagenow, R. R. Ramsay, Nuevos compuestos con capacidad antioxidante que combinan la inhibición e las enzimas monoaminoxidasas y colinesterasas y la interacción con el receptor de histamina 3, su prodecimiento de obtención y composiciones farmacéuticas que los contienen, No. P201731044 (Aug 23, 2017).

Miscellaneous
S. Hagenow, H. Stark, From Magic Bullet To Magic Pump Gun: Multi-Targeting Drugs For Neurodegenerative Diseases, *Science Trends*, sciencetrends.com (Oct 30, 2017).

S. Hagenow, H. Stark, Promiscuous drugs exemplified by dopamine receptor ligands, *Atlas of Science*, atlasofscience.org (Dec 7, 2016).

Poster
K. Szczepanska, T. Karcz, S. Mogilsky, K. Kuder, S. Hagenow, M. Kotanska, H. Stark, K. Kiéc-Kononowicz, Piperazine derivatives as novel, active histamine H_3 receptor ligands, European Histamine Research Society 47th Annual Meeting, 31 May - 02 June 2018, Dublin, Ireland, Abstract book, p. 70 (presenting author: K. Szczepanska).

S. Hagenow, O. Bautista-Aguilera, A. Palomino-Antolin, V. Farre-Alins, P.-J. Joffrin, M.L. Jimeno, O. Soukop, J. Janockova, A. Romero Martinez, F. Lopez-Munoz, L. Ismaili, L. Kalinowsky, E. Proschak, I. Iriepa, I. Moraleda, J.S. Schwed, M. Chioua, J. Egea, R.R. Ramsay, J. Marco-Contelles, H. Stark, Contilisant as multi-targeting ligand combining cholinesterase and monoamine oxidase inhibition with histamine H_3R antagonism for Alzheimer's disease, Düsseldorf-Jülich Symposium on Neurodegenerative Diseases, 27-29 November 2017, Düsseldorf, Conference Book, p. 64 (POST.14).

D. Lazewska, M. Bajda, S. Hagenow, E. Stawarska, P. Zareba, H. Stark, B. Malawska, K. Kiéc-Kononowicz, Acetyl- and Butyryl-cholinesterase Inhibitory Activity of Histamine H_3 Receptor Ligands, Histamine 2017 - Joint Meeting of the European and Japanese Histamine Research Societies, 11-13 May 2017, Amsterdam, The Netherlands, Abstract Book, p. 75 (presenting author: D. Lazewska); Inflamm. Res. 66 (Suppl. 1), S24-S24, 2017.

S. Hagenow, A. Stasiak, R.R. Ramsay, H. Stark, Ciproxifan directing for H_3R/MAO dual targeting ligands in therapy of Parkinson's disease, GLISTEN COST Action CM1207 Meeting, 29-31 March 2017, Porto, Portugal (presenting author: H. Stark)

S. Kassel, O. Saur, T. Kottke, H. Stark, Studies on biased signaling of novel dopamine D_2 and D_3 receptor ligands, DPhG Annual Meeting, 23-25 September 2015, Düsseldorf, Germany, Conference Book, p. 150 (POS.095).

Oral Presentations

S. Hagenow, A. Stasiak, O. Bautista-Aguilera, A. Palomino-Antolin, V. Farre-Alins, M.L. Jimeno, A. Romero Martãnez, F. López-Munoz, I. Iriepa, I. Moraled, O. Soukop, J. Janockova, L. Ismaili, L. Kalinowsky, E. Proschak, J.S. Schwed, M. Chioua, J. Egea, J. Marco-Contelles, P.-J. Joffrin, R.R. Ramsay, H. Stark, Design of multitargeting histamine H_3 receptor antagonists for neurodegenerative diseases, European Histamine Research Society 47th Annual Meeting, 31 May - 02 June 2018, Dublin, Ireland, Abstract book, p. 46 (O13). FIRST PRIZE, YOUNG INVESTIGATOR AWARD 2018

S. Hagenow, A. Stasiak, A. Affini, A. Zivkovic, W.A. Fogel, H. Stark, Dual MAO B and histamine H_3 receptor inhibitor ST1957, a potential drug candidate for therapy of neurodegenerative diseases, European Histamine Research Society 47th Annual Meeting, 31 May - 02 June 2018, Dublin, Ireland, Abstract book, p. 45 (O12, presenting author: W.A. Fogel).

H. Stark, A. Affini, J. Marco-Contelles, S. Hagenow, Novel indanone derivatives as MAO B/H_3R dual targeting ligands for treatment of Parkinson's disease, MuTaLig COST Action CA15135 WG Meeting, 15 - 16 March 2018, Tenerife, Spain (presenting author: H. Stark).

N. R. Filipovic, A. Visnjevac, J. M. Padrón, H. Stark, <u>S. Hagenow</u>, S. Markovic, T. R. Todorovic, Biological activity of novel benzylidene-based (1,3-selenazol-2-yl)hydrazones, MuTaLig COST Action CA15135 WG Meeting, 15-16 March 2018, Tenerife, Spain (presenting author: N. R. Filipovic).

<u>S. Hagenow</u>, A. Stasiak, R. R. Ramsay and H. Stark, The reference H_3 receptor antagonist Ciproxifan is a moderate inhibitor of human monoamine oxidase A and B, International PhD students/Postdocs meeting of the German Pharmaceutical Society (DPhG), 29 - 31 March 2017, Frankfurt a. M., Germany.

K. Szczepanska, T. Karcz, K. Kuder, A. Olejarz, A. Siwek, <u>S. Hagenow</u>, H. Stark, and K. Kiéc-Kononowicz, Piperazine derivatives as novel histamine H_3 receptor ligands, VII Meeting of the Paul Ehrlich Euro-PhD Network, 25 - 27 August 2017, Vienna, Austria, Abstract Book, p. 20. (presenting author: K. Kiéc-Kononowicz).

H. Stark, <u>S. Hagenow</u>, A. Affini, A. Stasiak, R. R. Ramsay, Histamine H_3 Receptor Antagonists Acting as Monoamine Oxidase Inhibitors, EpiChemBio (CM1406) and MuTaLig COST (CA15135) Joint Meeting, 22 - 24 September 2017, Porto, Portugal. (presenting author: H. Stark).

Acknowledgement

A scientific work is never the work of a single person. So I would like to take this opportunity to thank all who have accompanied me on the way to my PhD graduation.

First, I would like to acknowledge the assistance of Prof. Dr. Holger Stark, who gave me this interesting research topic to work on. My thanks go also to Prof. Dr. Holger Gohlke for taking over the mentorship. Particularly, I would like to thank Prof. Holger Stark for the guidance and steady promotion of my scientific career as well as the support in every respect during my time as a doctoral student.

My deepest appreciation goes also to Rona Ramsay for the host and assistance of my short-scientific missions, financially supported by the European Cooperation in Science and Technology (COST). These stays made a considerable contribution to the thematic development of my thesis as well as my scientific education. I am grateful for the intensive training in enzymology and provided guidance on any issue, not only during my stays in St Andrews.

I also thank my colleagues within the working group and the whole institute for the always friendly working atmosphere. In particular, I would like to mention Anna Affini, Jan Bandolik, Milica Elek, Annika Frank, Kathrin Grau, Alexandra Hamacher, David Reiner, Alexander Skerhut and Aleksandra Zivkovic. Thank you for the effective and good cooperation, the fruitful discussions, the friendly relationship beyond the work, as well as constant motivation and encouragement during my doctoral studies.

After all, my sincerest thanks go to my marvelous family for facilitating my scientific education and their untiring support in any situation. Last but not least, I owe my deepest gratitude to my husband, Jens. All of this would not have been possible without your unlimited support, care and love. Your faith in me has always encouraged me to do my best.

Eidesstattliche Erklärung

Name: Stefanie Hagenow

Ich versichere an Eides Statt, dass die Dissertation "Histamine H_3 receptor antagonists with multitargeting properties at GPCRs and enzymes" von mir selbstständig und ohne unzulässige fremde Hilfe unter Beachtung der "Grundsätze zur Sicherung guter wissenschaftlicher Praxis an der Heinrich-Heine-Universität Düsseldorf" erstellt worden ist. Ich erkläre weiterhin, dass die vorliegende Arbeit noch nicht im Rahmen eines anderen Prüfungsverfahrens eingereicht wurde.

Düsseldorf, den   Unterschrift: